



**UNIVERSIDADE ESTADUAL DE CAMPINAS**

**INSTITUTO DE BIOLOGIA**

**Natalia Novoselova**

**ANALYSIS OF THE EFFECT OF METEOROLOGICAL, SUPERFICIAL AND ANTHROPOGENIC CONDITIONS ON THE SOARING ACTIVITY OF THE BLACK VULTURE (*Coragyps atratus*, *CATHARTIDAE*) BY MEANS OF GIS AND REMOTE SENSING AND ITS IMPLICATION FOR THE REDUCTION OF BIRD STRIKE RISKS**

**ANÁLISE DO EFEITO DAS CONDIÇÕES METEOROLÓGICAS, SUPERFICIAIS E ANTROPOGÊNICAS SOBRE ATIVIDADE DE VOO DO URUBU-DE-CABEÇA-PRETA (*Coragyps atratus*, *CATHARTIDAE*) POR MEIO DE SIG E SENSORIAMENTO REMOTO E SUAS IMPLICAÇÕES PARA A REDUÇÃO DO RISCO DE COLISÕES COM AERONAVES**

Campinas, 2016

**Natalia Novoselova**

ANALYSIS OF THE EFFECT OF METEOROLOGICAL, SUPERFICIAL AND ANTHROPOGENIC CONDITIONS ON THE SOARING ACTIVITY OF THE BLACK VULTURE (*Coragyps atratus*, CATHARTIDAE) BY MEANS OF GIS AND REMOTE SENSING AND ITS IMPLICATION FOR THE REDUCTION OF BIRD STRIKE RISKS

ANÁLISE DO EFEITO DAS CONDIÇÕES METEOROLÓGICAS, SUPERFICIAIS E ANTROPOGÊNICAS SOBRE ATIVIDADE DE VOO DO URUBU-DE-CABEÇA-PRETA (*Coragyps atratus*, CATHARTIDAE) POR MEIO DE SIG E SENSORIAMENTO REMOTO E SUAS IMPLICAÇÕES PARA A REDUÇÃO DO RISCO DE COLISÕES COM AERONAVES

Dissertation presented to the Institute  
of Biology of the University of Campinas  
in partial fulfillment of the  
requirements for the degree of Master  
in Ecology

Dissertação apresentada ao Instituto de  
Biologia da Universidade Estadual de  
Campinas como parte dos requisitos  
exigidos para a obtenção do Título de  
Mestra em Ecologia

ESTE ARQUIVO DIGITAL CORRESPONDE À  
VERSÃO FINAL DA TESE DEFENDIDA PELA  
ALUNA NATALIA NOVOSELOVA E ORIENTADA  
PELO PROF. DR. WESLEY RODRIGUES SILVA.

Orientador: Dr. Wesley Rodrigues Silva

Campinas, 2016

**Agência(s) de fomento e nº(s) de processo(s):** CAPES

Ficha catalográfica  
Universidade Estadual de Campinas  
Biblioteca do Instituto de Biologia  
Mara Janaina de Oliveira - CRB 8/6972

N859a Novoselova, Natalia Sergeevna, 1980-  
Analysis of the effect of meteorological, superficial and anthropogenic conditions on the soaring activity of the black vulture (*Coragyps atratus*, Cathartidae) by means of GIS and remote sensing and its implication for the reduction of bird strike risks / Natalia Sergeevna Novoselova. – Campinas, SP : [s.n.], 2016.

Orientador: Wesley Rodrigues Silva.  
Dissertação (mestrado) – Universidade Estadual de Campinas, Instituto de Biologia.

1. Colisões entre aeronaves e aves - Prevenção. 2. Avaliação de riscos - Métodos. 3. *Coragyps atratus*. 4. Sistemas de informação geográfica. 5. Sensoriamento remoto. I. Silva, Wesley Rodrigues, 1955-. II. Universidade Estadual de Campinas. Instituto de Biologia. III. Título.

Informações para Biblioteca Digital

**Título em outro idioma:** Análise do efeito das condições meteorológicas, superficiais e antropogênicas sobre atividade de voo do urubu-de-cabeça-preta (*Coragyps atratus*, Cathartidae) por meio de SIG e sensoriamento remoto e suas implicações para a redução do risco de colisões com aeronaves

**Palavras-chave em inglês:**

Aircraft bird strikes - Prevention

Risk assessment - Methods

*Coragyps atratus*

Geographic information systems

Remote sensing

**Área de concentração:** Ecologia

**Titulação:** Mestra em Ecologia

**Banca examinadora:**

Wesley Rodrigues Silva

Milton Cezar Ribeiro

Diego Fernando Ducart

**Data de defesa:** 26-07-2016

**Programa de Pós-Graduação:** Ecologia

Campinas, 26 de julho de 2016

### **COMISSÃO EXAMINADORA**

Prof.Dr.Wesley Rodrigues Silva (orientador)

Prof. Dr. Milton Cezar Ribeiro

Prof. Dr. Diego Fernando Ducart

*Os membros da Comissão Examinadora acima assinaram a Ata de defesa, que se encontra no processo de vida acadêmica do aluno.*



*I wish to dedicate my work to the Environmental movement of the World*

## ACKNOWLEDGEMENTS

I am very grateful to my advisor Prof. Dr. Wesley Rodrigues Silva for the excellent academic guidance, important ideas about the project implementation, correction of the text and assistance with the finalization of the thesis.

I am very thankful to the ornithologists Guilherme Ortiz and Arthur Macarrão Montanhini for their professionalism in the bird's census and to biologist Angelo Benaglia for his assistance in developing of the field observations methodology.

Also I thank the following people for their technical assistance, advices and valuable contribution in the project:

Alexey Novoselov, Dr. in Geochemistry, post-doctoral researcher of the Institute of Geosciences (UNICAMP), for his valuable help in statistical analyses, discussion of the project ideas and text corrections.

Prof. Igor Belov, Dr. in Technical Sciences, a senior lecturer of the Department of Astronomy and Space Geodesy in Kazan Federal University (Russia) for accurate astronomic calculation of the local sunrise, sunset and noon for the studied areas.

I am very thankful to all members of the professional Internet community GIS-Lab: <http://gis-lab.info> for their valuable assistance in solution of numerous technical and scientific questions of GIS and remote sensing technologies, which I needed to solve for the project implementation. Especially I want to thank the following persons:

Maxim Dubinin – for creation and administration of this incredible professional community, for assistance of my effective work there, for his personal help, advices and moral support.

Anton Novichikhin, Alexander Cherepanov, Ericsson N., Nikita Lawrentyew, Alexander Muriy, Anatoliy Saveliev, Ivan Strelnikov, Nadejda Vladimirova, Timur Gimranov, Igor Bavshin, Andrey Pirogov, Alexander Manisha – for their technical and educational help, discussion of the project implementation and moral support.

Also I want to thank Prof. Dr. Carlos Roberto de Souza Filho (Institute of Geosciences, UNICAMP) for allowing me to take his discipline “Geotecnologias Aplicadas ao Estudo de Recursos Naturais (GA235)”, which helped me a lot in familiarization with the remote sensing technology for the project implementation.

I thank all professors of the Biology Institute of UNICAMP and all my colleagues of the laboratory LIVEP for their help and advices.

I thank the CAPES Brazilian Foundation for the financial support.

## RESUMO

O incremento do número de colisões de aeronaves com pássaros perto de aeroportos, causado principalmente pelo aumento do tráfego de aeronaves juntamente com o crescimento de populações de aves, são um grande problema para muitos países em todo mundo. Programas de pesquisas nacionais dedicados à elaboração dos métodos de redução do número de colisões com aves foram lançados em vários países.

A maioria das colisões entre aeronaves e pássaros ocorre durante os processos de decolagem e desembarque de aviões dentro da zona de 10 - 20 km ao redor de aeroportos, onde os aviões voam em altitude baixa. No Brasil este problema também é grave e urgente. O urubu-de-cabeça-preta (*Coragyps atratus*, Cathartidae) é uma das espécies mais abundantes nos arredores de aeroportos brasileiros e, ao mesmo tempo, a espécie que causa a maioria das colisões de aviação com pássaros no Brasil. Geralmente os urubus voam em bandos sobre as térmicas (os fluxos de ar ascendentes) durante as horas do dia, subindo a altitudes que trazem perigo para os aviões. Devido ao seu grande tamanho e às características comportamentais, os métodos gerais de controle não funcionam contra esta espécie. Esses conflitos provocam a necessidade de elaboração de abordagens eficazes que sejam capazes de diminuir o risco de colisões com urubus sem danos às populações destas aves.

Nossa investigação foi dedicada ao aperfeiçoamento da elaboração de métodos que permitam reduzir o risco de colisões de aeronaves com urubus. Ela teve duas partes distintas consideradas em dois capítulos. Na primeira parte (Capítulo II) nós estudamos a relação entre a atividade de voos de urubus e as características meteorológicas. Na segunda parte (Capítulo III) nós exploramos a dependência da atividade de voo de urubus das condições superficiais e antrópicas. O estudo de ambas as partes foi implementado nos arredores de dois aeroportos do sudeste do Brasil, escolhidos como áreas modelo.

Nós desenvolvemos as novas abordagens metodológicas combinadas de SIG e Sensoriamento remoto com tecnologias para processamento de dados espaciais, que foram utilizadas na nossa investigação como o instrumento de pesquisa principal. Por meio destas metodologias nós juntamos aos bancos de dados georreferenciados (shapefiles) os dados de observação de urubus e de três tipos de fatores ambientais: (i) condições meteorológicas coletadas juntamente com as observações de urubus; (ii) características superficiais (temperatura superficial e relevo) obtidas a partir de produtos de imagens ASTER; (iii) parâmetros de pressão humana e tipo de cobertura superficial obtidos a partir de imagens de satélite de resolução alta. Através das análises dos bancos de dados georreferenciados foi estudada a relação entre a

atividade de voo de urubus e os fatores ambientais. Bem como foram revelados os padrões comportamentais das aves em voo planado, os tipos de paisagem altamente atrativas para urubus e as grandes concentrações destas aves sobre eles. A partir dessas informações foram construídos mapas de avaliação do risco de colisão entre urubus e aeronaves nos arredores dos aeroportos e feitas recomendações práticas sobre a sua diminuição.

Nossos resultados mostraram que a altitude de voo planado dos urubus varia entre 13 a 550 metros. Existem dois padrões temporais de voo planado dos urubus: um apresentando um platô na maior parte do dia e outro com dois picos distintos, de manhã e à tarde, com uma queda notável entre eles. Em ambos os padrões, a atividade de voo tem início cerca de 1 - 1,5 horas após o amanhecer e se encerra cerca de 1 - 1,5 horas antes do poente. O forte stress antropogênico em combinação com uma área urbana grande e contínua torna-se um fator negativo para os urubus, ocasionando uma redução no número de urubus voando. Em contraste, zonas urbanas pequenas, cercada por territórios naturais e rurais, são muito atraentes para estas aves. Corpos d'água e rodovias são elementos da paisagem atraentes para urubus em voo. Foi confirmada a hipótese de que urubus tendem a planar mais sobre as térmicas mais fortes em seus arredores.

Acreditamos que os resultados da nossa investigação e as novas metodologias elaboradas ajudarão a desenvolver métodos eficazes para a redução do número de colisões de aeronaves com urubus e outras aves nos aeroportos brasileiros.

## **Palavras-chaves**

Problema de colisões de aeronaves com pássaros, perigo de aviões, mapa de avaliação do risco de colisões, redução de risco de colisões, Urubu-de-cabeça-preta, *Coragyps atratus*, comportamento de voo, altura de voo, variação diária de atividade de voo, variação sazonal de atividade de voo, térmicas, Sistema de Informação Geográfica, SIG, sensoriamento remoto, ASTER, imagens de satélite.

## ABSTRACT

The increasing numbers of aircraft collisions with birds near airports, caused mainly by growth of aircraft traffic and increase of bird populations are a big problem for many countries all over the world. The national research programs have been launched in several countries in order to solve the Bird Strike Problem. Most of bird-strike events occur during takeoff and landing operations within zone of 10-20 km around airports, where airplanes fly at low altitude. In Brazil this problem is also serious and urgent. The Black vulture (*Coragyps atratus*, Cathartidae) is the most abundant species in airports surroundings and, at the same time, the species that causes most of collisions with aviation in Brazil. These birds usually soar in flocks on thermals (the upward air flows) during daily hours, ascend highly at sky and cause the hazard of strikes for aviation. Due to its large size and behavioral features, the most common control approaches (falconry, ground deterrents) do not work against it. These conflicts cause the necessity of elaboration the effective measures, which can decrease the risk of strikes with Black vultures without harming these birds.

Our investigation was devoted to moving forward in elaboration of the methods allowing to reduce the risk of collision with Black vultures. It had two separate parts considered in two chapters. In the first one we studied the relationship between soaring activity of vultures and meteorological characteristics (Chapter II); in the second one we explored the dependence of soaring activity of vultures on superficial and anthropogenic factors (Chapter III). The both parts were implemented within surroundings of two airports of southeast of Brazil taken as case studies.

We developed the methodological approaches combining application of GIS and remote sensing technologies for data processing, which were used as the main research instrument. By dint of them we joined in the georeferenced databases (shapefiles) the data of bird's observation and three types of environmental factors: (i) meteorological characteristics collected together with the bird's observation, (ii) superficial parameters (relief and surface temperature) obtained from the products of ASTER imagery; (iii) parameters of surface covering and anthropogenic pressure obtained from the satellite images of high resolution. Based on the analyses of the prepared georeferenced databases, the relationship between soaring activity of vultures and environmental factors was studied; the behavioral patterns of vultures in soaring flight were revealed; the landscape types highly attractive for this species and forming the increased concentration of birds over them were detected; the maps giving a numerical estimation of

hazard of bird strike events over the airport vicinities were constructed; the practical recommendations devoted to decrease the risk of collisions with vultures were formulated.

Our results showed that the altitude of soaring flights of Black vultures ranges from 13 to 550 metres. There were two types of schedule of daily soaring activity: plateau-like plot and plot with two peaks at morning and afternoon with a notable drop between them. At both types, about 1- 1.5 hours after local sunrise the soaring activity starts and about 1 - 1.5 hours before local sunset the soaring activity finishes. The strong anthropogenic stress in combination with large area of uninterrupted urbanized lands is a negative factor for Black vultures, which decrease the number of soaring birds. In contrast, small islands of urban zones, surrounded by natural and rural territories, are highly attractive to these birds. Water bodies and automobile roads are the most attractive objects for soaring Black vultures. The hypothesis, stating that Black vultures tend to soar over the strongest thermals in their surroundings was confirmed.

We believe, that the results of our investigation and elaborated methodologies will help to develop the effective set of measures allowing to decrease the number of aircraft collisions with Black vultures and other bird species.

### **Key words**

Bird strike problem, aviation hazard, risk assessment map, reduction of bird strike risks, Black vulture, *Coragyps atratus*, soaring behaviour, altitudes of flights, daily variation of flying activity, seasonal variation of flying activity, thermals, Geographical Information System, GIS, remote sensing, satellite imagery, ASTER.

## STRUCTURE OF THE DISSERTATION

The Dissertation has the following structure. In the **Chapter I** we presented the preamble of our investigation. In the “**General introduction**” section we described the bird strike problem: its extent in the world, consequence, history and measures, which were realized in Brazil and other countries for its solution. There we designated the objectives and justification of our research. In the “**Ecological and behavioural traits of the Black vulture**” section we gave a short review of ecological and behavioural properties of Black vultures with a special focus on the behavioral traits, which were important for our investigation.

The results we presented in form of papers intended for peer reviewed journals. In the **Chapter II** we considered the dependence of soaring activity of Black vultures on meteorological conditions and behavioral patterns of vultures in soaring flight. In the **Chapter III** we considered the relationship between abundance of soaring Black vultures and superficial characteristics. Also there we gave some practical recommendations about the possibilities to reduce the number of aircraft collisions with vultures. In the **Chapter IV** we highlighted the key points of the novel methodological approaches elaborated during our research and their possible application for the solution of bird strike problem.

We resumed all findings obtained in our investigation in the “**Final conclusions**” section. The bibliography and Internet resources specialized on remote sensing and GIS technologies and applied in our study are given in the “**Reference**” section. The “**Appendices**” section contains the additional figures and tables, mentioned in the text. Also it includes the descriptions of several technical operations of data preparation for analyses and risk maps construction, implemented in ArcGIS software.

The “**Description of the Supplementary Files**” tabular section contains the description of various files applied in our research and link for download on the “**Supplementary Files**” folder representing those files as online archive. In the dissertation we marked each link on file from the “Supplementary Files” archive and its description by letters “SF” with a number of supplementary file in the list (like “SF1”, “SF2”).

# LIST OF FIGURES

## CHAPTER I

Figure 1.1 Geographical range of Black vulture ( <i>Coragyps atratus</i> , Cathartidae) (The IUCN Red list, 2015).....	28
--	----

## CHAPTER II

Figure 2.1 Location of the Amarais and Presidente Prudente airports in the state of São Paulo of Southeastern Brazil .....	35
Figure 2.2 Study area and observation points around the Amarais airport .....	36
Figure 2.3 Study area and observation points around the Presidente Prudente airport .....	37
Figure 2.4 Scheme of detection of the distance interval to an adult Black vulture in soaring flight by binoculars .....	38
Figure 2.5 Estimation of the distance interval to a bird using the size of this bird in binoculars .....	39
Figure 2.6 Calculation of the geographical coordinates (latitude, longitude) and height of flight parameter of a mid-point location of each registered bird.....	41
Figure 2.7 The registered birds georeferenced as vector points (example from Amarais site) .....	42
Figure 2.8 The average monthly temperature for daily hours (8:00-18:00), °C.....	43
Figure 2.9 The total amount of birds registered in each viewpoint during the observation period .....	48
Figure 2.10 Comparing of the studied populations by the number of flying birds recorded at each month by ANOVA test.....	48
Figure 2.11 Distribution of the recorded altitudes of soaring Black vultures nearby the Amarais and Presidente Prudente airports during the period of observation .....	50
Figure 2.12 Comparison of real and log-normal (theoretical) functional relationship between the “altitude of flight” and the “sum of birds recorded at this altitude” parameters .....	50
Figure 2.13 Daily variation in the soaring activity of Black vultures at the year of observations: from September 2012 to August 2013 .....	51
Figure 2.14 Daily variation in the soaring activity of Black vultures and meteorological conditions in the Amarais site (data averaged for each 15-min interval over 13 viewpoints for July).....	52
Figure 2.15 Daily variation in the soaring activity of Black vultures and meteorological conditions in the Amarais site (data averaged for each 15-min interval over 13 viewpoints for December) .....	52
Figure 2.16 Daily variation in the soaring activity of Black vultures and meteorological conditions in the Prudente site (data averaged for each 15-min interval over 13 viewpoints for June) .....	53
Figure 2.17 Daily variation in the soaring activity of Black vultures and meteorological conditions in the Prudente site (data averaged for each 15-min interval over 13 viewpoints for December) .....	54
Figure 2.18 Number of Black vultures recorded at each month.....	55
Figure 2.19 Annual variation of $F_{bird}$ index for study sites. The median, first and third quintile of $F_{bird}$ , averaged for each month over the 13 viewpoints. The result of ANOVA test comparing months by $F_{birds}$ index in each study site .....	55
Figure 2.20 Functional relationship between air temperature and soaring activity of Black vultures in Amarais site.....	56



Figure 2.21 Functional relationship between air temperature and soaring activity of Black vultures in Prudente site .....	57
Figure 2.22 Functional relationship between relative humidity and soaring activity of Black vultures in Amarais site.....	57
Figure 2.23 Functional relationship between relative humidity and soaring activity of Black vultures in Prudente site .....	58
Figure 2.24 Functional relationship between wind speed and soaring activity of Black vultures in Amarais site .....	58
Figure 2.25 Functional relationship between wind speed and soaring activity of Black vultures in Prudente site .....	59
Figure 2.26 The DigitalGlobe image of high resolution representing the vicinity of Campinas (-22.78724, -47.09007), where the observation of Black vulture behaviour near the fresh carcass of large animal was conducted. The red point shows the location of the dead animal .....	65
<b>CHAPTER III</b>	
Figure 3.1 The principle of thermals work (by Prem and Mackley, 2005) .....	79
Figure 3.2 The general scheme of calculation of “contrast of surface temperature”, “slope inclination” and “slope exposure” superficial parameters from original rasters (AST_08, ASTER GDEM v2) .....	81
Figure 3.3 Projected polygons for all distance ranges: 0-6000 m (Amarais site).....	84
Figure 3.4 Projected polygons for three first distance ranges: 0-700 m (Amarais site) .....	84
Figure 3.5 Overlapping of the projected polygons .....	85
Figure 3.6 Examples of projected polygons. Circular shape corresponds to projected polygons with a vertical angle to a bird equal to 90° .....	85
Figure 3.7 Relationship between soaring activity of Black vultures ( $W_{birds}$ ) and contrast of surface temperature in Prudente (a) and Amarais (b) sites.....	95
Figure 3.8 Relationship between soaring activity of Black vulture ( $W_{birds}$ ) and surface temperature in Prudente (a) and Amarais (b) sites .....	97
Figure 3.9 Landscape types and soaring activity of Black vultures (Amarais) .....	99
Figure 3.10 Landscape types and soaring activity of Black vultures (Presidente Prudente) .....	100
Figure 3.11 Deviation from the mean density of $W_{birds}$ of each landscape type.....	100
Figure 3.12 Risk assessment map of aircraft collisions with Black vultures within the 13 km radius around the Amarais airport .....	103
Figure 3.13 Risk assessment map of aircraft collisions with Black vultures within the 13 km radius around the Presidente Prudente airport.....	104
Figure 3.14 Risk assessment map (a); true-color band composition of high resolution imagery (b); surface temperature (c); contrast of surface temperature (d); landscape types (e) for 700 meter zone around the viewpoint № 11 of Amarais site.....	106
Figure 3.15 Risk assessment map (a); true-color band composition of high resolution imagery (b); surface temperature (c); contrast of surface temperature (d); landscape types (e) for 700 meter zone around the viewpoint № 7 of Amarais site.....	109

## LIST OF TABLES

### CHAPTER II

Table 2.1 Distribution of the registered altitudes of soaring Black vultures nearby the Amarais and Presidente Prudente airports during the period of observation .....	49
Table 2.2 Result of the Principal component analysis estimated the relationship between soaring activity of Black vultures ( $F_{bird}$ ) and meteorological condition (Amarais).....	59
Table 2.3 Result of the Principal component analysis estimated the relationship between soaring activity of Black vultures ( $F_{bird}$ ) and meteorological condition (Presidente Prudente) .....	60
Table 2.4 Result of the Multiple regression analysis estimated the dependence of soaring activity of Black vultures on meteorological conditions (Amarais). Dependent variable: $F_{birds}$ .....	60
Table 2.5 Results of the Multiple regression analysis estimated the dependence of soaring activity of Black vultures on meteorological conditions (Presidente Prudente). Dependent variable: $F_{birds}$ .....	61
Table 2.6 Pearson correlation coefficients between values of meteorological characteristics and soaring activity of Black vulture ( $F_{birds}$ ) in Amarais site.....	63
Table 2.7 Pearson correlation coefficients between values of meteorological characteristics and soaring activity of Black vultures ( $F_{birds}$ ) in Prudente site .....	63
Table 2.8 The Pearson correlation coefficients between (i) Wind speed and Solar radiation, (ii) Wind speed and Solar energy (Amarais).....	63

### CHAPTER III

Table 3.1 Identified numbers (ID) of the remote sensing products used in the investigation .....	77
Table 3.2 Main characteristics of the remote sensing products used in the study.....	77
Table 3.3 Classification of landscape types used in the landscape analysis.....	82
Table 3.4 Result of the Principal component analysis estimated the relationship between soaring activity of Black vultures ( $W_{bird}$ ) and superficial characteristics (Amarais, Prudente) .....	93
Table 3.5 Result of the Multiple regression analysis estimated the dependence of soaring activity of Black vulture ( $W_{birds}$ ) on superficial parameters (Amarais). Dependent variable: $W_{birds}$ .....	94
Table 3.6 Result of the Multiple regression analysis estimated the dependence of soaring activity of Black vulture ( $W_{birds}$ ) on superficial parameters (Prudente). Dependent variable: $W_{birds}$ .....	94
Table 3.7 Summary table of the Spearman rank correlation analysis studied the relationship between soaring activity of Black vultures ( $W_{birds}$ ) and contrast of surface temperature (Prudente) .....	96
Table 3.8 Summary table of the Spearman rank correlation analysis studied the relationship between soaring activity of Black vultures ( $W_{birds}$ ) and contrast of surface temperature (Amarais).....	96
Table 3.9 Summary table of the Spearman rank correlation analysis studied the relationship between soaring activity of Black vultures ( $W_{birds}$ ) and surface temperature (Amarais).....	97

Table 3.10 Summary table of the Spearman rank correlation analysis studied the relationship between soaring activity of Black vultures ( $W_{birds}$ ) and surface temperature (Prudente) .....	97
Table 3.11 The soaring activity of Black vulture over the landscape types with different levels of anthropogenic pressure (Amarais) .....	98
Table 3.12 The soaring activity of Black vulture over the landscape types with different levels of anthropogenic pressure (Prudente) .....	99

# LIST OF SCRIPTS

## CHAPTER III

Script 3.1 Algorithm of calculation of the slope inclination parameter for each pixel of the original raster performed by Slope Tool of ArcGIS software .....	81
Script 3.2 Algorithm of calculation of the slope exposure parameter for each pixel of the original raster (ASTER GDEM v2) performed by the Aspect Tool in the ArcGIS software	81

# LIST OF APPENDICES

## APPENDIX A - FIGURES

Figure A.1 Portable meteorological station “WeatherLink Vantage Pro2” .....	137
Figure A.2 Altitude above sea level for surrounding of the Amaraïs airport. Raster map produced from the ASTER GDEM v2 .....	138
Figure A.3 Surface temperature for surrounding of the Amaraïs airport. Raster map produced from the ASTER On-Demand L2 Surface Kinetic Temperature or “AST_08” product of ASTER image made in 11.05.2013, 13:28 .....	139
Figure A.4 Contrast of surface temperature for surrounding of the Amaraïs airport. Raster map produced from the ASTER On-Demand L2 Surface Kinetic Temperature or “AST_08” product of ASTER image made in 11.05.2013, 13:28.....	140
Figure A.5 Contrast of surface temperature for surrounding of the Amaraïs airport (viewpoints 1, 2, 3, 6). Raster map produced from the ASTER On-Demand L2 Surface Kinetic Temperature or “AST_08” product of ASTER image made in 11.05.2013, 13:28.....	141
Figure A.6 Altitude above sea level for surrounding of the the Presidente Prudente airport. Raster map produced by ASTER GDEM v2 .....	142
Figure A.7 Surface temperature map for surrounding of the Presidente Prudente airport. Raster map produced from the ASTER On-Demand L2 Surface Kinetic Temperature or “AST_08” product of ASTER image made in 20.08.2013, 13:46.....	142
Figure A.8 Contrast of surface temperature for surrounding of the Presidente Prudente airport. Raster map produced from the ASTER On-Demand L2 Surface Kinetic Temperature or “AST_08” product of ASTER image made in 20.08.2013, 13:46.....	143
Figure A.9 Daily variation in the soaring activity of Black vultures at each month during the period of study (Prudente, XII – V).....	144
Figure A.10 Daily variation in soaring activity of Black vultures at each month during the period of observation (Prudente, VI - XI) .....	145
Figure A.11 Daily variation in soaring activity of Black vultures at each month during the period of observation (Amaraïs, XII – V) .....	146
Figure A.12 Daily variation in soaring activity of Black vultures at each month during the period of observation (Amaraïs, VI - XI).....	147
Figure A.13(a) Daily variation in soaring activity of Black vultures ( $F_{birds}$ ), wind speed and solar radiation for III, IV and V months of the period of study (Amaraïs)...	148
Figure A.13(b) Daily variation in soaring activity of Black vultures ( $F_{birds}$ ), wind speed and solar radiation for VI, VII and VIII months of the period of study (Amaraïs).....	149
Figure A.13(c) Daily variation in soaring activity of Black vultures ( $F_{birds}$ ) and wind speed for IX, X and XI months of the period of study (Amaraïs) .....	150
Figure A.13(d) Daily variation in soaring activity of Black vultures ( $F_{birds}$ ) and wind speed for XII, I and II months of the period of study (Amaraïs).....	151
Figure A.14(a) Daily variation in soaring activity of Black vultures ( $F_{birds}$ ) and wind speed for III, IV and V months of the period of study (Prudente).....	152
Figure A.14(b) Daily variation in soaring activity of Black vulture ( $F_{birds}$ ) and wind speed for VI,VII and VIII months of the period of study (Prudente) .....	153
Figure A.14(c) Daily variation in soaring activity of Black vultures ( $F_{birds}$ ) and wind speed for IX, XI and XI months of the period of study (Prudente).....	154

Figure A.14 (d) Daily variation in soaring activity of Black vultures ( $F_{birds}$ ) and wind speed for XII, I and II months of the period of study (Prudente) .....	155
---	-----

## **APPENDIX B – TABLES**

Table B.1 Geographical coordinates of the observation points (viewpoints) around the Amarais airport .....	156
Table B.2 Geographical coordinates of the observation points (viewpoints) around the Presidente Prudente airport .....	156
Table B.3 Number of Black vultures registered around the viewpoints during each month and the whole period of observation (from September 2012 to August 2013) in Presidente Prudente study area .....	157
Table B.4 Number of Black vultures registered around the viewpoints during each month and the whole period of observation (from September 2012 to August 2013) in Amarais study area .....	157

## **APPENDIX C – TECHNICAL ALGORITHMS**

### **CHAPTER II**

Algorithm C1. Preparation of the “Georeferenced birds and meteorological parameters” database as a base for implementation of analyses .....	158
Algorithm C2. Transformation of timescale to the relative biological timescale and normalized relative biological timescale .....	161

### **CHAPTER III**

Algorithm C3. Georeferencing of the recorded birds through the projected polygons .....	162
Algorithm C4. Preparation of the “Wbirds and superficial parameters” georeferenced database for statistical analyses implementation .....	166
Algorithm C5. The technique of cartographic visualization of the abundance of soaring Black vultures and the risk of collisions with these birds over the territory .....	170

## **APPENDIX D - DECLARATIONS**

Declaração bioética e biossegurança .....	189
Declaração referente a direitos autorais .....	190

# CONTENTS

ACKNOWLEDGEMENTS.....	
RESUMO.....	
ABSTRACT.....	
STRUCTURE OF THE DISSERTATION.....	
CONTENTS.....	
LIST OF FIGURES.....	
LIST OF TABLES.....	
LIST OF SCRIPTS.....	
LIST OF APPENDICES.....	
<b>CHAPTER I.....</b>	<b>23</b>
1. General introduction.....	23
1.1 “Bird strike problem” and actuality of the research topic .....	23
1.2 Justification .....	25
1.3 Objectives .....	26
1.4 Scientific contribution .....	26
1.5 Application .....	27
2. Ecological and behavioural traits of the Black vulture.....	27
2.1 Taxonomy.....	27
2.2 Anatomy .....	27
2.3 Range and habitat .....	28
2.4 Reproduction .....	28
2.5 Natural enemies and interaction with other species .....	29
2.6 Cycle of daily activity .....	29
2.7 Communal roosts.....	29
2.8 Foraging behaviour.....	30
<b>CHAPTER II. Study of the soaring behaviour of Black vulture (<i>Coragyps atratus</i>, <i>Cathartidae</i>) and its dependence on meteorological conditions in southeast Brazil using GIS technologies .....</b>	<b>31</b>
1. Introduction .....	32
2. Material and methods .....	34
2.1 Study areas.....	34
2.2 Field data gathering .....	36
2.3 Data preparation for analyses .....	40
2.3.1 Preparation of the summary database .....	40
2.3.2 Preparation of the summary georeferenced database .....	40
2.3.3 The “Frequency of soaring bird records” ( $F_{\text{birds}}$ ) index .....	42
2.3.4 Ranging months by average daily temperature .....	43
2.3.5 Application of relative biological timescale and normalized relative biological timescale.....	44
3. Data analyses .....	44
3.1 Study of the soaring Black vulture distribution and population size.....	44
3.2 Study of the height of flight of soaring Black vultures.....	44
3.3 Study of the influence of meteorological and seasonal changes on soaring activity of Black vultures.....	45
3.3.1 Study of the influence of seasonality on daily variation in soaring activity of Black vultures .....	45

3.3.2 Study of the influence of seasonality on the abundance of soaring Black vultures .....	46
3.3.3 Study of the dependence of soaring activity of Black vultures on basic meteorological characteristics .....	46
3.3.3.1. Graphical analysis of the functional relationship between meteorological conditions and soaring activity of Black vultures .....	46
3.3.3.2 Statistical analyses studying the dependence of soaring activity of Black vultures on meteorological conditions .....	46
4. Results .....	48
4.1 Comparing of the population size of Black vultures between studied sites .....	48
4.2 Height of flight of soaring Black vultures .....	49
4.3 Influence of meteorological seasonal changes on soaring activity of Black vultures .....	51
4.3.1 Influence of seasonality on daily variation in soaring activity of Black vultures .....	51
4.3.2 Influence of seasonality on the abundance of soaring Black vultures.....	54
4.3.3 Dependence of soaring activity of Black vultures on basic meteorological characteristics .....	56
4.3.3.1 Functional relationship between meteorological conditions and soaring activity of Black vultures.....	56
4.3.3.2 The revealed dependence of soaring activity of Black vultures on basic meteorological characteristics .....	59
4.4 Observation of Black vultures behaviour near abundant source of food.....	65
5. Discussion .....	66
5.1 Behaviour traits of the Black vulture in soaring flight .....	66
5.1.1 Altitudes of soaring flight.....	66
5.1.2 Daily variation in soaring activity of Black vulture .....	66
5.1.3 Behaviour of Black vultures near abundant source of food .....	67
5.2 Influence of meteorological conditions on soaring activity of Black vultures.....	69
5.2.1 Dependence of soaring activity of Black vultures on meteorological conditions .....	69
5.2.2 Seasonal changes in soaring activity of Black vulture.....	70
6. Conclusions.....	71
<b>CHAPTER III. Study of the influence of superficial natural and anthropogenic conditions on abundance of soaring Black vulture (<i>Coragyps atratus</i>, <i>Cathartidae</i>) using GIS and remote sensing technologies .....</b>	<b>72</b>
1. Introduction.....	73
2. Materials and methods.....	75
2.1 Data gathering and applied material.....	75
2.1.1 Satellite imagery applied for investigation.....	75
2.1.2 Thermals properties .....	78
2.2 Data preparation for analyses .....	79
2.2.1 Processing of the remote sensing products for detection of the surface parameters .....	79
2.2.1.1. Detection of the surface temperature and relief parameters .....	79
2.2.1.2 Detection of the landscape parameters .....	82
2.2.2 Georeferencing of the recorded birds as point shapefile .....	82



2.2.3 Georeferencing of the recorded birds as polygonal shapefile .....	83
2.2.4 The "Weight of birds" ( $W_{birds}$ ) index .....	85
2.2.5 Preparation of the georeferenced database as the basis for analyses and mapping .....	86
2.2.6 Data preparation for statistical analyses .....	88
2.2.7 Data preparation for landscape analysis .....	88
2.2.8 Cartographic visualization of the abundance of soaring Black vultures and risk of collision with these birds over the territory .....	89
2.3 Assumptions and limitations .....	90
2.3.1 Accuracy of the bird's calculation.....	90
2.3.2 Accuracy of the birds' georeference.....	90
2.3.3 Accuracy of the cartographic visualization of abundance of soaring birds over the territory .....	91
3. Data analyses.....	92
3.1 Study of the dependence of soaring activity of Black vultures on relief, surface temperature and anthropogenic pressure .....	92
3.2 Study of the dependence of soaring activity of Black vultures on landscape type.....	93
4. Results .....	93
4.1 Dependence of the soaring activity of Black vultures on relief, surface temperature and anthropogenic pressure.....	93
4.2 Dependence of the soaring activity of Black vultures on landscape type .....	98
4.3 Risk of collision with Black vultures over the studied territory .....	102
4.3.1 Risk of collision, estimated for the entire area of 13 km radius around the airports.....	102
4.3.2 Risk of collision, estimated for the circular zones of 700 m radius around the viewpoints .....	105
5. Discussion .....	111
5.1 Dependence of the soaring activity of Black vultures on relief, surface temperature and anthropogenic pressure .....	111
5.1.2 Confirmation of the hypothesis stating that Black vultures tend to choose the strongest thermals in surroundings .....	112
5.2 Dependence of soaring activity of Black vultures on landscape type (surface covering and anthropogenic pressure).....	114
5.3 Influence of anthropogenic pressure on soaring activity of Black vultures .....	116
5.4 The cartographical assessment of risk of collision with Black vultures over the territory .....	118
5.5 Practical recommendations.....	119
5.5.1. General recommendations .....	119
5.5.2 Proposed measures for reduction the risk of collision with Black vultures .....	119
6. Conclusions .....	121
<b>CHAPTER IV. Application of GIS and remote sensing technologies in the analysis studying the relationship between spatial distribution of flying birds and environmental factors .....</b>	<b>122</b>
1. Introduction .....	122
2. General stages of investigation, basing on the elaborated methodological approaches.....	123
3. Linking the different types of parameters in a single georeferenced database.....	124
4. Method of georeference of birds registered as points and as polygons.....	125

5. Implementation of analyses and risk assessment maps basing on the summary georeferenced database.....	126
6. Technique of remote sensing data processing allowing to detect the possible locations of the strongest thermals .....	127
7. Discussion .....	128
8. Conclusions .....	129
<b>FINAL CONCLUSIONS .....</b>	<b>130</b>
<b>REFERENCES .....</b>	<b>132</b>
<b>APPENDICES .....</b>	<b>137</b>
<b>DESCRIPTION OF THE SUPPLEMENTARY FILES.....</b>	<b>172</b>

# CHAPTER I

## 1. General introduction

### 1.1 “Bird strike problem” and actuality of the research topic

The number of airplane collisions with birds is increasing in many countries all over the world, strongly impacting the safety of aircraft flying. This happens mainly due to the general increase of aircraft traffic coupled with the growth of bird populations. Only in USA from 1990 to 2003, 97% of 52493 of the recorded wildlife collisions with aircrafts were caused by birds (Blackwell, 2006). Those bird strike events led to the death of dozens of people, destruction of dozens of aircrafts and costs were estimated in more than 500 million dollars (Kelly, 2005). Rising concerns about nature conservation coupled with tightening of environmental legislation attract the additional interest to the issue. The aviation safety experts of many nationalities try to solve or reduce the hazard to aircraft from birds.

In Brazil this problem is also serious and urgent. The Brazilian aviation industry has grown considerably during the recent years, the aircraft fleet and traffic reached volumes comparable to the most developed economies in the world. However, the Brazilian statistics of bird collisions are alarming. The Aeronautical Accident Prevention and Investigation Center (CENIPA)<sup>1</sup> is collecting the database of all accidents with aircrafts happened in Brazil due to bird strike events. It reported that from 1980 to 2000s have been registered 2198 aircrafts collisions with birds in the country. So long as the aviation fleet and traffic volumes in the country is continuing to grow, the potential risk of bird strike crashes becomes higher (Bastos, 2001).

According to the CENIPA researchers, the most abundant feathery inhabitant of the airports surroundings and at the same time the species accounted for the highest percentage of collision (54.97% from 1126 reports) was the Black vulture (*Coragyps atratus*), a large scavenger bird about 1.5 m of wingspan, 65 cm of length and 1.6 kg of weight (Buckley, 1999; Bastos, 2001). Strikes with Black vultures are considered a substantial hazard to aviation in both Americas (DeVault et al., 2005, 2011; Zakrajsek and Bissonette, 2005; Blackwell and Wright, 2006; Avery et al., 2011; USAF, 2014). It was revealed that more than 79% of all bird strikes in Brazil occurred at the airports and its proximities. This allowed concluding that the area where a bird

---

<sup>1</sup> CENIPA - Aeronautical Accidents Investigation and Prevention Center (Portuguese: Centro de Investigação e Prevenção de Acidentes Aeronáuticos) is a unit of the Brazilian Air Force that investigates aviation accidents and incidents in Brazil. It is headquartered in Brasília.

strike event has the maximal probability is a circle surrounding the airport with a radius of 10-20 km (Bastos, 2001).

The analysis of the Black vulture behavioural properties in conjunction with the general unfavorable situation in the airports surroundings allowed to explain why those birds were more frequently stricken by aircrafts in almost all big cities of Brazil. The real estate prices in the neighborhood of airports are cheap because of their locations. For this reason these lands are often occupied by numerous low-income families, which live in shantytowns without adequate sanitary conditions and their garbage utilization. Moreover, waste landfills, slaughterhouses, tanning and fishing industries are often located there. Whereas Black vultures eat meat in deterioration, such activities near the airports attract them to the aircraft's routes. Black vultures usually soar in flocks on thermals (upwelling air flows) and remain for long periods in the air, disturbing the airports' traffic paths. Due to its large size and behavioral traits, the most common control approaches (falconry, ground deterrents) do not work against it. As there are no natural predators for Black vultures, their population growth depends on the food abundance (Bastos, 2000).

A number of special measures were implemented to reduce the bird strike hazard in Brazil. In 1995 the Ministry of Environment of Brazil signed the resolution on the creation of the bird strike risk zones (Área de Gerenciamento de Risco Aviário or AGRA), which include all territories around airports in a 13 - 20 km radius. The establishment and operation of any activity attractive for vultures (such as the waste open dumps, slaughterhouses, tanning and fish industries, some agriculture plantations) became prohibited there (Bastos 2001). To minimize the risk of bird strikes, the checklist of main information about the problem and simple maps outlining the areas attributed to large bird flocks were developed and given to airline pilots and airports' administrations. Also a wide information campaign explaining the essence of the problem for distinct parts of society was conducted, which included short seminars, educational films, informational materials, publications and educational activities for children (Bastos, 2000). These efforts brought some positive results, however they did not solve this problem completely.

The failure of attempts to reduce the risk of collisions was caused by the following reasons. Firstly, despite the approved resolution and informational campaigns, many objects attractive for those birds were not removed from the airports surroundings. Most probably, due to interfering economic and social factors, this will not be done in the nearest future as well. Secondly, even a complete removing of all abundant food sources from the ground may not clean the sky from soaring vultures (Bastos, 2001; Novaes and Cintra, 2013; Avery and Cummings, 2004; our

observation). This happens for the reason that vultures always soar at sky searching for food in all region of their habitat. They soar all daily hours when they cannot find the abundant food for them. In case of absence of abundant food sources, they soar for search dead animals over the roadways and fields surrounding the cities.

Considering the possible measures of reduction the threat of Black vultures for airplanes, it is important to understand the general situation with vulture species in the world. Presently, 14 of 23 (61%) of vulture species (New World and Old World groups) are threatened with extinction due to considerable human-caused changes in conditions of their habitats. The most rapid declines have occurred in Asia (especially India), Africa and Europe. (Deygout et al., 2009; Cortés-Avizanda et al., 2010; Ogada et al., 2012; Buechley and Şekercioğlu, 2016). The problem of Brazil and other countries, where vultures are so numerous that pose a threat to aircrafts, contrasts with the situation of many other countries, which are now struggling against the catastrophic decline in the numbers of vulture populations in their territory. The reasons for the dramatic decline of vulture populations vary among different regions. The most important causes are the poisoning of carcasses of domestic livestock containing specific drugs, human persecution and hunting, disappearance or sharp reduction of the dead domestic and wild animals on open surface (Ogada et al. 2012; Cortés-Avizanda et al. 2010).

As avian scavengers, all vulture species implement the important role in natural ecosystems and traditional agriculture. By feeding on meat in deterioration they participate in ecological processes affecting soil, vegetation and consumers from invertebrate to large vertebrates (Cortés-Avizanda, 2010). Additionally, vultures prevent the spread of epizootic diseases that could be harmful to nature, livestock farming and human health. The regions where the dramatic decline of vulture populations occurred have a huge environmental and economic damage.

## **1.2 Justification**

Due to the growing risk of aircraft collisions with Black vultures and the failed attempts to reduce this hazard it is necessary to find a compromise – an acceptable solution that will be able to work in this situation. The high threat for aircrafts caused by vultures can provoke the desire to solve this problem by hard measures destructive for birds' population. It's important to warn against it, reminding the abundant species which completely or nearly disappeared for a short time since of strong human impact (the Old World Vultures, the Passenger pigeon, the Canadian and European beavers and others). In order not to repeat these tragic examples, people need to avoid harmful measures of influence on Black vultures. Instead of them it should be necessary to elaborate the soft methods, which will allow to reduce the risk of collision with vultures without

damage for their population. To achieve this, it is important to identify the environmental factors causing the high density of soaring vultures over the territory, to learn how to estimate the risk of collision and how to predict it for airports vicinities.

Our investigation was devoted to moving forward in elaboration of the soft methods allowing to reduce the risk of collision aircrafts with Black vultures and other avian species. We studied the relationship between the soaring activity of Black vultures and the environmental factors in the surroundings of two airports taken as case studies. The elaborated methodology of combined application of GIS and remote sensing technologies were applied as the main research instrument. They allowed to construct the maps giving a numerical estimation of hazard of bird-strike event over the territory. Also they allowed to reveal the dependence of distribution of soaring Black vultures on various environmental parameters.

We believe that the results of our work will help to elaborate the effective set of reasonable soft measures which will allow to decrease the number of aircraft strikes with Black vultures and other bird species.

### **1.3 Objectives**

Our investigation had the following objectives:

1. To analyze the superficial, meteorological and anthropogenic factors of the environment within the circular zones of 13 km radius of two airports (Amarais and Presidente Prudente) and estimate their influence on the distribution of soaring Black vultures over the territory.
2. To test the hypothesis that Black vultures tend to soar over the strongest thermals in their surroundings.
3. To study the behavioral patterns of vultures in soaring flight (altitudes of flights, daily and seasonal variation in soaring activity).
4. To develop a methodology for numerically estimation and mapping the risk of bird strike event over the territory.
5. To formulate the practical recommendations of possibilities for the reduction of the number of aircraft collisions with Black vultures.

### **1.4 Scientific contribution**

- ❖ We elaborated a set of novel methodological approaches of data processing basing on combined application of GIS and remote sensing technologies. They allowed to numerically estimate and cartographically visualize the risk of aircraft collisions with

birds over the airports vicinities as well as to study the relationships between the distribution of flying birds and various environmental factors.

- ❖ We clarified and detailed the several behavioral traits of Black vultures, which were not previously described in the literature.

## 1.5 Application

- ❖ The formulated practical recommendations proposed for airport administration, aircraft pilots and researchers could help to reduce the number of aircraft collisions with Black vultures and Turkey vultures in Brazil and other countries.
- ❖ The elaborated methodological approaches can be used for reduction the hazard of collisions with various avian species in any geographical region. This technique can be applied directly or can be adopted for specific objectives.

## 2. Ecological and behavioural traits of the Black vulture

### 2.1 Taxonomy

The Black vulture (*Coragyps atratus*, Cathartidae), also known as the American Black vulture, as well as “Urubu-de-cabeça-preta” or simply “urubu” in Portuguese - is a bird of the New World vulture or condor family Cathartidae whose range extends from the south eastern United States to Central Chile and Uruguay in South America. This family includes five genera, which contain seven species (five vultures and two condors).

The New World vultures were widespread in both the Old World and North America during the Neogene. However, the New World group of vultures is considered as not closely genetically relative to the externally similar family of the Old World vultures. The later belong to the family *Accipitridae* including eagles, hawks, kites and harriers. Similarities between those two groups can be resulted by the convergent evolution. Albeit, the degree of their affinity is still a matter of scientific debates (Buckley, 1999; Stewart, 1983).

### 2.2 Anatomy

The Black vulture is a large bird reaching 56–74 cm in length with about 150 cm (from 133 to 167 cm) of wingspan. The weight for Black vultures ranges from 1.6 - 2.75 kg in North America and the Andes to 1.18–1.94 kg in the tropical lowlands (Osofsky, 1990; Buckley, 1999).

The head and neck are featherless, the skin is dark grey and wrinkled, the plumage is mainly glossy black. The eye iris is brown and has a single incomplete row of eyelashes on the upper lid and two rows on the lower lid. The legs are greyish white, while the two front toes of the foot are long and have small webs at their bases. The feet are flat, relatively weak, and are

poorly adapted to grasping; the talons are also not designed for grasping, as they are relatively blunt. It has broad wings with a distinctive whitish coloured tip at the ends and a short square-shaped tail (Peterson, 2001, Buckley, 1999).

The Black vulture does not have a good sense of smell, but it has keen eyesight that they use for finding their food. Also it lacks the vocal organ of birds known as syrinx and therefore its only vocalizations are grunts or low hisses when it is irritated (Buckley, 1999; Mandel et al, 2007).

### 2.3 Range and habitat

The geographical range of Black vulture includes the southern United States, Mexico, the Central America and most of the South America (to central Chile and Argentina). It also is found as a vagrant on the islands of the Caribbean (Fig. 1.1).

The Black vulture is usually a permanent resident throughout its range, although birds may migrate for short distances at unfavourable conditions (Buckley, 1999; Peterson, 2001).

This species prefers open lands interspersed with areas of woods or brush. It is also found in moist lowland forests, scrublands and grasslands, wetlands and swamps, pastures, and heavily degraded former forests. Preferring lowlands, it is rarely seen in mountainous areas (Buckley, 1999).



**Figure 1.1 Geographical range of the Black vulture (*Coragyps atratus*, Cathartidae) (The IUCN Red list, 2015)**

### 2.4 Reproduction

Black vultures do not have the specific pairing season and their mating patterns are varying with the latitude. Whereas birds in northern regions do not begin mating till March, vultures in southern regions can start mating in January.



Black vultures do not build nests. Instead, they lay their eggs, between 1 to 3 in each clutch, on the bare ground in a suitable cavity, hollow tree or abandoned building. Both parents incubate eggs, which hatch after 28 to 41 days. Next, they feed nestlings regurgitating food at the nest site. The young remain in the nest for two months. After 75 to 80 days they are able to fly skillfully. However, it was noted that parents might feed their young during eight months after fledging.

Pairs use the same nest site for many years as long as their breeding is successful. Black vultures are monogamous and maintain long-term pair bonds. This prolonged dependence of the young on their parents may, in part, be responsible for the strong social bonds with relatives that Black vultures maintain throughout their lives (McHargue *et al.*, 1981; Buckley, 1999).

## **2.5 Natural enemies and interaction with other species**

Due to its aggressiveness and size, adult Black vultures are endangered by very few predators. Some eagles may kill vultures in conflicts. Available literature reports that the Ornate Hawk-Eagle, a slightly smaller bird than the vulture, has preyed on adult black vultures (Environmental assessment., 2002). On the contrary, their eggs and nestlings can be attacked by a number of mammalian predators such as raccoons, coatis and foxes.

Black vultures can compete for carrion with other species of the family Cathartidae. A group of these birds gathering around carcasses can drive away the slightly larger Turkey vultures. However, Black vultures often use Turkey vultures and two others species of vultures of the genus *Cathartes* for search for food (Carrete *et al.*, 2010).

## **2.6 Cycle of daily activity**

The regime of the Black vulture activity is divided by two phases: the period of daily foraging activity and the night-time rest on the roosts. The phase of daily foraging activity starts at morning after sunrise and finishes at evening before the sunset. During this phase the birds soar at sky searching for food, periodically resting on trees. Before the sunset all birds finish their soaring and fly away to their roosts where they spend the night.

## **2.7 Communal roosts**

Black vultures spend night hours in communal roosts, which are defined as a complex of series of spatially closed roosts used by a local population (Stolen and Taylor, 2003) and the “aggregation of more than two birds that sleep together” (Beauchamp, 1999). A communal roost can contain from dozens to hundreds of individuals of Black vultures. These birds tend to roost in company with their genetic relatives (Parker, 1995).

Birds normally make communal roosts in protected areas where human activities are limited and near natural and anthropogenic objects generating updraft flows of air or thermals. Those thermals help birds to take wing in early morning (Coleman and Fraser, 1989, Thompson *et al.*, 1990). Black vultures can locate communal roost near technogenic thermals, like a thermal power station (Novaes and Cintra, 2013). Similar behavior was observed for Turkey vultures by Mandel and Bildstein (2007). Those authors suggest that proximity to thermal power plants might be favorable for forming of communal roosts of these birds.

In the wild Black vultures organize roosts in forests with large open areas and tend to congregate on dead trees without leaves and branches. In areas with high human population birds tend to gather at garbage dumps attracted by available source of food or beside highways to feed on road-killed animals.

The communal roost is an important aspect of the social life of Black vultures. It serves as a meeting place for adults and their young and as an assembly point for foraging groups. The communal roost also appears to function as an information center, a site from where unsuccessful foragers can find food by following roost mates to carcasses. Aggressive interactions between adults partially control roost membership. Hence, these interactions may serve to limit recruitment of non-kin to recently discovered food sources (Rabenold, 1987 ; Buckley, 1999).

## **2.8 Foraging behaviour**

In natural settings Black vultures eat mainly carrion. Otherwise, in areas populated by humans they may scavenge at garbage dumps. In both situations birds can also take eggs of other species and kill or injure newborn or incapacitated mammals (Buckley, 1999).

Black vultures often search for food by following other Cathartidae species: the Turkey vulture, the Lesser Yellow-headed vulture and the Greater Yellow-headed vulture. These three species, unlike Black vultures, have very good sense of smell (this ability is uncommon in the avian world), which they actively use for searching carrion on the ground.

In case of absence of these species, Black vultures rely on each other for searching food. This adaptation is a core reason why they live together in large groups. They do this in order to maximize feeding opportunities. However, in very large flocks they tend to scare away other scavengers from carrions. Another advantage of foraging in large groups is that during feeding they can be warned about any approaching danger by other individuals of the group.

## CHAPTER II

### **Study of the soaring behaviour of Black vulture (*Coragyps atratus*, *Cathartidae*) and its dependence on meteorological conditions in southeast Brazil using GIS technologies**

*Paper intended for "Biological Conservation" journal*

#### **Abstract**

The increasing risk of collision between aircrafts and Black vultures along with the impossibility to reduce this threat by traditional techniques requires special measures that would reduce this hazard without harming the birds. To elaborate these methods, the meteorological factors affecting the density of soaring vultures over the area should be detected. The behavioral patterns of vultures in soaring flight should be identified. The dependence of concentration of flying birds over area from thermal's strength should be explored.

Our investigation was devoted to moving forward in these objectives. The study was implemented within surroundings of two airports of southeastern Brazil taken as model areas. We joined the bird's census and the meteorological characteristics collected together with the bird's observation in the georeferenced databases (shapefiles) by dint of ArcGIS software. Based on the georeferenced databases, we analyzed the dependence of the soaring activity of Black vultures on meteorological and anthropogenic conditions, determined the behavioral patterns of soaring vultures (altitudes of flights, daily and seasonal variation in soaring activity).

We found that soaring activity of Black vultures is significantly dependent from solar activity and wind speed parameters, which can be interpreted as its dependence on thermals strength. This finding suggests that these birds tend to soar over the strongest thermals in their surroundings. Air temperature, air humidity, atmospheric pressure and wind direction do not affect the soaring activity of vultures. Seasonality affects the soaring flight notably, but its influence depends on level of anthropogenic stress. The altitudes of soaring flights range from 13 to 550 m, most probable up to 300 m. The period of soaring activity lasts from 1 - 1.5 hours after local sunrise to 1 - 1.5 hours before local sunset. It was revealed two types of daily variation in soaring activity: plateau-like plot and plot of two peaks at morning and afternoon with a notable drop within them. An abundant food source on the ground attracts vultures from a large distance, which lead to a complete disappearance of soaring vultures above a large area.

## Key-words

*Aviation hazard, bird hazard control, bird strike problem, Black vulture, Coragyps atratus, soaring behaviour, thermals, meteorological factors, GIS, ArcGIS, ArcMap.*

## 1. Introduction

The rising number of aircraft collisions with birds all over the world makes it necessary to develop a set of specific measures to control on bird populations. The majority of bird strike events occur in a circular zone with radius of 10-20 km surrounding airports, where aircrafts conduct of landing and takeoff operations and fly at low altitudes (Bastos, 2001).

In Brazil the avian species creating the greatest hazard for airplanes is the Black vulture (*Coragyps atratus*, *Cathartidae*). Strikes with this species are considered a significant threat to aircraft in both Americas (Bastos, 2001; DeVault et al., 2005, 2011; Zakrajsek and Bissonette, 2005; Blackwell and Wright, 2006; Avery et al., 2011; USAF, 2014). This is a large scavenger bird about 1.5 m of wingspan, 65 cm of length and 1.6 kg of weight (Buckley, 1999; Bastos, 2001). Due to the large size and behavioral traits, the most common control approaches, i.e. falconry, ground deterrents, do not work against it (Bastos, 2001; Blackwell and Wright, 2006). During daily hours Black vultures usually soar in flocks on upward air flows or thermals at high altitudes searching for food and threatening to aircrafts. Because there is no natural predator for this species, the population growth can depend on the food abundance (Bastos, 2000). Some researchers believe that presence of soaring Black vultures at sky is caused mainly by waste of food located on the surface (e.g. Novaes and Alvarez, 2014). However, as it was revealed recently, even a complete removing of all abundant food sources from the ground may not clean the sky from soaring vultures (Bastos, 2001; Novaes and Cintra, 2013; Avery and Cummings, 2004; our observation).

The increasing hazard of collision with Black vultures, together with failed attempts to decrease this threat, leads to the necessity to find a compromise – an acceptable solution that will be able to work in this situation. However, these measures should be thoughtful and not harm to birds, since harsh actions can be disastrous to vultures populations. All avian scavengers implement the important function in natural ecosystem and traditional agriculture, preventing the spread of epizootic diseases that could be harmful to nature, livestock farming and human health (Cortés-Avizanda et al., 2010). Currently Black vulture is not endangered species. However, we must consider that during the last decades human impact on the environment caused the catastrophic reduction of many vulture species. Presently, 14 of 23 (or ~60%) of both New World and Old World vulture species are threatened with extinction. The most rapid declines have occurred in Asia (especially in India), Northern Africa and Southern Europe. The reasons

of dramatic extinction of vulture population are varied in different regions; i.e., poisoning of carcasses of domestic livestock containing specific drugs, human persecution and disappearance or sharp reduction of the dead domestic and wild animals on open space lands (Deygout et al., 2009; Cortés-Avizanda et al., 2010; Ogada et al., 2012).

For elaboration of the soft methods of reduction the risk of collision with vultures it is strictly important to outline the environmental factors impacting the temporal and spatial distribution of flying birds and pay a special attention to the dependence of soaring vultures on thermals.

Several authors observed the clear dependence of soaring activity of Black vultures and its close species, Turkey vultures (*Cathartes aura*) on thermals. It was observed that both species use the ascending air fluxes for takeoff and upward flights at morning and soaring flights in daily hours. The soaring activity of vultures coincides accurately with hours of thermals work. It starts after 1-1.5 hours after the local sunrise and finishes at 1-1.5 before the local sunset (Mandel and Bildstein, 2007; Freire *et al*, 2015; Pennycuick 1971, 1983; Akos, 2010; Parrott, 1970; Newman, 1957, our observations). Usually, vultures locate their large roosts near the structures generating thermals (Thompson *et al*, 1990). The lack of sufficient (strong and constant) assistant thermal can keep Turkey vultures on the ground several days or more (Mandel and Bildstein, 2007). Both species use soaring flight most of the time, the flapping flight is rarely used by birds and mainly at small (about 10 m over the ground) altitudes (Buckley, 1999; our observations). Since the soaring flight is possible only in presence of thermals, both species apply thermals for flight most of the time of their daily activity. This behavioural pattern can be explained by adaptation to minimize energy loss in flights, as occurs in most avian scavengers (Schoener, 1971; Ruxton and Houston, 2002).

The hypothesis which should be tested is the following: *do Black vultures tend to soar over the strongest thermals in their surroundings?*

It was evidenced that Black vulture can choose technogenic thermals (i.e. thermals produced by artificial heating) for soaring flight in their surroundings (Mandel and Bildstein, 2007; Freire *et al*, 2015; Novaes and Cintra, 2013). For Turkey vultures was found even prolongation of soaring activity over the technogenic thermals with illumination for 90-120 minutes after sunset (Mandel and Bildstein, 2007). Since technogenic thermals are always much stronger than natural ones, this finding suggests, that vultures actively search for strongest thermals for soaring flight. However, this behavioural trait was not confirmed statistically and examined in details. Also, the behavioral patterns of vultures dwelling in habitats with the occurrence of natural thermals only were not studied at all. Meanwhile, it would be very important to make clear this issue, aiming

the reduction of the hazard of collision with these birds. If vultures have this behavioural trait, the strongest thermals in the surroundings (and especially technogenic thermals) can form a zone of enormous concentration of soaring birds above them. Furthermore, technogenic thermals can form an extremely high density of birds not only at daily hours, but at night time as well.

Our investigation was devoted to moving forward in elaboration of soft methods of reduction the risk of collision with Black vulture. The study was implemented within surroundings of two airports of southeast of Brazil and was consists from two parts. Here we considered the first part of our investigation which was devoted to study of the dependence of soaring activity of Black vultures on meteorological conditions. Also we explored the daily and seasonal variation of soaring activity of birds, altitudes of their soaring flights and obtained the first confirmation of the hypothesis, stating that Black vultures tend to soar over the strongest thermals in their surroundings.

## 2. Material and methods

### 2.1 Study areas

We studied the behaviour traits of soaring Black vultures in the vicinities of two airports of southeast of Brazil, intended for small and medium sized airplanes (Fig. 2.1, Supplementary Files SF4). The **Amarais airport** (-22.86293°, -47.10528°) is located in Campinas city, in the southeastern part of the São Paulo state (Fig. 2.2). The relief has transitional characteristics between large depression on the west from the city and the plateau coming to the city from the east. The altitudes of the area range from 451 to 974 metres above the sea level (Fig. A.2). The average annual temperature is 22.4°C and average annual precipitation is 1424.5 mm. The **Presidente Prudente airport** (-22.17656°, -51.427389°) is located at a distance of 7 km from Presidente Prudente city, in the western part of the São Paulo state (Fig. 2.3). The relief is slightly undulating, turning into low hills somewhere, the borders of which serve as riverbeds to streams. The altitudes range from 295 to 541 m above the sea level (Fig. A.6). The average annual temperature is 23.6°C and average annual precipitation is 1256.5 mm. Both airports locate very close to dense residential areas: the Amarais airport is located inside this area, whereas the Presidente Prudente airport is distant 1.9 km from town (Fig. 2.2; Fig. 2.3).

Natural and rural features of the landscapes are similar in both study sites. Pastures and agricultural fields occupy the main part of the area. Native ecosystems are presented by small fragments of residual native forest, strait corridors of degraded native vegetation along rivers and scattered trees. Degree of anthropogenic disturbance of the two study sites is different. The dominating landscape around Amarais airport is composed of highly urbanized lands (the urban

areas – 58.5%, the natural and agricultural areas – 41.5%), while around the Presidente Prudente airport - natural and rural landscapes (urban areas – 16.5%, natural and agricultural areas – 83.5%)<sup>2</sup>. Due to this difference, we attribute the studied populations of Black vultures as having the “natural and rural” type of habitat around the Presidente Prudente airport, and “urban” type of habitat around the Amarais airport. The large distance between two study sites (~450 km, Fig. 2.1) allows asserting that Black vultures inhabiting both areas belong to different populations. Therefore should not be migration of birds between two sites.

For brevity, we call the populations of Black vultures inhabiting the surrounds of Presidente Prudente airport as the “Prudente population” and inhabiting the surrounds of Amarais airport as the “Amarais population”.

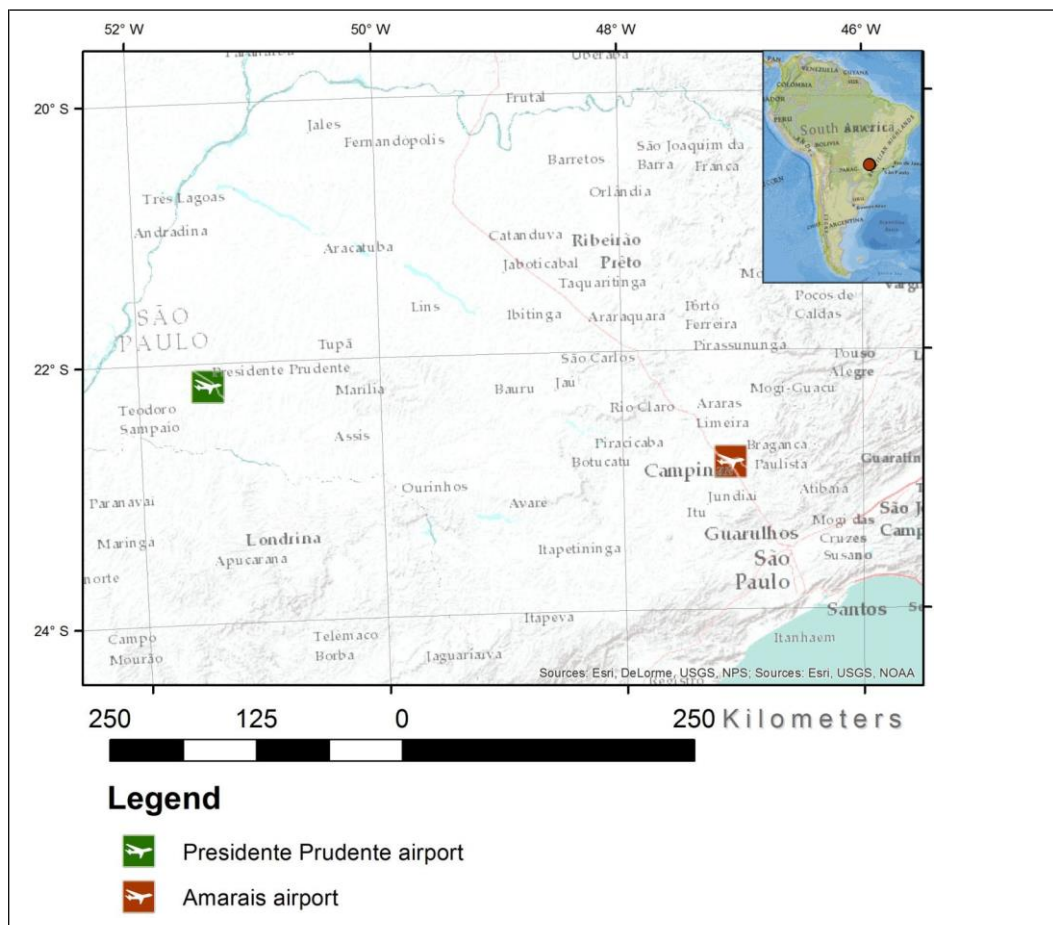


**Figure 2.1 Location of the Amarais and Presidente Prudente airports in the state of São Paulo of Southeastern Brazil (Supplementary Files SF4)**

<sup>2</sup> We obtained this conclusion by means of digitizing of landscape types and calculating the ratio between areas of different landscape types within zones of 700 m around 26 observation points of both studied sites according to our classification of landscape types (Chapter III, Table 3.3). The digitizing was implemented manually, basing on high-resolution DigitalGlobe imagery of Basemap gallery in ArcGIS. The close conclusion we obtained by visual analyses of high resolution imagery of the entire studied areas (Supplementary Files, SF3).





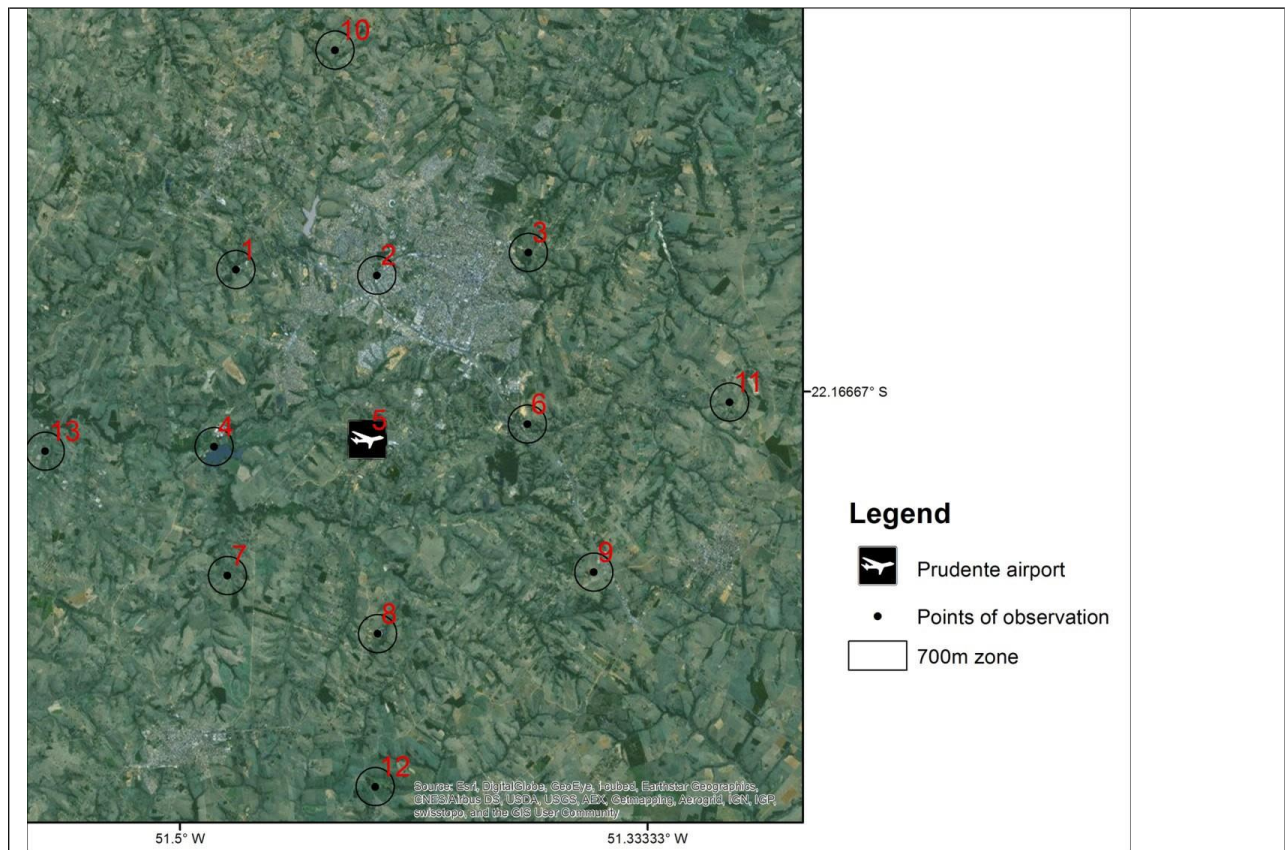


**Figure 2.3 Study area and observation points around the Presidente Prudente airport**

In each viewpoint the observations of birds were conducted during one day of each month from 8:00 to 18:00 excepting short periods of rainy weather when Black vultures do not fly. The sky around a viewpoint was reviewed every 15 minutes and parameters of geographical position of all vultures within the binocular field of vision were recorded as interval of values. When birds were located close to each other they were recorded as a single object, entitled as the “*ornithological object*”. All individuals in a single ornithological object have the identical parameters of registration. For each ornithological object the following parameters of geographical position were registered as intervals of values:

- **direction** to ornithological object (circular degrees), was measured by a compass and fixed by 8 intervals (sectors of compass): 22.5-67.5°, 67.5-112.5°, 112.5-157.5°, 157.5-202.5°, 202.5-247.5°, 247.5-292.5°, 292.5-337.5°, 337.5-22.5°.
- **vertical angle** to ornithological object (angle degrees), was measured by inclinometer manual attached to the binoculars and fixed by 18 intervals: 2.5-7.5°, 7.5-12.5, 12.5-17.5... 82.5-87.5, 87.5-90°.
- **distance** between observer and ornithological object (metres) was measured by the 12-powered binoculars (CSR 12x50, 87m/1000m) and fixed by 4 intervals: 100-

200 m, 200-400 m, 400-700 m, 700-6000 m. Closer than 100 metres birds did not approach to the observer, since that the interval from 0 to 100 m was not included.

- **time of observation** – date and time of registration with accuracy of 15 minutes, like 21.10.2012 9:15; 21.10.2012 9:30; etc.
- **geographical coordinates** (measured by GPS) and **identification number** of observation point.

The distance to soaring bird was determined by its visual size in the binoculars that was divided in four classes of size by the special graticule lines marked on the eyepiece of binoculars (Fig. 2.4). It was assumed that the wingspan of adult Black vulture in soaring flight is about 150 cm (Buckley, 1999). Since this species use almost exclusively soaring flight at high altitudes (Buckley, 1999; our observations), this size was used for calculation of the distance to each soaring bird. The correspondence of each size class to distance interval was calculated by Eq. 1, explained within the Fig. 2.5<sup>3</sup>. Three distance intervals (100-200, 200-400 and 400-700 m) determined by Eq. 1 were tested empirically by comparing them with the distances to an artificial model of a soaring adult Black vulture with wingspan of 150 cm, measured by the “distance finder” option of GPS Montana650. The test showed the close correspondence between calculated and measured distances.

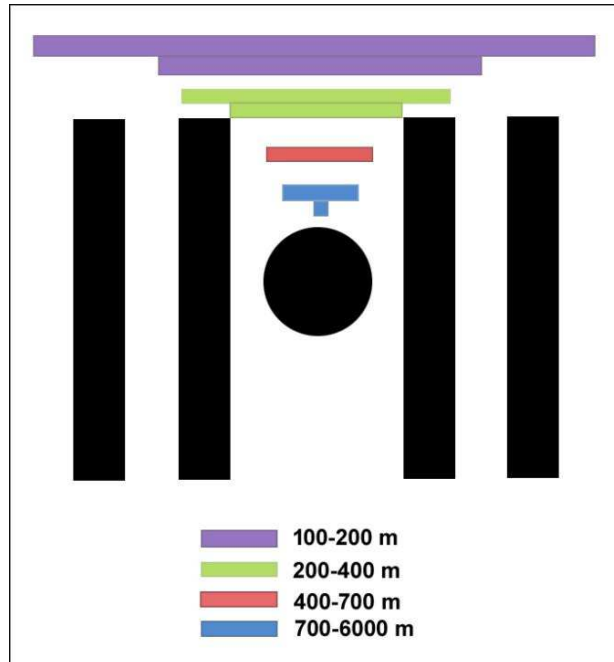


**Figure 2.4 Scheme of detection of the distance interval to an adult Black vulture in soaring flight by binoculars**

Black bars show the graticule lines marked on the eyepiece of binoculars. Colored bars correspond to the visible size of a bird.

<sup>3</sup>The upper limit of the fourth interval (6000 m) determined by the Eq. 1, must be considered only as the maximum limit beyond which the flying birds could not be located. The fourth interval because of its high inaccuracy in detection of number and geographical position of flying birds was excluded from several analyses. See details in "Assumptions and limitations" section of Chapter III. The applied dataset - "full" (includes 4 distance intervals from 100 to 6000 m) or "incomplete" (includes 3 intervals from 100 to 700 m) is specified in the methodology to each analysis.

The following meteorological characteristics were recorded by the portable weather station “WeatherLink Vantage Pro2” (Fig. A.1) synchronously with the bird’s observation (i.e. every 15 minutes) and in the same viewpoint:

- **air temperature**, degrees of Celsius (the maximum value in 15 minutes interval);
- **relative humidity**, percents;
- **wind speed**, km/h (the maximum value in 15 minutes interval);
- **wind direction**, compass degrees (the most frequent wind direction in a 15 minutes interval);
- **atmospheric pressure** (hPa);
- **solar radiation**, W/m<sup>2</sup> (the maximum solar radiation in a 15 minutes interval);
- **solar energy** (Ly)<sup>4</sup>;
- **time of observation**, i.e. date and time of registration (with the same accuracy as it was for birds census).

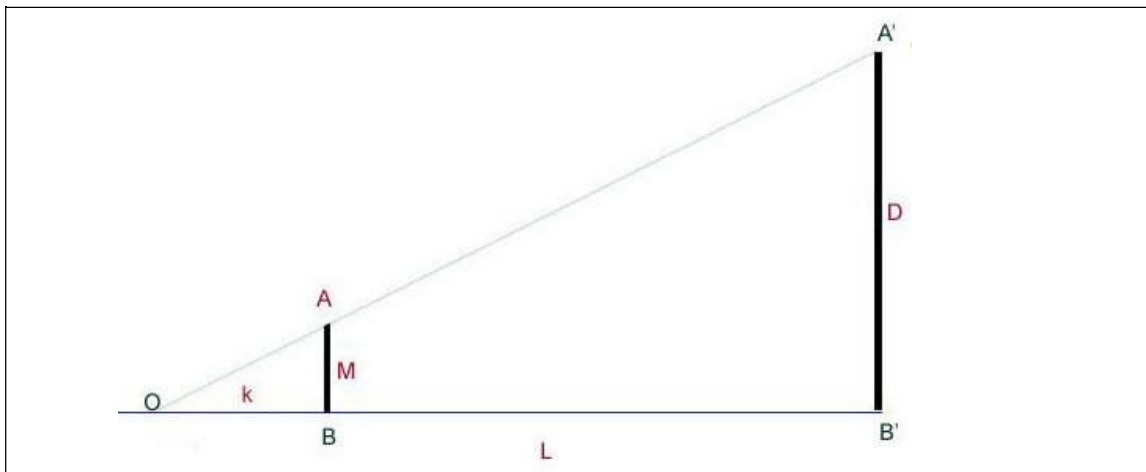


**Figure 2.5 Estimation of the distance interval to a bird using the size of this bird in binoculars**

O - observer

D – real object’s size (metres)

L - real distance to object (metres)

M - object’s size in binocular units

k - coefficient of binocular which was calculated experimentally by the same equation ( $k = 857,143$ )

From the triangle OA'B' (Fig. 2) follows:

$$k = OB, L = OB'$$

$$\frac{D}{M} = \frac{L}{k} \rightarrow$$

$$L = k \frac{D}{M} \quad (\text{Eq. 1})$$

<sup>4</sup> 1 Langley (Ly) = 11.622 Watt-hours per square meter = 41.84 kilojoules per square meter.

## 2.3 Data preparation for analyses

Data preparation for analyses was implemented in ArcGIS10.0 (ArcMap) and Excel software by several steps considered below. The most of calculation procedures were implemented directly in the attribute tables of corresponded shapefiles. The technical algorithms of data preparation in more details are considered in Appendix C (Algorithm C1, Algorithm C2).

### 2.3.1 Preparation of the summary datasets

At first, the field observations were organized in two summary datasets (Excel tables): (i) **“Number and locations of soaring birds”** dataset, consisting of ornithological objects and their recorded parameters: number of viewpoint, geographical coordinates of viewpoint, quantity of birds, direction, vertical angle, distance, time of observation; (ii) **“Values of meteorological parameters”** dataset, containing meteorological characteristics which were measured synchronously with the bird observation in each viewpoint. Then, both tables were connected with each other by the identical **“time of observation”** parameters in ArcGIS software into a single table, entitled as the **“Birds and meteorological parameters”** merged dataset (Supplementary Files SF26). To each ornithological object of this dataset the registered parameters of geographical position and meteorological characteristics measured simultaneously with birds’ observation were attributed.

### 2.3.2 Preparation of the summary georeferenced database

On the next step, the ornithological objects of the **“Birds and meteorological parameters”** merged dataset were georeferenced<sup>5</sup> as vector points on GIS map and saved as point shapefile (separately for each studied site) by dint of calculation of their geographical coordinates. The latitude and longitude of each flying bird were calculated in ArcGIS software within the attribute table of shapefiles by Eq. 4, Eq. 5 from average values of registered intervals of distance, direction, vertical angle and geographical coordinates of viewpoint, from which the observation were conducted. The *height of flight* parameter of each flying bird was calculated in ArcGIS software by Eq. 3 from average values of registered intervals of vertical angle and distance. The explanations of equations are presented within Fig. 2.7.

---

<sup>5</sup> To georeference of an object as a point means to determine its geographical coordinates (latitude and longitude) and put it as a vector point on a map of GIS software as a shapefile or file of any other GIS format.

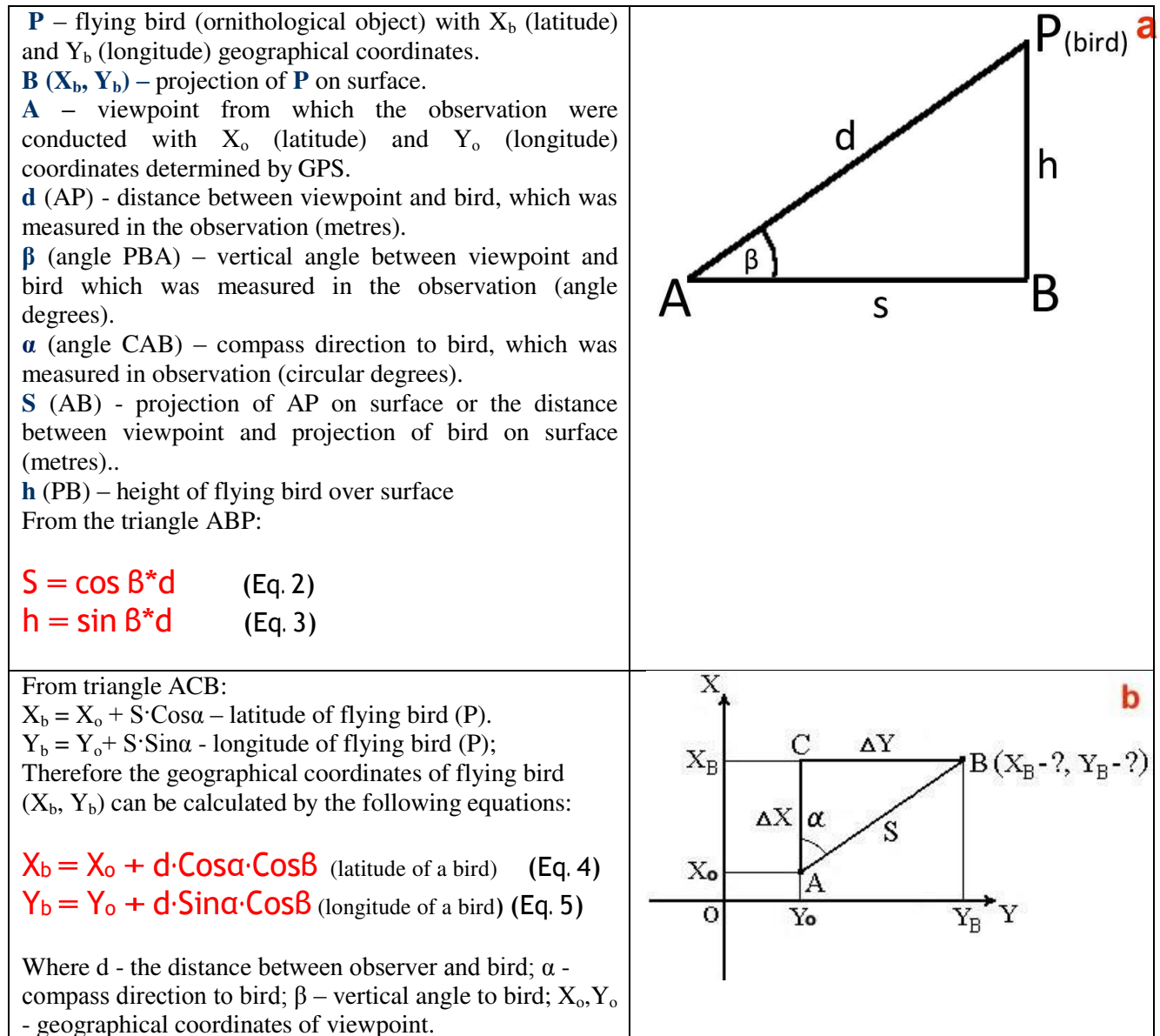


**Figure 2.7 Calculation of the geographical coordinates (latitude, longitude) and height of flight parameter of a mid-point location of each registered bird**

The resultant point shapefiles with their attribute tables constructed for both study sites (Supplementary Files SF2) became the [summary georeferenced database](#), which was the basis for all analyses and maps construction. We entitled it as the “**Georeferenced birds and meteorological parameters**” database<sup>6</sup>. Each point of those shapefiles represents on GIS map the projection on the earth's surface of an averaged (approximate) position in space of a

<sup>6</sup> The “Georeferenced birds and meteorological parameters” database and its attribute table (i.e. the “Birds and meteorological parameters” merged dataset) became the basis for both parts of our investigation. The “Birds and meteorological parameters” merged dataset was the basis for analyses, studying the relationship between soaring activity of Black vultures and meteorological conditions, considered in the Chapter II. The shapefiles themselves were the intermediate stage of the data preparation for statistical analyses, studying the dependence of abundance of soaring vultures on superficial characteristics, considered in Chapter III. Also they were used for construction of maps, predicting the risk of collision with Black vultures over territory.



registered flying ornithological object (Fig. 2.6). The attribute tables of those shapefiles contain for each point (i.e. each ornithological object) all registered parameters (quantity of birds, distance, vertical angle, direction, number and geographical coordinates of a viewpoint, time of observation); calculated parameters (height of flight, latitude and longitude of its geographical position) and all meteorological characteristics, measured synchronously with its registration. The technique of birds' georeference as points and "Georeferenced birds and meteorological parameters" database preparing is considered in more details the in the Appendix C (Algorithm C1).



**Figure 2.6 The registered birds georeferenced as vector points (example from Amarais site, Supplementary Files SF2)**

### 2.3.3 The "Frequency of soaring bird records" ( $F_{\text{birds}}$ ) index

The parameter entitled as the **Frequency of soaring birds records or  $F_{\text{birds}}$**  calculated by Eq.6 can be considered as a relative numerical measure of the abundance of soaring Black vultures over the territory in a chosen geographical area during the chosen period of the year.

$$F_{\text{birds}(j)} = \frac{\sum \text{birds}(j)}{\sum \text{reviews}(j)} \quad (\text{Eq. 6})$$

Where:

$\sum \text{birds}(j)$  - is a total amount of birds recorded in a given (j) 15-minutes time interval (j=7:01 -7:15; 7:16-7:30; 7:31-7:45;...17:46 -18:00) or a given hour (j=7:00-8:00; 8:01-9:00; 9:01-10; ...17.01-18:00) of a day in a chosen geographical area (which can be a single viewpoint or several viewpoints) during a chosen period of the year (which can be a month or a few month);

$\Sigma_{\text{reviews}(j)}$  – is a total amount of sky reviews that were implemented by the observer at the same time interval of a day, geographical area and period of the year, as the  $\Sigma_{\text{birds}(j)}$ .

Hence, the  $F_{\text{bird}(j)}$  - is the average number of birds that were recorded in a given (j) 15 minutes time interval or a given 60 minutes time interval of a day in a chosen geographical area during a chosen period of the year.

The  $F_{\text{birds}}$  index was applied in several analyses, studying the relationship between soaring activity of vultures and meteorological characteristics. The use of  $F_{\text{birds}}$  index allowed to consider in analyses the difference in total amount of sky reviews done in each viewpoint, caused by weather and human factor.

The  $F_{\text{birds}}$  index was calculated by different ways according to the purposes of the analyses. It was determined for all viewpoints (i.e. the “chosen geographical area” was the 13 viewpoints of each study site), for entire year of observation and for single month (i.e. the “chosen period of the year” was 12 months and one month); for time interval 15 minutes and 60 minutes. Those details are specified in the methodology to each analysis.

#### 2.3.4 Ranging months by average daily temperature

Some analyses of our investigation were conducted separately for cold and warm period of the year with the purpose to estimate the seasonal fluctuation in the flying behavior of Black vultures. To determine the warm and cold months, the months of the observed period (09.2013 – 08.2013) were compared with each other by the average daily (from 8:00 to 18:00) temperature. It was conducted by means of meteorological measurements, which were implemented along with the birds' observations. As the result, months from April to August were detected as the "cold months"; months from September to March were defined as the "warm months"; June and July were identified as the coldest months of the year of observation (Fig. 2.8).

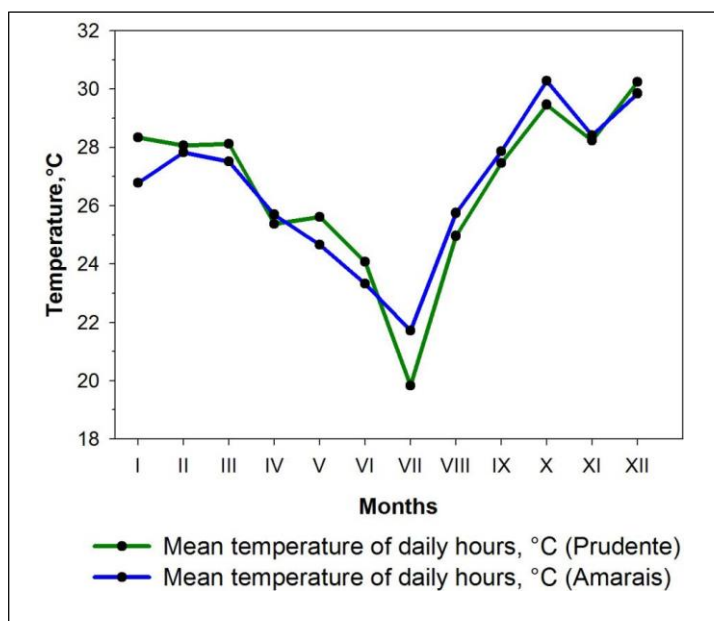


**Figure 2.8** The average monthly temperature for daily hours (8:00-18:00), °C

### 2.3.5 Application of relative biological timescale and normalized relative biological timescale

To the study of flying activity of birds during a day and throughout a year, the ordinary timescale was transformed to a *relative biological timescale* where time of local sunrise was taken as zero point. To compare abundance of soaring birds by months, the relative biological time normalized to a day length of 12 hours was applied. It allowed confronting the peaks and drops of the birds soaring activity, values of meteorological parameters and their dependence from sun position. The methodology of transformation of the ordinary timescale to the relative biological timescale and normalized relative biological timescale is considered in Appendix C (Algorithm C2).

## 3. Data analyses

### 3.1 Study of the soaring Black vulture distribution and population size

The Repeated Measures ANOVA was applied to compare the distributions of total amount of vultures recorded in each month between Amarais and Prudente sites. The summary tables for test was prepared from the “Birds and meteorological parameters” full database. To illustrate the result of ANOVA the boxplots of both distributions were constructed. These analyses allowed estimating the difference between size of studied populations.

To estimate the character of distribution of soaring vultures within study sites, the total amount of flying recorded birds at each point of observation was calculated and the summary histograms were constructed (Fig. 2.9).

### 3.2 Study of the height of flight of soaring Black vultures

For assessment the altitudes of the vultures soaring flight, the distribution of the “height of flight” parameter, calculated by Eq. 3 for three first distance intervals of the “Birds and meteorological parameters” database was analyzed. For graphical illustration of the character of flying altitudes distribution, all values of the “height of flight” parameter were ranged by the intervals of 50 metres and for each interval the sum of birds recorded in this altitude was calculated.

The functional relationship between “height of flight” and “sum of birds recorded at this altitude” parameters was compared with the log-normal theoretical distribution built by LOGNORMDIST function in Microsoft Excel by Mean and Standard Deviation parameters of the real distribution (Supplementary Files SF32, SF33).



### 3.3 Study of the influence of meteorological and seasonal changes on soaring activity of Black vultures

To study the influence of meteorological conditions on soaring activity of Black vulture, the  $F_{\text{birds}}$  index was applied as the relative numerical measure of the intensity of soaring flights of birds over the area. The summary tables for analyses were prepared from the “Birds and meteorological parameters” full database. The research question was formulated as the following *“What relationship does exist between  $F_{\text{birds}}$  index and meteorological characteristics”?*

At first we explored the influence of seasonal and diurnal variations of meteorological characteristics on the soaring activity of Black vultures. Together with this question the pattern of daily soaring activity of this species was studied.

At second, we analyzed the dependence of soaring activity of vultures from specific meteorological characteristics. The  $F_{\text{birds}}$  index and the total amount of recorded birds were applied as the relative numerical measure of the abundance of soaring vultures over the area. Firstly, the graphic analysis of functional relationship between meteorological conditions and soaring activity was implemented. It was done in order to get the visual representation of the general character of this relationship. Then the Principal component analysis and the Multiple regression analysis were conducted to clarify the results of graphical analysis and to detect the dependence of  $F_{\text{birds}}$  index from meteorological characteristics. Finally the Pearson correlation test was implemented to clarify the results of both previous analyses.

#### 3.3.1 Study of the influence of seasonality on daily variation in soaring activity of Black vultures

The daily variation of the soaring activity of Black vultures and the influence of seasonality on it was estimated graphically. The histograms and plots were built from the “Birds and meteorological parameters” full database and presented on the normalized biological timescale.

The histograms of  $F_{\text{birds}}$  index calculated for each month and for the whole period of observation were constructed. The  $F_{\text{birds}}$  index was calculated as a number of birds recorded during one hour in a month, averaged over 13 viewpoints (Figs.A.9-A.12, Supplementary Files SF35) and the whole year averaged over 13 viewpoints and 12 months (Fig. 2.13) of each study site.

The combined plots of meteorological characteristics (air temperature, relative humidity, wind speed, atmospheric pressure and solar radiation) and  $F_{\text{birds}}$  index were built to estimate the relationship between daily variation of meteorological condition and daily schedule of soaring activity (Figs. 2.14 – 2.17; Supplementary Files SF36). The  $F_{\text{birds}}$  index was calculated as a number of birds recorded during a 15 minutes interval of a given month, averaged over 13

viewpoints. The plots were yielded for two months contrasting by the average daily temperature<sup>7</sup>, which allowed estimating the seasonal difference in the weather impact on the character of daily soaring activity of the Black vulture.

### **3.3.2 Study of the influence of seasonality on the abundance of soaring Black vultures**

The influence of seasonality on the intensity of soaring flights of Black vulture was estimated by plotting the total amount of birds recorded at each month (Fig. 2.18). The ANOVA test comparing months by the  $F_{\text{birds}}$  index was conducted to clear the seasonal impact on the intensity of soaring activity. The data for both analyses were prepared from the “Birds and meteorological parameters” full database.

### **3.3.3 Study of the dependence of soaring activity of Black vultures on basic meteorological characteristics**

#### **3.3.3.1. Graphical analysis of the functional relationship between meteorological conditions and soaring activity of Black vultures**

The graphical analysis was conducted for the [air temperature](#), [relative humidity](#) and [wind speed](#) parameters. The plots of functional relationship between each meteorological parameter and the soaring activity was built by a sample, prepared from the “Birds and meteorological parameters” full database by the following way. For each sample, the curves of theoretical normal and log-normal distributions were constructed by NORMDIST and LOGNORMDIST Microsoft Excel functions by use of “Mean” and “Standard deviation” parameters of the real bird’s distribution. The adequate number of ranges for analyses and graphical presentation was determined using the Sturges’ formula:  $k=1+3.3221*\text{LOG10}(n)$ , where “n” is the number of observations (a sum of recorded birds). Each sample was converted into a table with the uniform scale of ranks. For each rank of each meteorological parameter the following values were calculated: (i) the total amount of birds recorded in it; (ii) the total number of sky reviews made in it; (iii) the  $F_{\text{birds}}$  index (which here is the number of birds recorded during a single sky review at a given range of values, averaged over 13 viewpoints). Based on these data the resultant plots were constructed (Figs. 2.20 – 2.25, Supplementary Files SF37).

#### **3.3.3.2 Statistical analyses studying the dependence of soaring activity of Black vultures on meteorological conditions**

The Principal component analysis (PCA), the Multiple regression analysis (MRA) and the Pearson correlation analysis were conducted for Amarais and Prudente sites to clarify the results of graphical analysis and estimate the dependence of soaring activity of Black vultures

---

<sup>7</sup> July and June were determined as the coldest months, December – as the warmest month of the period of observation (Fig. 2.8, Supplementary Files SF38).

(expressed in  $F_{\text{birds}}$  index) on weather conditions. The statistical analyses were carried out in SPSS 20.0 and R 3.1.0. The plots were constructed in SigmaPlot10.

PCA was applied to reveal the meteorological factors which have the strong relationship with each other and  $F_{\text{birds}}$ , MRA was used to outline the meteorological characteristics strongly affecting on  $F_{\text{birds}}$ . The following meteorological parameters were studied in both tests: [air temperature](#), [wind speed](#), [relative humidity](#), [solar energy](#) and [solar radiation](#)<sup>8</sup>. These characteristics were chosen as the most presumably affecting the soaring activity of Black vultures and, at the same time, promising to be useful to monitor the distribution of flying birds and reduce the risk of collisions. In MRA the meteorological parameters were considered as independent variables, whereas  $F_{\text{birds}}$  - as variable depending from those meteorological parameters. Otherwise, in PCA all variables including  $F_{\text{birds}}$  assumed to be independent. We use PCA in this context in order to identify links between soaring activity of birds and meteorological characteristics, including those ones which caused by some other factors. We implemented PCA and MRA separately for warm months (from April to August) and cold months (from September to March). This allowed to estimate the influence of seasonality on the relationship between soaring activity of vultures and weather condition. In addition, we conducted both tests for a sample of the coldest months of the year (June and July).

The Pearson correlation analysis between  $F_{\text{birds}}$  and meteorological characteristics, as well as between parameters meteorological themselves, was conducted to confirm and detail of the PCA and MRA results and to provide the further insights to the links between soaring activity of vultures and meteorological conditions, as well as between meteorological parameters themselves.

Thus, three statistical tests were implemented on the basis of the “Birds and meteorological parameters” full database (Supplementary Files SF27), which was prepared for those analyses by the following way. For each 15 minutes interval of each month the following parameters were detected and organized as a table: (i) [value of each meteorological parameter](#), calculated as the arithmetic mean by a month over 13 viewpoints of a study site; (ii) [F<sub>birds</sub> index](#) calculated by Eq. 6 for 13 viewpoints of a study site.  $F_{\text{birds}}$  index here means the number of birds recorded during a given 15 minutes interval of a day (7:01 -7:15; 7:16-7:30; 7:31-7:45;....17:46-18:00) in all viewpoints of the study site in a given month (sep. 2012, oct. 2012, ... aug. 2013). Those calculations were implemented in ArcGIS software (by means of Dissolve tool and Field Calculator) within attribute tables of shapefiles entitled as the “Georeferenced birds and meteorological parameters” database (Supplementary Files SF1). The attribute tables of the final

---

<sup>8</sup> Solar energy and solar radiation parameters were measured only for Amaraïs site from April to August 2013.

shapefiles became the summary tables for implementation of statistical tests. Their copies as Excel tables can be found in Supplementary Files SF39.

## 4. Results

### 4.1 Comparing of the population size of Black vultures between studied sites

The soaring Black vulture distribution within the airports vicinities was non-uniform. The contrast between minimum and maximum quantity of vultures recorded in a viewpoint is **15.71%** (4171 ind., from 3.04% to 18.75%) in Prudente; and **34.21%** (6202 ind., from 1.9% to 36.11% in Amaraïs (Fig. 2.9, Tables A.3, A.4). The studied populations had strong differences in size. From the total amount of recorded birds in both sites (**44201** individuals), 59% (**26072**) were observed in Prudente and 41% (**18129**) - in Amaraïs (Table B.3, Table B.4).

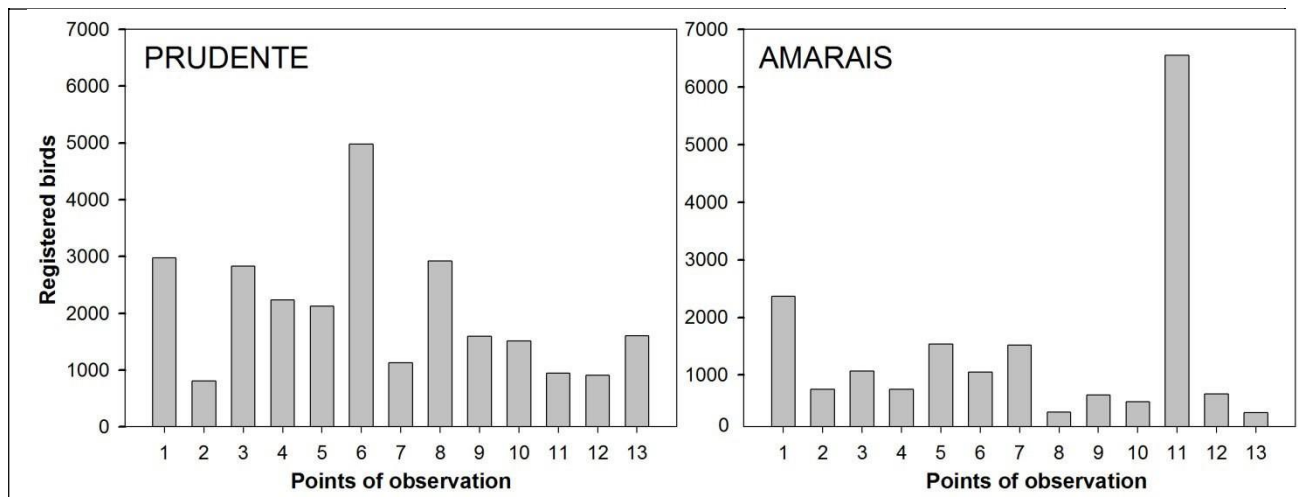


**Figure 2.9** The total amount of birds registered in each viewpoint during the observation period

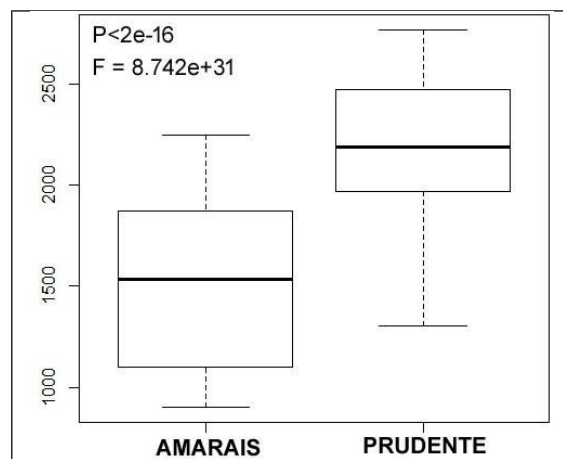


**Figure 2.10** Comparing of the studied populations by the number of flying birds recorded at each month by ANOVA test

The two studied populations differ significantly from each other by the number of flying birds recorded at each month ( $P < 2e-16$ ,  $F = 8.742e+31$ ). The boxplot shows that the total amount

of soaring birds recorded at each month in Prudente site was much higher than it was in the Amaraís site (Fig. 2.10).

#### 4.2 Height of flight of soaring Black vultures

The distributions of flight altitudes have small difference in the study areas. The median of altitudes in Prudente (129.9 m) is slightly lower than in Amaraís (192.8 m), while maximum in both areas is the same (550 m). In Prudente it has a pronounced peak between 50 and 150 m, where 64% of birds were observed. The number of recorded birds decreases sharply at altitudes higher than 150 meter: at altitudes of 150-300 m - 29%, at altitudes of 300-550 m – 8% of birds were recorded. In Amaraís it has two small peaks located in the intervals of 100-150 m (18.2% of recorded birds) and 250-300 m (15% of recorded birds) (Fig. 2.11, Table 2.1). The functional relationship between altitude of soaring flight and the total number of birds recorded at this altitude are close to the log-normal distribution, the correlation coefficient between real and theoretical log-normal distribution is 0.91 for Prudente and 0.78 for Amaraís (Fig. 2.12).

**Table 2.1 Distribution of the registered altitudes of soaring Black vultures nearby the Amaraís and Presidente Prudente airports during the period of observation (Supplementary Files SF32)**

Altitude of flight (m)	Birds, Amaraís (%)	Birds, Prudente (%)
13.0 - 50.0	4.5	9.76
50.1- 100	13.2	22.69
100.1-150	18.2	31.51
150.1-200	12.7	8.75
200.1-250	7.1	8.94
250.1-300	15.0	10.84
300.1 - 350	3.6	1.62
350.1-400	8.7	2.76
400.1-450	4.3	0.90
450.1- 500	4.7	0.91
500.1 - 550	8.0	1.32

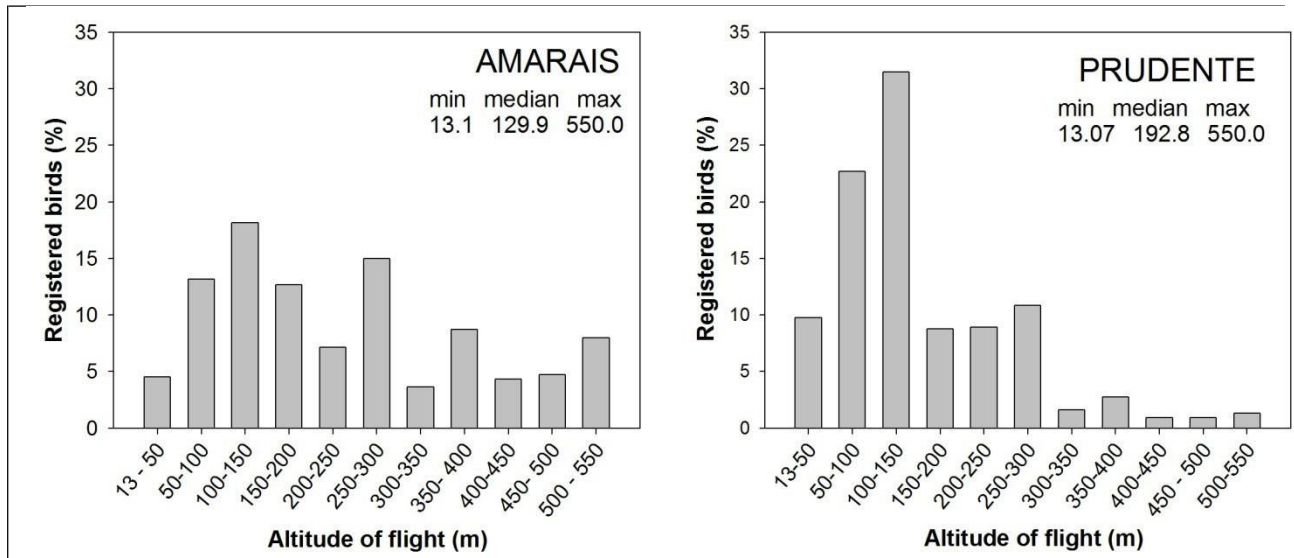


**Figure 2.11** Distribution of the recorded altitudes of soaring Black vultures nearby the Amarais and Presidente Prudente airports during the period of observation

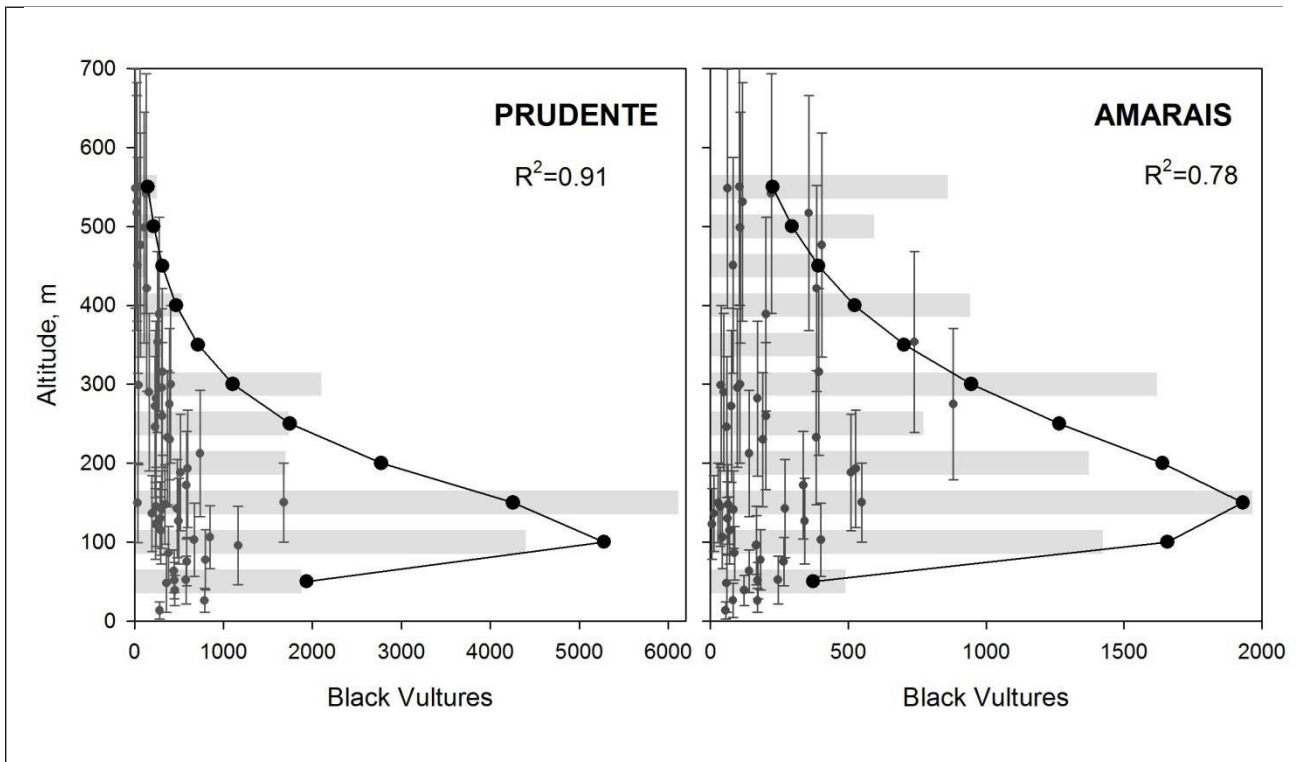


**Figure 2.12** Comparison of real and log-normal (theoretical) functional relationship between the “altitude of flight” and the “sum of birds recorded at this altitude” parameters

The grey histograms represent the real distribution of the registered birds. The black curves represent the theoretical log-normal distribution calculated by Mean and Standard Deviation parameters (Excel) of the real distributions of the registered birds as a function of the “altitude of flight” parameter. Small dark grey points with uncertainty intervals correspond to the “sum of vultures recorded at this altitude” parameter and represent the raw data for analyses.

### 4.3 Influence of meteorological seasonal changes on soaring activity of Black vultures

#### 4.3.1 Influence of seasonality on daily variation in soaring activity of Black vultures

The resulting plots (Figs.A.9 - A.12; Fig. 2.13; Figs.2.14-2.17) reveal two types of schedule of the soaring activity of Black vultures on the study areas: (i) with two strong peaks of daily activity at morning and afternoon with notable depression in local midday (about 6-7 hours after local sunrise); (ii) with plateau-like graph or plot with a single weak smooth peak at local midday. The first type occurred for most of the months in the Amarais site (Fig.2.13<sub>(right)</sub>; Fig. 2.14; Figs. A.11, A.12), the second type - for most of the months in the Prudente site (Fig.2.13<sub>(left)</sub>; Fig.2.16 ; Fig.2.17; Figs. A.9, A.10). In both types about 1- 1.5 hours after sunrise the soaring activity starts and about 1-1.5 hours before sunset the soaring activity finishes. The soaring activity grows drastically for about 1.5 hours after sunrise, which clearly concurs with the increase of solar radiation and air temperature (Figs. 2.14-2.17).

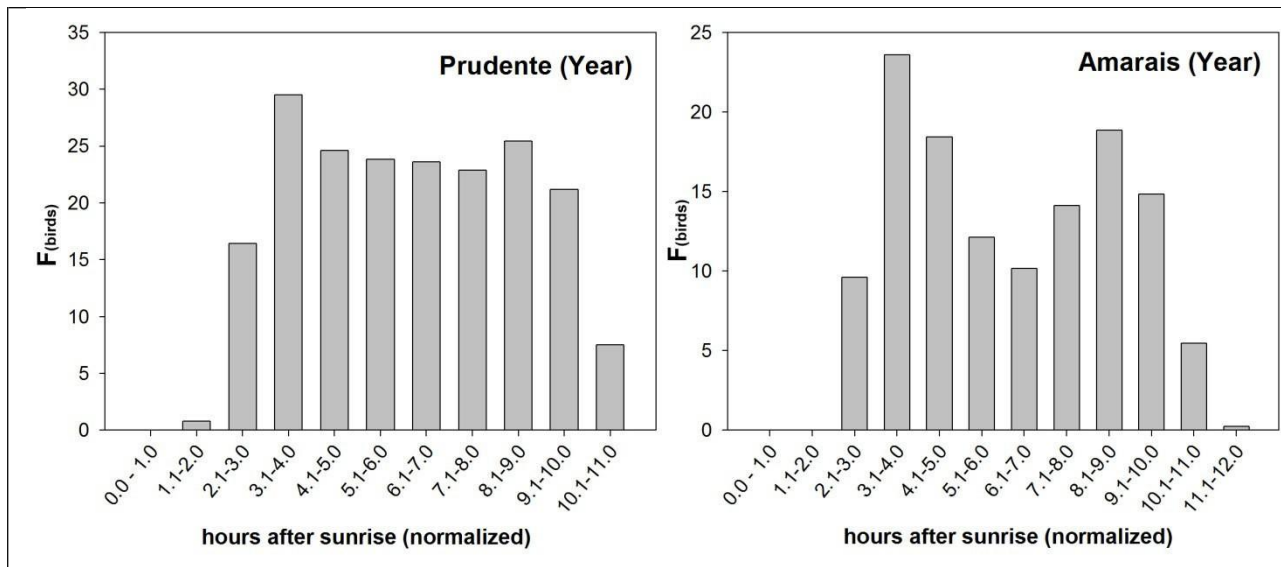


**Figure 2.13 Daily variation in the soaring activity of Black vultures at the year of observations: from September 2012 to August 2013 (Supplementary Files SF35)**

OY: Frequency of birds records ( $F_{birds}$  index) is a number of birds recorded during an hour of the year, average over 13 viewpoints and 12 months

There were few small peaks of the relative humidity parameter probably caused by rain, which correspond with the decrease of the soaring activity (Figs. 2.14-2.17). Due to the fact that the number of those cases was small, the correlation coefficient between these parameters did not evidence this relationship (Table 2.6).



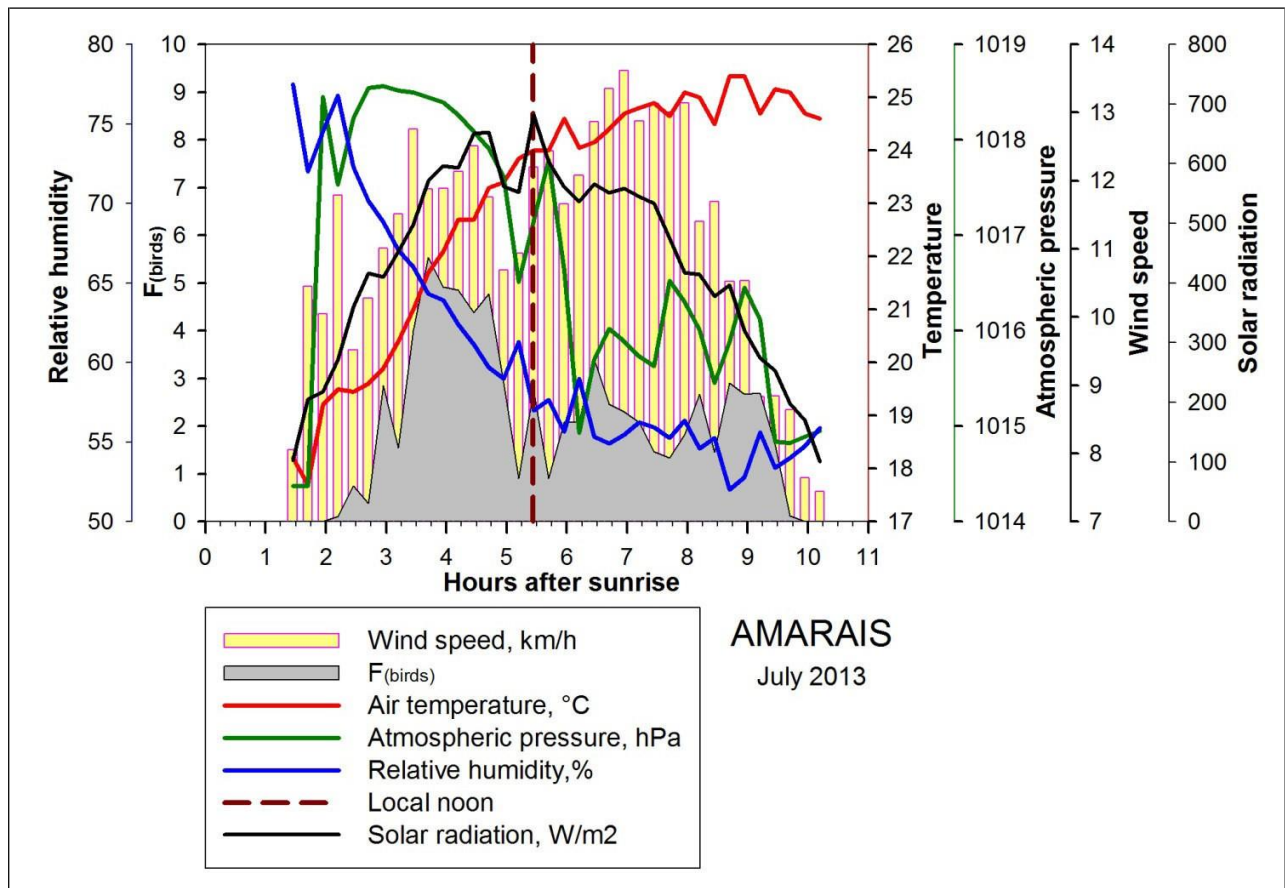


**Figure 2.14** Daily variation in the soaring activity of Black vultures and meteorological conditions in the Amaraïs site (data averaged for each 15-min interval over 13 viewpoints for July)

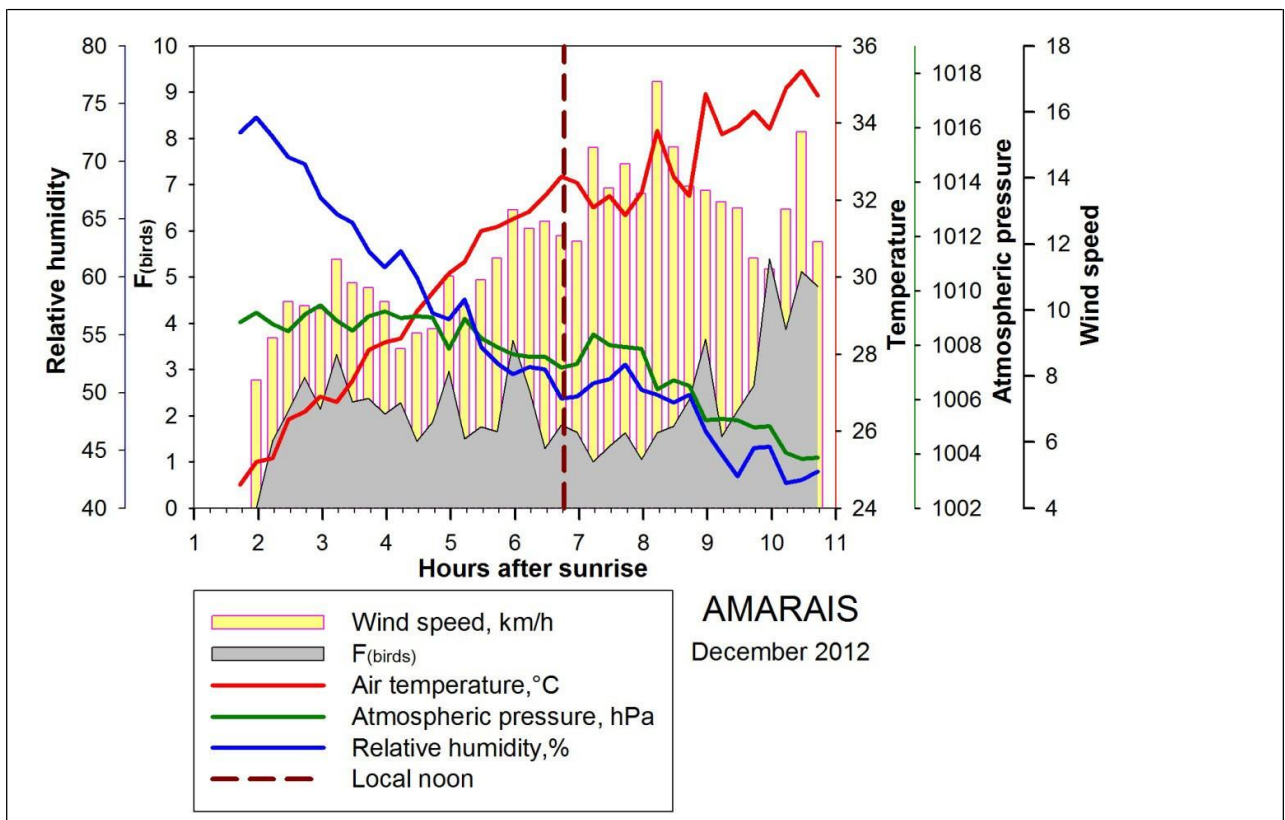


**Figure 2.15** Daily variation in the soaring activity of Black vultures and meteorological conditions in the Amaraïs site (data averaged for each 15-min interval over 13 viewpoints for December)



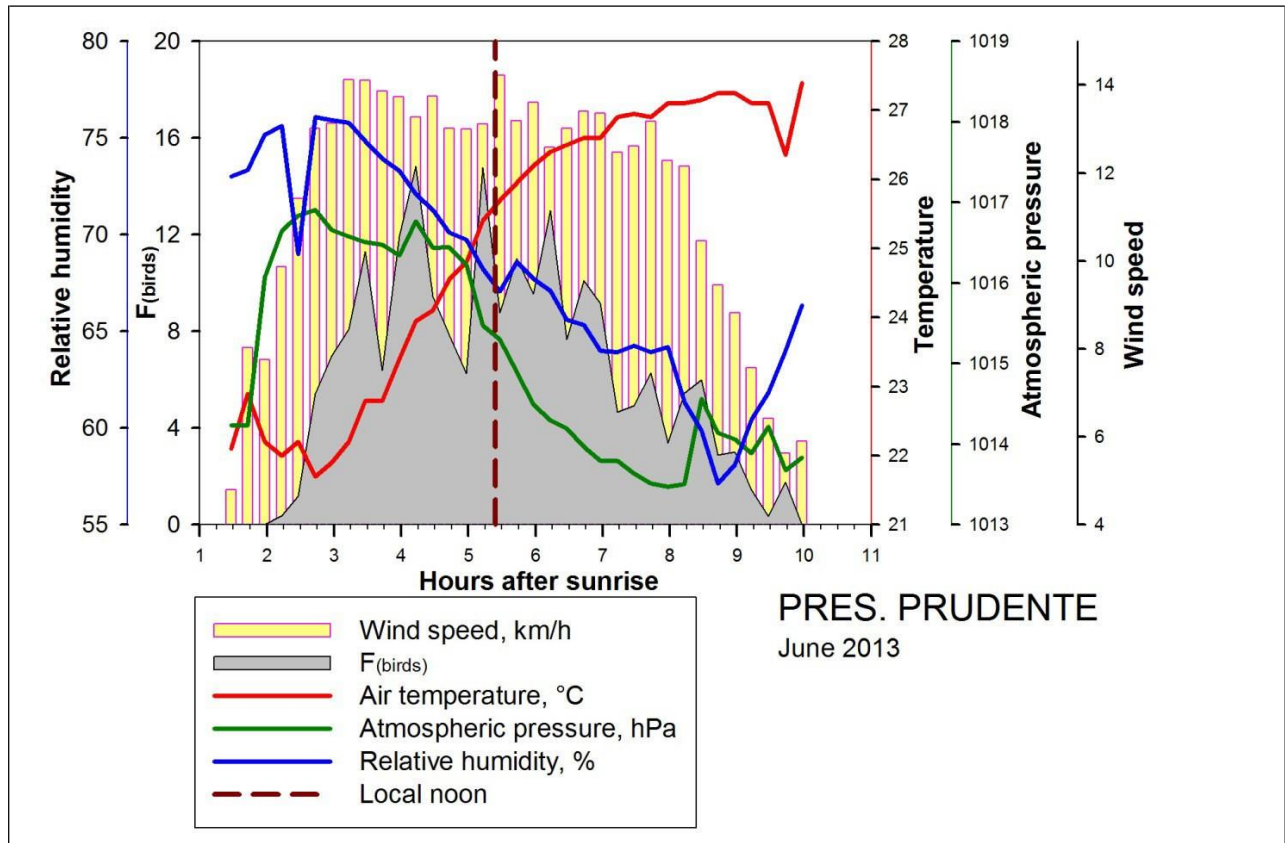


**Figure 2.16** Daily variation in the soaring activity of Black vultures and meteorological conditions in Prudente site (data averaged for each 15-min interval over 13 viewpoints for June)

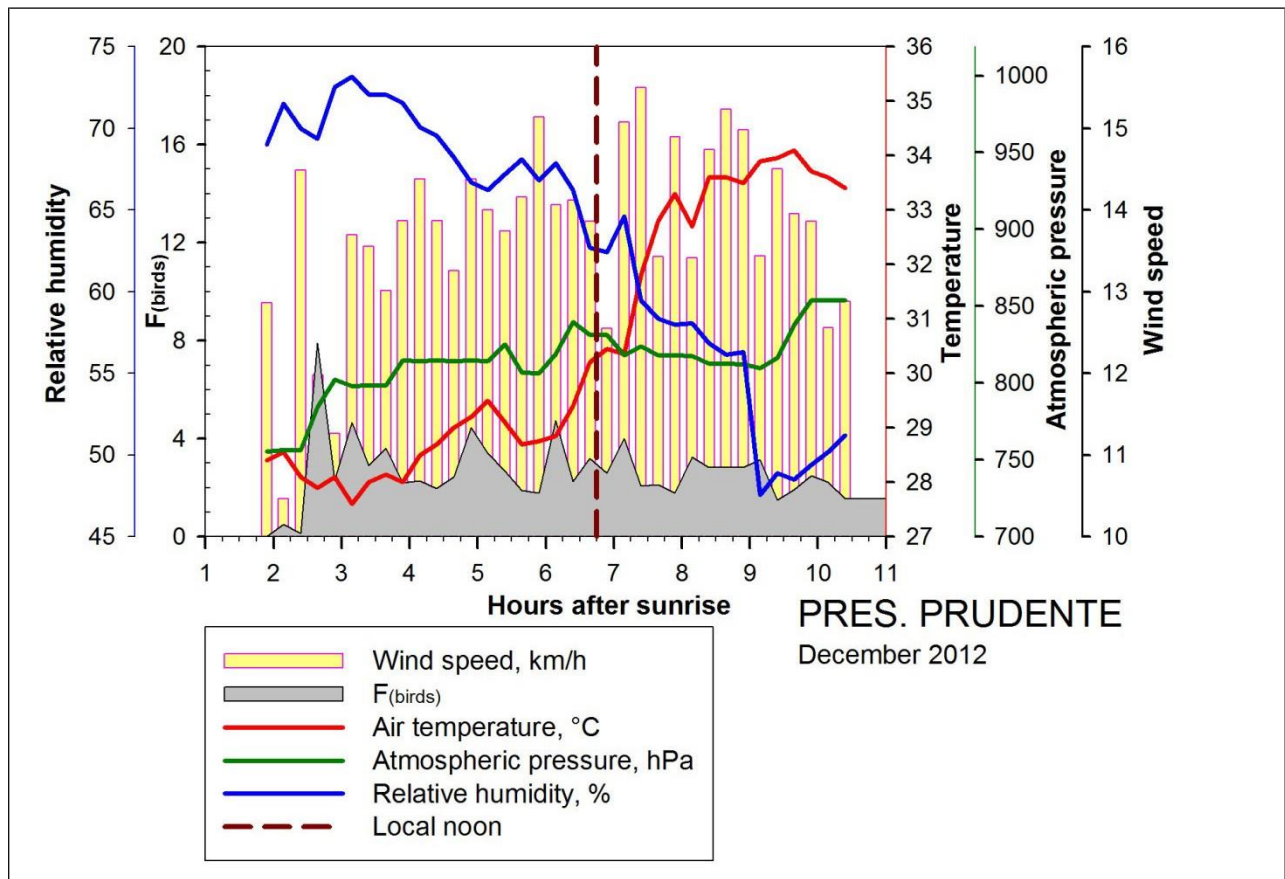


**Figure 2.17 Daily variation in the soaring activity of Black vultures and meteorological conditions in the Prudente site (data averaged for each 15-min interval over 13 viewpoints for December)**

The each meteorological parameter of the Figs. 7.9-7.12 indicates the highest value of this parameter during a given 15-minutes period of a day, averaged over 13 viewpoints of a given month (December, June or July). Here the  $F_{birds}$  index is a number of birds that were recorded during a given 15 minutes interval of a day, averaged over 13 viewpoints of the same month.

Local noon – is time of a day when the Sun is at zenith. For each study site the time of local noon was calculated as the average time of local noon over 13 viewpoints (see details in Appendix C (Algorithm C2)). The summary tables for construction of Figs 7.9-7.12 can be found in the Supplementary Files SF36.

#### 4.3.2 Influence of seasonality on the abundance of soaring Black vultures

The resulting plots reveal that abundance of soaring vultures in both populations had strong irregularity with smooth peaks and valleys continued for several months (Fig. 2.18). The ANOVA test comparing months by  $F_{birds}$  index separately in each study site shows a significant difference between samples in both populations (for Amaraïs  $p\text{-value} = 5.06e-09$ ,  $F = 5.938$ , for Prudente  $p\text{-value} = 0.0031$ ,  $F = 2.616$ ). The boxplot representing annual variation of  $F_{birds}$  index (Fig. 2.19) shows that studied populations had the mutually inverse trends in the abundance of soaring birds. The period of increasing of soaring activity in Prudente coincides with the period of decreasing of soaring activity in Amaraïs and vice versa. The plot representing the total amount of the recorded birds at each month shows the same result (Fig. 2.18). The negative correlation of those trends is stronger in cold months from April to August. In those months the Amaraïs population had high values of  $F_{birds}$ , while Prudente had low values of  $F_{birds}$ . In other

words, we found that the period of reduction of the soaring activity in Amaraís site coincides with the period of growth of soaring activity in the Prudente site. This is a remarkable phenomenon, taking into account the large distance between both studied sites.

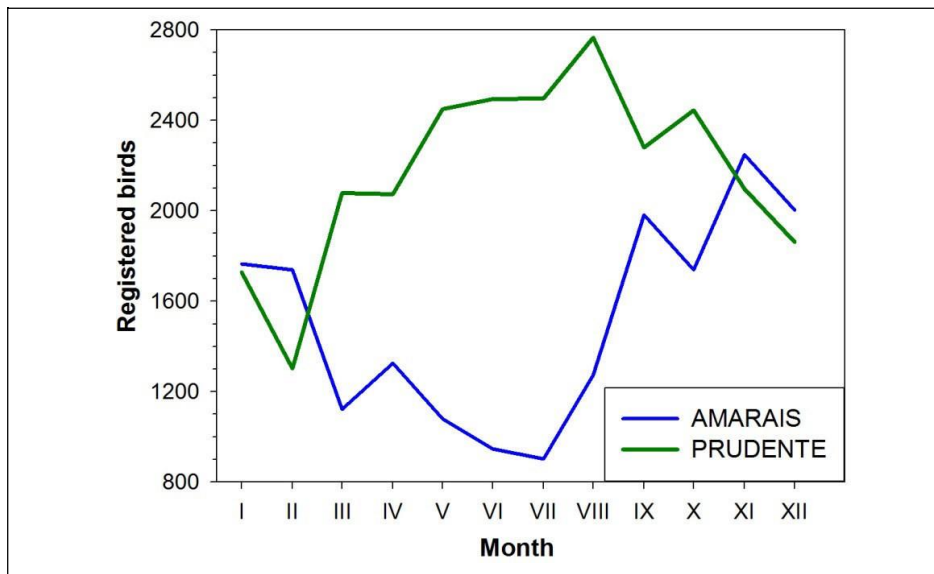


**Figure 2.18** Number of Black vultures recorded at each month (Supplementary Files SF34)

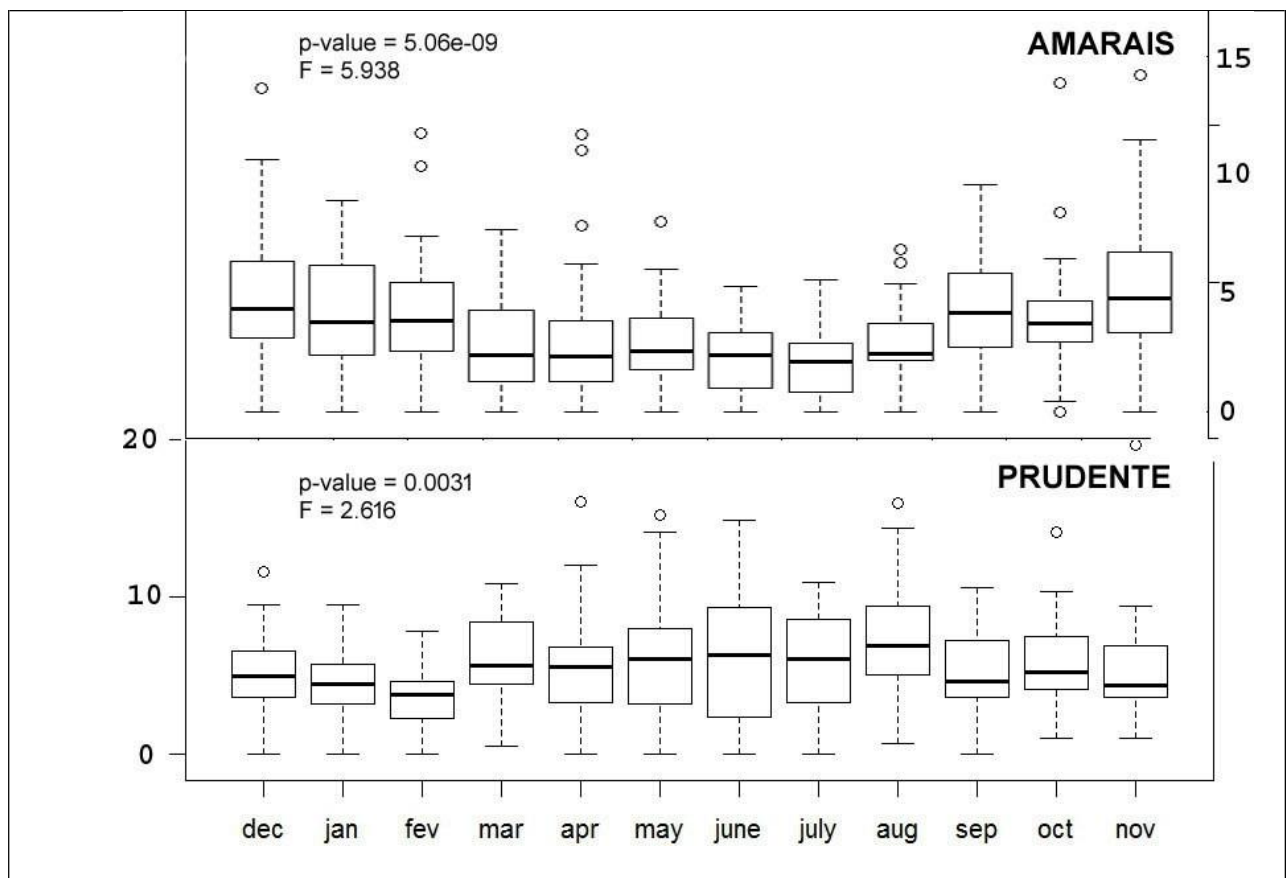


**Figure 2.19** Annual variation of  $F_{bird}$  index for study sites. The median, first and third quintile of  $F_{bird}$ , averaged for each month over the 13 viewpoints. The result of ANOVA test comparing months by  $F_{birds}$  index in each study site (Supplementary Files SF31)

### 4.3.3 Dependence of soaring activity of Black vultures on basic meteorological characteristics

#### 4.3.3.1 Functional relationship between meteorological conditions and soaring activity of Black vultures

The result of analysis studying the functional relationship between meteorological conditions and soaring activity of Black vultures is presented on Figs. 2.20 – 2.25 and Supplementary Files SF37. On these figures the **grey histogram** shows the total amount of birds recorded at a given range of values of meteorological parameter. It corresponds to the observed distribution of soaring vultures and represents the functional relationship between meteorological condition and number of registered birds. For **air temperature** and **relative humidity** parameters this distribution is close to the Gaussian (normal) distribution (Figs. 2.20– 2.23), for **wind speed** parameter it is close to a log-normal distribution (Figs. 2.24, 2.25). The **red curve** represents the theoretical (normal or log-normal) distribution of the accounted birds. The **dotted brown line** represents the **number of sky reviews** at a given range of values of meteorological parameter. It shows that distribution of this parameter is close to normal and log-normal. The **green histogram** represents the  $F_{\text{birds}}$  index or the average number of birds that were recorded during a single sky **review** at a given range of values of meteorological parameter. The distribution of  $F_{\text{birds}}$  index is close to the uniform distribution.

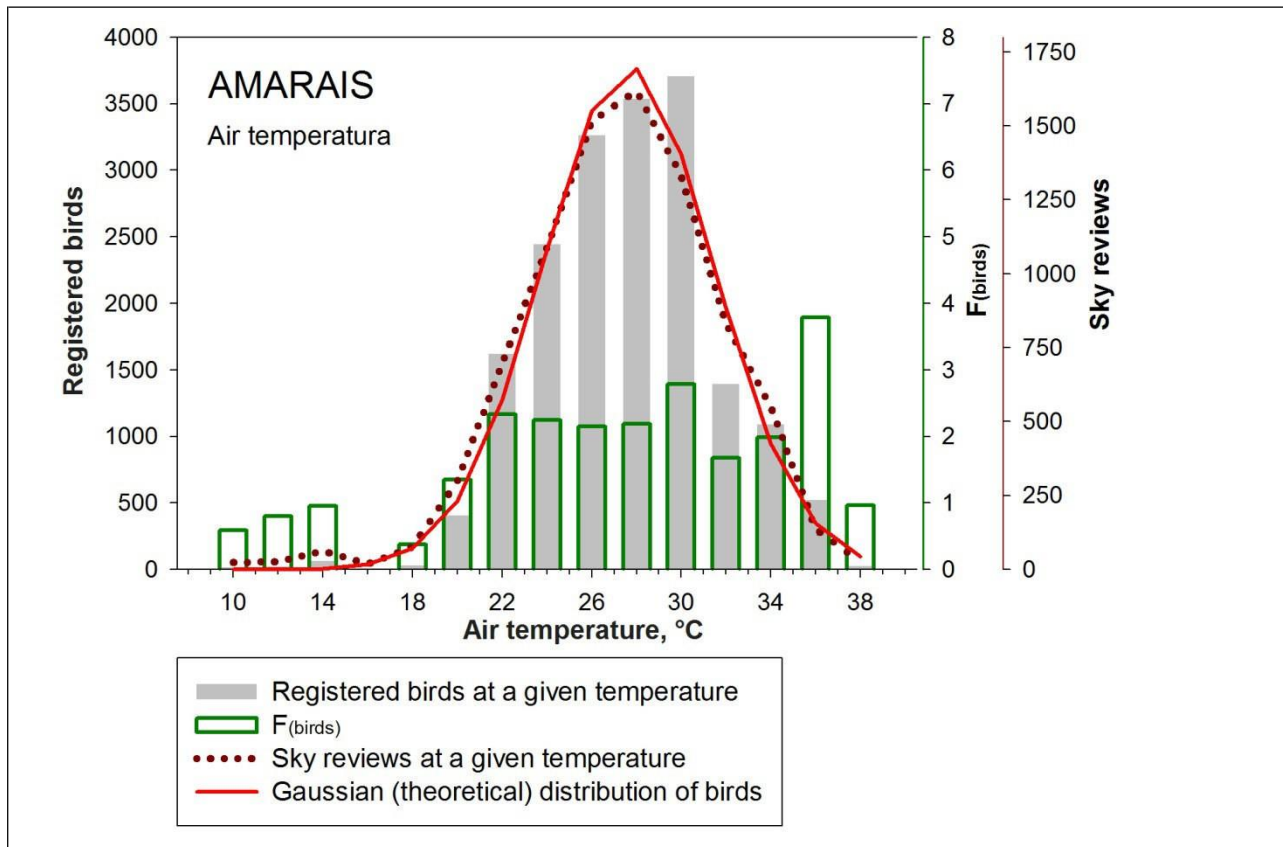


**Figure 2.20** Functional relationship between air temperature and soaring activity of Black vultures in Amaraïs site (Supplementary Files SF37)

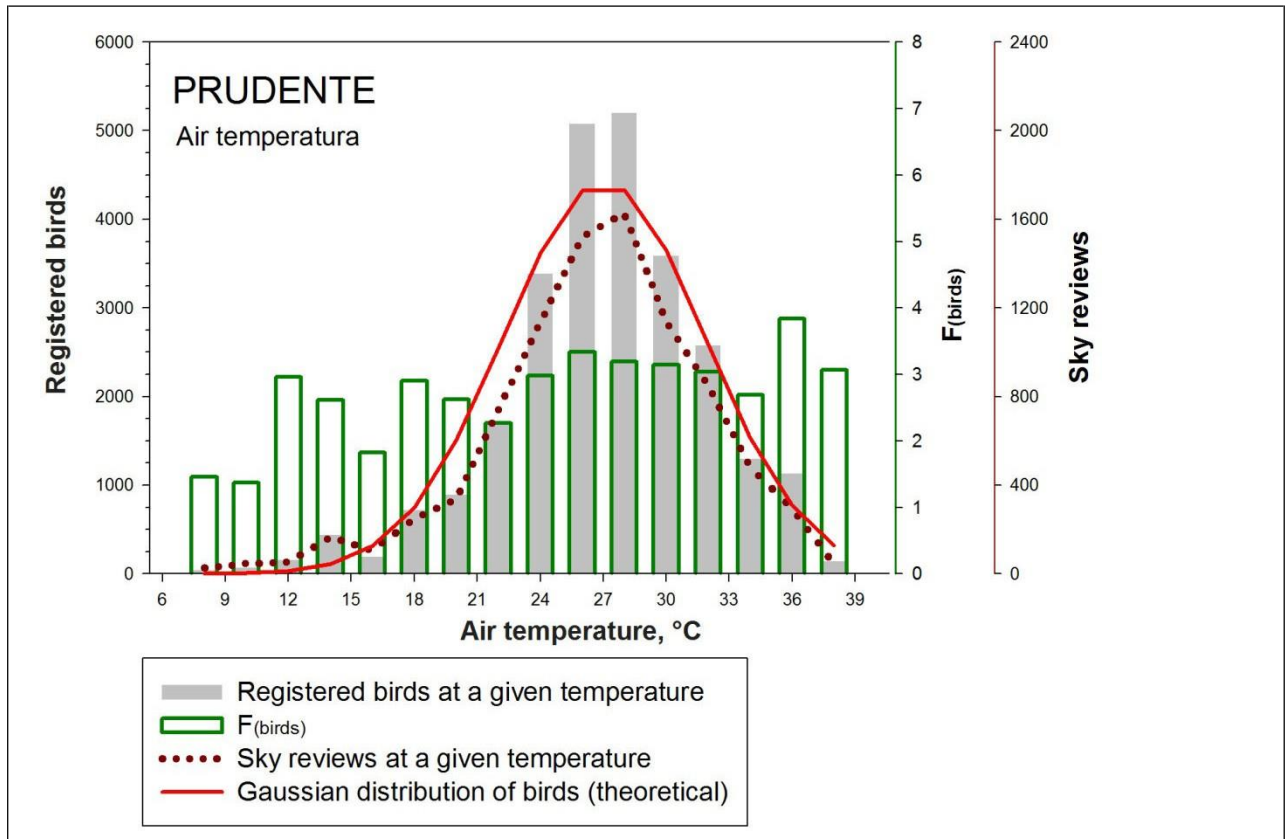


**Figure 2.21 Functional relationship between air temperature and soaring activity of Black vultures in Prudente site (Supplementary Files SF37)**

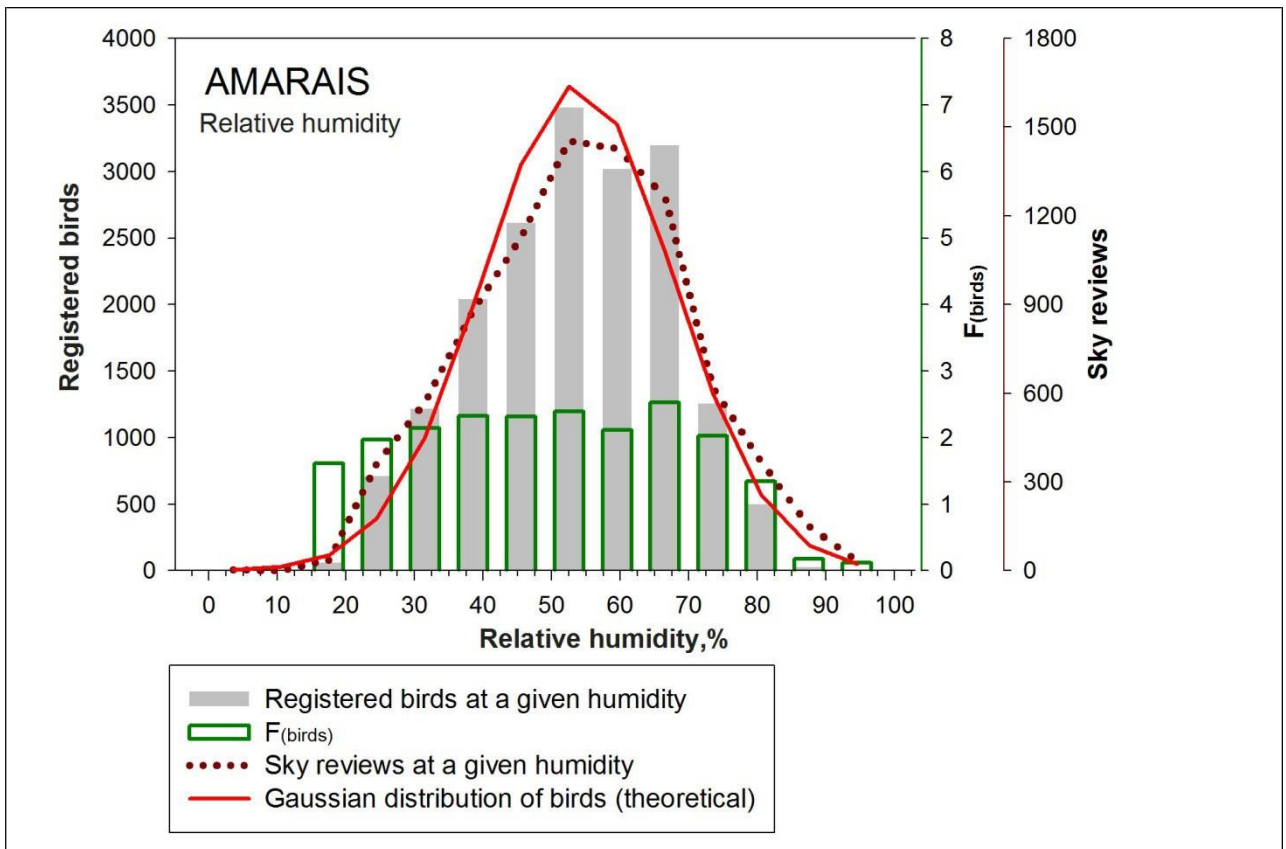


**Figure 2.22 Functional relationship between relative humidity and soaring activity of Black vultures in Amaraís site (Supplementary Files SF37)**



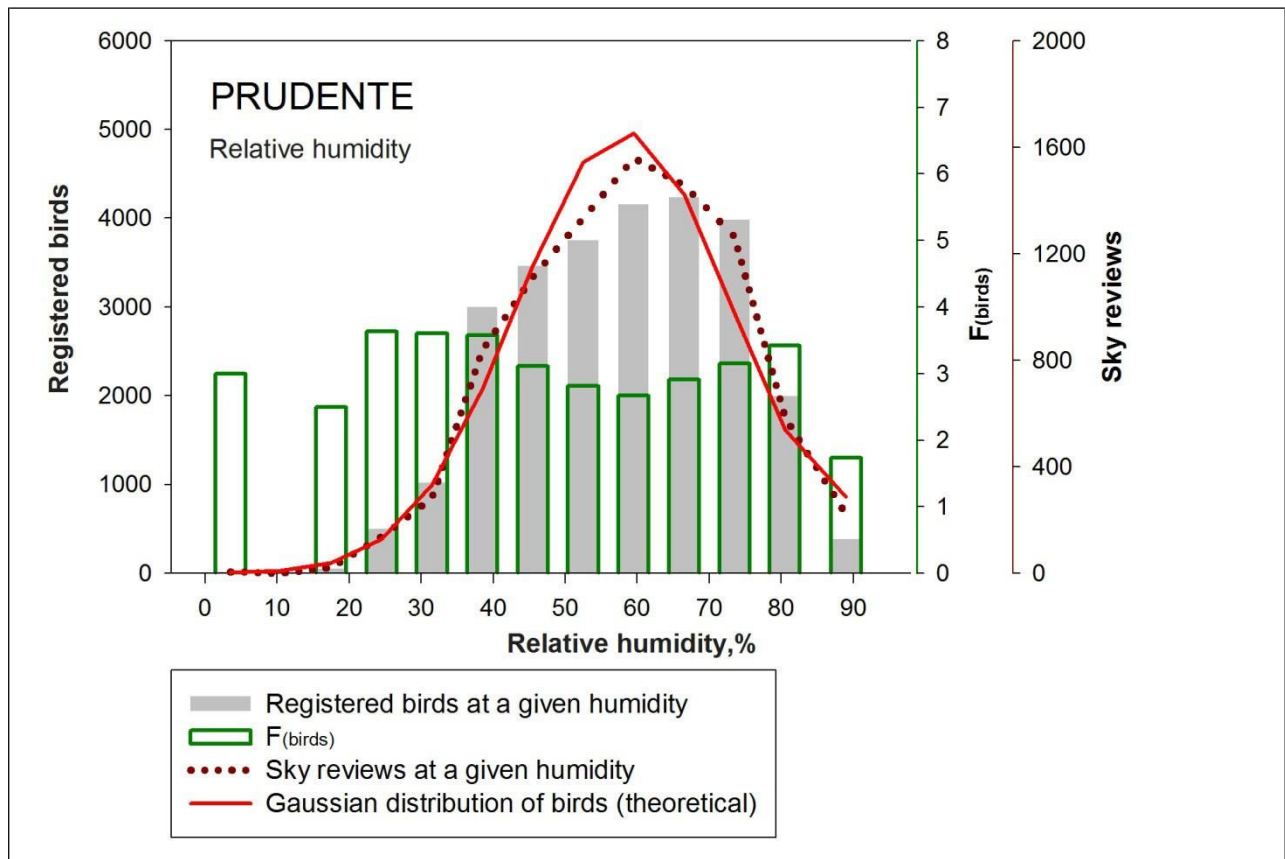


**Figure 2.23** Functional relationship between relative humidity and soaring activity of Black vultures in Prudente site (Supplementary Files SF37)

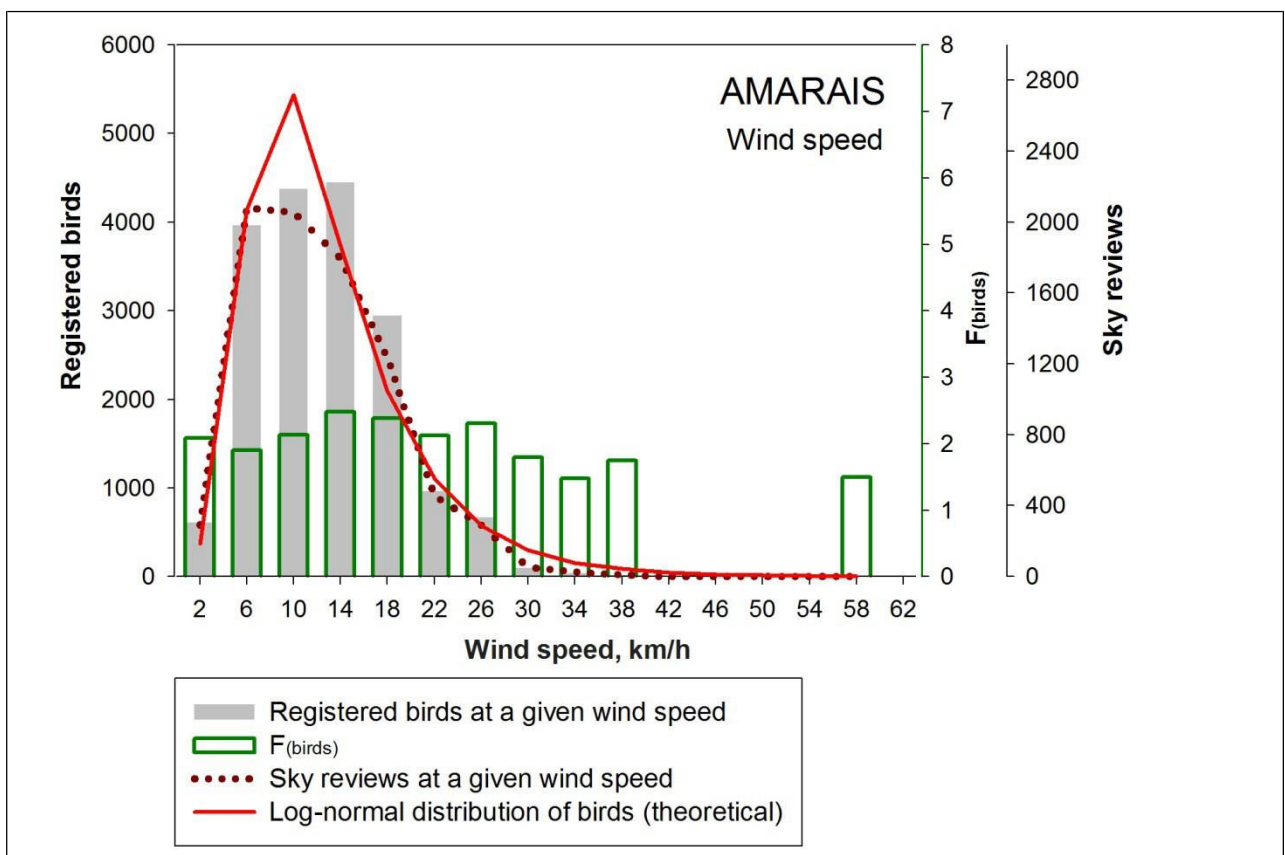


**Figure 2.24** Functional relationship between wind speed and soaring activity of Black vultures in Amaraïs site (Supplementary Files SF37)

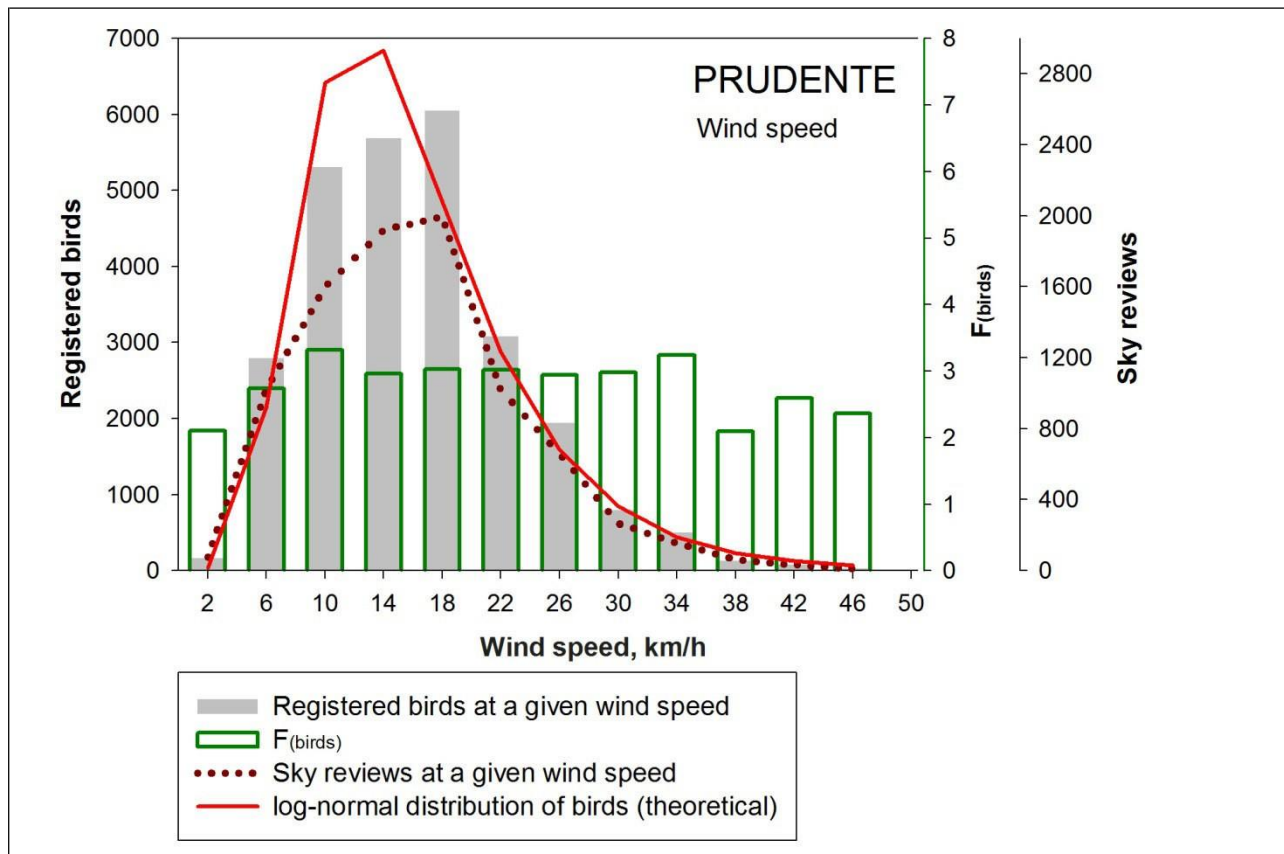


**Figure 2.25 Functional relationship between wind speed and soaring activity of Black vultures in Prudente site (Supplementary Files SF37)**

#### 4.3.3.2 The revealed dependence of soaring activity of Black vultures on basic meteorological characteristics

I. The results of Principal component analysis (PCA) are given in the Tables 2.2 and 2.3; the results of Multiple regression analysis (MRA) are given in the Tables 2.4 and 2.5; the results of Pearson correlation analysis are given in the Tables 2.6 and 2.7. The summary tables prepared for analyses you can find in Supplementary Files SF39.

**Table 2.2 Result of the Principal component analysis estimated the relationship between soaring activity of Black vultures ( $F_{bird}$ ) and meteorological condition (Amarais)**

Variables	April-August		June-July		September-March
	Principal component 1	Principal component 2	Principal component 1	Principal component 2	Principal component 1
$F_{bird}$	0.524	0.169	0.640	0.359	0.348
Air temperature	0.205	0.876	0.112	0.856	0.817
Wind speed	0.783	0.380	0.809	0.141	0.807
Relative humidity	-0.132	-0.928	-0.074	-0.854	-0.826
Solar radiation	0.951	0.081	0.966	0.036	
Solar energy	0.963	0.080	0.974	0.004	

**Table 2.3 Result of the Principal component analysis estimated the relationship between soaring activity of Black vultures (Fbird) and meteorological condition (Presidente Prudente)**

Variables	April-August		June-July	
	Principal component 1	Principal component 2	Principal component 1	Principal component 2
F <sub>bird</sub>	0.280	0.578	0.170	0.732
Air temperature	0.938	-0.207	-0.863	0.451
Wind speed	-0.200	0.914	0.921	0.300
Relative humidity	-0.789	-0.349	0.184	-0.736

**Table 2.4 Results of the Multiple regression analysis estimated the dependence of soaring activity of Black vultures on meteorological conditions (Amarais). Dependent variable: F<sub>birds</sub><sup>9</sup>**

Independent Predictors	Months	R <sub>reg</sub>	R <sub>sq</sub>	Adjusted R Square	Std. Error of the Estimate
Wind speed	Apr-Aug	0.394	0.155	0.150	1.03
ALL: Solar Energy, Relative humidity, Air temperature, Wind speed, Solar Radiation	Apr-Aug	0.450	0.203	0.179	1.01
Solar Radiation	Jun-Jul	0.564	0.318	0.309	0.83
Solar Radiation, Air temperature,	Jun-Jul	0.620	0.385	0.367	0.80
ALL: Solar Energy, Relative humidity, Air temperature, Wind speed, Solar Radiation	Jun-Jul	0.622	0.386	0.340	0.82
ALL: Relative humidity, Wind speed, Air temperature	Sep-Mar	0.,217	0.047	0.037	1.13

<sup>9</sup> R<sub>sq</sub> – R square, R<sub>reg</sub> - multiple correlation coefficient



**Table 2.5 Results of the Multiple regression analysis estimated the dependence of soaring activity of Black vultures on meteorological conditions (Presidente Prudente). Dependent variable:  $F_{birds}$**

Independent Predictors	Months	$R_{reg}$	$R_{sq}$	Adjusted R Square	Std. Error of the Estimate
Wind speed	Apr-Aug	0.234	0.055	0.049	1.49
Wind speed, Air temperature	Apr-Aug	0.371	0.137	0.128	1.43
ALL: Relative humidity, Wind speed, Air temperature,	Apr-Aug	0.439	0.193	0.179	1.38
Wind speed	Jun-Jul	0.254	0.064	0.051	1.52
Wind speed, Air temperature	Jun-Jul	0.561	0.314	0.295	1.31
ALL: Relative humidity, Wind speed, Air temperature,	Jun-Jul	0.653	0.426	0.400	1.21
ALL: Relative humidity, Air temperature, Wind speed	Sep-Mar	0.166	0.028	0.017	1.94

#### April-August

In April-August for Amarais, the PCA shows a high positive correlation between **wind speed** (0.783), **solar radiation** (0.951), **solar energy** (0.963),  $F_{birds}$  (0.524) variables and the corresponding first component; the high negative correlation between **air temperature** (0.876), **relative humidity** (-0.928) and corresponding second component (Table 2.2). MRA detects the **wind speed** as the most important predictor for  $F_{birds}$  variable, explaining its dispersion on 15,5% ( $R_{sq} = 0.155$ ). The multiple correlation coefficient between **wind speed** and  $F_{birds}$  is relatively strong ( $R_{reg} = 0.394$ ). All included predictors explain the dispersions of  $F_{birds}$  on 20.3% ( $R_{sq} = 0.203$ ) with the strong multiple correlation coefficient ( $R_{reg} = 0.45$ ) (Table 2.4).

In April-August for Prudente, the PCA identifies a high positive correlation between **wind speed** (0.914),  $F_{birds}$  (0.578) and corresponding second component; the high negative correlation between **air temperature** (0.938), **relative humidity** (-0.789) and the corresponding first component (Table 2.3). MRA determines **wind speed** as the most important predictor for  $F_{birds}$  variable which explains its dispersion on 5,5% ( $R_{sq} = 0.055$ ). However the multiple correlation coefficient between **wind speed** and  $F_{birds}$  is not very strong ( $R_{reg} = 0.234$ ). All included predictors explain the dispersions of  $F_{birds}$  on 19.3% ( $R_{sq} = 0.193$ ) with the multiple correlation coefficient  $R_{reg} = 0.439$  (Table 2.5).

#### June-July

In Amarais for June and July, the dependence of  $F_{birds}$  on meteorological variables is stronger than in other months. PCA shows a high positive correlation between **wind speed** (0.809), **solar radiation** (0.966), **solar energy** (0.974),  $F_{birds}$  (0.640) and corresponding first

component; the high negative correlation between **air temperature** (0.856), **relative humidity** (-0.854) and the corresponding second component (Table 2.2). MRA determines **solar radiation** as the most important predictor for  $F_{\text{birds}}$ . It explains the  $F_{\text{birds}}$  dispersion on 31,8% ( $R_{\text{sq}}=0.318$ ) and has strong multiple correlation coefficient with  $F_{\text{birds}}$  ( $R_{\text{reg}}=0.564$ ). Other important predictor is **air temperature**. Together with **solar radiation** they explain the dispersion of  $F_{\text{birds}}$  on 38,5% ( $R_{\text{sq}}=0.385$ ) with  $R_{\text{reg}} = 0.620$  (Table 2.4).

The multiple regression analyses of data belonging to these months does not determine the **wind speed** parameter as the significant variable for  $F_{\text{birds}}$  for Amarais site. However, the factor analyses showed a strong correlation between **wind speed** and both parameters of solar activity (Table 2.2). It allows concluding that **wind speed** affects  $F_{\text{birds}}$  variable during June and July as well.

In Prudente for June and July, the PCA shows a positive correlation between **wind speed** (0,3),  $F_{\text{birds}}$  (0.732) and the corresponding second component; the high negative correlation between **relative humidity** (-0.736),  $F_{\text{birds}}$  (0.732) and second component; the high negative correlation between **air temperature** (-0.863), **wind speed** (0.921) and the first component (Table 2.3). MRA determined **wind speed** as the most important predictor for  $F_{\text{birds}}$ . It explains its dispersion on 6,4% ( $R_{\text{sq}}=0.064$ ) and has the small multiple correlation coefficient with  $F_{\text{birds}}$  ( $R_{\text{reg}}=0.254$ ). Other important predictor is **air temperature**. Together with **wind speed** they explain the dispersion of  $F_{\text{birds}}$  on 31,4% ( $R_{\text{sq}}=0.314$ ) with  $R_{\text{reg}} = 0.561$  (Table 2.5).

### September - March

In September – March for Amarais site PCA shows a weak positive correlation between  $F_{\text{birds}}$  (0.348), **air temperature** (0.817), **wind speed** (0.807) and the corresponding component (Table 2.2). In MRA all predictors (**relative humidity**, **air temperature**, **wind speed**) explain the dispersion of  $F_{\text{birds}}$  only on 4,7% with the  $R_{\text{reg}} = 0.217$  (Table 2.4).

In September – March for Prudente site PCA does not show any significant correlation between  $F_{\text{birds}}$  and predictors. In MRA all predictors (**relative humidity**, **air temperature**, **wind speed**) explain the dispersion of  $F_{\text{birds}}$  only on 2,8% with  $R_{\text{reg}} = 0.166$  (Table 2.5).

II. The Pearson correlation analysis of meteorological characteristics and soaring activity ( $F_{\text{birds}}$ ) conducted for both sites does not show any constant significant correlation between estimated parameters. The high correlation coefficients with  $F_{\text{birds}}$  were detected for **wind speed** and **solar activity** parameters, but not for all months. Other meteorological characteristics (**air temperature**, **relative humidity**, **atmospheric pressure**) do not show any positive correlation with the soaring activity of vultures (Tables 2.6, 2.7).

**Table 2.6 Pearson correlation coefficients between values of meteorological characteristics and soaring activity of Black vultures ( $F_{birds}$ ) in Amarais site**

Month	Air temperature	Wind Speed	Relative Humidity	Solar radiation	Solar energy	Atmospheric pressure
sep, 2012	0.27	0.32	-0.28	no data	no data	-0.06
oct, 2012	0.17	-0.21	-0.26	no data	no data	-0.02
nov, 2012	0.26	0.09	0.09	no data	no data	0.20
dec, 2012	0.38	0.15	-0.38	no data	no data	-0.54
jan, 2013	0.17	<b>0.53</b>	-0.54	no data	no data	-0.22
fev, 2013	-0.12	0.16	-0.07	no data	no data	-0.37
mar, 2013	0.04	0.30	0.05	no data	no data	0.00
apr. 2013	0.159	0.31	0.19	0.31	0.33	0.30
may, 2013	0.49	<b>0.58</b>	-0.48	0.14	0.14	0.01
jun, 2013	0.43	<b>0.62</b>	-0.33	<b>0.48</b>	<b>0.49</b>	0.25
july, 2013	0.29	<b>0.52</b>	-0.18	<b>0.68</b>	<b>0.66</b>	0.28
aug, 2013	-0.19	0.33	0.18	0.22	0.21	0.11

**Table 2.7 Pearson correlation coefficients between values of meteorological characteristics and soaring activity of Black vultures ( $F_{birds}$ ) in Prudente site**

Month	Air temperature	Wind Speed	Relative Humidity
sep, 2012	0.06	<b>0.55</b>	0.02
oct, 2012	0.28	-0.13	-0.28
nov, 2012	0.18	0.18	-0.16
dec, 2012	-0.13	-0.02	0.13
jan, 2013	<b>0.47</b>	0.10	-0.51
fev, 2013	0.35	-0.05	-0.30
mar, 2013	0.29	-0.11	-0.26
apr. 2013	-0.08	0.32	0.27
may, 2013	0.07	<b>0.52</b>	-0.09
jun, 2013	-0.15	<b>0.79</b>	0.11
july, 2013	<b>0.52</b>	0.17	-0.40
aug, 2013	<b>0.45</b>	-0.18	-0.44

III. The Pearson correlation analysis shows a significant correlation ( $R^2=0.51-0.81$ ) between solar activity (solar radiation and solar energy) and wind speed parameters for all month of Amarais site, during which the solar activity observation was conducted (Table 2.8).

**Table 2.8 The Pearson correlation coefficients between (i) Wind speed and Solar radiation, (ii) Wind speed and Solar energy (Amarais)**

Month	Wind speed & Solar radiation	Wind speed & Solar energy
April	0.78	0.81
May	0.58	0.53
June	0.79	0.78
July	0.84	0.85
August	0.78	0.76

This result is confirmed and supplemented by PCA and MRA results, which evidence the strong positive relationship between **wind speed**, **solar activity** and  $F_{\text{birds}}$ . For both sites in cold months PCA shows that  $F_{\text{birds}}$  refers to the same component as the **wind speed** and (for Amarais) **Solar activity** (**solar radiation**, **solar energy**) variables. While **air temperature** and **relative humidity** variables are always located in another component, where they have high negative correlation with corresponding factor (Tables 2.2, 2.3). MRA for both sites determines **wind speed** as the most important predictor for  $F_{\text{birds}}$  variable in the cold months (Tables 2.4, 2.5).

Also the strong positive relationship between **wind speed** and **solar activity** is confirmed by visual comparing of the daily variation plots of those parameters. In most of the months the daily plot of **wind speed** is very close to the measured and expected shape of the daily plot of **solar radiation and solar energy**<sup>10</sup> parameters, the similarity was especially stronger in cold months. Those parameters start to grow about 1 hour after sunrise; they have the maximum at midday; then they begin to decline and reach the minimum during the sunset (Figs. A.13<sub>(a, b, c, d)</sub>; Figs. A.14<sub>(a, b, c, d)</sub>). The following details are important:

a. In both airports the general trend of the registered **wind speed** parameter resembles the variation of solar parameters through a day. However, for various months it might fluctuate significantly. In Amarais the **wind speed** deviated from the generalized trend during September, October and November. In Prudente the considered trend was typical only for March, May, June, August and September.

b. Both study sites showed a stronger similarity in the **wind speed** and **solar activity** parameters (measures or expected) for the cold months.

The strong positive relationship between **wind speed** and **solar activity** implies that the **wind speed** parameter reflects the daily circulation of atmosphere and it relates very closely with the intensity of solar radiation. Since thermals are directly determined by the intensity of solar radiation and, for this reason, should have the same shape of daily curve that solar activity (Angevine, 1998; 2014), **in both study sites, during most of the year (and all cold months), the Wind speed parameter reflected partly or completely the strength of thermals activity.**

---

<sup>10</sup> Here we use the statement, that curves of daily variation of solar activity parameters (solar radiation and solar energy) should be identical considering the time of day (i.e. the sun position above the horizon) during all months of the year. It has shape of the inverted parabola with peak at true noon (time of the highest position the sun above the horizon). This occurs due to the fact that for any geographical region the intensity of solar radiation depends mainly from the sun position above the horizon. Weather conditions (clouds, precipitation) can make only a slight decrease in solar activity, but do not change the underlying trend. The plots constructed for all months when the solar activity parameters were measured confirm this statement (Figs. A.13<sub>(a, b)</sub>).

#### 4.4 Observation of Black vultures behaviour near abundant source of food

The observation of Black vulture behaviour near the abundant source of food (a fresh carcass of large animal) was conducted<sup>11</sup>. The carcass was located at the edge between a large agricultural field and the stripe of forest fragments, wetland and several water bodies (large ponds and narrow river) close to several buildings of the working farm (Fig. 2.26).

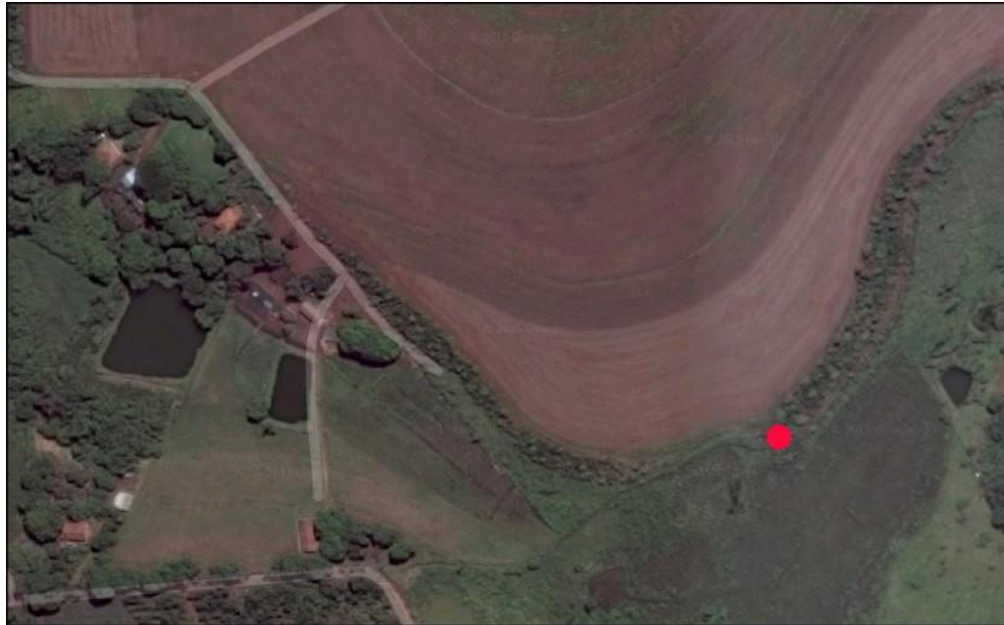


**Figure 2.26** The DigitalGlobe image of high resolution representing the vicinity of Campinas (-22.78724, -47.09007), where the observation of Black vulture behaviour near the fresh carcass of large animal was conducted. The red point shows the location of the dead animal.

We observed a lot of Black vultures (approximately 150-200 individuals) gathered around the carcass. We suppose that these birds arrived to carcass from surrounding lands. A few of them pecked the carcass, but most of birds were sitting in a small distance from the carcass on the ground and trees. There were no conflicts between birds for a place near the dead animal, therefore they rested after the eating. After the human appearance, vultures moved away with flapping flight about ten metres of height and sat on the ground and on the trees nearby the carcass. During the hour of observations, we saw only four Black vultures simultaneously soaring at sky low to the ground and most of the time there were no soaring birds at all.

A month later<sup>12</sup> we again visited this place. We saw that the carcass of the pig was almost eaten and didn't attract any more of vultures. There were no birds around it at all. At sky we counted about 10 Black vultures, which soared above the border between agricultural field and stripe of forest fragments, wetlands and water bodies. There were no soaring vultures above the huge field and town within limits of visibility.

<sup>11</sup> The observation was conducted in the vicinity of Campinas (-22.787237, -47.090074) on 17.05.2015 from 14:55 to 16:05 (weather: cloudy 60%, a slight wind, 28 °C).

<sup>12</sup> 20.06.2015, from 13:30 to 14:25, weather: cloudy 0%, a middle wind, 31°C

## 5. Discussion

Our study was focused on those aspects of the flying behaviour of Black vultures, which are associated with the threat of collision between these birds and aircrafts and which could be used for reduction this hazard. At the same time, our findings highlight the several aspects of flying behavior of the species, which were not previously described in the literature.

### 5.1 Behavior traits of the Black vulture in soaring flight

#### 5.1.1 Altitudes of soaring flight

Our results showed that the most common altitude of the soaring flight of Black vulture ranges from 50 to 300 metres. The height of 300 to 550 metres is less used and the probability of encounter with Black vultures at altitudes higher than 550 metres is negligible.

This range of altitudes corresponds to the estimations yielded by Walter et al. 2012, Avery et al. 2011, who observed the flying behavior of 11 Black vultures and 7 Turkey in South Carolina, USA, using satellite telemetry (GPS backpack harness technology) and three-dimensional modeling in ArcMap. They reported the mean altitude of the Black vulture flight as  $200 \pm 203$  m (SD) and for the Turkey vulture  $108 \pm 95$  m (SD); the median altitude of in-flight locations within FACOD was 125 m and 83 m for Black vulture and Turkey vulture, respectively

#### 5.1.2 Daily variation in soaring activity of Black vulture

We showed two types of daily schedule of soaring activity of Black vultures: (i) two strong peaks of daily activity at morning and afternoon with a notable depression at local midday (about 6-7 hours after local sunrise); and (ii) plateau-like plot with a single weak smooth peak at local midday. Both findings agree with the results reported in literature.

Avery *et al.* 2011 observed the single-peak schedule of flying activity of Black vulture occur at local midday during their study of the flying behavior of Black vultures and Turkey vultures in South Carolina of USA. While Freire et al. 2015 detected the two-peaks type of soaring activity occurring at the morning and afternoon, with notable decrease at midday, observing the flying behavior of both species in Manaus, Central Amazon, Brazil. Our results allow concluding that both types of the schedule of daily soaring activity are inherent to Black vultures.

In both types of schedule the soaring activity starts about 1- 1.5 hours after local sunrise and finishes about 1-1.5 hours before local sunset. Therefore, the sky is completely safe from soaring vultures in dark and twilight hours between local sunset and sunrise. However, this schedule of flying activity is validated only for territories that do not have technogenic thermals working during dark hours. For the areas having strong artificial thermals especially in

combination with illumination it cannot be asserted for sure. It is an open question, which has to be specially studied in each individual case.

### ***Ecological interpretation of two types of soaring activity schedule***

We suppose that the notable distinction between daily variation plots of soaring activity of vultures can be explained by difference in anthropogenic pressure of their habitats. The first “two-peaks” type of daily soaring activity occurred in most months of Amarais site (Fig.2.13<sub>(right)</sub>; Fig. 2.14; Figs. A.11, A.12), where highly urbanized lands predominate and generate a strong anthropogenic pressure. Around Amarais airport may not be enough quiet natural areas acceptable for resting of all vultures of local populations. Thus, a part of birds may need to fly away for looking the appropriate places for rest in the remote natural areas. This may decrease the soaring activity in the middle of the light period.

The second “plateau-like” type of daily soaring activity was observed for most months of Prudente site (Fig.2.13<sub>(left)</sub>; Fig. 2.16, Fig. 2.17, Figs. A.9, A.10), where natural and rural landscapes predominate and generate a small anthropogenic pressure. Around Presidente Prudente airport vultures can have enough quiet natural refuges for resting. Hence, birds may not need to fly away from feeding area. Since that, the breaks in vultures’ flight for their rest can be distributed evenly throughout the period of daily activity and do not form a large depression at midday. However, this interpretation is only a hypothesis of possible explanation of the obtained results. To say this exactly, more research is needed on this topic.

### **5.1.3 Behaviour of Black vultures near abundant source of food**

Our observation of the Black vulture behaviour near the large dead animal shows that a single fresh carcass (or probably any other source of abundant food) attract these birds from large distances, which leads to complete disappearance of soaring vultures above large areas. Being near the food, the birds used only flapping flight rising at low altitude to get closer to the food or to move away from human. Despite our observation was not a controlled scientific experiment and our interpretations can only be considered as a hypothesis, they consistent closely with the results of several other authors. The overall conclusions gave a new practical idea about the possibility of reduction the risk of collisions with vultures.

Buckley (1996) resumed that when food location is known to Black vultures, they approach the feeding site using rather flapping flight than soaring, which evidences that in this case they do not depend on thermals. Other researchers reported about the similar behavior of Black vultures. Coleman and Fraser (1989) wrote that Black Vultures can roost in small and medium sized woodlots located near the feeding sites. Novaes and Cintra (2013) observed the Black vulture’s roosts in a small spot of remnant vegetation (0.3 ha) in areas of intense human



activity (street markets), but close to large garbage containers with constant source of food for birds. These observations allow to suppose, that a permanent source of abundant food can cause the absence of soaring vultures at sky near it, since these birds can place their nocturnal roost nearby and do not use soaring flight. Instead of soaring, vultures will move only by flapping flight from roost to food location. This hypothesis can be confirmed by the results of Novaes and Cintra (2013), who identified that the distance to feeding sites is the only factor that significantly determines the Black vulture's roosts location. In their opinion, other variables - size and shape of natural areas, distance to strong thermals, human disturbance, do not influence on it.

Summarizing our observation and the results of other researchers we can assert, that high concentration of soaring vultures at sky most likely means that at the moment the territory lacks any abundant source of food for these birds. It may be a notable mistake to look for a link between high concentration of soaring vultures and presence of alimentary attractive objects on the surface. This statement has the following practical conclusions:

- An abundant source of food (like carcasses) can cause the complete or partial disappearance of soaring birds from the sky.
- If we remove all possible source of food from the surface, we can reduce the density of soaring birds, but we will not remove all vultures from the sky, because they soar for search for food.
- Probably we can clean sky from soaring vultures or strongly decrease their number over the area, by means of placement an abundant food for this species in suitable places far away from important lands.

It should be noted that in Europe the method of feeding vultures by placing food for them on the ground are widely used in practice. It is called the “vulture restaurants” or “supplementary feeding stations”, these are the special places on the ground dispersed within the area where the domestic livestock carcasses are located (Cortés-Avizanda et al. 2010, Piper, 2006). It is implemented for the purpose to restore the populations of those species, many of which are now classified as threatened with extinction (Deygout et al. 2009; Ogada et al. 2012). The experience of “vulture restaurants” probably can be applied in Brazil and other countries for creating the net of feed stations that will remove soaring vultures from sky over the territories intensively used by aircrafts.



## 5.2 Influence of meteorological conditions on soaring activity of Black vultures

### 5.2.1 Dependence of soaring activity of Black vultures on meteorological conditions

a. The graphical analysis shows that the functional relationship between meteorological characteristics and the recorded number of soaring vultures are close to normal distribution for **air temperature** and **relative humidity** parameters and log-normal distribution for **wind speed** parameter.

Since the distributions of **number of sky reviews** at a given range of values of a meteorological parameter is close to normal and log-normal distributions, while the distribution of  $F_{\text{birds}}$  index (the average number of birds which were recorded during a single sky review and the relative numerical measure of the intensity of soaring flights of vultures over the area) - is close to uniform distribution, the limits of meteorological characteristics, shown as a niche for Black vultures, do not reflect the preferences of the species. They only show the climate properties itself in a given geographical area. In other words, the Black vulture inhabit within the revealed range of climatic conditions (Figs. 2.20-2.25) because they are adapted to them, not because the species intentionally choose this niche.

Consequently, the graphical analysis shows the ecological niche of the meteorological conditions occupied by Black vulture in the study region, but it does not identify the significant impact of meteorological parameters on the soaring activity of this species.

b. The statistical tests confirm the independence of soaring activity of vultures (expressed in  $F_{\text{birds}}$  index) from **air temperature** and **relative humidity** parameters. However, they detect the dependence of soaring activity ( $F_{\text{birds}}$ ) on **wind speed** and solar activity (**solar radiation** and **solar energy**) parameters. The difference in conclusions of two approaches can be caused by their different possibilities in data analysis. The graphical method represents the general relationship between meteorological conditions and soaring activity of Black vultures. The statistical tests reveal the weak relationships, which are important for understanding the pattern of flying behaviour of birds.

The **wind speed** parameter reflects partly or completely the strength of thermals works in most months of the year. This statement was based on the high correlation between **wind speed** and **solar activity** parameters, revealed by Pearson correlation test for most of the months of the year (and all cold months) in both study sites (Table 2.8). Based on this statement, the dependence of  $F_{\text{birds}}$  on **wind speed** and **solar activity** parameters was interpreted as a **positive relationship between the intensity of soaring flights of Black vultures and thermal strength**. Also it was found, that the positive correlation between soaring activity of Black vultures and thermals strength is more pronounced in the cold period of the year. This finding can be

interpreted as the tendency of Black vulture movement toward thermals with the highest strength in surroundings. We consider this result as the **first confirmation of the hypothesis, stating that Black vultures tend to choose for soaring flight the strongest thermals in surroundings**<sup>13</sup>.

### 5.2.2 Seasonal changes in soaring activity of Black vulture

Our results show that seasonality impacts notably on the soaring activity of Black vultures. This is proved by smooth peaks and valleys of the intensity of soaring flights extended for several months. Also we showed that the studied populations had the mutually inverse trend in the soaring activity of birds, which was stronger in the cold period of the year, from April to August (Figs. 2.18, 2.19). The large distance between Amarais and Prudente areas (about 450 km, Fig. 2.1) prevents the explanation of this finding by interchanging of vultures between them. Rather, this difference can be attributed to their differences in anthropogenic pressure. In the vicinities of Amarais airport, the highly urbanized lands expanded on large areas without natural landscapes. It contrasts notably with the vicinities of Presidente Prudente airport, which consists mainly from natural and rural lands with relatively small spots of urbanized territories. From this we can suppose, that **in cold months as the most difficult period of the year, Black vultures tend to migrate from highly urbanized lands (as the less comfortable habitats<sup>14</sup>) to more natural territories (as the more comfortable habitats).**

This is consistent with other of our finding, stating that the direct relationship between  $F_{birds}$  index and wind speed (parameter associating with thermals work and force) was stronger and more clear in cold months in both sites, than in rest of the year (Tables 2.4, 2.5, 2.6, 2.7). It means that the direct relationship between soaring activity of Black vultures and thermals strength is more pronounced in the cold period of the year. This also can be explained by the fact, that in colder months vultures tend to spend less energy on flights. Since thermals save energy for birds during takeoff and flying, in cold months vultures may have the larger tendency to soar over the strongest thermals for saving more energy, than in warm period of the year.

---

<sup>13</sup> The second confirmation of this hypothesis basing on the analysis of the surface temperature, we obtained in the second part of our investigation, which is considered in Chapter III.

<sup>14</sup> We came to the conclusion, that highly urbanized areas are less comfortable for Black vulture than natural and rural lands in both parts of the study. The first reason for the conclusion we considered here (section 5.2.2). The second reason we obtained studying the dependence of the soaring activity of vultures from superficial conditions, including the anthropogenic stress. It considered in Chapter III.

The both behavioural patterns can be interpreted as a form of ecological adaptation of Black vulture as avian scavenger species to minimize energy loss in flights (Schoener, 1971; Ruxton and Houston, 2002).

## 6. Conclusions

1. The most common altitude of soaring flight of Black vultures ranges from 13 to 300 metres, the height from 300 to 550 metres is less used, and above 550 metres is improbable.
2. Two types of schedule of daily soaring activity were detected: (i) plot with morning and afternoon peaks and notable drop at local midday; and (ii) plateau-like plot with a single weak smooth peak at midday. At both types, about 1- 1.5 hours after local sunrise the soaring activity starts and about 1 - 1.5 hours before local sunset the soaring activity finishes. The sky should be completely safe from soaring vultures in dark and twilight hours between local sunset and sunrise at normal conditions (i. e. without presence of technogenic thermals).
3. The abundant food on the ground attracts Black vultures from large distances, which leads to temporal disappearance of soaring birds above a large area. It means that concentration of soaring vultures at sky evidences the lack of abundant food for these birds in availability.
4. Seasonality impacts notably on the soaring activity of Black vultures, but its influence depends on anthropogenic pressure of the territory. In cold months the number of soaring vultures decreases above continuous highly urbanized lands, but increases above natural and rural lands with inclusion of small urbanized islands. Most likely it means that in cold months as the most difficult period of the year, Black vultures tend to migrate from highly urbanized lands (as the less comfortable habitats) to more natural territories (as the more comfortable habitats) to save their energy.
5. The intensity of soaring flights of vultures has a significant dependence only from solar activity and wind speed parameters, both of which were interpreted as the indicator of thermal strength. This finding was considered as the first confirmation of the hypothesis, stating that Black vultures have a tendency to choose the strongest thermals in their surrounding for soaring flight.

## CHAPTER III

### **Study of the influence of superficial natural and anthropogenic conditions on abundance of soaring Black vulture (*Coragyps atratus*, *Cathartidae*) using GIS and remote sensing technologies**

*Paper intended for "Biological Conservation" journal*

#### **Abstract**

The increasing risk of collision with Black vultures for aircrafts, coupled with the impossibility to reduce this threat by traditional methods, requires the development of special measures that would reduce this hazard without harming the birds. To achieve these objectives, it is important to identify the environmental factors impacting on the spatial distribution of soaring vultures and pay a special attention to study the relationships between vultures and thermals.

Our research was devoted to the study of the influence of superficial and anthropogenic conditions on the soaring activity of Black vultures and to the numerically estimation and mapping the risk of collision with vultures over the airports surroundings. The study was implemented around two airports of southeastern Brazil, taken as model areas.

We developed the new methodological approaches combining application of GIS and remote sensing technologies for spatial data processing. By dint of them we joined in the georeferenced databases (shapefiles) the data of bird's census and superficial parameters (relief, surface temperature, surface covering type and anthropogenic pressure) revealed from the satellite images. Basing on the prepared georeferenced databases, the relationship between soaring activity of vultures and environmental factors was analyzed; the maps representing the numerical assessment of risk of collision with Black vultures over the territory were constructed for vicinities of model airports.

We found that the contrast of surface temperature affects significantly on the intensity of soaring flights of Black vultures. This observation supports the hypothesis stating that vultures tend to choose for soaring flight the strongest thermals in surroundings. The natural water bodies and automobile roads were detected as the most attractive landscape types for soaring birds. Anthropogenic pressure also demonstrates the notable influence on the soaring activity of vultures. The number of soaring birds shows the inverse ratio with the area of uninterrupted highly urbanized lands. The relief parameters (altitude above sea level, slope exposure and slope inclination) do not show notable influence on the soaring activity of birds.

Basing on the results of both parts of our investigation we formulated the practical recommendations which can help to reduce the number of collision with Black vultures and other bird species. We recommend (i) to consider our findings of vultures soaring behavioural pattern in tracking the aircraft routes; (ii) to build maps predicting the risk of collision with vultures or other avian species for airports surroundings and to use them for choosing the more safety routes for landing and takeoff operations; (iii) to study carefully two perspective directions for soaring vultures management: (a) the dependence of soaring activity of vultures from thermal strength and (b) the ability of vultures to clean the sky in case of presence of abundant food source on the ground.

## Key-words

*Aviation hazard, bird hazard control, bird strike problem, risk assessment, risk assessment map, Black vulture, Coragyps atratus, soaring behaviour, thermals, GIS, remote sensing, satellite imagery, ASTER.*

## 1. Introduction

The threat of aircraft collisions with birds increases together with rising air traffic around the globe. Strikes with Black vultures (*Coragyps atratus*, Cathartidae), because of their large size and specific flight behavior, pose a substantial hazard to aviation safety in both Americas (Bastos, 2001; DeVault et al., 2005, 2011; Zakrajsek and Bissonette, 2005; Blackwell and Wright, 2006; Avery et al., 2011; USAF, 2014). Neither avian deterrents nor removal of food garbage from airport surroundings can provide the reliable protection for landing and takeoff aircrafts (Bastos, 2001; Avery and Cummings, 2004; Blackwell and Wright, 2006; Novaes and Cintra, 2013;). For these reasons, the development of new approaches which can effectively reduce this hazard is strongly required. Despite of the urgency, these measures should be thoughtful and do not harm to vulture populations which implement the essential function in natural ecosystem and traditional agriculture (Cortés-Avizanda et al., 2010). We must remember that 14 of 23 (or ~60%) vulture species living all over the world are threatened with extinction due to considerable human-caused changes in conditions of their habitats (Deygout et al., 2009; Cortés-Avizanda et al., 2010; Ogada et al., 2012; Buechley and Şekercioğlu, 2016). In this regard, study the environmental factors impacting on the spatial distribution of soaring vultures and assessment of the dependence of soaring activity of these birds on thermal strength can provide the promising approaches to progress in the issue.

A few factors control the soaring foraging activity of Black vultures. Like the majority of avian scavengers, these birds use thermals (the upward flows of warm air) for takeoff and

foraging flying to minimize the energy losses (Newman, 1957; Parrott, 1970; Coleman and Fraser, 1989; Thompson et al., 1990; Mandel and Bildstein, 2007; Akos, 2010; Freire et al., 2015; our observations). Thermals are formed above hotspots, or zones with high contrast in surface temperatures (Angevine, 2014). Hence, the patterns of vultures' distribution can be linked to the uneven heating of surface objects. The abundance of food is often considered as the main attracting factor for Black vultures (e.g. Novaes and Cintra, 2013). Besides, this species needs in perching sites (Blackwell and Wright, 2006). The suitable quiet locations are more available in natural and agricultural landscapes. However, vultures can even roost in areas of intense human activity, such as street markets (Novaes and Cintra, 2013). Black vulture can adapt to life even in big cities and forages above areas strongly impacted by human activities (Avery, 2004; Blackwell et al., 2007; Carrete et al., 2010; Novaes and Cintra, 2013; Novaes and Alvarez, 2014; Freire et al., 2015).

Our study was devoted to moving forward in elaboration of soft methods of reduction the risk of collision with Black vulture. In the first part of our investigation we focused on the links between meteorological factors and soaring behavioral traits of Black vultures, studied of the seasonal and daily soaring activity patterns and altitudes of soaring flights. Here we continue our investigation and explore the dependence of soaring activity of Black vultures on superficial natural and anthropogenic parameters. Also we carry on the study of influence of thermals on abundance of soaring birds, which was started in the first part of the research.

We explored the dependence of soaring activity of vultures from relief, surface temperature, surface covering and atmospheric pressure characteristics, which were revealed from the remote sensing products. The study was implemented in the surroundings of two Brazilian airports. The methodological approaches of combined application of GIS and remote sensing technologies for data processing were developed and used as the main research instrument. They allowed to build the maps giving a numerical estimation of hazard of bird-strike event over the airport vicinities, as well as to explore the various parameters of the environment in their relationship with distribution of soaring birds. We clarified the issue of behavioural specific of vultures in relation of thermal and obtained the second confirmation of the hypothesis that Black vultures tend to soar over the strongest thermals in their surroundings.

## 2. Materials and methods

### 2.1 Data gathering and applied material

The study was based on two types of data – the field observation of soaring vultures and data of superficial characteristics obtained from the remote sensing products<sup>15</sup>. The field observations were implemented from September 2012 to August 2013 in the adjacent areas of Amarais and Presidente Prudente airports of southeast of Brazil, and included two elements: recordings of all Black vultures flying around 13 viewpoints in a radius of visibility through the binoculars and measurement of the meteorological characteristics.<sup>16</sup> The unit of vulture censuses was “*ornithological object*” - one individual or a few birds located at sky close to each other in the moment of registration. For each ornithological object the following parameters were recorded as interval of values: **direction** (was measured by a compass and fixed by 8 intervals (22.5-67.5°, 67.5-112.5°, 112.5-157.5°, 157.5-202.5°, 202.5-247.5°, 247.5-292.5°, 292.5-337.5°, 337.5- 22.5°); **vertical angle** (was measured by inclinometer manual and fixed by 18 intervals: 2.5-7.5°, 7.5-12.5, 12.5-17.5... 82.5-87.5, 87.5-90°); **distance** (was determined by a size of a bird in a binoculars with a help of graticule lines marked on the eyepiece and fixed by 4 intervals: 100-200 m, 200-400 m, 400-700 m, 700-6000 m); **number of birds**; **time of observation** (date and time of registration with accuracy of 15 minutes); geographical coordinates and identification number of observation point.

The study areas and methods of field data gathering are considered in details in Chapter II. Here we focus on the data acquirement from the remote sensing products and their preparing for the statistical analyses and constructing of risk assessment map. The elaborated methods combining GIS and remote sensing technologies were applied for this procedure.

#### 2.1.1 Satellite imagery applied for investigation

We studied the relationships between abundance of soaring Black vultures over the territory and the following superficial characteristics: **surface temperature**, **contrast (or gradient) of surface temperatures**, **relief (altitude above sea level, slope exposure, slope inclination)**; **landscape type** (surface covering type linked with its level of anthropogenic pressure). Those parameters were obtained from the following remote sensing products:

**ASTER On-Demand L2 Surface Kinetic Temperature (AST\_08)**. It is the raster derivative product of ASTER satellite image, representing the surface temperature characteristic

<sup>15</sup> Remote sensing product is a raster image produced from satellite imagery by dint of special algorithm of data processing and representing a single surface characteristic.

<sup>16</sup> The meteorological data were applied only in the first part of our investigation and were considered in the Chapter II.

in Kelvin degrees at 90 metres per pixel spatial resolution. It is produced from five thermal infrared (TIR) bands of ASTER satellite image located between 8 and 12  $\mu\text{m}$  of the electromagnetic spectrum (“On Demand Surface Kinetic Temperature AST\_08” web page). The original ASTER image was made during the midday time in 2013 and well suited for analyze of temperature distribution in the studied areas (Table 3.1)

**ASTER Global Digital Elevation Model (ASTER GDEM v2 or ASTGTM).** It is the raster digital elevation model of the Earth surface designed for the entire World from the collection of ASTER satellite images of 2000 to 2011 years. It represents the altitude above sea level at 30 metres per pixel spatial resolution. It has the vertical error equal to 12.6 metres (standard deviation), horizontal errors - 0.11 arc-seconds to west and 0.20 arc-seconds to north, and horizontal resolution – 2.4 arc-seconds<sup>17</sup> (“Routine ASTER Global Digital Elevation Model ASTGTM” web page; Tachikawa et al., 2011).

The both derivative products were produced from images of ASTER (Advanced Spaceborne Thermal Emission and Reflection Radiometer) sensor of the Terra NASA satellite. ASTER obtains high-resolution (15 to 90 square metres per pixel) images of the Earth in 14 different wavelengths of the electromagnetic spectrum, ranging from visible to thermal infrared light. The ASTER data are used to create of the detailed maps of land surface temperature, emissivity, reflectance, and elevation (“Terra. The EOS Flagship” web page; “ASTER” web page; “ASTER Products Table” web page).

**DigitalGlobe imagery of high resolution.** It is the true-colour band composition raster image, provided for free by Basemap gallery in ArcGIS for online application.

The [surface temperature](#) and the [contrast of surface temperature](#) parameters were revealed from AST\_08 raster image. The relief parameters ([altitude above sea level](#), [slope exposure](#) and [slope inclination](#)) were detected from ASTER GDEM v2 raster image. The DigitalGlobe images were used for manual digitizing of landscape objects and obtainment of the [landscape type](#) parameter.

The main characteristics of the remote sensing products applied in our study are presented in the Table 3.2. The ID numbers of the used scenes are presented in the Table 3.1.

---

<sup>17</sup> 1 arc-second corresponds to 30 metres



**Table 3.1 Identified numbers (ID) of the remote sensing products used in the investigation**

Derivative products of the satellite imagery used for data processing	ID of the scenes (used for Amarais site)	ID of the scenes (used for Presidente Prudente site)
<b>ASTER GDEMv2</b>	SC:ASTGTM.002:2088830049 SC:ASTGTM.002:2088830127	SC:ASTGTM.002:2088813568
<b>AST_08</b>	AST_L1A#00305112013132753_05132013034738.hdf 11.05.2013, 13:27:53 UTC cloudiness = 0.0%  AST_L1A#00305112013132802_05132013034746.hdf 11.05.2013, 13:28:02 UTC cloudiness = 0.0%	AST_L1A#00308202013134626_08212013131509.hdf 20.08.2013, 13:46, cloudiness = 1%
<b>DigitalGlobe imagery</b>	Online application in ArcGIS	Online application in ArcGIS

**Table 3.2 Main characteristics of the remote sensing products used in the study.**

Derivative products of the satellite imagery used for data processing	Description	Access	Year of data production	Spatial resolution (metres in 1 pixel)	Data obtained * - initial data, others-calculated from the initial data
<b>ASTER GDEMv2</b>  Digital Elevation Model of the Earth Surface	Derivative product of ASTER images produced since 2000 to 2011	Scenes selection and order for download - Reverb. ECHO or GIOVIS services	Produced from the collection of ASTER images since 2000 to 2011	30	Altitude above sea level (metres)*  Slope direction (compass degrees)  Slope inclination (angle degrees)
<b>AST_08</b> Surface Temperature	Derivative product of a single ASTER image	ASTER scenes selection - Reverb. ECHO or GIOVIS services  Order for download - LP DAAC service need to mark "AST08" in the order registration	2013	90	Surface temperature (Kelvin degrees)  Gradient of surface temperature, i.e. the maximum surface temperature contrast between pixels adjacent (angle degrees)
<b>DigitalGlobe imagery of high resolution</b>  The true-color band composition	Product of DigitalGlobe high resolution imagery, provided by ArcGIS software	Through the "Add Basemap" option of ArcGIS only in Online form	2010-2013	about 1 m	The true-colour image of very high resolution (it was used for manual digitizing of the landscape objects)

### 2.1.2 Thermals properties

The physical properties of thermals were laid in the basis of study the influence of thermals on soaring activity of Black vultures. Since information of thermal's traits is not generally known, we gave a brief description of these properties.

Thermal is a column of rising warm air in the lower layers of the atmosphere. Thermal is never set alone. It always belongs to a field of upwelling airflows (Fig. 3.1). Thermal forms over “*hotspot*” – a relatively small piece of surface, which has the higher superficial temperature than adjoining lands. The hotspots form due to non-uniform heating of the Earth's surface by solar radiation, which is caused by different reflectivity (the albedo coefficient)<sup>18</sup> of distinct ground objects (Angevine, 1998; Angevine, 2014). Air above the hotspot is more intensively heated in comparison with adjacent lands, which makes its density smaller than density of adjoining air mass. The surrounding colder and denser air force out the warmer and lighter air over the hotspot and it ascend. The rising warm air cools and becomes more denser. At the same time the colder air mass with higher density descends and replaces the lighter air. The circulation convective cell forms (Fig. 3.1) (Angevine, 2014).

Thermals are driven by temperature contrast between ground and air. Air stops its rising as soon as it has cooled to the same temperature as the surrounding air. For this reason natural thermals **work only in daily hours when sun is shining**. They start their work a bit after sunrise and finish their work a bit before sunset. During the cloudy weather thermals are weaker or do not work at all. The high surface temperature is not necessary for thermal formation. The contrast of superficial temperatures between hotspot and its surrounds is the only factor that determines the possibility of thermal creation and its force. The following statement, arisen from the thermals properties, was used for study the dependence of soaring activity of vultures on thermals strength: **The higher is the contrast between surface temperature of a hotspot and surface temperature of its adjacent lands, the larger is the possibility of thermal formation over this hotspot and the stronger could be this thermal** (Angevine, 2014).

The thermals generation often occurs above “*triggers*” - the surface object which heated faster than adjacent territories and become hotspots for surrounding lands. The triggers may be contrasting fields, buildings, asphalt road, ploughland, hills, borders of mountains with high temperature contrast caused by different slope direction.

---

<sup>18</sup> Albedo – is a reflection coefficient or “reflectivity” of surface, measured from “0” (no reflection) that is typical for a perfectly black surface to “1” – is a complete reflection of a perfectly white surface. The smaller is the value of albedo of surface covering, the less it reflects the solar radiation incoming to it, and the more it heats up itself and air above it due to absorption of the solar radiation.

If a territory has rather uniform surface and equal albedo coefficient of all surface objects it does not have triggers, but also will have thermals. However, in this case, they would not have permanent location. The position of those thermals can change and they can move with the wind. The strength of such natural thermals might be weaker than the strength of thermals generated above triggers. **Only if an area has triggers, its thermals form over the permanent places** (Angevine, 2014).

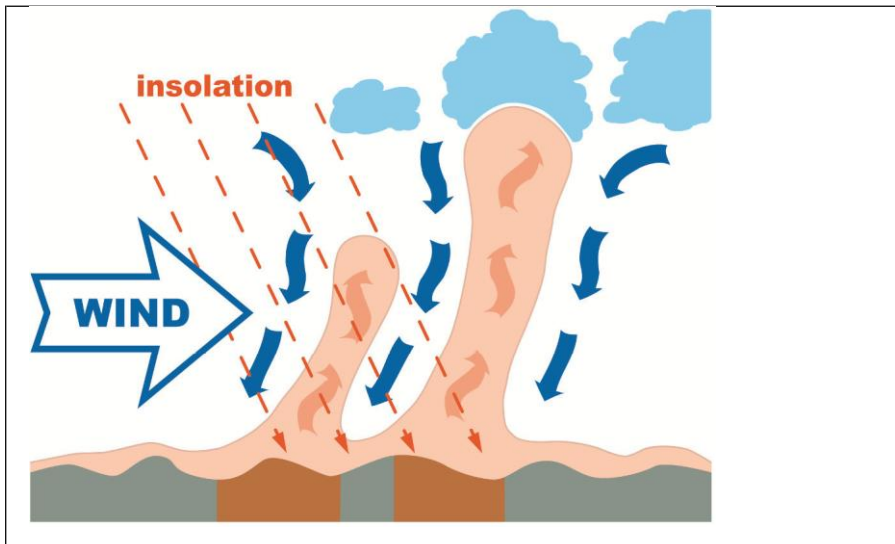


**Figure 3.1 The principle of thermals work (by Prem and Mackley, 2005)**

## **2.2 Data preparation for analyses**

The initial data gathered in the field and derived from the remote sensing products were prepared for analyses and mapping by several steps considered below. The data preparation was implemented in ArcGIS 10.0 (ArcMap) and Excel software, the most of calculation procedures were conducted directly in corresponded shape and raster files. Several complicated technical algorithms of data preparation are considered in details in Appendix C (Algorithms C3-C5)

### **2.2.1 Processing of the remote sensing products for detection of the surface parameters**

#### **2.2.1.1 Detection of the surface temperature and relief parameters**

The surface temperature and relief characteristics were detected by means of special processing in ArcGIS software of the original remote sensing products. As a result of processing, the georeferenced raster maps, each of which represents a single surface characteristic, were obtained. The final summary tables for implementation of statistical analyses were prepared from these raster maps by means of subsequent processing conducted in ArcGIS. The methodology of data processing is considered below (Fig. 3.2, Script 3.1, Script 3.2, div. 2.2.5). The surface characteristics obtained from the remote sensing products and used for analyses were the following:

- **Surface temperature** (Celsius degrees) was detected directly from the raster AST\_08 as the original parameter of this product. The original Kelvin degrees ( $T_k$ ) of AST\_08 were recalculated in Celsius degrees ( $T_c$ ) by the formula:  $T_c = T_k - 273.15$  using the Raster Calculator tool of ArcGIS software. The resultant surface temperature maps of both study sites are presented in Supplementary Files SF22, SF24 and visualized on Figs A.3, A.7 of Appendix A.
- **Gradient of surface temperature** (angle degrees). It is the rate of maximum change in temperature value from each cell to its eight adjacent pixels, i.e. it is also the **highest temperature contrast** between each cell and its eight adjacent pixels. Below we call this parameter “*contrast of surface temperature*”. It was detected from raster AST\_08 by dint of *Slope tool* of ArcGIS software where for each pixel of the original raster the calculation was conducted according to the algorithm “Script 1” and general scheme of calculation, presenting on Fig. 3.2. The resultant contrast of surface temperature maps for both study sites are presented in Supplementary Files SF21, SF25 and visualized on Figs A.4, A.5, A.8 of Appendix A.
- **Altitude above sea level** (metres) was detected directly from the raster ASTER GDEM v2 as the original parameter of this product. The resultant altitude above sea level maps for both study sites are presented in Supplementary Files SF23, SF26 and visualized on Figs. A.2, A.6 of Appendix A.
- **Slope exposure** (compass degrees, 0-360°), is measured clockwise from north of the maximum rate of change in z-value from each cell in a raster surface. It was derived from the raster ASTER GDEM v2 by dint of *Aspect tool* of ArcGIS, where for each pixel of initial raster the calculation was conducted according to the Script 2 and the general scheme of calculation (Fig. 3.2).
- **Slope inclination** (angle degrees) is a slope angle. It was obtained from the raster ASTER GDEM v2 by *Slope tool* of ArcGIS where for each pixel of initial raster the calculation was conducted according to the algorithm of Script 1 and the general scheme of calculation (Fig. 3.2).

a	b	c
d	e	f
g	h	i

**Figure 3.2 The general scheme of calculation of “contrast of surface temperature”, “slope inclination” and “slope exposure” superficial parameters from original rasters (AST\_08, ASTER GDEM v2).**

The value of each surface parameter was calculated for central pixel (“e” on the scheme) from eight adjacent pixels by the formulas, considered in the Scripts 1-2. The calculation was implemented for each pixel of the initial raster, except of the pixels of raster’s boundaries (they did not receive the correct value of surface parameter and were not applied in the study).

$$\text{slope\_degrees} = \text{ATAN} \left( \sqrt{[\text{dz}/\text{dx}]^2 + [\text{dz}/\text{dy}]^2} \right) * 57.29578$$

where:

The rate of change in the x direction for cell with value “e”:

$$[\text{dz}/\text{dx}] = ((c + 2f + i) - (a + 2d + g)) / (8 * x\_cellsize)$$

The rate of change in the y direction for cell with value “e”:

$$[\text{dz}/\text{dy}] = ((g + 2h + i) - (a + 2b + c)) / (8 * y\_cellsize)$$

a,b,c,d,f,g,h,i – are temperature values of eight cell adjacent to cell “e”

**Script 3.1 Algorithm of calculation of the slope inclination parameter for each pixel of the original raster performed by Slope Tool of ArcGIS software (“Slope (Spatial Analyst)” web page; “How Slope works” web page)**

The Slope tool was used to calculate two parameters: slope inclination itself (from raster ASTER GDEM v2) and contrast of surface temperature (from raster AST\_08).

The rate of change in the x direction for cell e is calculated with the following algorithm:

$$[\text{dz}/\text{dx}] = ((c + 2f + i) - (a + 2d + g)) / 8$$

The rate of change in the y direction for cell e is calculated with the following algorithm:

$$[\text{dz}/\text{dy}] = ((g + 2h + i) - (a + 2b + c)) / 8$$

Taking the rate of change in both the x and y direction for cell e, aspect is calculated using:

$$\text{aspect} = 57.29578 * \text{atan2}([\text{dz}/\text{dy}], -[\text{dz}/\text{dx}])$$

The aspect value is then converted to compass direction values (0-360 degrees), according to the following rule:

if aspect < 0

$$\text{cell} = 90.0 - \text{aspect}$$

else if aspect > 90.0

$$\text{cell} = 360.0 - \text{aspect} + 90.0$$

else

$$\text{cell} = 90.0 - \text{aspect}$$

**Script 3.2 Algorithm of calculation of the slope exposure parameter for each pixel of the original raster (ASTER GDEM v2) performed by Aspect Tool of ArcGIS software (“Aspect (Spatial Analyst)” web page; “How Aspect works” web page)**

### 2.2.1.2 Detection of the landscape parameters

We evaluated the impact of landscape type on the soaring activity of Black vulture, understanding this term as a type of *surface covering* coupled with its *level of anthropogenic pressure*. Those parameters were detected by manually digitizing of high-resolution DigitalGlobe imagery within the circular zones of a radius of 700 metres around 26 viewpoints of both studied sites. The digitizing was conducted in ArcGIS software according to the elaborated simple classification, containing seven types of surface covering linked with four levels of anthropogenic pressure (Table 3.3). The rank of the anthropogenic stress according to this classification varying from “1” the smallest to “4” the greatest.

**Table 3.3 Classification of landscape types used in the landscape analysis**

Type of surface covering	Level of anthropogenic stress	Description
natural area	1	agricultural fields, grassy wasteland, forest fragments, vegetation areas along the river banks
natural water object	1	water objects with clean water (rivers, lakes)
soft urbanized zone	2	moderately urbanized zone (natural lands with the inclusion of scattered buildings)
technical water object	2	water objects with polluted water <sup>19</sup>
roadway	2	automobile roads
heavy urbanized zone (dense residential area)	3	densely populated residential areas
heavy urbanized zone (industrial area)	4	industry, waste treatment facilities, power station

The resultant polygonal shapefiles (Fig.3.14(e), Fig. 3.15(e); Supplementary Files SF19) became the basis for the landscape analyses, studying the influence of surface covering and anthropogenic pressure on soaring activity of Black vultures<sup>20</sup>.

### 2.2.2 Georeferencing of the recorded birds as point shapefile

At first, for each study site the raw datasets of the bird’s census and meteorological characteristics were joined with each other in a single table, entitled as the “**Birds and meteorological parameters**” merged dataset (Supplementary Files SF27) by means of identical “time of observation” parameter. The geographical coordinates (latitude and longitude) of each recorded bird were calculated within the merged dataset from the geographical coordinates of observation point and average values of the recorded parameters, i.e. intervals of distance, vertical angle and compass direction.

<sup>19</sup> The polluted water was identified only logically through the location of the water object within the industrial zones

<sup>20</sup> The data preparation for the landscape analysis is considered below in div. 2.2.7.

Then, basing on the merged dataset, the *summary georeferenced databases* (point shapefile) entitled as the “**Georeferenced birds and meteorological parameters**” database was constructed (Supplementary Files SF2). In those shapefiles, each registered ornithological object is represented by two elements. The first one is the vector point on GIS map, which marks the projection on the earth's surface of its averaged (approximate) position in space. The second one is the records in the attribute table, containing its registered parameters (quantity of birds, distance, vertical angle, direction, number and geographical coordinates of a viewpoint, time of observation), its calculated parameters (height of flight, latitude and longitude) and all meteorological characteristics, measured synchronously with its registration.

The technical details of birds' georeference as vector points and “Georeferenced birds and meteorological parameters” database preparing are considered in the Chapter II (div. 2.3.2) and Appendix C (Algorithm C1).

### 2.2.3 Georeferencing of the recorded birds as polygonal shapefile

At the next step, the ornithological objects georeferenced as points (in point shapefile) were transformed into the ornithological objects georeferenced as polygons (in polygonal shapefile). Those polygons we entitled as the “*projected polygons*”. Each projected polygon was constructed by the entire values of the registered parameters of a flying bird (i.e. intervals of the distance, vertical angle and direction) and represents the projection on surface of three-dimension figure within which a recorded bird was located in the moment of registration. Thus, a projected polygon of each ornithological object can be interpreted as a *region above which all birds attributed to it were located at the moment of registration*. This transformation allows to determine the uncertainty of spatial position of flying birds caused by the interval character of the recorded parameters<sup>21</sup>. Also it permits to include this uncertainty into analyses, which improved the accuracy of their results.

The forms of projected polygons are defined by the geometry of a circle with observer in its center, which is caused by the specific of bird's census conduction from the viewpoints within radius of visibility. It looks like *annular sector* (when vertical angle to a bird was 5-85°), and *circle* (when the vertical angle to a bird was equal to 90°, i.e. bird was located exactly above the viewpoint)<sup>22</sup> (Figs. 3.3 - 3.6). The total number of projected polygons is determined by sum of all possible combinations of intervals of the recorded parameters (18 – by vertical angle; 8 - by

<sup>21</sup> The distance, vertical angle and direction parameters measured as interval of values allow to determine only a region (not a point) above which a bird was located at the moment of registration. A projected polygon represents this region for each recorded bird in GIS environment.

<sup>22</sup> When a vertical angle to a bird was 90° it was no value of “direction to a bird” parameter, because a bird was located exactly above the observer. In this case the projected polygon is a circle above the viewpoint with a radius equal to the height of a flying bird above the ground.



direction and 4 - by distance), and taking into account that the vertical angle equal to  $90^\circ$  produces a circular projected polygon. Thus, the total number of projected polygons is the following: for each viewpoint:  $(18 \times 8 \times 4) - (4 \times 7) = 548$ ; for each airport:  $13 \times 548 = 7124$ ; in total  $= 7124 \times 2 = 14248$ .

The procedure of georeferencing of the ornithological objects to projected polygons was implemented in two stages. At first, the projected polygons were constructed. At second, for each projected polygon all ornithological objects, registered above it during the year of observation, were attributed. Both stages were implemented separately for Amarais and Prudente sites in ArcGIS software through the technical algorithm considered in Appendix C (Algorithm C3).

As a result of Algorithm C3 application, the polygonal shapefiles of projected polygons, constructed for all distance intervals were created (Supplementary Files SF9). In those shapefiles each projected polygon contains the number of birds, which were recorded over it during the observation. Those shapefiles and their attribute tables became the basis for analysis studying the relationship between soaring activity of Black vultures and superficial parameters. Also basing on those shapefiles, the maps, predicting the risk of collision with vultures were constructed.

The projected polygons superpose each other (Fig. 3.5), which is caused by the geometry of their construction and four distance intervals from a viewpoint to birds. The number of superposed polygons varies from three above the viewpoint to several dozen at the periphery of the studied zone.

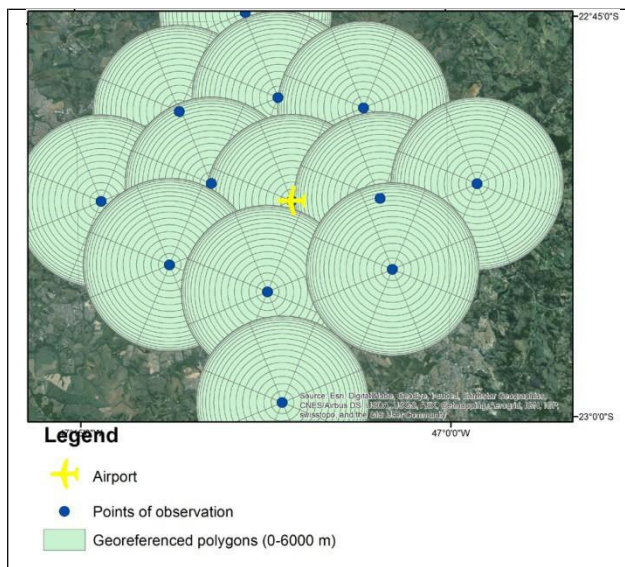


**Figure 3.3 Projected polygons for all distance ranges: 0-6000 m (Amarais site)**

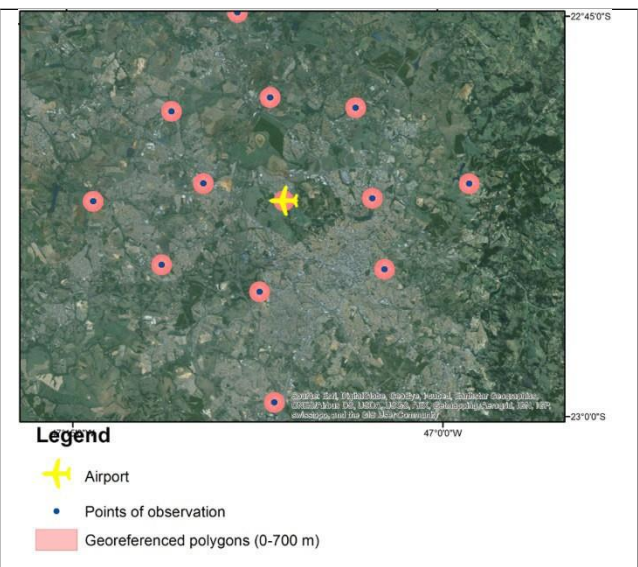


**Figure 3.4 Projected polygons for three first distance ranges: 0-700 m (Amarais site)**





the value of  $W_{\text{birds}}$  index at each point to position of viewpoint, representing the actual number of birds that can be located over this point during the observation hours<sup>24</sup>.

The biological interpretation of  $W_{\text{birds}}$  index for a given *spatial unit*<sub>(i)</sub> is a total number of flying birds that were registered (i.e. can be located) exactly above this spatial unit during a chosen period of time (a month, a set of months, a year, etc). In other words,  $W_{\text{birds}}$  index depicts the relative numerical indicator of the abundance of flying birds above a chosen spatial unit in a chosen period of time. This statement allow to consider  $W_{\text{birds}}$  index as a relative numerical measure of risk of aircraft collision with Black vultures over the study area and use it for predicting the probable hazard for aviation.

The uncertainty of  $W_{\text{birds}}$  index definition (we tell that the number of birds "can be located" above the spatial unit instead of "was for sure") caused by the interval character of registered parameters. As a bird was georeferenced to a polygon (not to a point) any interpretation of those data in terms of points has probabilistic character. It is important to note that the sum of all  $W_{\text{birds}}$  of all cells of the study areas is much higher than the real number of all recorded birds. It also happens because of the interval character of the collected data: for each bird the indicator of its presence (its "weight") above the surface was "stretched" from a point to a polygon and then averaged between polygons. For this reason,  $W_{\text{birds}}$  is not the number of vultures above this cell, but only the relative measure of the probable abundance of flying birds.

### 2.2.5 Preparation of the georeferenced database as the basis for analyses and mapping

To study the relationships between soaring activity of Black vultures and superficial conditions, the statistical tests (Principal component analysis (PCA), Multiple regression analysis (MRA) and Spearman rank correlation analysis as well as the Landscape analysis) were implemented.

The  $W_{\text{birds}}$  index was applied as the relative numerical measure of the abundance of soaring Black vultures over the area in statistical analyses. Also we visualized the  $W_{\text{birds}}$  index on a map as a quantitative measure of the probable hazard of aircraft collision with birds over the territory. In contrast, we used the "**Sum of birds recorded in each landscape type**" parameter as the numerical indicator of the abundance of soaring birds in the landscape analysis.

---

<sup>24</sup> The viewpoint, as a centre of spatial half-sphere reviewed by the observer, are assumed as the "standard" point, because it has the real number (3) of overlapped projected polygons over it, which caused by three distance range used for birds registration (100-200, 200-400 and 400-700 m). We can imagine it as a column of space over the viewpoint divided by three intervals with length identical of the same three ranges. When a flying bird was located directly above the observer (i.e. over the viewpoint itself), the distance to it was equal to a height of this bird over the ground. The fourth distance range (700-6000 m) can't be the altitude of flight, because according to our results considered in the Chapter II, the maximum altitude of vulture's flight was 550 m. Therefore we can assert that a "standard point" has only three projected polygon overlap over it.

This difference in the approach is caused by different objectives of the analyses. The purpose of the landscape analysis is to compare the attractiveness for vultures of various surface covering types. For this objective, it is more effectively to use a simple sum of birds, instead of  $W_{\text{birds}}$  index. Application of  $W_{\text{birds}}$  index allows to remove the incorrect increase of number of registered birds attributed to some areas because of the geometry of projected polygons. For this reason, we used  $W_{\text{birds}}$  index for mapping (i.e. the detailed visual analysis of the territory) and statistical tests, where landscape parameters were studied with other environmental characteristics. However, as any averaging,  $W_{\text{birds}}$  index increases the inaccuracy of the analysis studying the distribution of flying birds. Therefore, in landscape analysis, where there was no need for such smoothing, we used a simple sum of birds registered.

The research question of spatial analyses can be formulated as the following: *What relationship does exist between  $W_{\text{birds}}$  index (or “sum of birds recorded” parameter) and superficial parameters (surface temperature, relief, surface covering and anthropogenic pressure)?*

The study area of all spatial analyses were the three distance intervals, i.e. the circular zones of 700 m radius around 13 viewpoints in each airport’s surroundings. The fourth distance interval (700 - 6000 m) was excluded from spatial analyses due to the high inaccuracy in determination of number and geographical positions of flying birds<sup>25</sup>.

The data preparation for the spatial analyses were conducted in ArcGIS 10.0 (ArcMap) software separately for Amarais and Prudente site. The general principle of data preparation was the following. Using a common template the polygonal shapefiles, consisting of *spatial units* of analyses for which the studied territory was divided, were created in ArcGIS. The spatial units of analyses were represented by square cells of 30 x 30 m for MRA and PCA, square cells of 100 x 100 m for Spearman rank correlation analysis and digitized polygonal objects corresponding to landscape types for landscape analysis. Then, for each spatial unit the  $W_{\text{birds}}$  index or “sum of birds recorded” parameter was calculated and superficial parameters (surface temperature, contrast of surface temperatures, altitude above sea level, slope inclination, slope exposure, level of anthropogenic pressure) were attributed.

The resulting polygonal shapefiles entitled as the “ $W_{\text{birds}}$  and superficial parameters” georeferenced database (or, in short, the “ $W_{\text{birds}}$  database”) and their attribute tables became the basis for analyses implementation.

---

<sup>25</sup> See details in "Assumptions and limitations" section.

### 2.2.6 Data preparation for statistical analyses

The technical algorithms of **W<sub>birds</sub> database** preparation for statistical tests are considered in the Appendix C (Algorithm C4). In the result of implementation of the considered procedures, the **W<sub>birds</sub> database**, i.e. the polygonal shapefiles containing the spatial units with attributed values of superficial parameters (**surface temperature**, **contrast of surface temperatures**, **altitude above sea level**, **slope inclination**, **slope exposure**, **level of anthropogenic pressure**) and the **W<sub>birds</sub>** index, calculated by Eq.7, was constructed for each studied site. You can find those shapefiles in Supplementary Files SF15 (for PCA and MRA); SF16, SF17, SF18 (for Spearman rank correlation analysis). Their attribute tables became the basis for implementation of statistical tests. You can find those tables in Supplementary Files SF40 (for PCA and MRA); Supplementary Files SF42 and Tables 3.7- 3.10 (for Spearman rank correlation analysis).

### 2.2.7 Data preparation for landscape analysis

The technique of **W<sub>birds</sub> database** preparing for the landscape analysis is considered in the Appendix C (Algorithm C4). The polygonal shapefiles produced by considered operations (Supplementary Files SF20) became the basis for subsequent data preparation for landscape analysis. The attribute table of those shapefiles contains the total amount of vultures that were registered above each landscape type during the observation period.

In order to prepare data for landscape analysis, the parameters listed below were calculated for each landscape type in the attribute tables of the **W<sub>birds</sub> database** (Supplementary Files SF20) and Excel tables (Supplementary Files SF41).

- **S**, ha - the total area in hectares of lands occupied by each landscape type within study site.
- **S**, % - the percent of area of each landscape type, where 100% is the total area of study site (i.e. area of the circular zones of 700 m radius around 13 viewpoints in each airport's surroundings).
- **S<sub>(birds)</sub>** – the total amount of birds that were registered above each landscape type during the observation period.
- **S<sub>(birds)</sub>**, % - the percent of **S<sub>(birds)</sub>** of each landscape type, where 100% is a sum of **S<sub>(birds)</sub>** for the study site.

Using those parameters the relative density of soaring vultures (**q**, birds ha<sup>-1</sup>) above all landscape types were calculated:

$$q = \frac{S(birds)}{S} \quad (Eq. 8)$$

To compare the attractiveness of distinct landscapes, the percent deviation from the mean density ( $\hat{q}$ , %) was calculated:

$$\hat{q} = \frac{q - \bar{q}}{\bar{q}} \cdot 100\% \quad (\text{Eq. 9})$$

where  $\bar{q}$  depicts the mean density of soaring vultures (birds ha<sup>-1</sup>) registered in the study sites:

$$\bar{q} = \frac{\sum S(\text{birds})}{\sum S} \quad (\text{Eq. 10})$$

where  $\sum S(\text{birds})$  is a sum of all  $S(\text{birds})$  parameters of all landscape types;  $\sum S$  is a sum of areas of all landscape types (or the total area of the studied site). The mean density ( $\bar{q}$ ) found for the Amarais vicinity is of 14.9 birds ha<sup>-1</sup> and for Prudente – 28.5 birds ha<sup>-1</sup> (Tables 3.12, 3.13).

### 2.2.8 Cartographic visualization of the abundance of soaring Black vultures and risk of collision with these birds over the territory

The cartographic visualization of  $W_{\text{birds}}$  index produced the maps, representing the numerical estimation of abundance of the recorded Black vultures over the airport's vicinities during the period of observation. Those maps (entitled as the “risk assessment maps”) represent the intensity of soaring flights of vultures over the studied territory, which can be interpreted as the cartographic prediction of the risk of collision with these birds over this area at future.

In order to construct the risk assessment maps, the polygonal grid shapefiles, consisting from square cells with size 100 by 100 metres was created in ArcGIS software for each airport's surrounding (Supplementary Files SF11). For each cell the  $W_{\text{birds}}$  index was calculated by the Eq. 7. Basing on those grids the two types of risk assessment maps were constructed.

The first type is the risk assessment map built for the whole area around 13 km zone around each airport. Those maps were produced in a raster format by dint of Natural Neighbourhood interpolation method applied on the grid with attributed  $W_{\text{birds}}$  indices. Those maps are presented in Supplementary Files SF13 and visualized on the Fig. 3.12, Fig. 3.13. The second type is the risk assessment map of high accuracy constructed for the circular zones of 700 m radius around 26 viewpoints. This kind of map was built without any interpolation just by visualization values of  $W_{\text{bird}}$  indices. Those maps can be found in Supplementary Files SF14. Examples of those maps constructed for two viewpoints are presented on the Fig. 3.14<sub>(a)</sub>, Fig. 3.15<sub>(a)</sub>. The technical details of risk assessment maps construction in ArcGIS software is considered in Appendix C (Algorithm C5).

Since the accuracy of bird's number seen by the observer is reducing exponentially with increasing the distance to a bird, the accuracy of map of the range up to 700 m from the viewpoints is much higher than the accuracy beyond that zone. The elaborated methodology of

risk assessment maps construction can be applied for any avian species or various species and for any geographical region for predicting the probability of collision with birds over the area. However, it is important to take into account our recommendation about the possibility of creating maps of high accuracy for all studied territory, which are considered below in the “Practical recommendations” sections.

## **2.3 Assumptions and limitations**

The question of accuracy in our study consists from three components - the accuracy of bird's calculation, the accuracy of bird's georeference and the accuracy of risk assessment maps. The uncertainty of conducted analyses and estimates of hazard plotted on maps stems from human factor, the equipment used for birds' observation, the traits of the georeference procedure, and the cartographic visualization of the registered birds.

### **2.3.1 Accuracy of the bird's calculation**

The human factor doubtless impacted the quality of birds' records. The probability to miss a bird increases exponentially with rising distance from the observer. This is difficult to numerically estimate this effect. It is small or even absent on a small distance in case of well-qualified observer and good technique, but it increases sharply when distance to observed birds approaching to horizon of visibility. Since the bird's census in our study were conducted by two professional ornithologists, we assumed that this error was negligible at the first three distance intervals, i.e. between 100 and 700 m. The 4-th interval (700-6000 m) was eliminated from most of analyses as the interval stretching into the horizon, where the error of birds' calculation and the uncertainty of birds' georeferencing increase sharply. The data of the 4-th interval were applied only in study the relationship between flying activity of birds and meteorological conditions<sup>26</sup>. Here it was left for the reason, that for those analyses the exact georeference of each flying bird was not used, the linking was conducted only by a viewpoint<sup>27</sup>.

### **2.3.2 Accuracy of the birds' georeference**

The large size of both study areas and stated objectives to record all flying birds in a range of visibility around 26 viewpoints, caused the limitation of our technical opportunities. We can't use GPS or radio collars in our observations. The complexity of the observed objects (groups of birds flying at different altitudes) allowed to register parameters of birds' position (distance,

<sup>26</sup> The analyses of flights altitude of Black vultures and study the relationship between soaring activity and meteorological characteristics are considered in the Chapter II.

<sup>27</sup> A mathematical and statistical model probably can be applied for estimation this type of error more precisely. It may allow to detect the multiplier for recalculation the number of birds registered to a real number of birds located at sky in the moment of registration (by personal communication of Dr. A. Saveliev). However, the developing of a good model which will allow estimating this type of error is a very complicated task, which should be solved by the experts in mathematical statistics with the help of specialists of geotechnology and ornithology.

vertical angle and compass direction) only as intervals of values. For this reason, only a polygon of surface can be identified for each flying bird as the geographical position of its location in the moment of registration.

We elaborated and used in analyses the technique of flying bird georeference to a polygon above which it was located in the moment of registration. Each polygon represents the projection on surface of three-dimension figure within which the bird was located in the moment of registration. The subsequent data preparation for analyses and maps constructions was based on the georeferencing birds to projected polygons. These methods allowed not only determine the uncertainty of spatial position of flying birds, but include this uncertainty into analyses, which improved the accuracy of their results.

### **2.3.3 Accuracy of the cartographic visualization of abundance of soaring birds over the territory**

The accuracy of risk assessment maps is an important methodological issue. The building of risk assessment maps for the entire territory within radius of 13 km around airports required the data of bird's observation obtained in all distance intervals (from 100 to 6000 m). This happened because of the large distance between adjacent viewpoints (~6 km). However, as we mentioned above, the data of the 4-th interval has a large error of bird's calculation and large uncertainty of bird's georeference. This caused the low precision of the risk assessment maps constructed for the whole studied areas (Figs-dis. 3.12; 3.13). The risk assessment maps of the small circular zones of 700 m radius around the viewpoints (Figs-dis. 3.14(a), 3.15(a)) were built using the data only of first three distance ranges (100-700 m). For this reason the accuracy of those maps is much higher, that the accuracy of the large maps. We formulated our recommendations about the desirable changes in the methodology of field data gathering which will allow constructing the risk assessment map of high accuracy for the entire territory around airports in the "Practical recommendations" section.

To compare the risk of collisions between different areas, the calculated  $W_{\text{birds}}$  indices should comprise the records collected during approximately equal time intervals. In our case, the investigations were designed to satisfy this condition. Otherwise, the additional recalculations should be yielded.

The superficial characteristics derived from satellite imagery AST\_08 and ASTER GDEM v2 have a specific spatial resolution. In order to compare those data with birds records, various averaging procedures have been employed. The temperature parameters obtained from the AST\_08 raster with resolution of 100 m were transformed to the grid with a cell size of 30 m.



Besides, all used satellite products tied to specific shooting dates and do not show the variation of parameters in time.

The implemented statistical tests revealed that activity of vultures correlates with strength of thermals approximated by contrast of superficial temperature. However, the multiple regression analysis (MRA) indicated that only a part of records can be directly attributed to upwelling air flows. The estimated confidence level can be diminished by the following factors. (i) If the territory does not have strong triggers producing thermals, they will also be formed, but at variable positions (Angevine, 2014). In this case, methods analyzing the contrast in surface temperatures may not detect correctly the locality of thermals. (ii) There may be a threshold value for thermal strength that is able to impose the behavior of Black vultures. Vultures may not prefer the strongest thermal if it is only a bit stronger than its counterparts. (iii) Thermals attract soaring vultures, but this is not the only factor governing their behavior. (iv) Whereas highly urbanized vast lands of Amarais site provide the strongest thermals, Black vultures avoid them because of their unfavorable environmental conditions.

### 3. Data analyses

#### 3.1 Study of the dependence of soaring activity of Black vultures on relief, surface temperature and anthropogenic pressure

The Principal component analysis (PCA) and the Multiple regression analysis (MRA) and the Spearman rank correlation analysis were conducted to study the dependence of soaring activity of Black vultures expressed in  $W_{\text{birds}}$  index on superficial characteristics (surface temperature, contrast of surface temperatures, altitude above sea level, slope inclination, slope exposure and level of anthropogenic pressure). The statistical tests were carried out in SPSS 20.0 and R 3.1.0. The plots were constructed in SigmaPlot10.

In the course of MRA the superficial characteristics were considered as independent variables, whereas  $W_{\text{birds}}$  index was chosen as a variable depending on those surface parameters. In contrast, all variables including  $W_{\text{birds}}$  were assumed to be independent in the course of PCA. We use PCA in this context to indicate links between abundance of soaring vultures and superficial characteristics including those ones which caused by some other factors.

The Spearman rank correlation analysis was conducted to identify links between abundance of soaring vultures over area ( $W_{\text{birds}}$ ) and two temperature parameters (surface temperature and contrast of surface temperature). This test was conducted to confirm and detail the results of PCA and MRA which detect the dependence of  $W_{\text{birds}}$  index on those superficial characteristics.



The algorithms of preparation of summary tables for statistical analyses were considered above and in Appendix C (Algorithm C4). The resulting summary tables collected for PCA and MRA can be found in Supplementary Files SF40. The resulting summary tables which were processed with the Spearman correlation analysis can be found in Tables 3.7 - 3.10 and Supplementary Files SF41.

### 3.2 Study of the dependence of soaring activity of Black vultures on landscape type

The dependence of soaring activity of Black vulture on landscape type was studied by dint of evaluation of the relative attractiveness of each landscape types for soaring birds within studied sites. It was implemented by the elaborated approach of landscape analysis, basing on the same principle that was applied for statistical tests, but with own specifics. The “Sum of birds recorded in each landscape type” ( $S_{(birds)}$ ) parameter was applied as the relative numerical measure of soaring activity of vultures above territory.

The attractiveness of different landscape types was estimated using the ratios between following parameters: the percent of area of each landscape type ( $S$ , %); the percent of  $S_{(birds)}$  parameter of each landscape type ( $S_{(birds)}$ , %); the density of soaring vultures ( $\rho$ , birds ha<sup>-1</sup>) (Figs 3.9, 3.10; Tables 3.11, 3.12) and the percent deviation from the mean density ( $\hat{q}$ , %) (Fig. 3.11).

## 4. Results

### 4.1 Dependence of the soaring activity of Black vultures on relief, surface temperature and anthropogenic pressure

Results of PCA and MRA are presented in the tables 3.4 - 3.6, the results of Spearman correlation analysis are given in the Tables 3.7-3.10 and Fig. 3.7, Fig. 3.8.

**Table 3.4 Result of the Principal component analysis estimated the relationship between soaring activity of Black vultures ( $W_{bird}$ ) and superficial characteristics (Amarais, Prudente)**

Variables	Amarais		Prudente		
	Principal component 1	Principal component 2	Principal component 1	Principal component 2	Principal component 3
anthropogenic pressure	0.663	0.409	0.570	0.134	0.504
altitude above sea level	0.209	0.800	-0.194	-0.048	0.876
slope inclination	-0.189	0.270	-0.157	0.829	-0.062
surface temperature	0.762	-0.186	-0.264	-0.635	-0.063
contrast of surface temperature	0.046	-0.744	0.665	0.113	-0.039
$W_{birds}$	-0.738	0.004	0.650	-0.069	-0.143

**Table 3.5 Result of the Multiple regression analysis estimated the dependence of soaring activity of Black vulture ( $W_{birds}$ ) on superficial parameters (Amarais). Dependent variable:  $W_{birds}^{28}$**

Independent Predictors	$R_{reg}$	$R_{sq}$	Adjusted R Square	Std. Error of the Estimate
surface temperature	0.322	0.104	0.103	14.21
surface temperature, anthropogenic pressure	0.378	0.143	0.143	13.89
surface temperature, anthropogenic pressure, slope inclination	0.386	0.149	0.149	13.84
surface temperature, anthropogenic pressure, slope inclination, altitude above the sea level	0.389	0.152	0.151	13.82

**Table 3.6 Result of the Multiple regression analysis, estimated the dependence of soaring activity of Black vulture ( $W_{birds}$ ) on superficial parameters (Prudente). Dependent variable:  $W_{birds}$**

Independent Predictors	$R_{reg}$	$R_{sq}$	Adjusted R Square	Std. Error of the Estimate
contrast of surface temperature	0.159	0.025	0.025	11.97
contrast of surface temperature, anthropogenic pressure	0.176	0.031	0.031	11.94
contrast of surface temperature, anthropogenic pressure, surface temperature	0.185	0.034	0.034	11.92
contrast of surface temperature, anthropogenic pressure, surface temperature, altitude above sea level	0.190	0.036	.036	11.90
contrast of surface temperature, anthropogenic pressure, surface temperature, altitude above sea level, slope inclination	0.191	0.036	.036	11.90

### Amarais

For Amarais population PCA shows a high negative correlation between  $W_{birds}$  (-0.738) and [surface temperature](#) (0.762) with [anthropogenic pressure](#) (0.663) variables and corresponding first component (Table 3.4). MRA confirms and supplements the result of PCA. It identifies [surface temperature](#) and [anthropogenic pressure](#) variables as the most significant predictors determining  $W_{birds}$ . Together they explain 14.3% of the  $W_{birds}$  dispersion ( $R_{sq}=0.143$ ) with rather high multiple correlation coefficient ( $R_{reg}=0.378$ ) (Table 3.5).

The Spearman rank correlation analysis does not found any significant relationship between [contrast of surface temperature](#) and  $W_{birds}$  for the full range of values of this surface characteristic. It should be noted that PCA and MRA provide the same results. However, the

<sup>28</sup>  $R_{sq}$  – R square,  $R_{reg}$  – multiple correlation coefficient

Spearman rank correlation analysis demonstrates a very high correlation ( $R = 0.9$ ) between  $W_{\text{birds}}$  and contrast of surface temperature for the first five ranks of the last parameter (where range of its values lasts from 0.21 to 0.60°). On the contrary, for another five ranks (for values from 0.60 to 4.45°) the Spearman rank correlation analysis shows a small inverse correlation between these parameters ( $R = -0.3$ ) (Fig. 3.7<sub>(b)</sub>)

### Presidente Prudente

For Prudente population PCA outlines a high positive correlation between  $W_{\text{birds}}$  (0.65), contrast of surface temperature (0.665) and anthropogenic pressure (0.570) variables and corresponding first component (Table 3.4). MRA completely confirms the PCA result. It identifies the contrast of surface temperature, anthropogenic pressure and surface temperature as the most significant predictors affecting on  $W_{\text{birds}}$ . However, together they explain the  $W_{\text{birds}}$  dispersion only on 3.4% ( $R_{\text{sq}} = 0.034$ ) (Table 3.6). The Spearman rank correlation analysis fully confirms the results of PCA and MRA. It detects the strong correlation ( $R = 0.94$ ) between contrast of surface temperature and  $W_{\text{birds}}$  (Fig. 3.7<sub>(a)</sub>; Tables 3.7, 3.8)<sup>29</sup>.

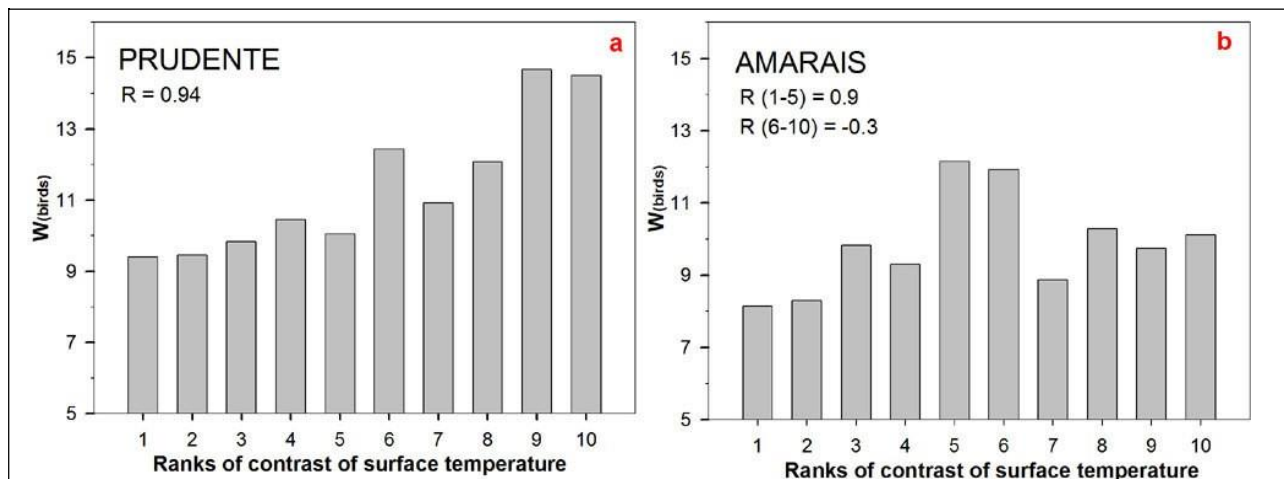


**Figure 3.7 Relationship between soaring activity of Black vultures ( $W_{\text{birds}}$ ) and contrast of surface temperature in Prudente (a) and Amarais (b) sites**

The plotted parameters are presented in the Tables 3.7 and 3.8. The axis OX represents the ranks of the contrast of surface temperature parameter. Each rank corresponds to 10% of the whole range of its values, i.e. in each rank the value of contrast of surface temperature is higher than in the rank before. “R” shows the Spearman's rank correlation coefficient between  $W_{\text{birds}}$  and contrast of surface temperature.

**Table 3.7 Summary table of the Spearman rank correlation analysis studied the relationship between soaring activity of Black vultures ( $W_{\text{birds}}$ ) and contrast of surface temperature (Prudente)**

<sup>29</sup> The mean values of  $W_{\text{birds}}$  attributed to each rank considering due to the Spearman rank correlation analyses are rather uncertain. The standard deviation of  $W_{\text{birds}}$  is comparable to calculated means. However, whereas the reviewing tests are not mathematically rigorous, they provide new evidences about traits of the soaring activity of vultures and its dependence on thermals strength.

Rank each interval - 10% of all data	Contrast of surface temperature averaged for the interval	Soaring activity of Black vultures recorded above the area ( $W_{birds}$ ) weighted mean for the interval
1	0.23	9.39
2	0.34	9.46
3	0.43	9.84
4	0.53	10.46
5	0.64	10.04
6	0.75	12.44
7	0.90	10.92
8	1.10	12.08
9	1.40	14.68
10	3.16	14.51

**Table 3.8 Summary table of the Spearman rank correlation analysis studied the relationship between soaring activity of Black vultures ( $W_{birds}$ ) and contrast of surface temperature (Amarais)**

Rank each interval - 10% of all data	Contrast of surface temperature averaged for the interval	Soaring activity of Black vultures recorded above the area ( $W_{birds}$ ) weighted mean for the interval
1	0.21	8.14
2	0.30	8.30
3	0.40	9.83
4	0.49	9.30
5	0.60	12.15
6	0.73	11.93
7	0.89	8.86
8	1.06	10.28
9	1.40	9.74
10	4.45	10.11

For both studied populations PCA shows the inverse relationship between [surface temperature](#),  $W_{birds}$  and corresponding component. It is higher for Amarais: [surface temperature](#) (0.762),  $W_{birds}$  (-0.738); and smaller for Prudente: [surface temperature](#) (-0.264),  $W_{birds}$  (0.65) (Table 3.4). These findings are confirmed by the Spearman rank correlation, which shows high coefficients of inverse correlation between  $W_{birds}$  and [surface temperature](#) for both populations (Fig. 3.8, Table 3.9, Table 3.10). At the same time for Amarais site PCA reveals a high direct relationship between [anthropogenic pressure](#) (0.663), [surface temperature](#) (0.762) and corresponding component, while for Prudente site it shows a weak negative relationship between [anthropogenic pressure](#) (0.57), [surface temperature](#) (-0.264) and corresponding component (Table 3.4).

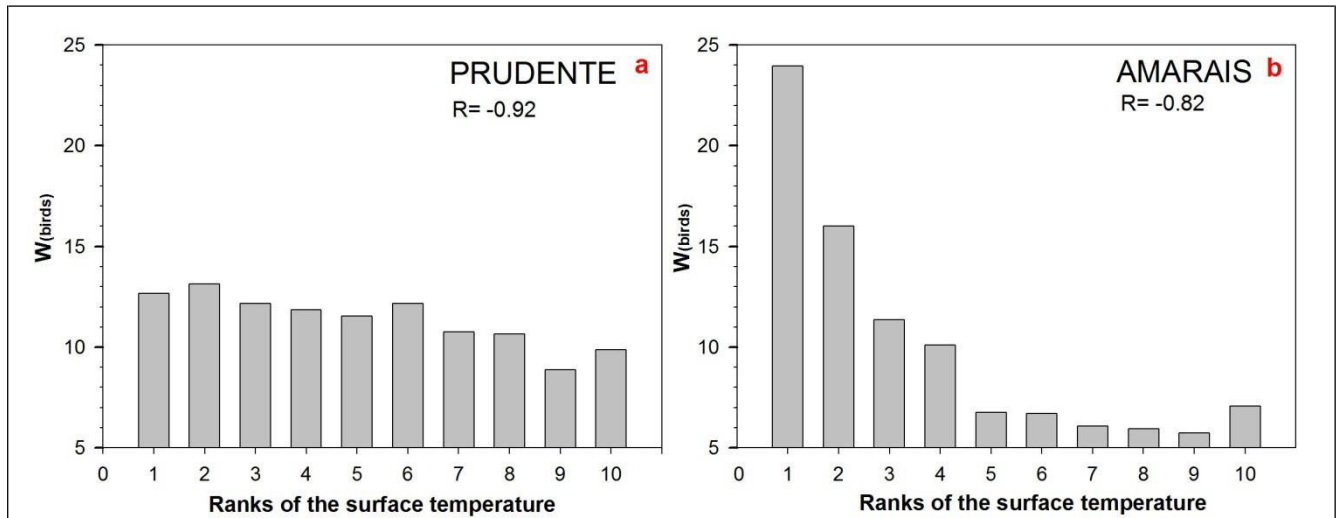


**Figure 3.8 Relationship between soaring activity of Black vulture ( $W_{birds}$ ) and surface temperature in Prudente (a) and Amaraïs (b) sites**

The plotted parameters are presented in the Tables 3.9 and 3.10. The axis OX represents the ranks of the surface temperature parameter. Each rank corresponds to 10% of the whole range of its values, i.e. in each rank the value of contrast of surface temperature is higher than in the rank before. “R” shows the Spearman's rank correlation coefficient between  $W_{birds}$  and surface temperature.

**Table 3.9 Summary table of the Spearman rank correlation analysis studied the relationship between soaring activity of Black vultures ( $W_{birds}$ ) and surface temperature (Amaraïs)**

Rank 10% of all data	Surface temperature averaged over the interval	Soaring activity of Black vultures recorded above the area ( $W_{birds}$ ) weighted mean over the interval
1	26.60	23.94
2	28.25	16.00
3	29.33	11.35
4	30.07	10.09
5	30.75	6.75
6	31.50	6.72
7	32.18	6.08
8	32.89	5.94
9	33.72	5.72
10	35.67	7.06

**Table 3.10 Summary table of the Spearman rank correlation analysis studied the relationship between soaring activity of Black vultures ( $W_{birds}$ ) and surface temperature (Prudente)**

Rank 10% of all data	Surface temperature averaged over the interval	Soaring activity of Black vultures recorded above area ( $W_{birds}$ ) weighted mean over the interval
1	25.5	12.65
2	28.2	13.07
3	29.4	12.08
4	30.3	11.85
5	31.0	11.37
6	31.5	12.09
7	32.1	10.75

8	32.7	10.65
9	33.4	8.86
10	34.8	9.86

Summarizing the results, it can be concluded that the lesser anthropogenic stress provide the higher soaring activity ( $W_{\text{birds}}$ ) over the Amarais site and a weaker soaring activity over the Prudente site. For both studied populations it was revealed the strong negative correlation between soaring activity ( $W_{\text{birds}}$ ) and surface temperatures; the strong positive correlation between soaring activity ( $W_{\text{birds}}$ ) and **contrast of surface temperature**. For Prudente population the last relationship was shown for full range of the **contrast of surface temperature**, for Amarais – only for five first ranks of its full range. At the same time, in Amarais site the higher anthropogenic stress provide the higher surface temperature, while in Prudente the increase of anthropogenic stress does not provide the increase of surface temperature.

#### 4.2 Dependence of the soaring activity of Black vultures on landscape type

The parameters used for analysis of attractiveness of landscape types<sup>30</sup> for Black vultures, i. e. the percent of area of each landscape type (**S**, %); the percent of  $S_{\text{(birds)}}$  parameter of each landscape type ( **$S_{\text{(birds)}}$** , %); the density of soaring vultures ( **$\rho$** , birds ha<sup>-1</sup>) and the percent deviation from the mean density ( **$\hat{q}$** , %) are presented on Figures 3.9-3.11 and Tables 3.11, 3.12.

**Table 3.11 The soaring activity of Black vultures over the landscape types with different level of anthropogenic pressure (Amarais)**

Landscape type	Attractiveness	Anthropogenic pressure	S, ha	S, %	$S_{\text{(birds)}}$	$S_{\text{(birds)}}$ , %	$\rho$ , $S_{\text{(birds)}}$ /ha	$\hat{q}$ , %
natural land	neutral	1	784.58	39.56	7906	40.07	10.08	1.30
natural water body	very high	1	39.12	1.97	1337	6.78	34.18	243.57
roadway	high	2	122.08	6.16	2008	10.18	16.45	65.35
soft urbanized land	neutral	2	215.32	10.86	2450	12.42	11.38	14.38
technical water body	high	2	39.27	1.98	608	3.08	15.48	55.64
dense residential land	less than neutral	3	611.20	30.82	3530	17.89	5.78	-41.94
industrial land	neutral	4	171.74	8.66	1890	9.58	11.01	10.63
Mean							<b>14.91</b>	

<sup>30</sup> Preparing data for landscape analysis and definition of those parameters are considered in div. 2.2.7. Methodology of detection of the landscape parameters is considered in div. 2.2.1.2 .

**Table 3.12 The soaring activity of Black vultures over the landscape types with different level of anthropogenic pressure (Prudente)**

Landscape	Attractive ness	Anthropog enic stress	S, ha	S, %	$S_{(birds)}$	$S_{(birds)}, \%$	$\rho, S_{(birds)}/ha$	$\hat{Q}, \%$
natural land	less than neutral	1	1551.18	77.85	17511	57.83	11.29	-25.72
natural water body	very high	1	112.56	5.65	4579	15.12	40.68	167.68
roadway	high	2	90.60	4.55	2547	8.41	28.11	84.99
soft urbanized land	high	2	88.36	4.43	4204	13.88	47.58	213.07
dense residential land	less than neutral	3	129.57	6.50	668	2.21	5.16	-66.08
industrial land	high	4	20.20	1.01	771	2.55	38.16	151.15
<b>Mean</b>							<b>28.5</b>	

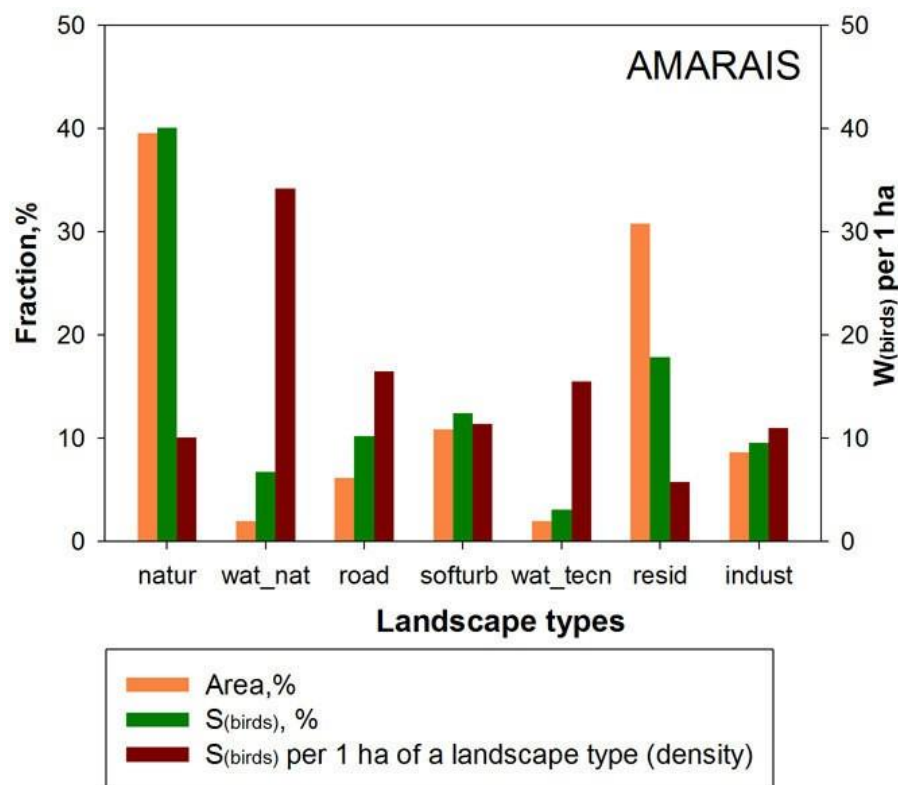


**Figure 3.9 Landscape types and soaring activity of Black vultures (Amarais)**

Landscape types: natur - natural land, wat\_nat - natural water object, road - roadway, softurb - soft urbanized land, wat\_tecn - technical water object, resid - dense residential land, indust - industrial land.

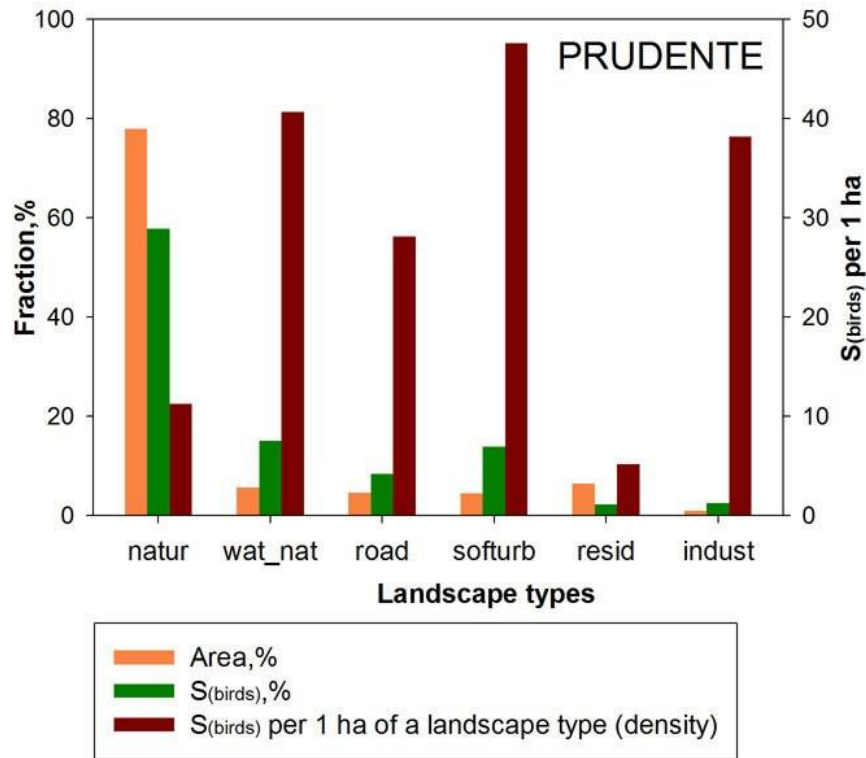


**Figure 3.10**  
**Landscape types and**  
**soaring activity of Black**  
**vultures (Presidente**  
**Prudente)**

Landscape types: natur - natural land, wat\_nat - natural water object, road - roadway, softurb - soft urbanized land, resid - dense residential land, indust - industrial land

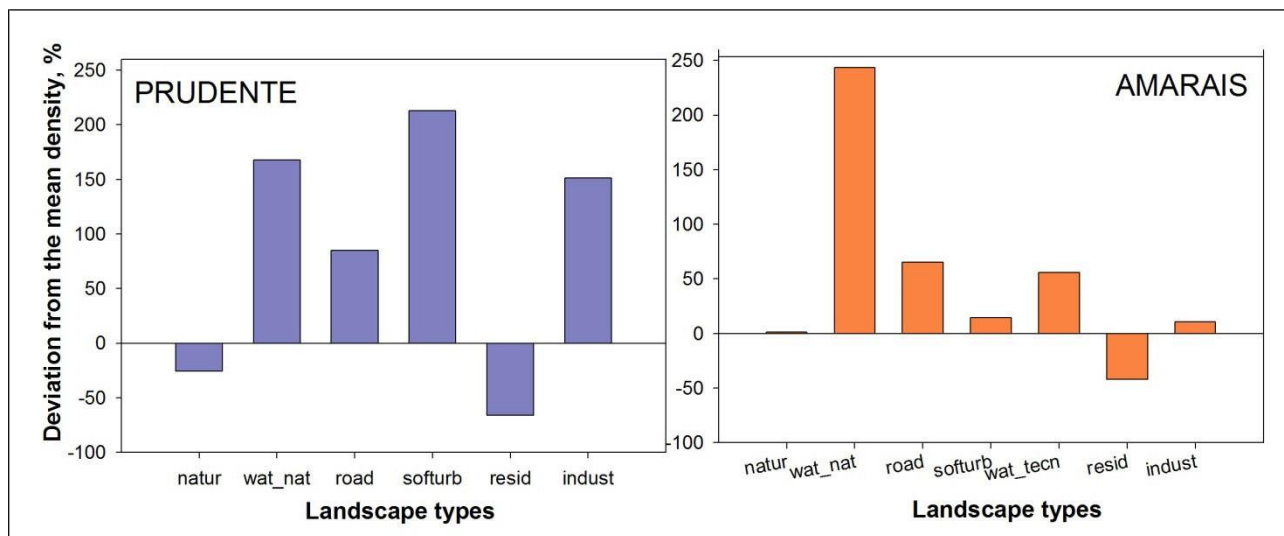


**Figure 3.11 Deviation from the mean density of  $S_{(birds)}$  of each landscape type**

1. The analysis of ratio between  $S, \%$  and  $S_{(birds), \%}$  parameters allows to estimate the level of concentration of vultures above the different landscape types within each study site. Here we assume that the higher is the concentration of birds over the landscape, the stronger its attractiveness for vultures. The possible combinations of ratio between  $S, \%$  and  $S_{(birds), \%}$  parameters and interpretation of landscape attractiveness for birds are the following:

(i) If all landscape types would be equally attractive for Black vultures, the fraction of the area ( $S, \%$ ) would be equal to the fraction of birds recorded ( $S_{(birds), \%}$ ) and the density of soaring vultures ( $\rho$ ) would have the uniform distribution among all landscape types.



We found that both study sites reveal the non-uniform distribution of the density of soaring vultures ( $\rho$ ), which allows to conclude that attractiveness of landscape types for birds is different. However, a few landscapes show about equal fractions of the area and recorded birds ( $S, \% \approx S_{(birds)}, \%$ ). Those landscapes we entitled as having the “*neutral*” level of attraction. Those landscapes can be interpreted as the typical habitat<sup>31</sup> for Black vultures, which do not have especially attractive features providing the increased concentration of birds. In Amaraïs site the nearly *neutral* attraction was revealed for *soft urbanized* and *industrial* landscapes. The pure *neutral* attraction was detected for the *natural* landscape of Amaraïs site (Fig. 3.9, Table 3.11).

(ii) The landscapes with fraction of its area larger than fraction of recorded vultures ( $S, \% > S_{(birds)}, \%$ ) we entitled as having the “*less than neutral*” level of attraction. Those landscapes we interpreted as having the minimal attractiveness for Black vulture within considered set of landscape types. This means, that those areas contain some uncomfortable factor for birds. The *dense residential* areas have *less than neutral* attraction in both studied sites. In Prudente also the *natural* landscapes can be attributed to *less than neutral* attraction.

(iii) The landscapes with fraction of its area smaller than fraction of the recorded vultures ( $S, \% < S_{(birds)}, \%$ ) we entitled as having the “*higher than neutral*” (or just “*high*”) level of attraction. Those landscapes can be interpreted as having the maximal attractiveness for Black vulture within considered set of landscape types. This means, that those territories contain especially attractive characteristics for vultures providing the increased concentration of these birds over the surface.

2. The *percent deviation from the mean density* ( $\hat{q}, \%$ ) (Fig 3.11) parameter can also be used for detection the attractiveness of landscape types for birds. It can be applied in combination with method considered above (for control its results) or alone. The deviation parameter is about zero ( $\hat{q} \approx 0$ ) identifies landscapes with “*neutral*” level of attraction; higher than zero ( $\hat{q} > 0$ ) detect landscape with *high* level of attraction; and smaller than zero ( $\hat{q} < 0$ ) reveals landscape with “*less than neutral*” level of attraction.

Moreover, according to the absolute value of the deviation parameter we can compare the attractiveness of landscapes for vultures which were identified as having the “high level of attraction”. Value “0” of deviation parameter marks the mean of the density ( $\rho$ ) of all landscape types within the study region. Therefore, the higher is the value of deviation parameter from zero, the more attractive this landscape should be for vultures within studied territory.

According to this we revealed, that “*water body*” landscape has the strongest attractiveness for Black vulture around both airports. Vultures prefer both clean natural reservoirs like rivers

<sup>31</sup> The “typical” means here the “usual” area of soaring vultures, the area where it’s distribution is uniform.

and lakes and technically polluted water objects, like technical ponds of treatment facilities. The “natural water body” has the highest attractiveness; its deviation is 243.57% in Amaraïs (1<sup>st</sup> place, Table 3.11; Fig. 3.11) and 167.68% in Prudente (2<sup>nd</sup> place, Table 3.12; Fig. 3.11). The “technical water body” (which were found only in the vicinities of the Amaraïs airport) also has high level of attractiveness, but its deviation is smaller - 55.64% (3<sup>d</sup> place, Table 3.11; Fig. 3.9).

The second highly attractive landscape for Black vultures is the “roadway”. Roads are less attractive than water bodies. Its deviation is 65.35% in Amaraïs (the 2<sup>nd</sup> place) and 84.99% in Prudente (3<sup>d</sup> place) (Tables 3.11, 3.12; Fig. 3.11).

Prudente site has two more landscapes with high level of attractiveness: the “soft urbanized” landscape (its deviation is 213.07%, 1<sup>st</sup> place) and the “industrial” landscape (deviation is 151.15%, 3<sup>rd</sup> place). In Amaraïs those landscapes have quasi neutral attraction level with deviation 14.38% and 10.63% respectively.

Important to note, that the percent deviation from the mean density ( $\hat{q}$ , %) parameter can be also applied for comparing the attractiveness of landscape types for birds within the different geographical region. This can be used to highlight the landscapes, which are particularly important for these birds, i.e. which attractive for them everywhere. And, conversely, it allows to identify the landscapes with different attractiveness for vultures in various geographical regions. By comparing histogram of deviation parameter of both studied sites (Fig. 3.11) we can conclude, that water objects and roads are highly attractive for vultures in both regions, while soft urbanized and industrial lands reveal significant difference in their attraction for birds in two observed airport’s surroundings.

## 4.3 Risk of collision with Black vultures over the studied territory

### 4.3.1 Risk of collision, estimated for the entire area of 13 km radius around the airports

The risk assessment maps constructed for 13 km zone around each airport (Figs. 3.12, 3.13) give the general estimation of hazard of bird-strike event above this territory and identify the most dangerous and the less dangerous places for the aircraft takeoffs and landings. They depict the most vulnerable area, where most of collisions with birds can occur. We suppose that this assessment already should to be considered by the airports administration for planning the safety paths of takeoffs and landings operations. However, it is necessary to take into account the low accuracy of maps constructed for the entire area.

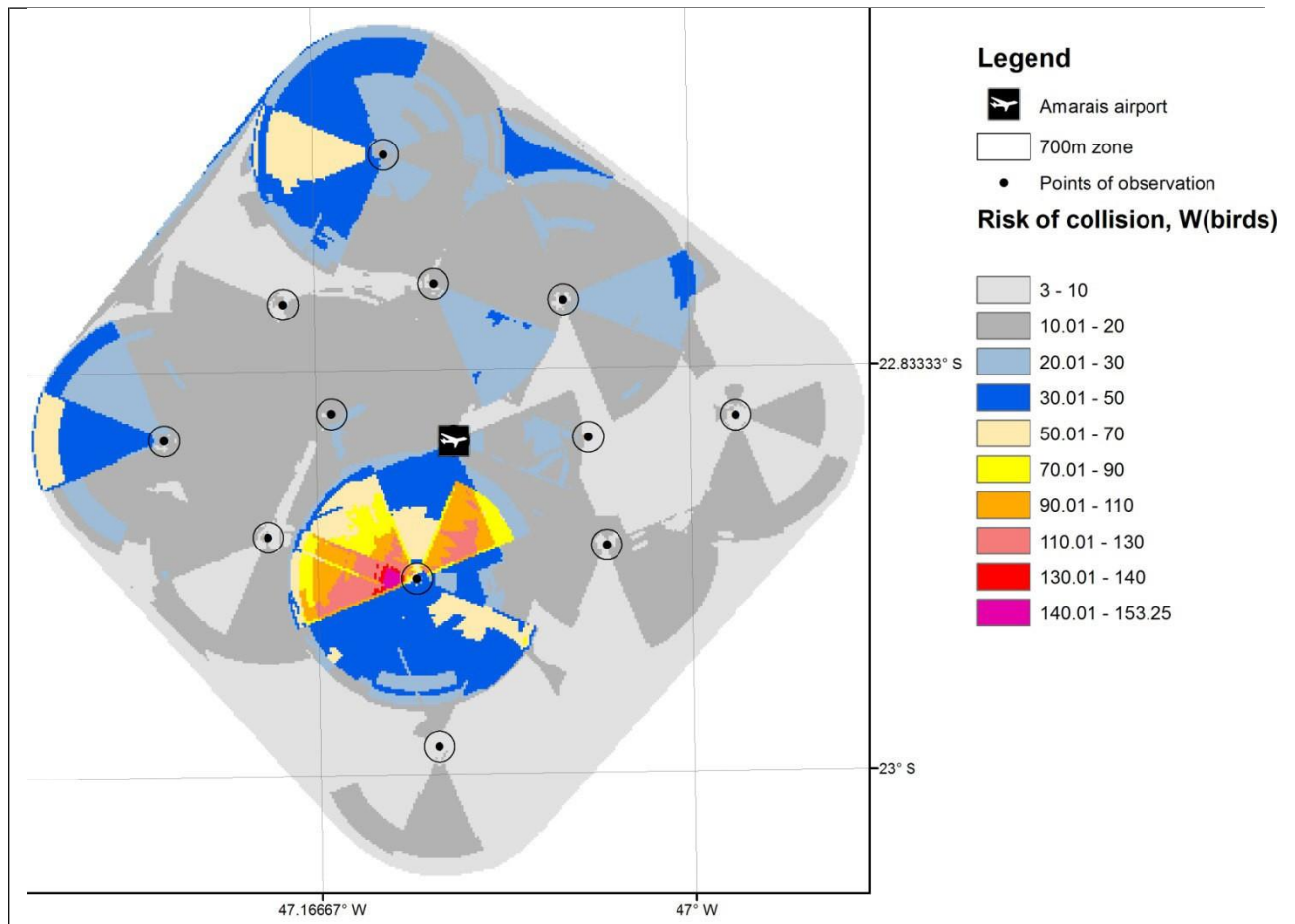


**Figure 3.12 Risk assessment map of aircraft collisions with Black vultures within the 13 km radius around the Amarais airport (Supplementary Files SF13)**

The  $W_{\text{birds}}$  index is the parameter, which we applied as the relative numerical indicator of the abundance of flying birds over the territory. It was calculated by Eq. 7 and considered in details in the text (div. 2.2.4, 2.2.5) and Appendix C (Algorithm C3, C4).

For any point of this map within 13 km zone around Amarais airport,  $W_{\text{birds}}$  depicts the estimated amount of birds which were registered and can be located over this point during the total period of study, i.e. 360 sky reviews or approximately 90 hours of pure observations distributed evenly from September 2012 to August 2013 (1 sky review lasts 15 minutes)<sup>32</sup>.

<sup>32</sup>Those values are the average number of sky reviews and hours of observations which were conducted above each vector point of the map. They were calculated from the total amount of sky reviews implemented in each site (Amarais -4683, Prudente - 4258) divided by 13), considering that one sky review lasted 15 minutes.

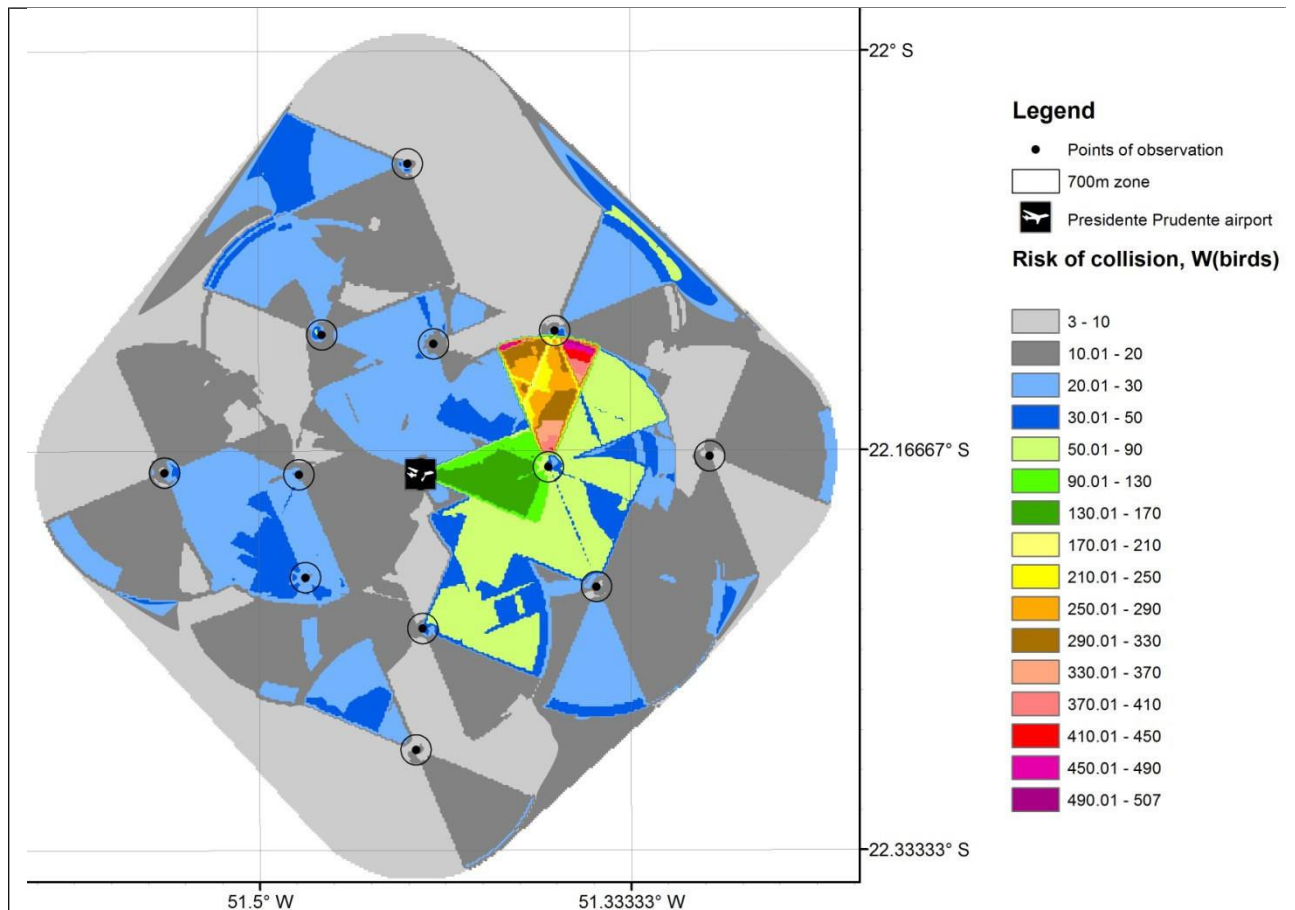


**Figure 3.13 The risk assessment map of aircraft collisions with Black vultures within the 13 km radius around the Presidente Prudente airport (Supplementary Files SF13)**

The  $W_{birds}$  index is the parameter, which we applied as the relative numerical indicator of the abundance of flying birds over the territory. It was calculated by Eq. 7 and considered in details in the text (div. 2.2.4, 2.2.5) and Appendix C (Algorithm C3, C4).

For any point of this map within 13 km zone around Presidente Prudente airport,  $W_{birds}$  depicts the estimated amount of birds which were registered and can be located over this point during the total period of study, i.e 328 sky reviews or approximately 82 hours of pure observations distributed evenly from September 2012 to August 2013 (1 sky review lasts 15 minutes).<sup>33</sup>

The maximum level of bird-strike hazard around Presidente Prudente airport is much higher than around the Amarais airport. The territories with the minimum risk (characterizing by values of  $W_{birds}$  index from 15 to 20) have approximately equal area in both sites.

For Amarais airport the most dangerous directions for takeoffs and landings are the south and southwest from the airport. The safest area is the east and north-west from the airport. In the Presidente Prudente airport the most dangerous are east, north-east and south-east directions. The safest areas locate from the west of the airport (Figs. 3.12, 3.13).

<sup>33</sup> See the previous footnote

#### **4.3.2 Risk of collision, estimated for the circular zones of 700 m radius around the viewpoints**

The risk assessment maps constructed for the circular zones of 700 metres radius around the viewpoints have the higher accuracy than the maps built for the entire area. We consider two examples taken as case-studies of those map constructed for the viewpoints №7 and №11 of Amarais site. They are given in combination with DigitalGlobe image and raster maps of surface temperature, contrast of surface temperature and landscape characteristics, constructed from the satellite imagery (Fig. 3.14, Fig. 3.15).

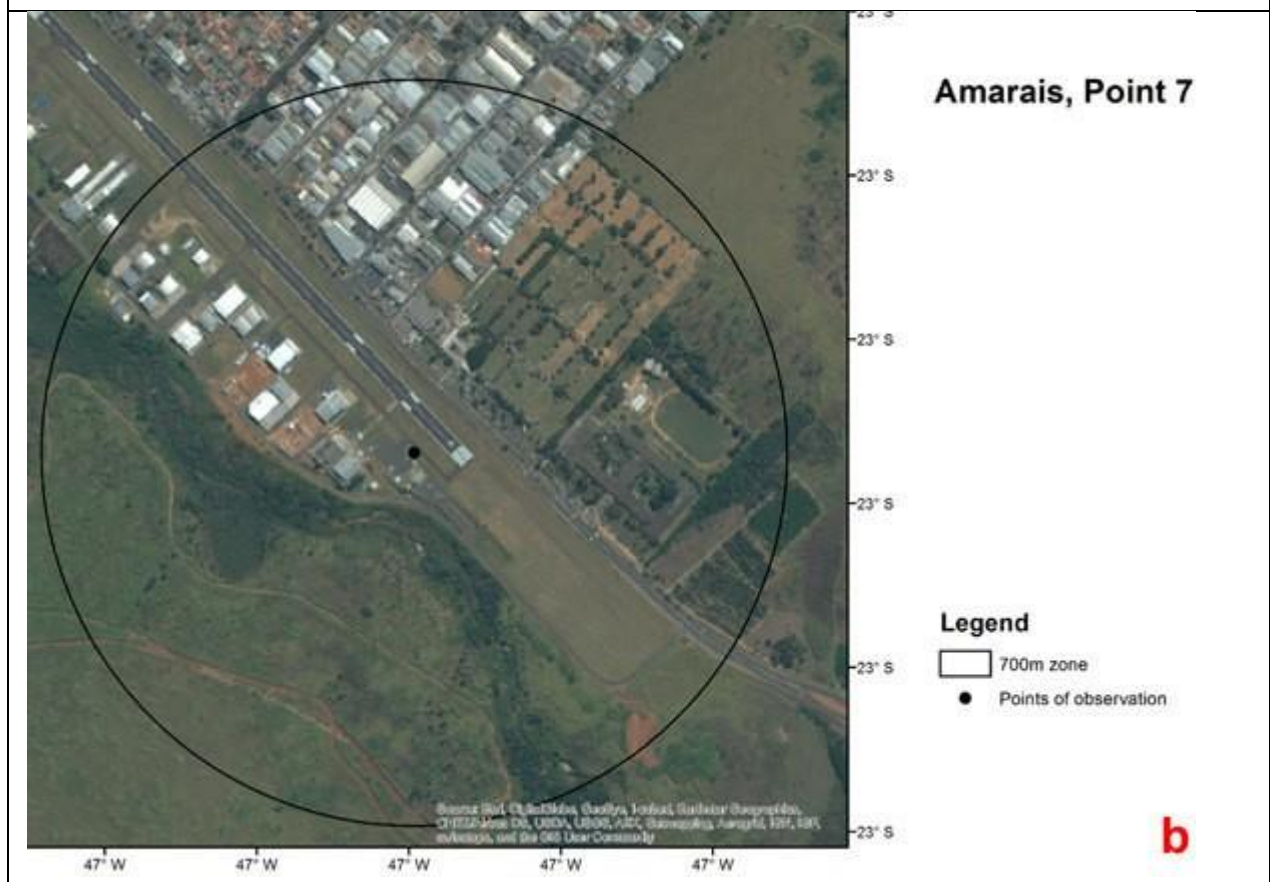
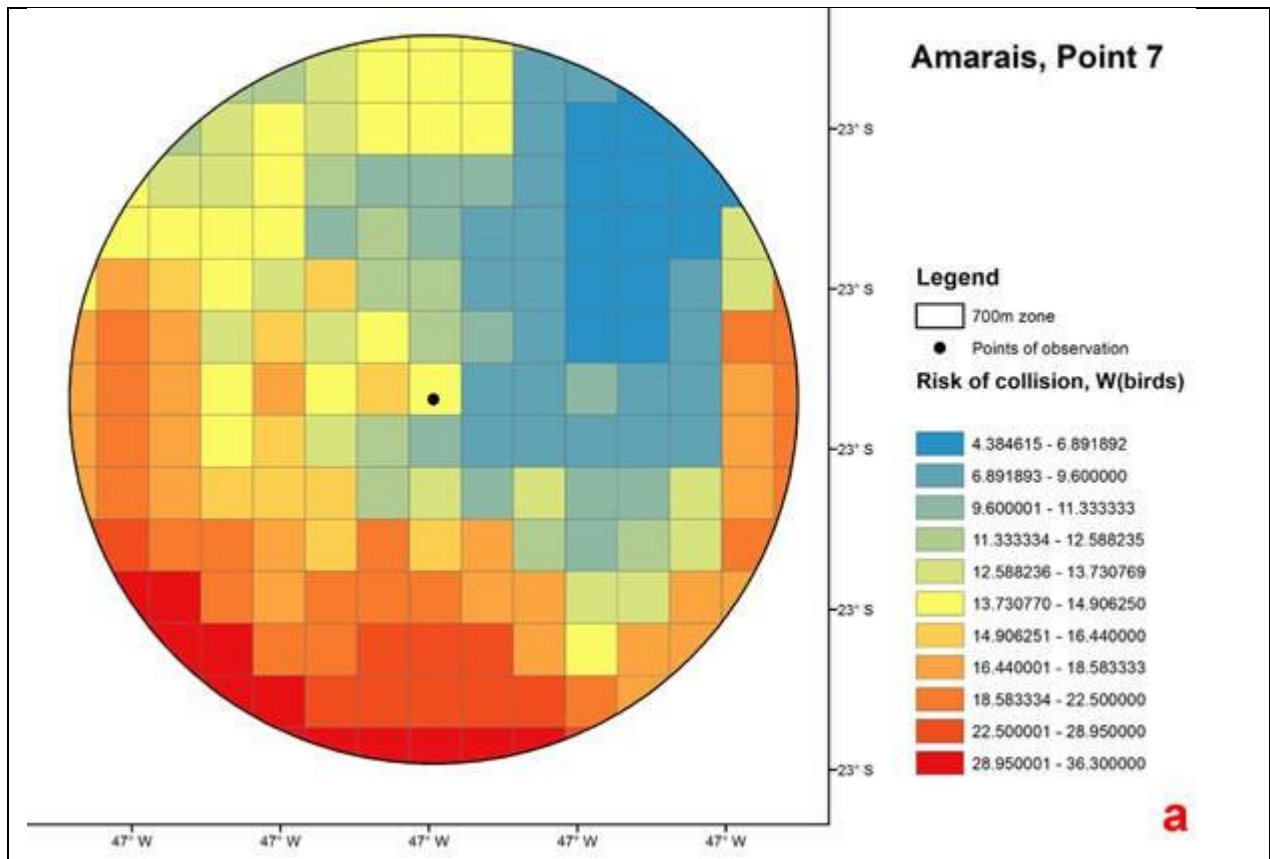
The visual analysis of risk assessment maps of two viewpoints together with superficial characteristics obtained from the remote sensing products reveals the following. (i) The concentration of flying birds over the rural and natural areas was higher than over the urban landscapes. (ii) The map of the surface temperature clearly shows that the surface temperature of urban areas is higher than surface temperature of rural and natural lands. It is the clear cartographic confirmation of the well-known effect of the “hot spots” forming over the cities. (iii) A high temperature contrast forms on the junction of the territories with low and high surface temperatures, i.e. on the boundary of the natural or agricultural lands and urban lands.

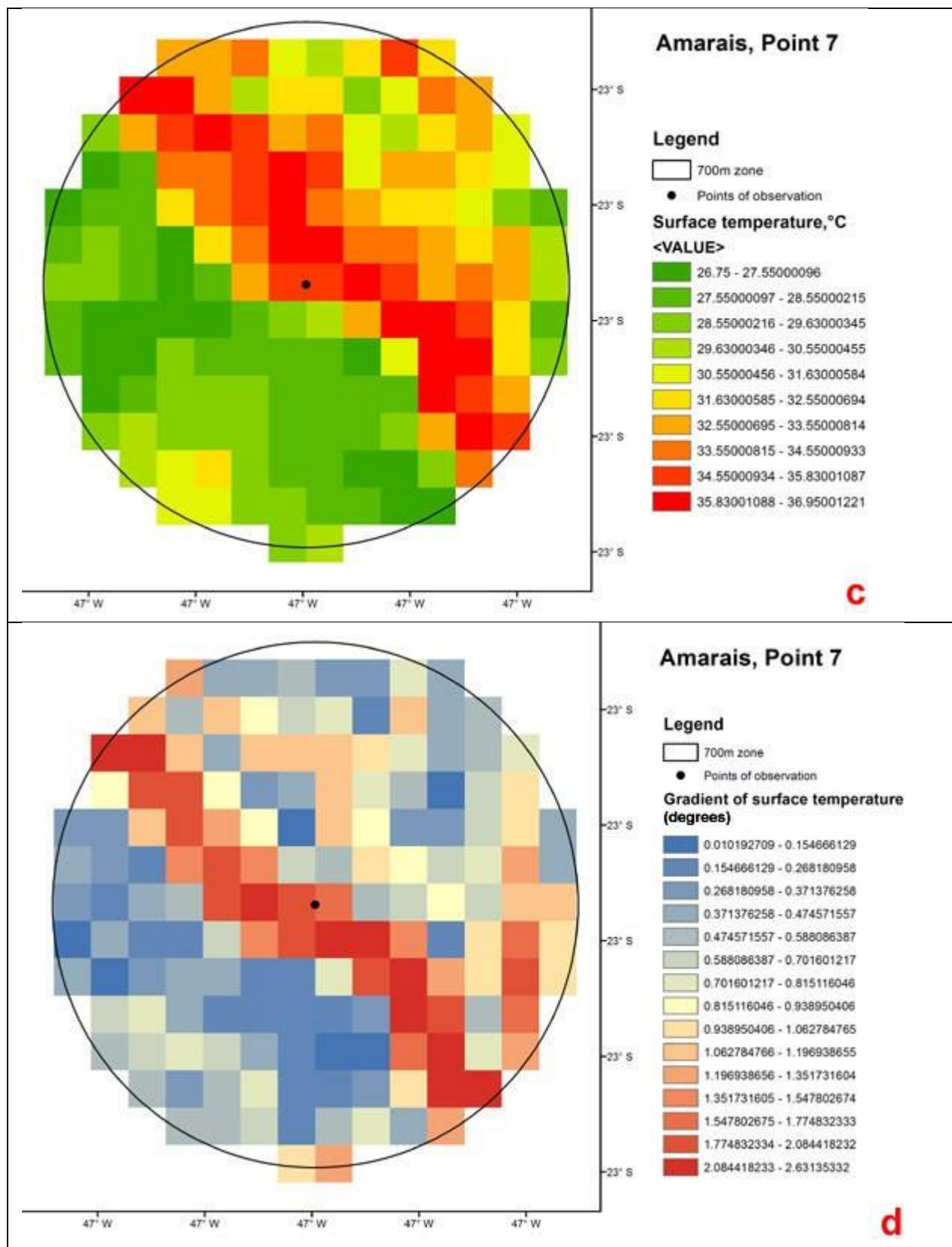
We considered those examples only as illustration of the technical ability of high-accuracy maps application for data analyzes and prediction of bird strike events. Since we were not able to construct the high-accuracy maps for the entire territory<sup>34</sup>, we did not manage to apply them for a complete analysis of the airport’s vicinities.

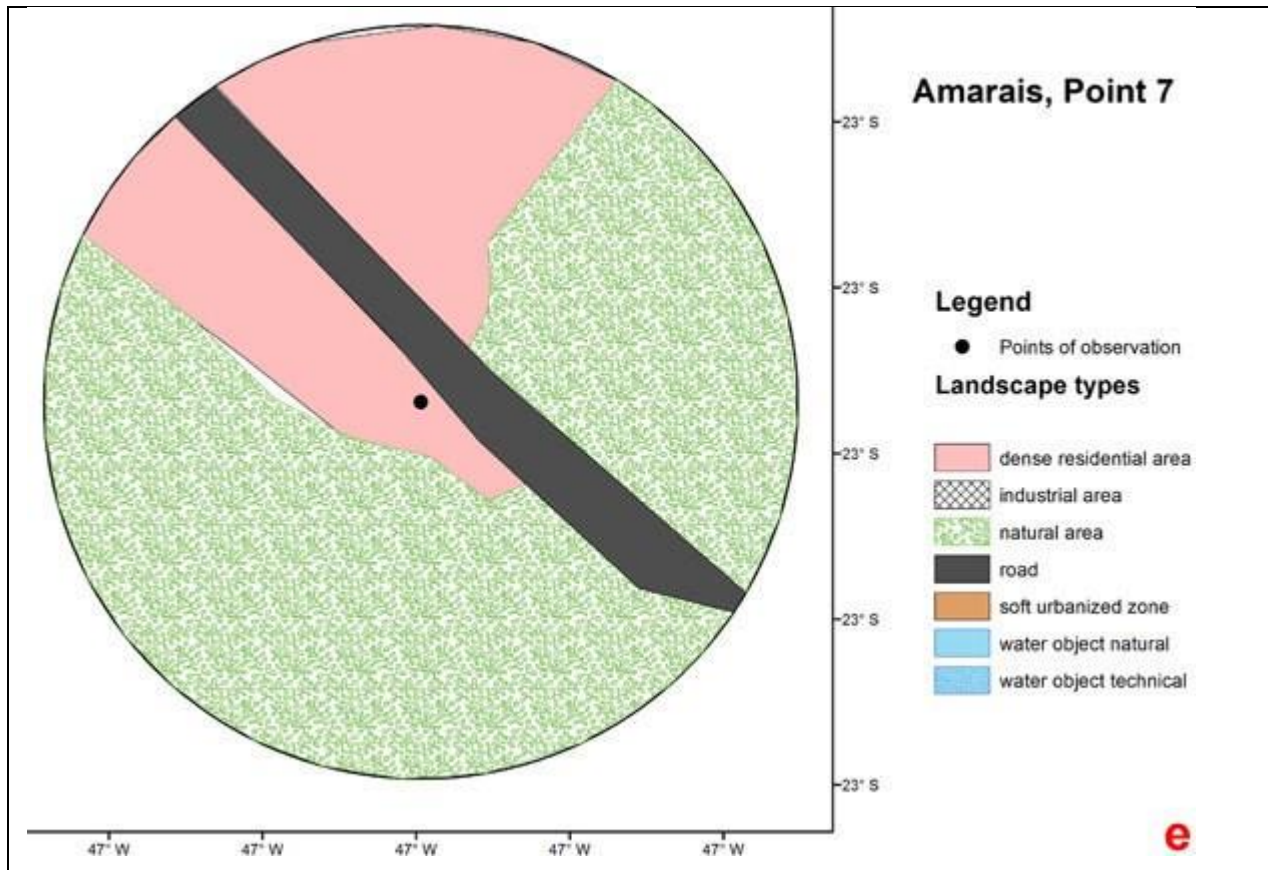
---

<sup>34</sup> The reasons of impossibility to construct the risk assessment maps of high accuracy for the entire territory are considered in “Assumptions and limitations” section. Our recommendations about the desirable changes in the methodology of field data gathering which will allow building the risk assessment map of high accuracy for the entire territory are considered in “Practical recommendations” section.



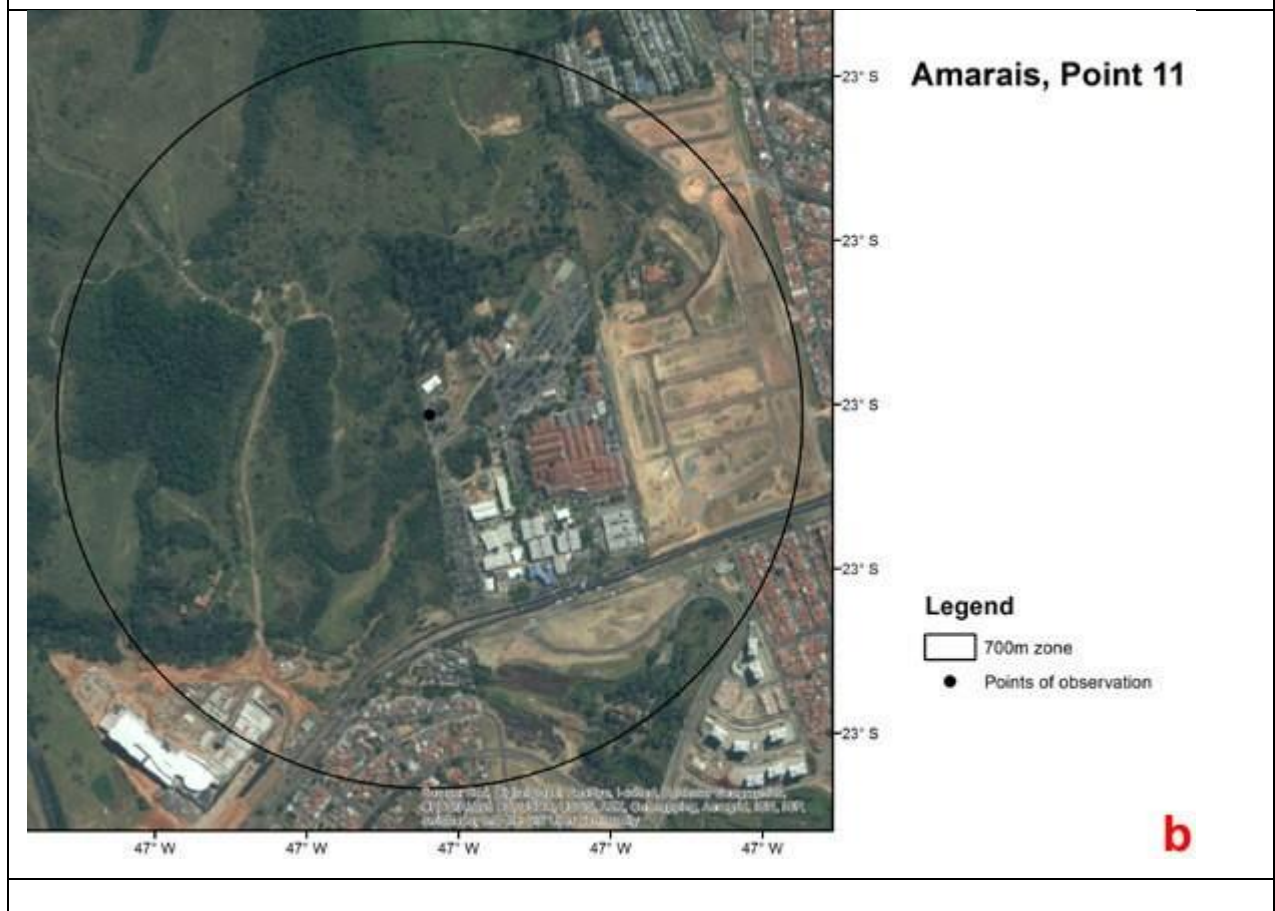
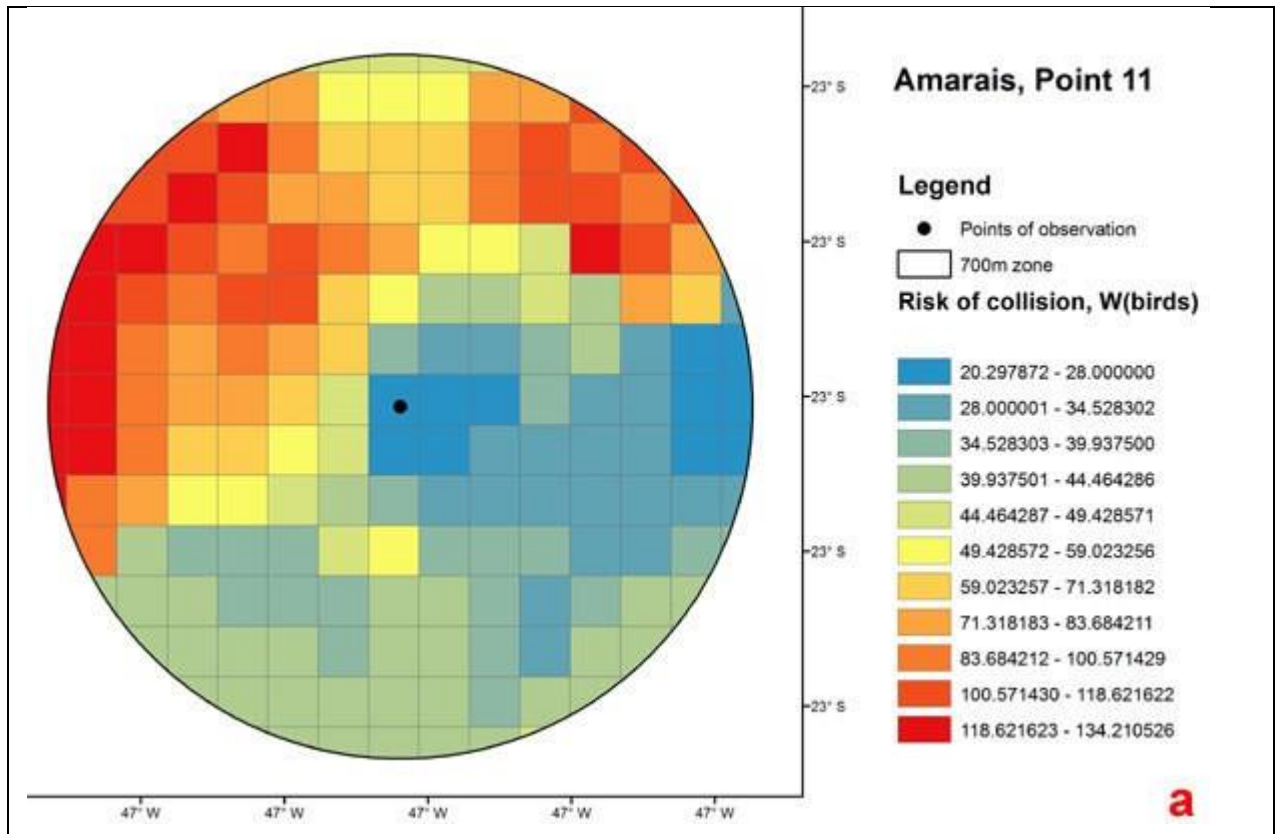


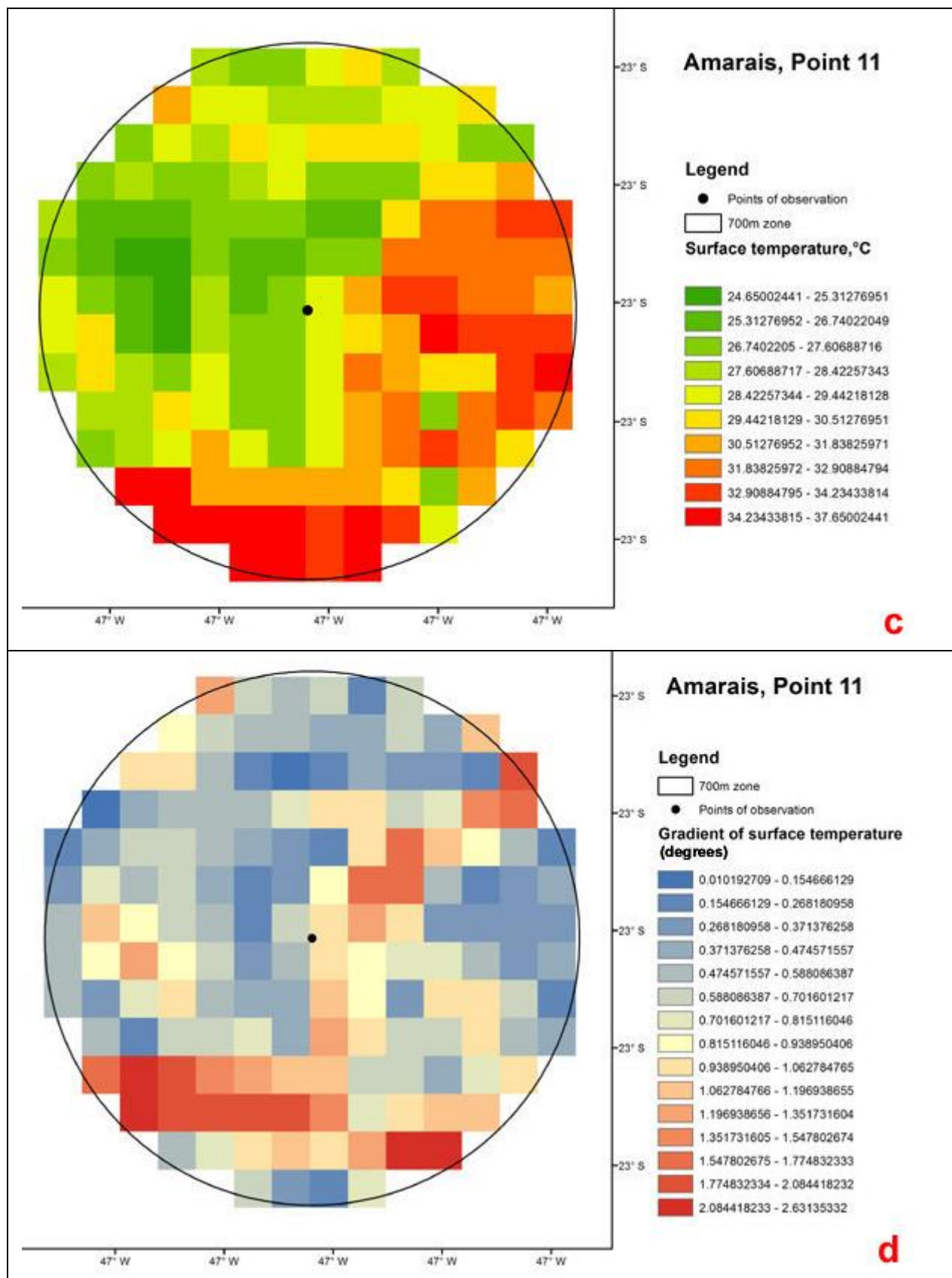




**Figure 3.14** Risk assessment map (a); true-color band composition of high resolution imagery (b); surface temperature (c); contrast of surface temperature (d); landscape types (e) for 700 meter zone around the viewpoint № 11 of Amarais site (Supplementary Files SF14)







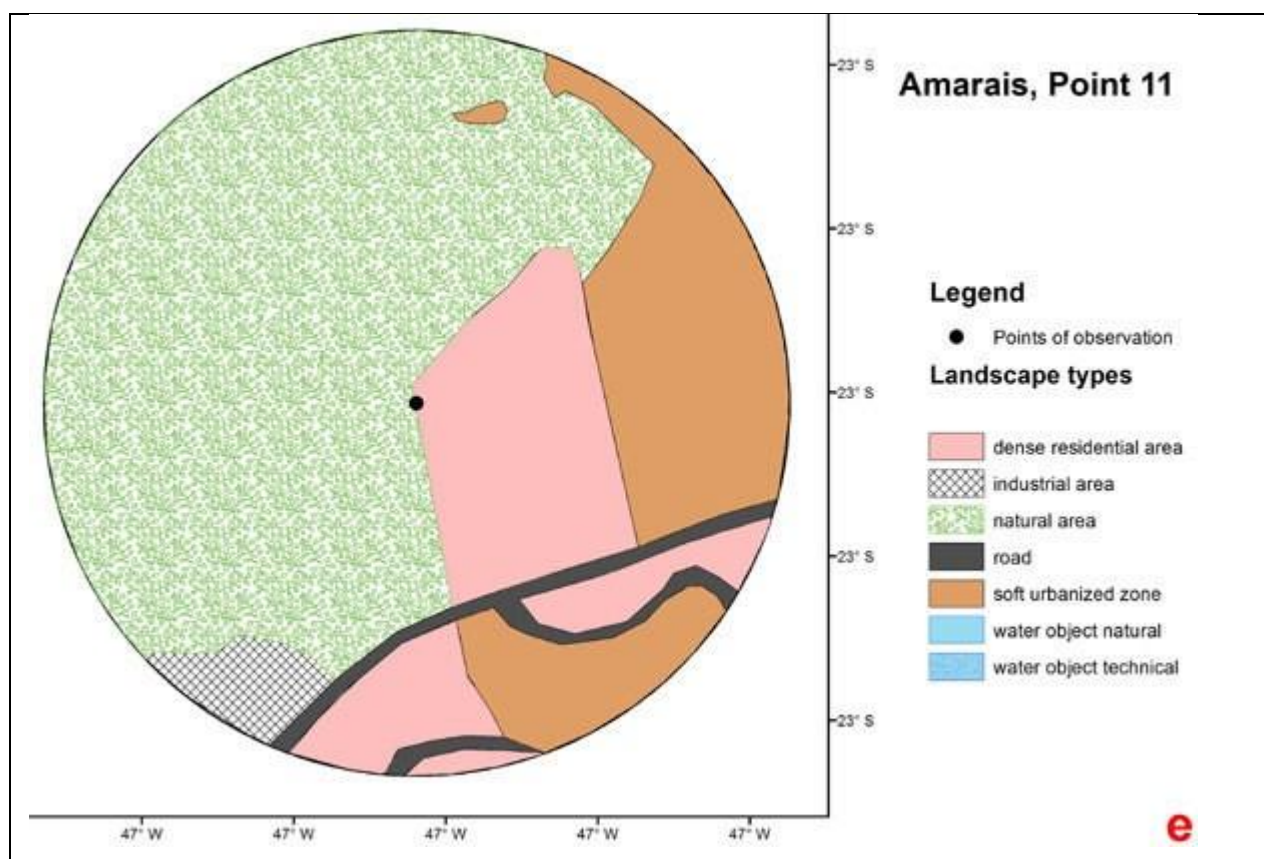


Figure 3.15 Risk assessment map (a); true-color band composition of high resolution imagery (b); surface temperature (c); contrast of surface temperature (d); landscape types (e) for 700 meter zone around the viewpoint № 7 of Amarais site (Supplementary Files SF14)

## 5. Discussion

### 5.1 Dependence of the soaring activity of Black vultures on relief, surface temperature and anthropogenic pressure

The surface temperature, contrast of surface temperature and level of anthropogenic pressure demonstrated the significant influence on the abundance of soaring Black vultures over the area, expressed in  $W_{birds}$  index. While the relief characteristics (slope inclination, slope exposure and altitude above the sea level) did not show any significant impact on soaring activity of these birds.

The strong dependence of  $W_{birds}$  index on contrast of surface temperature was detected for both study sites. For Prudente site it was revealed for the entire range of values of temperature contrasts (Fig. 3.7<sub>(a)</sub>). For Amarais site it was shown only for small values of this parameter, while its high values demonstrate a weak negative correlation with  $W_{birds}$  (Fig. 3.7<sub>(b)</sub>). Hence, we can conclude that vultures around Amarais airport are strongly attracted to the lands with small temperature contrast, but would rather avoid objects producing high contrast of surface temperatures. We suppose that this occur for the reason that the highest values of temperature contrast in Amarais site are typical for lands with strong anthropogenic pressure (like industrial

zones) producing technogenic heat, which usually much stronger than natural heating. This assumption was confirmed by the factor analysis which showed for Amarais site a high positive relationship between [anthropogenic pressure](#) and [surface temperature](#) (Table 3.4).

We can summarize that areas under heavy anthropogenic impact (like industrial lands), despite of extremely strong thermals forming over them, are less attractive to Black vultures than natural environments and lands with small anthropogenic pressure. This is consistent with the result of factor analysis of Prudente. PCA did not reveal any sufficient correlation between level of anthropogenic stress and surface temperatures, which can be interpreted as a weak negative impact of the urban areas on the environment around the Presidente Prudente airport. These conclusions are concord with the set of our findings illuminating the effect of reduction the number of soaring vultures over the large space of uninterrupted highly urbanized territories.

### **5.1.2 Confirmation of the hypothesis stating that Black vultures tend to choose the strongest thermals in surroundings**

We based our study of the dependence of soaring activity of vultures on thermals strength on the following statement, arisen from the thermals properties: “The higher is the contrast between surface temperature of a hotspot and surface temperature of its adjacent lands, the higher is the possibility of thermal formation over this hotspot and the stronger could be this thermal” (Angevine, 2014). The  $W_{birds}$  index was used in this study as the relative numerical measure of the abundance of soaring vulture over the territory.

Basing on this statement and conclusions considered above, we can assert that **the positive relationship between contrast of surface temperature and  $W_{birds}$  can be interpreted as the positive relationship between abundance of soaring vultures over the area and thermals strength of this area**. From this finding follows that Black vultures **tend to choose the strongest thermals in surroundings for soaring flight**. We consider this finding as the second confirmations of the testable hypothesis. The first confirmation of this hypothesis was considered in Chapter II, where it was based on the revealed dependence of the soaring activity of Black vultures on wind speed and solar activity characteristics. Important to note, that this hypothesis was confirmed in both parts of our investigation, which were implemented by the separate databases (meteorological characteristics registered synchronously with the birds’ observation and surface parameters revealed from the remote sensing products) and independent analyses.

The revealed positive relationship between intensity of soaring flights of Black vultures and thermals strength, which we interpreted as the tendency of Black vultures to choose the strongest thermals for soaring, can be explained by adaptation to minimize energy loss in flights, as occurs in most avian scavengers (Schoener, 1971; Ruxton and Houston, 2002).



Our result consists with the results of several authors who observed the high dependence of Black vulture and Turkey vulture on thermals in soaring flight. They evidenced that both species use thermals for upward flight in the morning and soaring flight in daily hours. The soaring activity coincides accurately with hours of thermals occurrence. It starts after local sunrise and finish before local sunset (Mandel and Bildstein, 2007; Freire *et al*, 2015; Newman, 1957; Coleman and Fraser, 1989, Thompson *et al.*, 1990). Usually, vultures locate their large roosts near the structures generating thermals (Thompson *et al*, 1990). The lack of sufficient (strong and constant) assistant thermal can keep Turkey vultures on the ground several days or more (Mandel and Bildstein, 2007). Both species use flapping flight very rarely and mainly at small altitudes (about 10 m over the ground), most of the daily time they soar (Buckley, 1999). The soaring type of flight are possible only on thermals, hence both species apply thermals for soaring flight most of the time of their daily activity. Several authors evidenced that vultures prefer technogenic artificial thermals (which are much stronger than natural ones) in surroundings (Freire *et al.*, 2015; Novaes and Cintra, 2013). For Turkey vultures was found even prolongation of their soaring activity over the technogenic thermals with illumination after sunset (Mandel and Bildstein, 2007).

However we did not find the researches exploring the dependence of vultures on thermals and their choice the strongest thermals by means of statistical or GIS analyses. We suppose that our investigation is the first confirmation of this behavioural pattern precisely by means of statistical and GIS methods.

### **The possible reasons of low positive relationship between intensity of soaring flights of Black vultures and thermal strength**

In both parts of our investigation we confirmed the hypothesis, stating that Black vultures tend to choose the strongest thermals in surroundings by the evidence of positive relationship between parameter, reflecting the intensity of soaring flights of vultures over the territory ( $F_{birds}$  index in the first part of the study, considered in Chapter II, and  $W_{birds}$  index in the second part of the study, considered here) and parameter, reflecting the strength of thermals (the [solar activity](#) and [wind speed](#) parameters in the first part of the study and the [contrast of surface temperature](#) in the second part). However, the degree of positive relationship was not strong in both cases. However, the following reason can lead to a decrease the degree of positive relationship between abundance of soaring vultures and thermal strength:

(i) The territory which does not have strong triggers producing thermals will also form thermals, but they may not locate in the permanent positions on the ground (Angevine, 2014).

Our spatial analysis, basing on the numerical estimation of the contrast of surface temperature, may not detect the bird's attraction to the strongest thermals for those areas.

(ii) The threshold value of thermal strength determining the behaviour of Black vultures may exist. Birds may not be attracted to a thermal if it is only slightly stronger than the nearest thermals.

(iii) Thermals are not the only factor governing the behavior of vultures. In some cases their flying behavior and spatial distribution over ground may depend on some other factors.

(iv) In Amarais site the highly urbanized lands were unattractive for Black vultures and, at the same time, they have the highest values of contrast of surface temperature.

Basing on these arguments it can be assumed, that even a low confidence level that was obtained allows suggesting that Black vultures tend to choose the strongest thermals in surroundings for soaring flight. For this reason the outlined direction has a great potential for further study in order to develop the practical application of these behavioural traits for reduction the hazard of collisions with vultures.

### **The possibility of forming the high risk of collision with vultures over the technogenic thermals**

Whereas natural thermals, as a result of solar heating, work only in daily hours, the technogenic thermals (generated by industrial heating, like power station, industrial pipe, etc.) may work during all night. We assume that over technogenic strong thermals with illumination (or maybe even without it) Black vultures can prolong their soaring activity even after sunset. The technogenic thermals may have the extremely high density of birds above them at night time, because all others thermal do not operate at dark hours and they can attract birds from large surroundings. This suggestion follows from observations of Mandel and Bildstein (2007) and Freire *et al.* (2015) as well as by our own results, which confirmed the hypothesis that Black vultures prefer the strongest thermal for soaring flight.

## **5.2 Dependence of soaring activity of Black vultures on landscape type (surface covering and anthropogenic pressure)**

The landscape analysis showed the attractiveness of various landscape types for soaring Black vultures within two study sites. The common features and the differences between them were identified.

### **Common features**

The following common features were detected:

1. In both study sites the high level of attractiveness was detected for areas containing **water reservoirs**. It was detected for both clean and polluted water objects. However above

clean water objects the concentration of vultures was higher than above water with technogenic pollution. This conclusion was confirmed by our observation of the clear preference of Black vultures the narrow strip of forest fragments, wetlands and clean water bodies (ponds and river) for soaring flight. Whereas sky above the large agricultural field and town (adjacent to this strip) was completely devoid of soaring vultures within the horizon of visibility<sup>35</sup>. We suppose that the high attractiveness of water bodies for soaring vultures can be explained by the increased contrast of superficial temperature forming in daily hours over the boundaries between cold water body and heated dry land. The high contrast of superficial temperature produces strong thermals, which can attract vultures from adjacent areas. Another possible reason of high attractiveness of areas containing water reservoirs for vultures is the needs of birds of clean drinking water. According to our personal observations in the area of Campinas city Black vultures specially sit on the ground near the pond with clean water and drink it.

2. For both study sites the high level of attractiveness of vultures was identified for the areas containing *automobile roadways*. This can be explained by food attractiveness of those objects, because the scavengers can often find dead animals on the highways. Also it can be caused by generation of thermals over roads, - the asphalt roads due to their increased heating in comparison with adjacent lands can become trigger for thermals.

3. In both sites the low attractiveness of soaring vultures - “neutral” (Amarais) and “less than neutral” (Prudente) level of attractiveness by our classification) were detected over the pure natural landscapes (without water reservoirs). However, most of the birds in both sites were recorded above natural landscapes: in Amarais - 57.83% , in Prudente - 40.07% of all recorded birds (Tables 3.11, 3.12). From this we can suppose, that natural landscapes are attractive for Black vulture, but the level of concentration of soaring birds above them is low in comparison with other landscapes for the reason that the flying birds scatter within the large expanse of these lands.

4. In both sites the low attractiveness (“less than neutral” by our classification) was detected for *dense residential* landscapes. It can be explained by several unfavourable factors of those lands for vultures: disturbance from people and vehicles, lack of high trees and clean water bodies, which are essential for resting and drinking, small quantity of food sources (animals killed by roads are quickly removed from the residential lands and the large food dumps were absent on the study sites).

---

<sup>35</sup> This observation was considered in Chapter II , div 4.4.

### Different features

The *soft urbanized* and *industrial* landscapes in Prudente have the higher level of attractiveness, than in Amarais. In Amarais the *natural* landscapes have the “neutral” level of attractiveness, while in Prudente – “less than neutral” (Figs. 3.9-3.11). Both differences can be explained by the reason that urban lands in Amarais site occupy large uninterrupted space and impact on the environment much more negatively than small urban zones in Prudente site surrounded by natural and rural territories. This difference causes that urban zone is unattractive for vultures in Amarais site and attractive for them in Prudente site<sup>36</sup>. The *soft urbanized* landscapes are mainly bordered by highly urbanized areas in Amarais, but surrounded by natural lands in Prudente. For those reasons, the *industrial* and *soft urbanized* landscapes can be less attractive for Black vultures in Amarais than the same landscapes in Prudente.

The higher attractiveness of natural landscapes in Amarais than in Prudente can be explained by the reason that in Amarais the area of natural lands is much smaller than in Prudente, as well as it is surrounded by highly urbanized territories, which are unattractive for vultures. This could cause the higher concentration of birds above natural lands in Amarais, than in Prudente.

### 5.3 Influence of anthropogenic pressure on soaring activity of Black vultures

For Amarais it was revealed, that increase of anthropogenic pressure of the environment leads to reduction of the intensity of soaring activity of vultures over the area. For Prudente it was detected the opposite - the increase of anthropogenic stress leads to the growth of the soaring activity of vultures over this area. Below are listed the evidences which allow to make this conclusion:

a. For both study sites the factor and correlation analyses detected the inverse relationship between the intensity of soaring flights (expressed in  $W_{birds}$  index) and [surface temperature](#). It was higher for Amarais and smaller for Prudente. At the same time, the factor analysis showed for Amarais a high positive relationship between [anthropogenic pressure](#) and [surface temperature](#), while for Prudente a small negative relationship between the same variables (Table 3.4). This allows concluding that in Amarais the stronger level of anthropogenic pressure corresponds to the higher surface temperature. This could be the evidence that impact of urban areas on the environment here is very strong, as they produce a lot of technogenic heat. In Prudente the level of anthropogenic pressure did not show a positive correlation with surface temperatures. That can be interpreted as a weak negative impact of the urban areas on the environment around the Presidente Prudente airport.

<sup>36</sup> We revealed this fact in our study by several evidences listed below.



b. The factor analysis detected for Amarais a high negative relationship between *level of anthropogenic pressure* and  $W_{\text{birds}}$ , while for Prudente a high positive relationship between the same variables (Table 3.4)

c. The opposite trends of the soaring activity of Black vultures during cold months occurred from April to August in Amarais and Prudente (Figs. 2.18, 2.19). It can be explained by the migration of part of the local populations of Black vultures from areas with high anthropogenic pressure to natural and rural territories (it was considered in Chapter II).

d. The landscape analyses showed that the *soft urbanized* and *industrial* landscapes in Prudente have a high level of attractiveness, while in Amarais – a small level of attractiveness (“neutral” or “less than neutral”). Also, it showed that in Amarais the *natural* landscapes have higher level of attractiveness than in Prudente.

We suppose that the different reaction of the intensity of soaring flights of Black vultures on the anthropogenic stress can be explained by the distinct level of negative impact on the environment of highly urbanized lands in both study regions.

In the Prudente site the highly urbanized landscapes consist from relatively small spots surrounded by natural and agricultural lands. They are probably not very aggressive to the environment. Also they can produce the increased heating. As a result, the birds from the neighbor natural lands can be attracted to thermals created by them. In contrary, in the Amarais site the highly urbanized lands, with the inclusion of large industrial zones, occupy huge uninterrupted territories. For this reason the negative influence of highly urbanized landscapes on the environment in Amarais is much stronger, than in Prudente. Hence, the highly urbanized lands are unattractive in Amarais and attractive in Prudente.

Summarizing this comparison, we can make the general conclusion **that highly urbanized landscapes (industrial and dense residential areas) can provide the increased attraction for vultures, but only if human impact on the environment is not very strong and if the urban districts occupy relatively small areas and surrounded by natural territories**. Urban areas, which provide a strong negative impact on the environment and, at the same time, occupy large uninterrupted territories, are unattractive for vultures, i. e. they have a low density of flying birds above them or none of them at all.

We suppose that several questions studied in our investigation are new input for the Black vulture behavior research. Among them there are the study of vulture’s migration between urban and natural landscapes; the study of the level of attractiveness for vultures on different types of surface covering; the influence of anthropogenic stress on soaring activity; the study of the seasonal difference on the soaring activity of both species and the dependence of vultures from

thermals. Those behavioural traits were considered in literature previously, but only as general description of species properties. Thus, many authors evidenced that Black vultures inhabit both natural and urbanized environment (Buckley, 1999; Novaes and Cintra, 2013; Mandel and Bildstein, 2007; Bastos, 2001) and note that these birds are active throughout the year (Buckley, 1999; Peterson, 2001). Several authors evidenced the dependence of vultures from thermals, which was considered above.

We explored these behavioural characteristics with more details and accuracy by statistical and GIS analysis. In this regard, we emphasize the importance of the elaborate methodological approaches that we used for our investigation. They consist in the preparation of birds' observation data to statistical analysis with various environmental characteristics by means of georeference of all data and preliminary processing through GIS software. These approaches allow to identify and accurately describe the various new features of the bird's behaviour.

#### **5.4 The cartographical assessment of risk of collision with Black vultures over the territory**

By means of cartographical visualization of  $W_{birds}$  index, we constructed the maps predicting the risk of collisions with vultures over the territory. We built those maps for both model airports in a small scale with less precision and details (Figs. 3.12, 3.13) and in a large scale with high precision and details (Fig. 3.14, Fig. 3.15). The maps show by color the value of  $W_{birds}$  index, which can be interpreted as the level of probable risk of collisions with Black vultures over each point of the surface at future.

This methodology can be used to construct the risk assessment maps for any airport's vicinities or other area to assess the threat of collisions with different avian species. Also those maps with combination of GIS and statistical analytical instruments can be applied to study the relationships between intensity of bird's flights over the territory and various superficial, atmospheric and anthropogenic characteristics.

The studied areas of most of previous researches which constructed the GIS databases and maps of flying birds in order to reduce the number of aircraft collisions with birds, were very large, about large part of a continent (Kelly, 2005; Anagnostopoulos, 2000; Gard et al., 2007; Gray, 2003; Leshem et al., 1998; Buurma, 1999; Walter et al. 2012). It is obviously that cartographical assessment in such a small scale will not allow to estimate the threat of collisions for each specific airport within the studied territory. This allows concluding that our methodology of mapping the risk assessment which can estimate this risk for a small area, provides a new and helpful methodological contribution for the solution of the problem of collision with birds.

## 5.5 Practical recommendations

Basing on the results of both parts of our investigation, we formulated the practical recommendations and suggestions about the possible measures of reduction the number of aircraft collisions with Black vultures, Turkey vultures and other bird species. They are intended for airport administrators, aircraft pilots, researchers and specialists working for bird strike problem.

### 5.5.1. General recommendations

1. To consider the daily period of soaring activity of vultures (1 - 1.5 hours after sunrise to 1 - 1.5 hours before sunset) and the altitudes used for soaring flights (13-300 m - the most probable; 300-550 m - the less probable) in tracking the routes for aircrafts of takeoffs and landings operations.
2. To consider that surface objects heating stronger than adjacent areas (*hotspots*), can become *triggers* for thermals formation over them. Thermals, in their turn, can form the increased concentration of soaring vultures, i.e. provide the high risk for aircraft flights. The main indicator of thermal strength is the **contrast of surface temperature**. The higher is the temperature contrast, the greater is the possibility of thermal formation over this hotspot and the stronger could be this thermal (Angevine, 2014). **Since vultures tend to soar within the strongest thermals in surrounds** (we confirmed this in our research), the biggest concentration of soaring vultures and associated risk of collisions can form over the places with **highest contrast of surface temperature** in surroundings. Triggers, launching the strong natural thermals, are represented by the boundaries between different types of surface covering, producing high contrast of surface temperature. These are the isolated technogenic construction made from concrete, asphalt or metal; the coastal line of water bodies; wood edge; ploughland edge; border between mountain slopes of different exposure. The **technogenic thermals** (i.e. thermals produced by industrial heating) can be the most threatening for aircrafts flying, since they can provide an extremely high concentration of birds within them. Also, they can attract birds and be dangerous for aircraft flights not only in daily hours (like natural thermals), but at night time as well.
3. To consider that **water bodies** and **automobile roads** were detected as the most attractive surface object for soaring vultures.

### 5.5.2 Proposed measures for reduction the risk of collision with Black vultures

1. We observed and confirmed by the results of other researches, that presence of abundant source of food on the surface almost completely cleans the sky in surroundings from

soaring Black vultures (Chapter II). This allows to suppose that presence of soaring vultures at sky means the absence of abundant food for these birds on the ground. Therefore, even if all food sources will be removed from the surface, the soaring vultures will be present at sky, since they soar for searching the food.

We suppose that complete removal of soaring vultures from sky over important lands can be achieved by placing of abundant food for birds (like carcasses) in special places. Those feeding points could attract vultures from neighborhoods and remove them from sky over the territories intensively used by aviation. The long-term experience of “vulture restaurants” established in European countries for the restoration of vulture populations (Cortés-Avizanda et al. 2010; Piper, 2006; Deygout et al. 2009; Ogada et al. 2012), may be helpful for elaboration the system of feeding stations cleaning the sky from soaring vultures over the most important lands.

2. The novel methodological approaches elaborated in our study, basing on combined application of GIS and remote sensing technologies for spatial data processing,<sup>37</sup> can be used for study the relationships between abundance of flying birds over the territory and various environmental factors; estimation the relative attractiveness of landscape types for flying birds; reveal the distribution of flying birds over territory, predicting and mapping the risk of collisions with birds for aircrafts. We recommend to involve these methods in solution of the bird strike problem for Black vulture and other bird species.

**To increase the precision of maps predicting the risk of collision with birds we recommend the following:**

- (i) To reduce the distance between observation points up to 1400-1500 meters. In this case, areas of high-accuracy observations will connect with each other and the whole area will be covered by the high quality monitoring. Examples of risk assessment maps of high accuracy constructed for the circular zone of 700 m radius around two observation points are presented on Fig. 3.14(a), Fig. 3.15(a). We did not build map of the high accuracy for all study territory because of the large distance between observation points in our study (about 6000 m).
- (ii) To apply the modern electronic equipment allowing the georeferencing of flying birds with high accuracy (the *electronic laser range finders*, *video registration*, *radiolocation*). However, we cannot say for sure that this equipment would allow recording all birds flying around the observer quickly enough; it should be tested.

---

<sup>37</sup> The methodological approaches are considered in the “Materials and methods” section of Chapter II and Chapter III. Also we considered them in general in the Chapter IV.

Also, it is necessary to take in mind that the use of these techniques will make the research more expensive.

## 6. Conclusions

1. The significant relationship between intensity of soaring flights of Black vultures and contrast of surface temperature was detected. Basing on the properties of thermals, this finding was interpreted as the dependence of soaring activity of vultures from thermals strength. At the same time it was considered as the second confirmation of the hypothesis, stating that Black vultures tend to soar over the strongest thermals in their surroundings. This hypothesis was confirmed in our study by dint of two independent methods basing on two different databases (meteorological characteristics and surface parameters), which proves the correctness of this conclusion.
2. Water bodies (both clean and polluted) and automobile roads were detected as the most attractive objects for soaring Black vultures.
3. The intensity of soaring flights of Black vultures demonstrated the inverse ratio with the area of uninterrupted highly urbanized lands together with their negative impact on the environment.
4. The novel methodological approaches of data processing, basing on the combined application of GIS and remote sensing technologies were elaborated. They allow to numerically estimate and cartographically visualize the risk of aircraft collisions with birds above the airports surroundings, as well as to study the dependence of intensity of soaring flights of birds over the territory from superficial, atmospheric and anthropogenic factors. Those methods can be used to reduce the hazard of aircraft collisions with various avian species in any geographical region. The techniques can be used directly or can be adopted for specific features of any airport and geographical region.
5. The practical recommendations and suggestions of reduction the number of aircraft's collisions with vultures were formulated.

## CHAPTER IV

### **Application of GIS and remote sensing technologies in the analysis studying the relationship between spatial distribution of flying birds and environmental factors**

*Paper intended for the Journal Applied Geography*

#### **Key-words**

*Geographical Information System, GIS, remote sensing, satellite imagery, ASTER, thermals, Black vulture, Coragyps atratus, aviation hazard, bird strike problem, bird hazard control, risk assessment map.*

#### **1. Introduction**

The increasing number of aircraft collisions with birds near airports, caused by general growth of aircraft traffic and birds populations, is a big problem for many countries all over the world. Most of strikes with birds occur during takeoffs and landings operations within zone of 10-20 km around the airports, where aircrafts fly at low altitudes. National research programs and international committees have been launched in several countries in order to find a solution of bird-strike problem and reduce the numbers of bird strike events (Buurma, 1999; Kelly, 2005; Herricks, 2005). Since this problem has a global international character, it is very important to join forces in its solution. First of all it is necessary to elaborate methods which would allow to study the factors causing the concentration of flying birds over a given area; to estimate, predict and map the risk of collision over the area; to clean the sky from flying birds from the areas intensively used by aircrafts for takeoff and landing operations where they fly at low altitudes and exposed to the danger of collision with birds.

We elaborated a set of novel methodological approaches of spatial data processing, basing on the combined application of GIS and remote sensing technologies, which will be helpful for the listed purposes. They allow to numerically estimate and cartographically visualize the risk of aircraft collisions with birds above the airports vicinities (or any other territory), as well as to study the relationships between intensity of bird's flying over the territory and various superficial, atmospheric and anthropogenic characteristics of the environment.

Here we consider the general principles of the elaborated methods and stages of their implementation for data processing in our investigation, which illustrate the capabilities of the approaches.

## 2. General stages of investigation, basing on the elaborated methodological approaches

The main objectives of our investigation was study the relationship between the intensity of soaring flights of Black vulture and basic meteorological, superficial and anthropogenic factors<sup>38</sup> of the environment. The study was implemented within surroundings of two Brazilian airports, taken as model areas. The elaborated methods, combining GIS and remote sensing technologies were used as a main research instrument. The principal stages of our investigation, basing on those methods, were the following.

1. We joined in the **summary georeferenced databases** (shapefiles<sup>39</sup>) three types of original data: (i) recorded and georeferenced<sup>40</sup> birds which were joined with meteorological characteristics measured synchronously with the bird's observation (Supplementary Files SF2); (ii) recorded and georeferenced birds which were joined with surface parameters obtained from satellite images<sup>41</sup> (Supplementary Files SF15). Those shapefiles for each observed bird contain in tabulated form its geographical coordinates (latitude, longitude, altitude above surface), time of observation, meteorological characteristics and superficial parameters of the “spatial unit” above which the bird was located in the moment of registration.

2. Two parameters indicating the intensity of soaring flights of vultures over the territory were applied for implementations the statistical and graphical analyses. Both of them were calculated by the specific equations, considered in Chapter II and Chapter III. The **“Frequency of soaring birds records”** or  $F_{birds}$  index (Eq. 6) was used to study the dependence of soaring activity of birds from meteorological conditions. It represents the number of birds recorded during a chosen period of time (15 min or 1 hour) averaged by a chosen number of months in a chosen geographical area. The **“Weight of birds” index or  $W_{birds}$**  index (calculated by Eq. 8) was used for studying the dependence of soaring activity of birds from superficial conditions. It was calculated for each “spatial unit” (a small piece of surface georeferenced in GIS) and

---

<sup>38</sup> The meteorological characteristics are the following: wind speed, wind direction, air temperature, solar radiation, solar energy, atmospheric pressure, relative humidity. Superficial parameters are the following: surface temperature, contrast of surface temperature, altitude above sea level, slope direction, slope inclination, landscape type (consists from type of surface covering and level of anthropogenic stress).

<sup>39</sup> The shapefile (or “shape file”) is a popular format of files in GIS software. It is a **georeferenced database** consists from two elements: the **georeferenced vector objects** (which can be of three types - point, line and polygon) and the **attribute table** which has all data of the objects in tabulated form of numerical or text format. The attribute table can be transferred to any other software for a subsequent processing (including statistical software, Excel, Word).

We call the shapefile as the **“summary georeferenced database”** and its attribute table as a **“summary database”**.

<sup>40</sup> The georeferenced object – object with determined geographical position (coordinates latitude and longitude) and represented in GIS map as a vector object (point, line or polygon) in a shapefile or other GIS format.

<sup>41</sup> The methodology of obtainment of surface parameters from the remote sensing products is considered in Chapter III

represents the total number of the flying birds that were recorded and could be located exactly above this unit of surface during the chosen period of time (a month, set of months, a year).

3. The statistical and graphical analyses were implemented on the basis of the [summary georeferenced databases](#) for each studied region. They were devoted to study the relationship between intensity of soaring flights of vultures above area and different meteorological, superficial and anthropogenic characteristics of this area. Also, the analysis estimating the different types of surface covering by their attractiveness for vultures was conducted and the most attractive landscapes for birds were showed.

4. Finally the maps, visualizing the  $W_{birds}$  indicator and giving the numerical estimation of the risk of collisions with birds for each spatial unit of the studied territory were constructed.

### 3. Linking the different types of parameters in a single georeferenced database

The main principle of the elaborated approach is the combination of **georeference** and **time reference** of different types of explored parameters and forming from them a [summary georeferenced database](#) (shapefile), which can be visualized and processed in GIS as a map; and can be processed and analyzed in statistical software as an attribute table. The procedure of georeference includes the determination of the geographical coordinates (latitude and longitude) of the observed objects and their representation in GIS. The time reference implies the linking of the observed objects by the *identical period of time*<sup>42</sup> of their observations.

The result of georeference and time reference procedures was obtainment of the [summary georeferenced database](#). It is a shapefile consists from all studied parameters linked with each other by the identical geographical position and identical time of observation. Its attribute table (entitled here as the “[summary database](#)”) contains all data in tabulated form of numerical or text format. This table is the basis of statistical and graphical analyses implementation, study the relationship between parameters included in it. The statistical processing can be realized in the special software (R, SPSS or other), as well as implemented in ArcGIS software. The latter has a rich set of tools permitting the different methods of geospatial analysis, mapping and 3d models creation, which greatly expand the capabilities of data investigation and allow visualising the samples of the summary georeferenced database in various combinations.

In our investigation we linked three types of parameters in a summary georeferenced database to study the relationship between flying bird’s activity and environmental

---

<sup>42</sup> The duration of the “identical period of time” for linking of gathered data is chosen by the researcher. It corresponds with the character of data and the objectives of the investigation. It can be year, month, date, date and hour, date and hour and interval of minutes or even smaller. In our study we joined data of the bird's census made in identical day and 15-minutes interval of a day. For example, we joined in two separate groups the birds registered in 20.09.2012 15:45 and the birds registered in 20.09.2012 16:00.



characteristics. These are the georeferenced bird's census, the meteorological characteristics collected together with the bird's observation and the surface parameters revealed from the satellite images. The set of the studied parameters is determined by the research's objectives and can be different.

#### 4. Method of georeference of birds registered as points and as polygons

The georeference of a studied object (a flying bird in our case) to a vector **polygon**, instead of its georeference to a vector **point**, - is one of the important findings of the elaborated approaches. We used it for taking into account the uncertainty of the geographical positions of the recorded birds, which we obtained in our investigation. The complexity of our observed object (the groups of birds flying at different altitudes) allowed detecting only the **intervals** of parameters, from which the geographical coordinates of birds were calculated (distance, vertical angle and compass direction). For this reason, only a **region of a surface** (a “polygon” in GIS terms) can be identified for each soaring bird as a position of its location at the moment of registration. In our case (our observation were conducted from the viewpoints in a radius of visibility through the binocular), each “*projected polygon*” – is a projection of the hemisphere's segment within which a flying bird was located at the moment of registration on the earth surface (the viewpoint where the observer stood was the center of this hemisphere). It is a sector truncated by two circumferences (when the vertical angle to a bird was 5-85°), and a circle (when the vertical angle to a bird was equal to 90°) (Fig. 3.5; Fig. 3.6). This method allows not only to determine the uncertainty of bird's georeference, but also to include it in the analyses and map constructions, which increase their accuracy<sup>43</sup>.

For clarification of the principle of georeference to polygons and their subsequent treatment, let's consider the example of a research task with two possible ways of georeference the movement of the explored animal: through a point (implemented by GPS collar, which records the precise geographical coordinates of animal location), and through a polygon (when the observed animal is determined only within a region of surface, like it was in our investigation). For both cases we want to study how the movement of this animal depends from the surface temperature.

In the first case the collected set of animal's positions recorded precisely by GPS collar we put on GIS map as vector points of the point shapefile. To show how the animal's movement depends from the surface temperature, we put the resultant shapefile of animal's positions on a

---

<sup>43</sup> Georeference of the observed flying Black vultures to polygons and preparation of the summary georeferenced databases which became the basis of the analyses and risk map's construction, are considered in Chapter III.

raster of superficial temperature (created, for example, from ASTER satellite image) and for each point of animal's location (for each vector point of the resultant shapefile) we obtain the unique value of the surface temperature. It will be the surface temperature value **of the pixel** of the raster on which this point stands.

In the second case, for each projected polygon of the studied animal we must assign the values of surface temperature of **all pixels** of the raster that **locate inside this polygon**. To prepare data for statistical analysis we can include in the table (instead of values of all pixels in the polygon) the average temperature of all pixels within the polygon, or the maximum temperature from of all pixels within the polygon; or the minimum temperature from all pixels within the polygon; or apply other processing procedure of values of a raster (or a vector) objects within the projected polygon. Our choice will be depended from the research objectives.

The spectrum of environmental factors, which can be investigated in their relationship with the distribution of the studied object by its georeference to polygons (or to points, in case of use of GPS collars or other technical equipment allowing the exact georeference), is very broad. Those parameters can be the relief, temperature and meteorological characteristics, anthropogenic pressure (for example, level of pollution, level of environmental perturbation), surface covering, as well as the observed data of others species of animal and plants. The “studied object” may also be very different – an individual of animal or plant, populations of animal or plant, a range of species or any other. We can study the separate locations of the object or its movement over the surface.

## 5. Implementation of analyses and risk assessment maps basing on the summary georeferenced database

The processing of the [summary georeferenced database](#) allowed conducting the statistical and graphical analyzes exploring the relationship between parameters included in it. By dint of several analyses we studied the dependence of the intensity of soaring flights of Black vultures from various meteorological and superficial conditions. For implementing those analyses the indicators of intensity of soaring flights of birds over the territory ( $W_{\text{birds}}$  and  $F_{\text{birds}}$ ) were applied.

Cartographical visualization of  $W_{\text{birds}}$  indicator in GIS allows constructing the maps of the numerical assessment of the risk of collision with vultures above each spatial unit of the territory surrounded airport. The “[risk assessment maps](#)” are one of the important results of our work, which can help to elaborate more secure aircraft tracks<sup>44</sup>.

---

<sup>44</sup> The methodology of the “risk assessment maps” construction, the accuracy questions and our recommendation about construction of high accuracy map for the entire territory of airport's surroundings are considered in Chapter III.

The combined application of  $W_{birds}$  index and the [summary georeferenced database](#) allows estimating the attractiveness of different types of surface covering for Black vultures. By this approach we detected the highly attractive types of surface covering which can form the increased concentration of vultures above them. We suppose that by dint of this approach it will be possible to implement a more accurate and detailed assessment of the attractiveness of various landscape types for bird species. This technique can be applied for comparing the attractiveness of several landscapes within the same region, and to compare the level of the relative attraction of the identical landscape in different regions. We suppose that the elaborated method of landscape analyses<sup>45</sup> provides the additional possibilities to predict the increased concentrations of birds in any specific region, which also can be used to reduce the risk of bird collisions with aircraft.

## **6. Technique of the remote sensing data processing for detect the possible locations of the strongest thermals**

Our results and data of other researchers allow to assert, that strong thermals may form the increased concentration of vultures soaring inside them and, for this reason, can be especially dangerous for aircrafts flights. Especially threatening could be the artificial thermals generated by technogenic heating. Unlike natural thermals they can be dangerous not only in daily hours but at night time as well (Chapter III). This information can be used to reduce the hazard of collision by means of mapping the location of strongest thermals (especially strong technogenic ones) and exclusion these spots from the aircraft routes.

To do this it is necessary to identify and mapping the location of the strongest thermals on the earth surface. This can be implemented either by analysis of the surface temperature of the territory and identification the *hotspots* (spots having the higher surface temperature than adjacent areas) or by identification the vertical warm air fluxes themselves.

We elaborated a simple technique of processing data of the remote sensing product, allowing to detect the spots on the surface with the higher probability of strong thermals formation over them. Those maps also can be considered as a prediction of the spots with high concentration of vultures over them (in contrast with the “risk assessment map” without field observation of flying vultures).

We calculated the “[contrast of surface temperature](#)” parameter from the surface temperature raster (AST\_08), produced from ASTER image<sup>46</sup>. This raster transformation was

---

<sup>45</sup> The method of landscape analysis is considered in Chapter III.

<sup>46</sup> We used directly the AST\_08 derivative product of ASTER image to be sure of the correctness of the surface temperature map preparation from the TIR bands of the image. Other satellite images may not have ready products

implemented in ArcGIS software by means of Slope Tool (Chapter III). The obtained **contrast of surface temperature** parameter represents a rate of maximum change in the temperature value from each cell to its eight neighbors or, in other words, it shows the **highest temperature contrast** between each cell to its eight neighbors for imaged territory.

According to the physical properties of thermals: “the higher is the contrast between surface temperature of a hotspot and surface temperature of its adjacent lands, the higher is the possibility of thermal formation over this hotspot and the stronger could be this thermal” (Angevine, 2014), we can suppose that the **strongest thermal will form over the highest value of the contrast of surface temperature parameter** represented on GIS map. This method can also help to reveal the location of the technogenic thermals, generated by industrial heating. These spots may have the extremely high (in compare with other territory) value of the contrast of surface temperature parameter on a map. The resultant contrast of surface temperature maps for both study sites are presented in Supplementary Files SF21, SF25 and visualized on Figs A.4, A.5, A.8 of Appendix.

It is important to note that we did not test this technical approach in practice, because it is a complicated task that requires an independent research. Also we suppose that application of satellite images with the spatial resolution of thermal bands higher than ASTER image will allow increasing the accuracy of thermal identification on the surface<sup>47</sup>.

## 7. Discussion

Comparison of the elaborated methodological approaches with methods applied in other researches, devoted to seeking the possibility of reduction the number of aircraft collisions with birds (Kelly, 2005; Anagnostopoulos, 2000; Gard et al., 2007; Gray, 2003; Leshem et al., 1998; Buurma, 1999; Walter et al. 2012), permits to conclude that our technical developments provide a new and helpful contribution for the solution of the bird strike problem. The reasons are the following:

- In most of the reviewed projects the GIS databases of flying birds and the resultant maps were implemented for a huge area (a large part of a country). It is obviously that study in such a small scale will not allow estimation the threat of collisions for each specific airport within the studied territory. Consequently, it cannot significantly help to elaborate methods

---

represented the surface temperature. In this case the preliminary image processing and the surface temperature map constructing from thermal bands will be necessary to implement by your own.

<sup>47</sup> The ASTER image used in our study has a spatial resolution of thermal infrared (TIR) bands equal to 90 meters (i.e. 1 pixel of image represents a square on surface with a side equal to 90 meters). It is possible to use satellite imagery with thermal bands with resolution much higher (up to few meters), however this kind of satellite imagery can be rather expensive.

of reduction the number of collisions with birds in airports vicinities where the most of the strikes with birds occur.

- We did not find works exploring the dependence of flying activity of birds from superficial, meteorological and anthropogenic characteristics of the territory. However, those features can be very important for understanding the causes of distribution of the bird's concentration over the territory and prediction the hazard of collisions. Also this knowledge can help to elaborate methods of management of the flying bird's location for cleaning from them the critical lands intensively used for aircrafts flying.
- Finally, we did not find any significant application of the remote sensing technologies and satellite images (which can give a lot of information about the superficial characteristics) in the studies related to the bird strike problem.

## 7. Conclusions

The elaborated methodologies permit to connect the heterogeneous parameters of the environment (differing by essence of data, accuracy and time of observation) through the identical geographical position of their objects, into a single system - summary georeferenced database or shapefile. Processing of this shapefile and its attribute table, containing the information about the explored parameters in tabulated form, in GIS and statistical software, allows to implement statistical, graphical and geospatial analyses; create maps and 3d-models; study the relationship between parameters included in this system.

The GIS instruments permit to choose samples from the full georeferenced database by time of observation, geographical position and characteristics of studied objects (for example, color, size, age, accuracy of observation, etc), which permit to conduct analyses and create related maps, 3D models and graphics with high flexibility.

We suppose that the developed methods can be a helpful practical contribution to the common fund of knowledge devoted to the solution of the bird strike problem. They can be applied to reduce the hazard of aircraft collisions with various bird species in any geographical region. The techniques can be used directly or can be adopted for specific features of any airport and geographical region. Also, they can be applied for various environmental investigations. They can permit to identify new scientific information about studied objects (that may be individuals, groups of individuals, populations, biome, a phenomenon of nature), which cannot be obtained without involvement of GIS and Remote sensing technologies.

## FINAL CONCLUSIONS

1. The most common altitude of soaring flight of Black vultures ranges from 13 to 300 metres, the height from 300 to 550 metres is less used, and above 550 metres is improbable.
2. There were two types of daily soaring activity: plot with morning and afternoon peaks and notable drop at midday and plateau-like plot with a single smooth peak at midday. At both types, about 1- 1.5 hours after local sunrise the soaring activity starts and about 1 - 1.5 hours before local sunset the soaring activity finishes. The sky should be completely safe from soaring vultures in dark and twilight hours between local sunset and sunrise at normal conditions (i.e. without presence of technogenic thermals).
3. The abundant source of food on the ground attracts Black vultures from large distances, which leads to temporal disappearance of soaring birds above a large area. It means that concentration of soaring vultures at sky evidences the lack of abundant food for these birds in availability.
4. The strong anthropogenic stress in combination with large area of uninterrupted highly urbanized lands is a negative factor for Black vultures that reduce the number of soaring birds. In contrast, small islands of highly urbanized lands, surrounded by natural and rural areas, are highly attractive to these birds. Most clearly this behavioural pattern is apparent in cold months. In this period of the year vultures tend to migrate from expanded highly urbanized lands to natural and rural regions with inclusion of small urban zones. This behavioural pattern can be explained by ecological adaptation of Black vulture as avian scavenger to minimize energy loss.
5. The air temperature, air humidity, atmospheric pressure, wind direction do not influence the soaring behaviour of vultures. The intensity of soaring flights demonstrates the significant dependence only on solar activity and wind speed parameters, both of which were interpreted as the indicator of thermal strength. This finding was considered as the first confirmation of the hypothesis stating that Black vultures have a tendency to choose the strongest thermals in their surrounding for soaring flight.

6. The significant relationship between intensity of soaring flights of Black vultures and contrast of surface temperature was found. Basing on the properties of thermals, this finding was interpreted as the dependence of soaring activity of vultures from thermals strength. At the same time it was considered as the second confirmation of the hypothesis, stating that Black vultures tend to soar over the strongest thermals in their surroundings. This hypothesis was confirmed in our study by dint of two independent methods basing on two different databases (meteorological characteristics and surface parameters), which proves the correctness of this conclusion.
7. Water bodies (both clean and polluted) and automobile roads were detected as the most attractive objects for soaring Black vultures.
8. The novel methodological approaches of data processing, basing on the combined application of GIS and remote sensing technologies were elaborated. They allow to numerically estimate and cartographically visualize the risk of aircraft collisions with birds above the airports surroundings, as well as to study the dependence of intensity of soaring flights of birds over the territory from superficial, atmospheric and anthropogenic factors. Those methods can be used to reduce the hazard of aircraft collisions with various avian species in any geographical region. The techniques can be used directly or can be adopted for specific features of any airport and geographical region.
9. The practical recommendations and suggestions of reduction the number of aircraft's collisions with vultures were formulated.

## REFERENCES

### Papers

- Akos Z, Nagy M, Leven S, Vicsek T, 2010. Thermal soaring flight of birds and unmanned aerial vehicles. *Bioinspiration and Biomimetics*, Volume 5. Number 4 , 12 pp.
- Akos Z, Nagy M, Vicsek T, 2008. Comparing bird and human soaring strategies. *Proc Natl Acad Sci USA*, 105: 4139-4143.
- Angevine W.M. 1998. The Flatland Boundary Layer Experiments. *Bulletin of the American Meteorological Society*.
- Avery, M. L., J. S. Humphrey, T. S. Daughtery, J. W. Fischer, M. P. Milleson, E. A. Tillman, W. E. Bruce, and W. D. Walter. 2011. Vulture flight behaviour and implications for aircraft survey. *Journal of Wildlife Management* 75:1581-1587.
- Avery M.L. , Cummings J.L., 2004. Livestock depredations by black vultures and golden eagles. *Sheep and Goat Research Journal* 19: 58-63.
- Bastos, L. C. M. 2000. Brazilian avian hazard control program - educational initiatives. *International Bird Strike Committee*, Amsterdam.
- Bastos, L. C. M. 2001. Successful actions for avian hazard control in Brazil. *Bird Strike Committee-USA/Canada, Third Joint Annual Meeting*, Calgary, AB. Paper 3.
- Beauchamp G. 1999. The evolution of communal roosting in birds: origin and secondary losses. *Behavioral Ecology* 10 (6): 675-687. doi:10.1093/beheco/10.6.675.
- Blackwell B. F. and Wright S. E. 2006. Collisions of Red-tailed Hawks (*Buteo jamaicensis*), Turkey Vultures (*Cathartes aura*), and Black Vultures (*Coragyps atratus*) with aircraft: implications for bird strike reduction. *Journal of Raptor Research* 40:76-80.
- Buckley N.J. 1996. Food finding and the influence of information, local enhancement, and communal roosting on foraging success of North American vultures. *The Auk* 113 (2):473-488.
- Buckley, N. J., 1999. Black vulture (*Coragyps atratus*). p. 1-19. *In*: A. Poole and F. Gill (eds.) *The Birds of North America*, No. 411. Philadelphia: The Birds of North America, Inc. Online edition.
- Buechley, E.R., Şekercioğlu, Ç.H., 2016. The avian scavenger crisis: Looming extinctions, trophic cascades, and loss of critical ecosystem functions. *Biological Conservation* 198 (2016) 220-228.
- Buurma L.S. 1999. The Royal Netherlands Air Force: two decades of bird strike prevention “en route”. *In*: Leshem Y., Mendelik Y., Shamoun-Baranes J. (eds) *Proc Int Semin on Birds and Flight Safety in the Middle East*. Tel Aviv University, Tel Aviv, pp 71-83.”
- Carrete, M., S. A. Lambertucci, K. Speziale, O. Ceballos, A. Travaini, M. Delibes, F. Hiraldo, and J. A. Donazar. 2010. Winners and losers in human-made habitats: interspecific competition outcomes in two Neotropical vultures. *Animal Conservation* 13:390-398.
- Coleman J.S., Fraser J.D. 1989. Habitat use and home ranges of Black and Turkey Vultures. *Journal of Wildlife Management* 53 (3): 782-792.



- Cortés-Avizanda A., Carrete M., Donázar J. A. 2010. Managing supplementary feeding for avian scavengers: Guidelines for optimal design using ecological criteria, *Biological Conservation* 143 (2010) 1707–1715
- DeVault, T.L., Reinhart, B.D., Brisbin, L., Rhodes, O., 2005. Flight behavior of Black and Turkey vultures: Implications for reducing bird-aircraft collisions. *Journal of Wildlife Management* 69, 601–608.
- Deygout C., Gault F., Sarrazin F., Bessa-Gomesa C. 2009. Modeling the impact of feeding stations on vulture scavenging service efficiency, *Ecological Modelling* 220 (2009) 1826–1835
- Dupont H., Mihouba J.B., Becub N, Sarrazina S. 2011. Modelling interactions between scavenger behaviour and farming practices: Impacts on scavenger population and ecosystem service efficiency, *Ecological Modelling* 222 (2011), 982–992.
- Environmental assessment for the management of vulture damage in the Commonwealth of Virginia. U.S. Department of Agriculture Animal and Plant Health Inspection Service (APHIS), Wildlife Services, 2002.
- Ferland-Raymond B. Bachand D. Thomas, Bildstein K. 2005. Flapping rates of migrating and foraging Turkey Vultures (*Cathartes aura*) in Costa Rica. *Vulture News* 53:1–5.
- Freire D.A, Rodrigues Gomes F.B, Cintra R, Novaes W.G. 2015, Use of Thermal Power Plants by New World Vultures (Cathartidae) as an Artifice to Gain Lift. *The Wilson Journal of Ornithology*: Vol. 127, No. 1, pp. 119-123.
- Kirk, D.A. & M.J. Mossman. 1998. Turkey Vulture (*Cathartes aura*). In *The Birds of North America*, No. 339. A. Poole & F. Gill, Eds. The Birds of North America, Inc. Philadelphia, PA.
- Lieury N., Gallardo M., Ponchon C., Besnard A., Millon A. 2015. Relative contribution of local demography and immigration in the recovery of a geographically-isolated population of the endangered Egyptian vulture. *Biological Conservation*, Vol. 191, Pages 349–356 .
- Mandel J.T., Bildstein K.L, 2007. Turkey Vultures Use Anthropogenic Thermals to Extend Their Daily Activity Period. *The Wilson Journal of Ornithology*. 119(1):102–105.
- McHargue, L. A. 1981. Black Vulture nesting behavior, and growth. *Auk* 98:182-185. [113\*\*]
- Newman B.G. 1957. Soaring and gliding flight of the Black vulture. Department of Engineering, University of Cambridge.
- Novaes W.G., Cintra R. 2013. Factors influencing the selection of communal roost sites by the Black Vulture *Coragyps atratus* (Aves: Cathartidae) in an urban area in Central Amazon. *Zoologia* 30:607–614.
- Novaes, W.G., Alvarez, M.R.D.V., 2014. Relação entre resíduo sólido urbano e urubus-de-cabeça-preta (*Coragyps atratus*): Um perigo para as aeronaves no Aeroporto de Ilhéus (SBIL). *Conexão Sipaer* 5, 22–29.
- Ogada, D. L., Keesing, F., and Virani, M. Z. 2012. Dropping dead: Causes and consequences of vulture population declines worldwide. *Ann. N.Y. Acad. Sci.* 1249:57–71.
- Osofsky, S. A., T. P. Brown, and C. B. Carrig. 1990. An ectopic wing in a wild Black Vulture (*Coragyps atratus*). *Avian Diseases* 34:765-769.
- Parker P. G. 1995. Kinship and association in communally roosting black vultures. *Animal Behavior*, 49, 395–401.

- Parrott G. C. (1970). Aerodynamics of gliding flight of a black vulture *Coragyps atratus*. J. exp. Biol. S3, 363-74.
- Pennycuik C. J. 1971 Gliding flight of the white-backed vulture *Gyps africanus* J. Exp. Biol. 55 13–38
- Pennycuik C. J. 1983 Thermal soaring compared in three dissimilar tropical bird species, *Fregata magnificens*, *Pelecanus occidentalis* and *Coragyps atratus*. J. Exp. Biol. 102 307–25
- Peterson, R. T., 2001. A Field Guide to Western Birds. Houghton Mifflin Field Guides. p. 182.
- Piper, S. E. 2006. Supplementary Feeding Programmes: How necessary are they for the maintenance of numerous and healthy vultures populations? In: Proceedings of the International Conference on Conservation and Management of Vulture Populations. Thessaloniki, Greece. Natural History Museum of Crete & WWF Greece, pp 41-50.
- Rabenold P.P., 1987. Recruitment to food in black vultures: evidence for following from communal roosts. Animal Behaviour, 35. 1775-1985.
- Ruxton G.D., Houston D.C. 2002. Modeling the energy budget of a colonial bird of prey, the Ruppell's Griffon Vulture, and consequences for its breeding ecology. African Journal of Ecology 40:260–266.
- Schoener T. W. 1971. Theory of feeding strategies. Annual Review of Ecology and Systematics 2: 369–404.
- Stewart P. A. 1983. The biology and communal behaviour of American Black Vultures. Vulture News 9-10:14-36.
- Stolen E.D., Taylor W. K.. 2003. Movements of black vultures between communal roosts in Florida. Wilson Bulletin 115 (3): 316-320.
- Tabor S.P, Mcallister C.T. 1988. Nocturnal flight by Turkey Vultures (*Cathartes aura*) in southcentral Texas. Journal of Raptor Research 22:91.
- Thompson W.L.; Yahner R.H.; Storm G.L. 1990. Winter use and habitat characteristics of vulture communal roosts. Journal of Wildlife Management 54 (1): 77-83.
- Wallington C.E. 1980. Meteorology for Glider Pilots. Transatlantic Arts.
- Walter D.W., Fischer J.W., Humphrey J.S., Daughtery T.S., Milleson M.P., Tillman E.A., Avery M. L. 2012. Using three-dimensional flight patterns at airfields to identify hotspots for avian–aircraft collisions. Applied Geography, Vol.35, Issues 1–2, pp. 53–59.
- Zakrajsek, E.J., Bissonette, J.A., 2005. Ranking the risk of wildlife species hazardous to military aircraft. Wildlife Society Bulletin 33, 258–264.

### Short reports

- Anagnostopoulos A. 2000. Monitoring Avifauna for risk analysis at Athens International Airport S.A. In the proceedings of the 25th IBSC Amsterdam 17-21 April 2000, Volume II: 125-138. [http://www.int-birdstrike.org/Warsaw\\_Papers/IBSC26%20WPAE2.pdf](http://www.int-birdstrike.org/Warsaw_Papers/IBSC26%20WPAE2.pdf)
- Buurma L.S. 1999. The Royal Netherlands Air Force: Two Decades Of Bird Strike Prevention “En Route”

Gard K., Groszos, M. S., Brevik E.C., Lee G. W. 2007. Spatial analysis of Bird-Aircraft Strike Hazard for Moody Air Force Base aircraft in the state of Georgia. Georgia Academy of Science ISSN: 0147-9369 <http://www.freepatentsonline.com/article/Georgia-Journal-Science/174751719.html>

Gray S. 2003. GIS and Wildlife Management Activities at Airports. USDA, Wildlife Service <http://digitalcommons.unl.edu/cgi/viewcontent.cgi?article=1010&context=birdstrike2003>

Kelly T.A. 2005. Managing Birdstrike Risk with Information Technologies: A Review of the State-of-the-Art in 2005. Detect, Inc. Panama City, Florida. USA.

Leshem Y., Shamoun-Baranes J, Yanai M, Tamir R., Yom-Tov Y. 1998. The development of a Global Database on bird movements and bird strikes in military and civilian flight/International Bird Strike Committee. Stars Lesna, Slovakia, 14 - 18 September 1998.  
<http://www.researchgate.net/publication/238073911> THE DEVELOPMENT OF A GLOBAL DATABASE ON BIRD MOVEMENTS AND BIRD STRIKES IN MILITARY AND CIVILIAN FLIGHT

United States Air Force (USAF), 2014. Top 50 USAF wildlife strikes by cost. USAF Safety Center.  
<http://www.afsec.af.mil/shared/media/document/AFD-141209-035.pdf>

### **Presentations, lectures**

Angevine W.M. 2014. Thermal Structure and Behavior  
[http://www.esrl.noaa.gov/csd/staff/wayne.m.angevine/wayne.m.angevine.presentations/thermals\\_2014.pdf](http://www.esrl.noaa.gov/csd/staff/wayne.m.angevine/wayne.m.angevine.presentations/thermals_2014.pdf)

Herricks E.E. 2005. Airport Wildlife Strike Hazard Management, Program Review. University of Illinois Center of Excellence and FAA WSM-R (AAR 411)

Prem H, Mackley W. Thermalling, 2005. Advance Pilot Training Lecture Series. Bacchus Marsh Airfield, Australia. [http://www.glidering.cz/souteze/2013/ppj\\_sk/doc/Thermalling.pdf](http://www.glidering.cz/souteze/2013/ppj_sk/doc/Thermalling.pdf)

### **GIS and Remote sensing data used in the project**

On Demand Surface Kinetic Temperature AST\_08//ASTER Products Table (Land Processes Distributed Active Archive Center)  
[https://lpdaac.usgs.gov/dataset\\_discovery/aster/aster\\_products\\_table/ast\\_08](https://lpdaac.usgs.gov/dataset_discovery/aster/aster_products_table/ast_08)

Routine ASTER Global Digital Elevation Model ASTGTM  
[https://lpdaac.usgs.gov/dataset\\_discovery/aster/aster\\_products\\_table/astgtm](https://lpdaac.usgs.gov/dataset_discovery/aster/aster_products_table/astgtm)

Tetsushi Tachikawa, Masami Hato, Manabu Kaku, Akira Iwasaki. 2011. Characteristics of ASTER GDEM Version 2, Earth Remote Sensing Data Analysis Center (ERSDAC), Mitsubishi Material Techno Corp., University of Tokyo.  
[https://lpdaac.usgs.gov/sites/default/files/public/aster/docs/Tachikawa\\_etal\\_IGARSS\\_2011.pdf](https://lpdaac.usgs.gov/sites/default/files/public/aster/docs/Tachikawa_etal_IGARSS_2011.pdf)

The IUCN Red list of threatened species//Coragyps atratus, American Black Vulture, data on 2015: <http://maps.iucnredlist.org/map.html?id=22697624>

Terra. The EOS Flagship (NASA).  
<http://terra.nasa.gov/>

ASTER (Advanced Spaceborne Thermal Emission and Reflection Radiometer) sensor of the Terra NASA satellite.

<http://terra.nasa.gov/about/terra-instruments/aster>

ASTER Products Table/ The Land Processes Distributed Active Archive Center (LP DAAC) web site.

[https://lpdaac.usgs.gov/dataset\\_discovery/aster/aster\\_products\\_table](https://lpdaac.usgs.gov/dataset_discovery/aster/aster_products_table)

## **ArcGIS10.0 help pages**

The help pages are available in the “Help” section inside the ArcGIS10 software and in the ArcGIS Resource Centre web site. Below the each article the link on the web variant is presented.

Adding an ArcGIS Online basemap into ArcGlobe

<http://help.arcgis.com/en/arcgisdesktop/10.0/help/index.html#//00q80000012v000000>

Slope (Spatial Analyst)

<http://help.arcgis.com/en/arcgisdesktop/10.0/help/index.html#//009z000000v2000000.htm>

How Slope works

<http://resources.arcgis.com/en/help/main/10.1/index.html#//009z000000vz000000>

Aspect (Spatial Analyst)

<http://help.arcgis.com/en/arcgisdesktop/10.0/help/index.html#//009z000000tr000000.htm>

How Aspect works

[http://help.arcgis.com/en/arcgisdesktop/10.0/help/index.html#/How\\_Aspect\\_works/009z000000vp000000/](http://help.arcgis.com/en/arcgisdesktop/10.0/help/index.html#/How_Aspect_works/009z000000vp000000/)

## APPENDIX

### APPENDIX A – FIGURES



Figure A.1 Portable meteorological station “WeatherLink Vantage Pro2”

**Raster maps of superficial parameters (relief, surface temperature and contrast of surface temperature), obtained from the remote sensing products:**

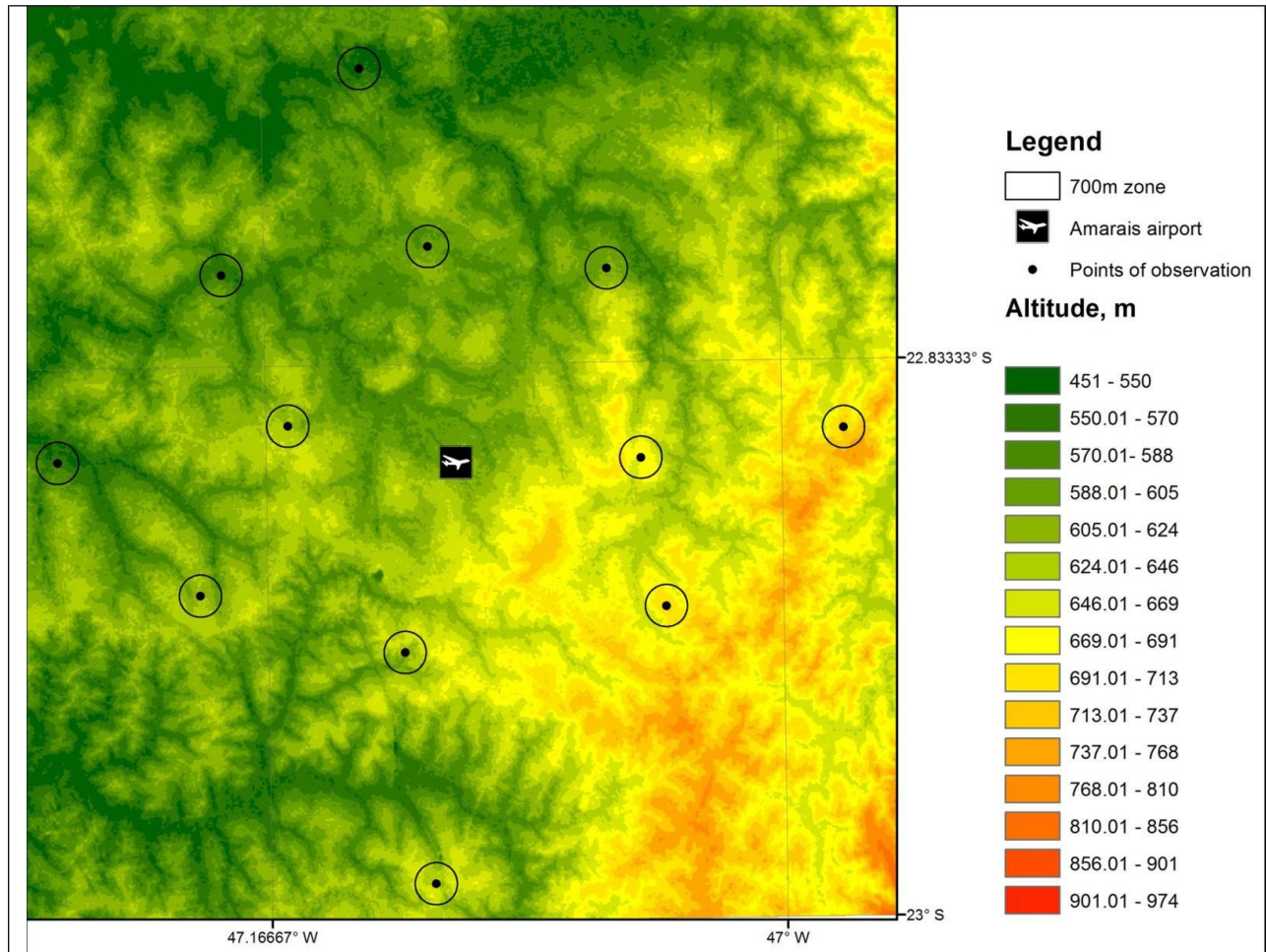


**Figure A.2 Altitude above sea level for surrounding of the Amarais airport. Raster map produced from the ASTER GDEM v2 (Supplementary Files SF23)**



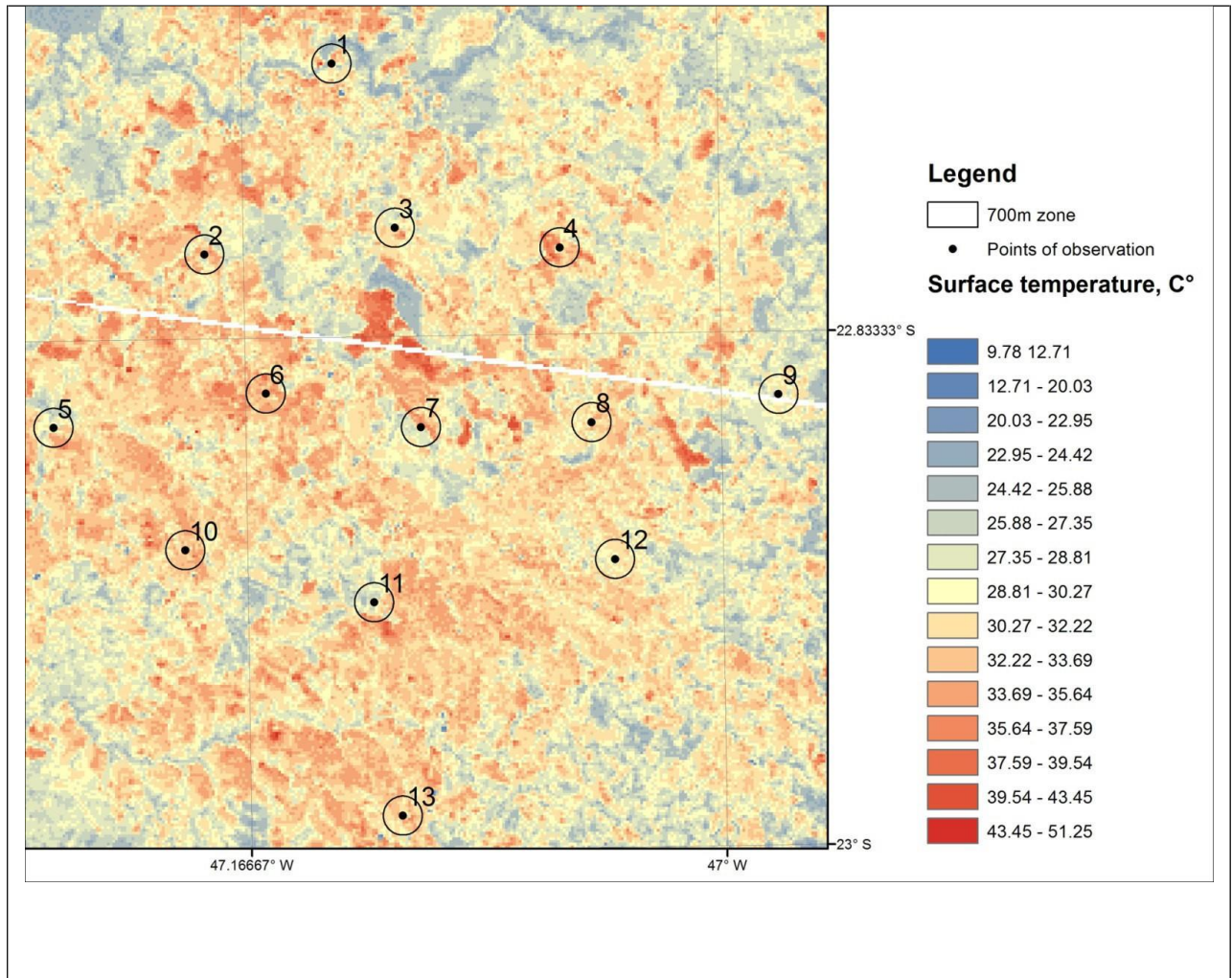


**Figure A.3 Surface temperature for surrounding of the Amarais airport. Raster map produced from the ASTER On-Demand L2 Surface Kinetic Temperature or “AST\_08” product of ASTER image made in 11.05.2013, 13:28 (Supplementary Files SF22)**

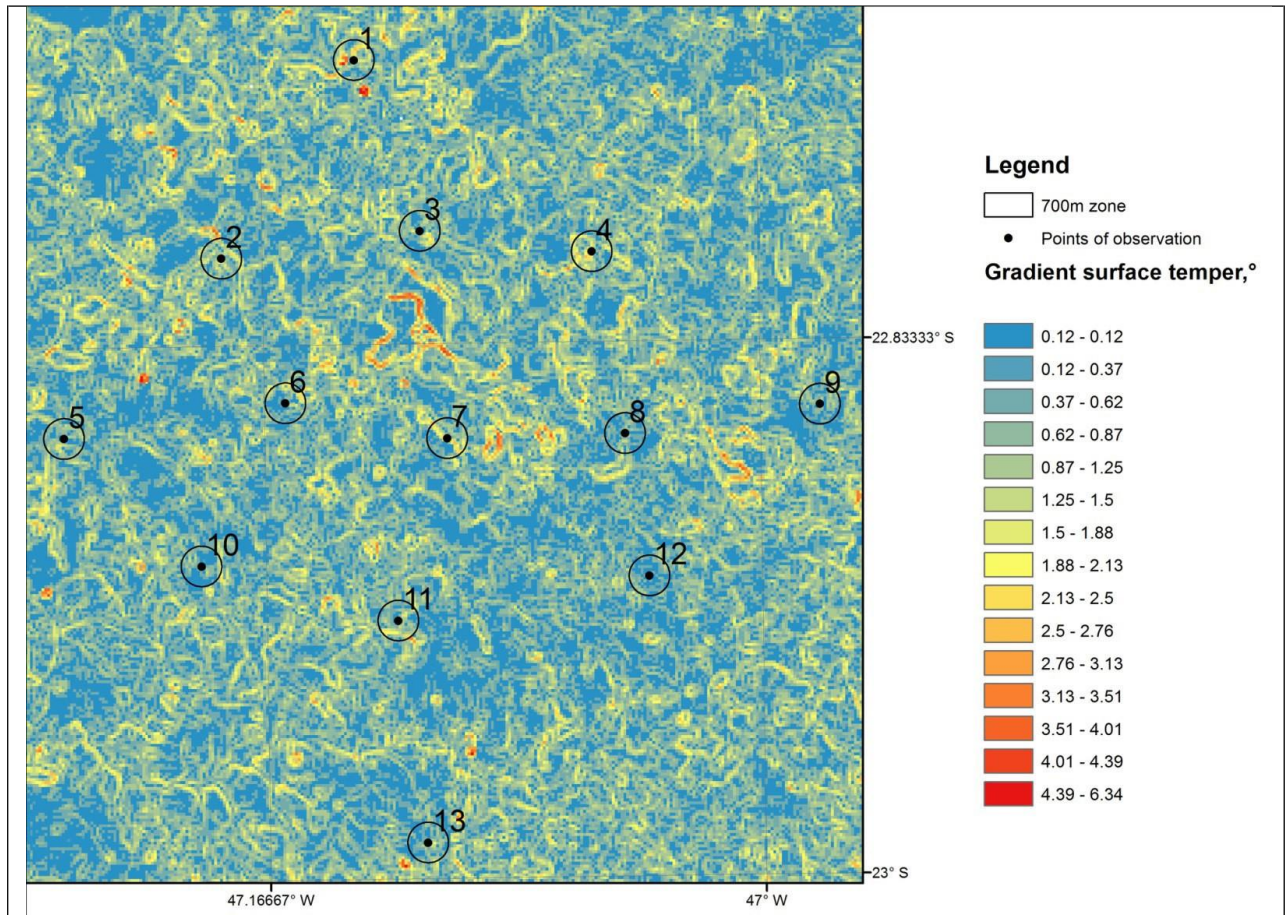


**Figure A.4 Contrast of surface temperature for surrounding of the Amarais airport. Raster map produced from the ASTER On-Demand L2 Surface Kinetic Temperature or “AST\_08” product of ASTER image made in 11.05.2013, 13:28 (Supplementary Files SF21)**



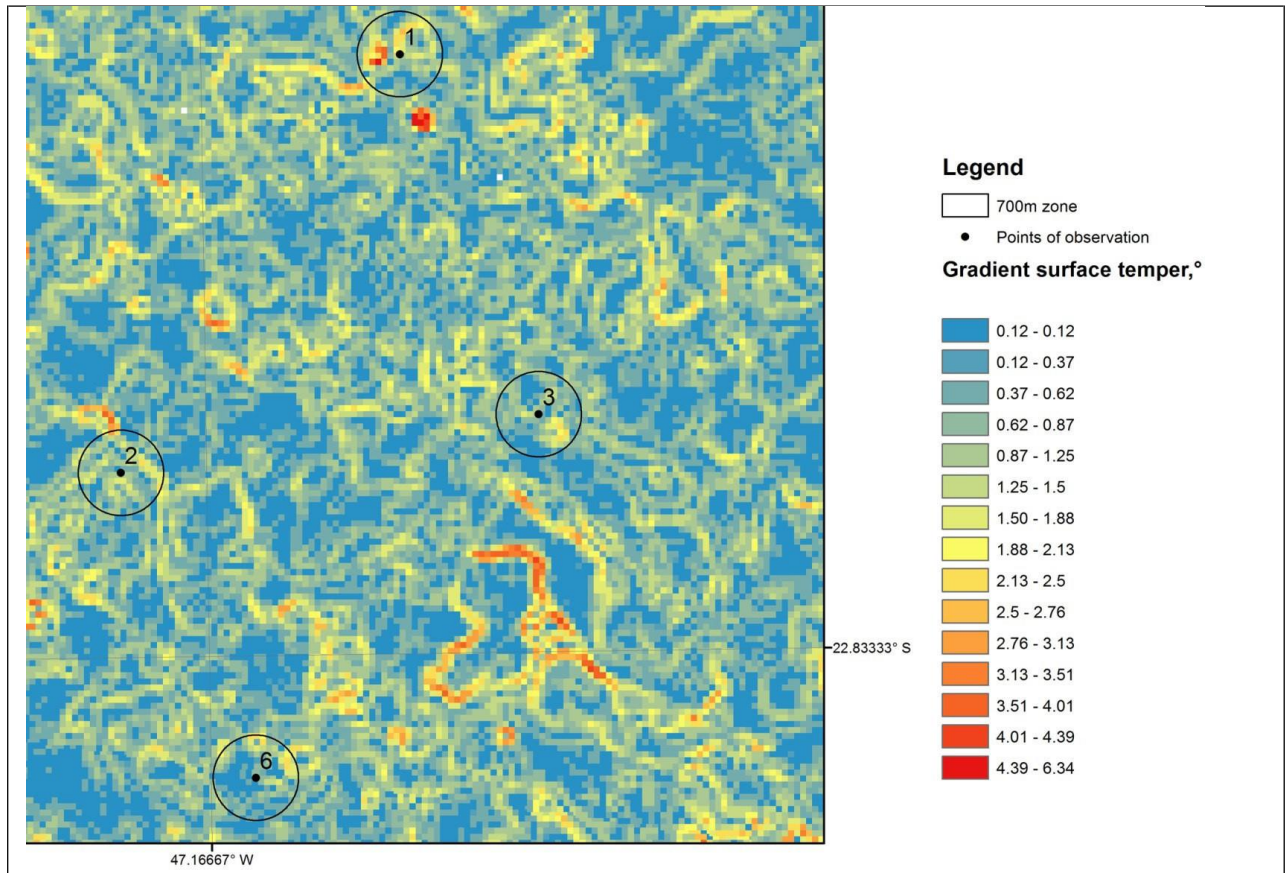


**Figure A.5 Contrast of surface temperature for surrounding of the Amaraï airport (viewpoints 1, 2, 3, 6). Raster map produced from the ASTER On-Demand L2 Surface Kinetic Temperature or “AST\_08” product of ASTER image made in 11.05.2013, 13:28 (Supplementary Files SF21)**

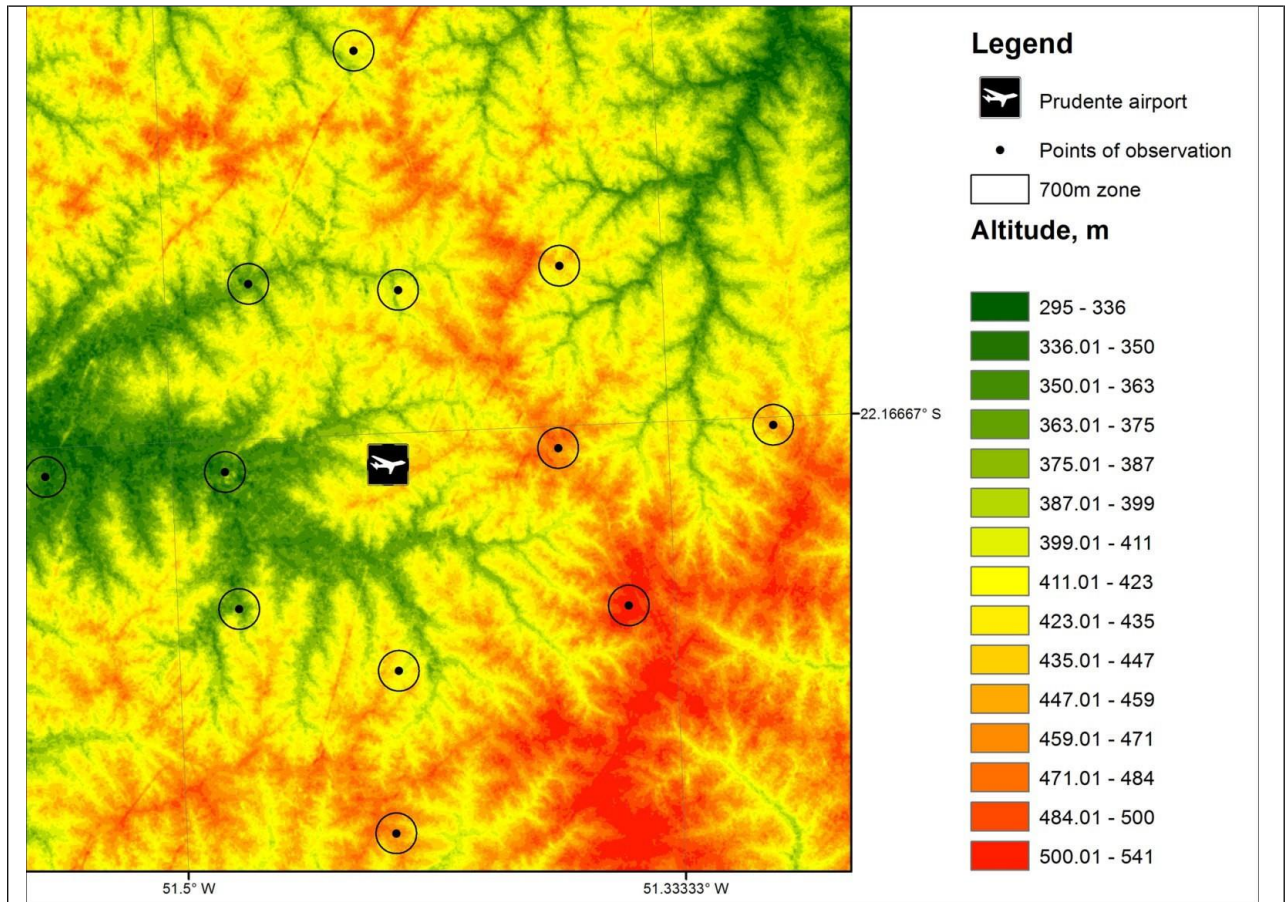


**Figure A.6** Altitude above sea level for surrounding of the Presidente Prudente airport. Raster map produced by ASTER GDEM v2 (Supplementary Files SF26)

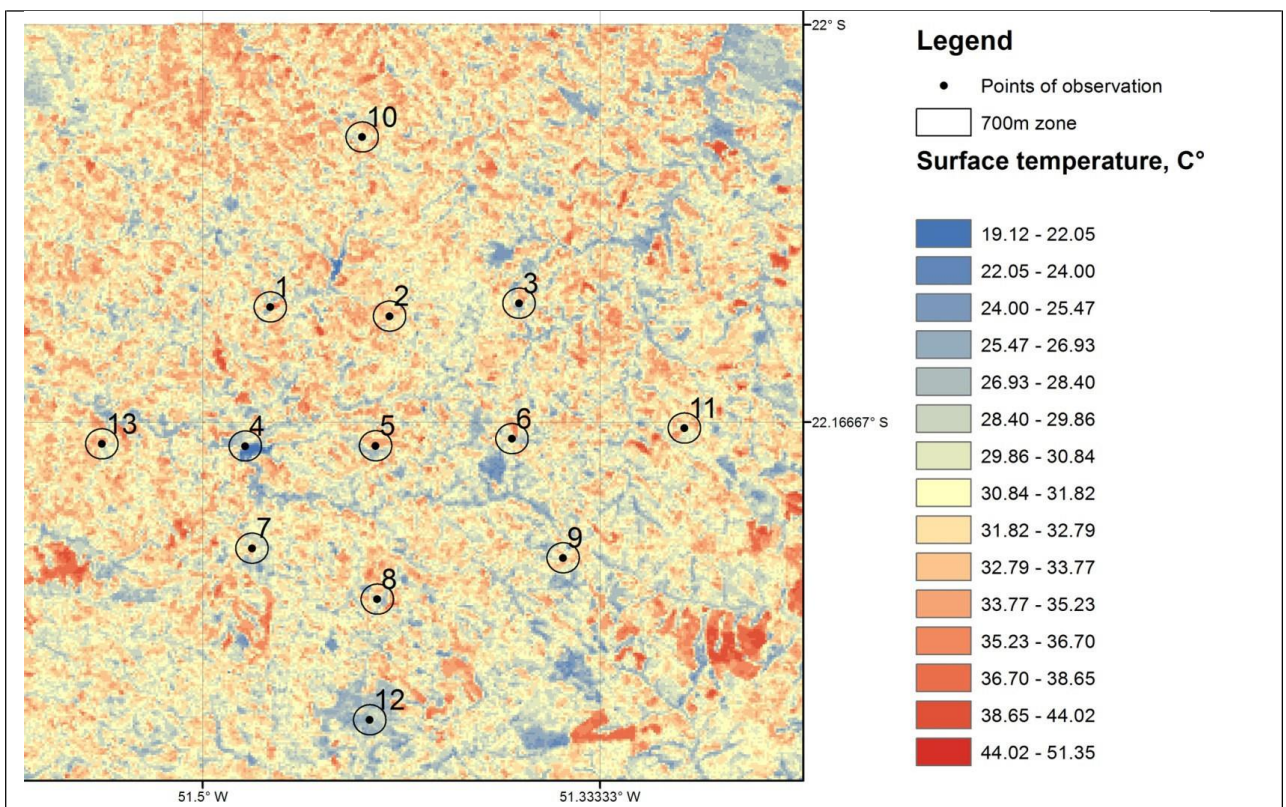


**Figure A.7** Surface temperature for surrounding of the Presidente Prudente airport. Raster map produced from the ASTER On-Demand L2 Surface Kinetic Temperature or “AST\_08” product of ASTER image made in 20.08.2013, 13:46 (Supplementary Files SF24)



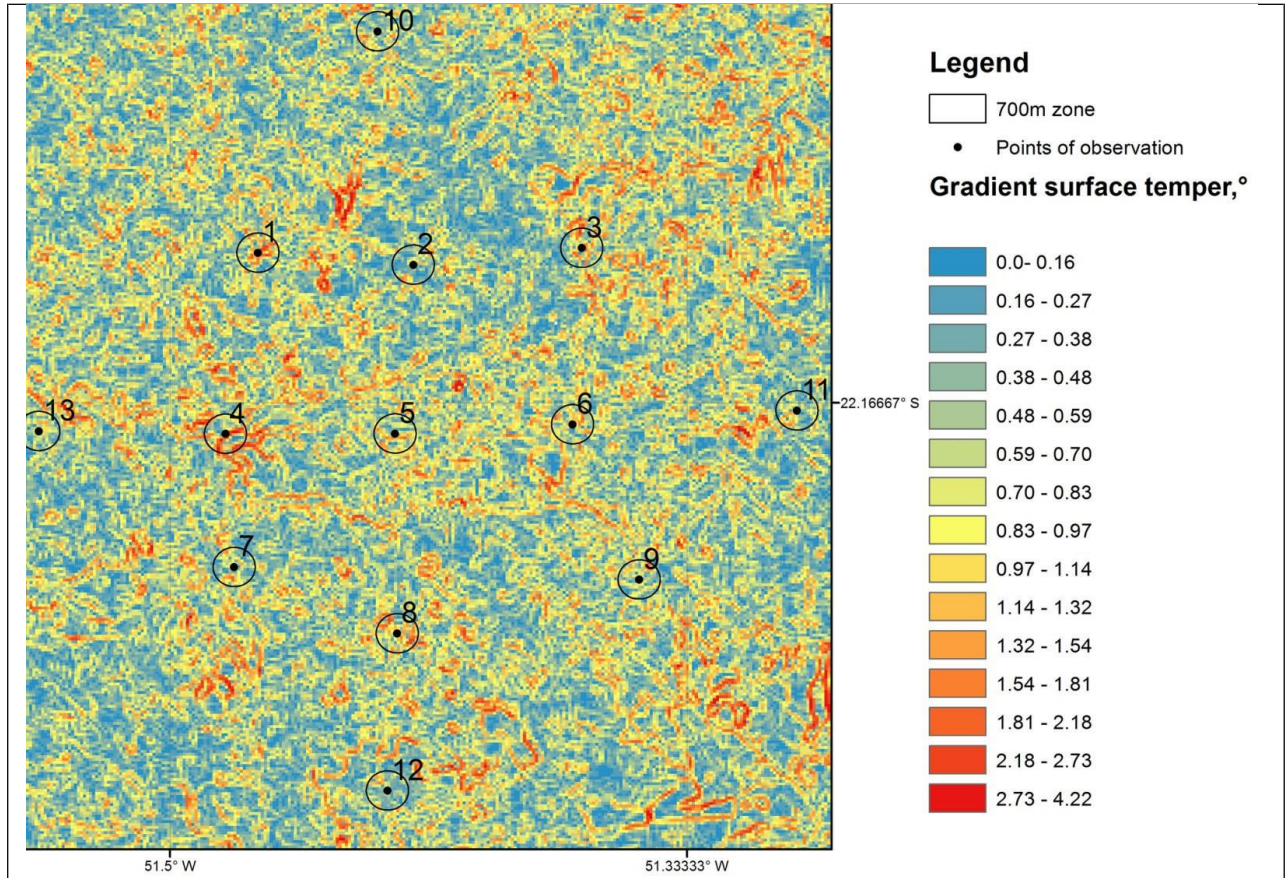


**Figure A.8 Contrast of surface temperature for surrounding of the Presidente Prudente airport. Raster map produced from the ASTER On-Demand L2 Surface Kinetic Temperature or “AST\_08” product of ASTER image made in 20.08.2013, 13:46 (Supplementary Files SF25)**

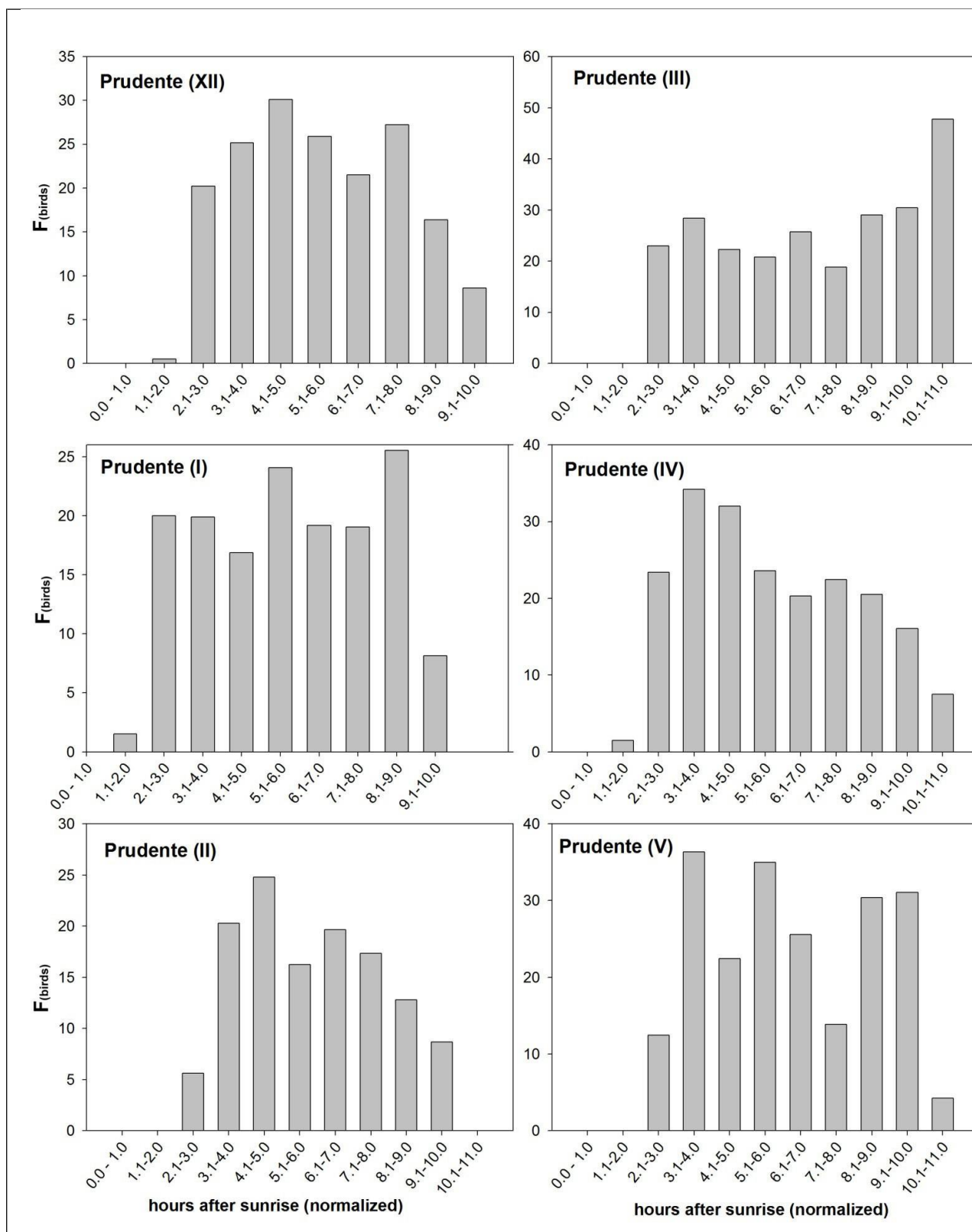


**Figure A.9 Daily variation in the soaring activity of Black vultures at each month during the period of study (Prudente, XII – V) (Supplementary Files SF35)**

OY: Frequency of birds records ( $F_{birds}$ ) or a number of birds recorded during an hour of a month average over 13 viewpoints.

OX: Scale of time biological normalized to 12 hours. It shows the hours after sunrise. Value “0”, “6”, “12” of each month of this scale is equivalent to a local sunrise; noon and sunset, respectively.

...

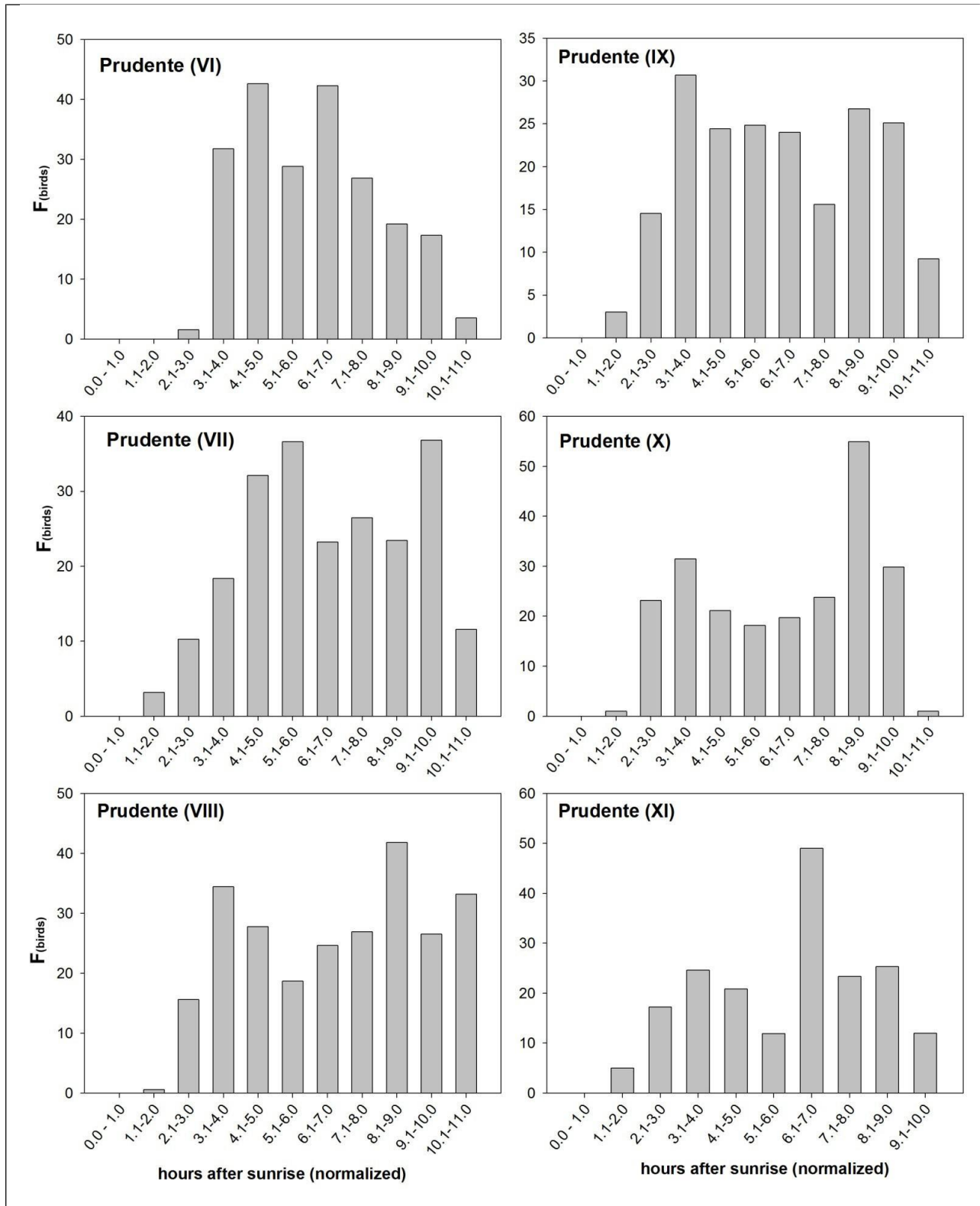


**Figure A.10 Daily variation in soaring activity of Black vultures at each month during the period of observation (Prudente, VI - XI) (Supplementary Files SF35)**

OY: Frequency of birds records ( $F_{birds}$ ) or a number of birds recorded during an hour of a month average over 13 viewpoints.

OX: Scale of time biological normalized to 12 hours. It shows the hours after sunrise. Value “0”, “6”, “12” of each month of this scale is equivalent to a local sunrise; noon and sunset, respectively.

...

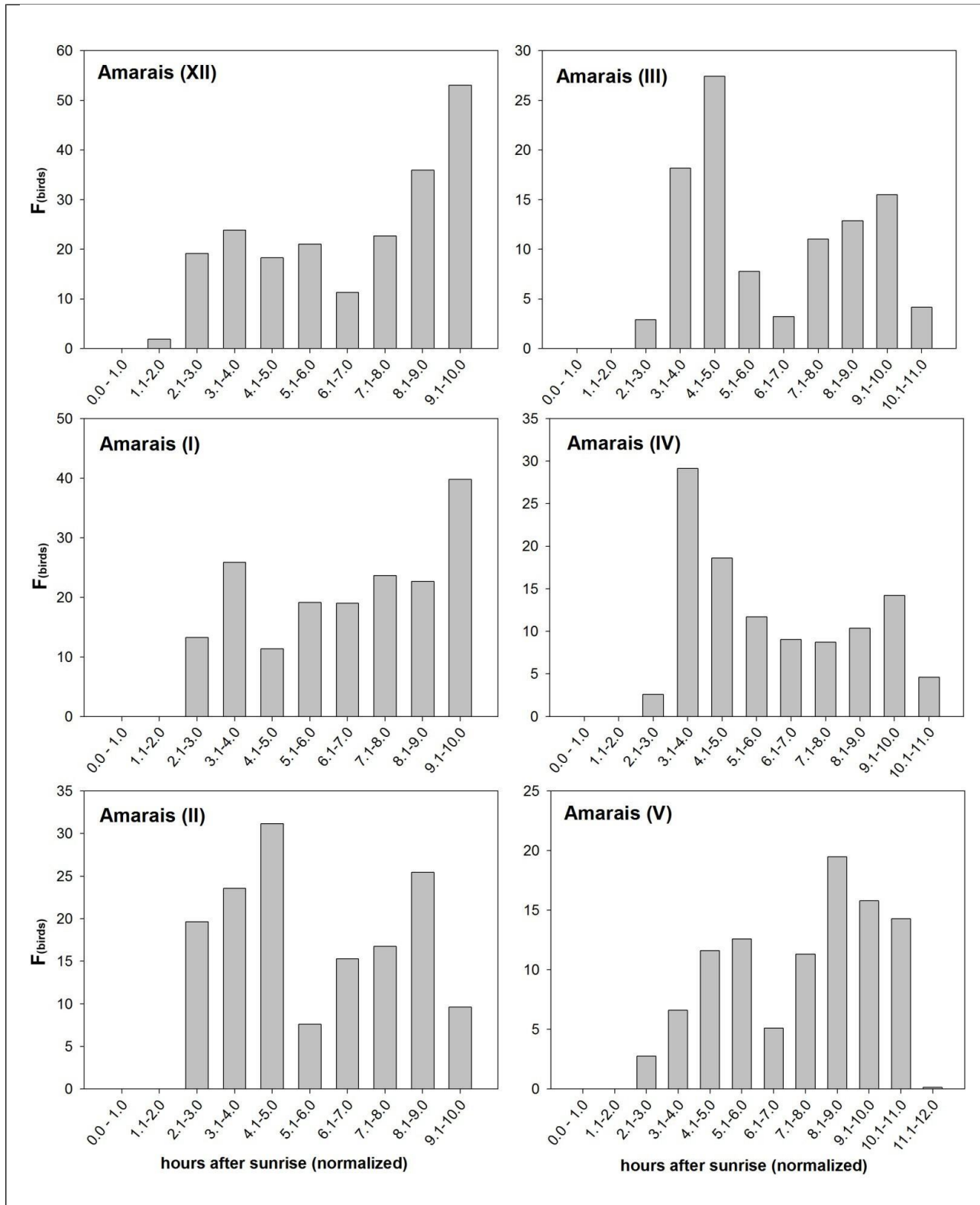


**Figure A.11 Daily variation in soaring activity of Black vultures at each month during the period of observation (Amarais, XII – V) (Supplementary Files SF35)**

OY: Frequency of birds records ( $F_{birds}$ ) or a number of birds recorded during an hour of a month average over 13 viewpoints.

OX: Scale of time biological normalized to 12 hours. It shows the hours after sunrise. Value “0”, “6”, “12” of each month of this scale is equivalent to a local sunrise; noon and sunset, respectively.

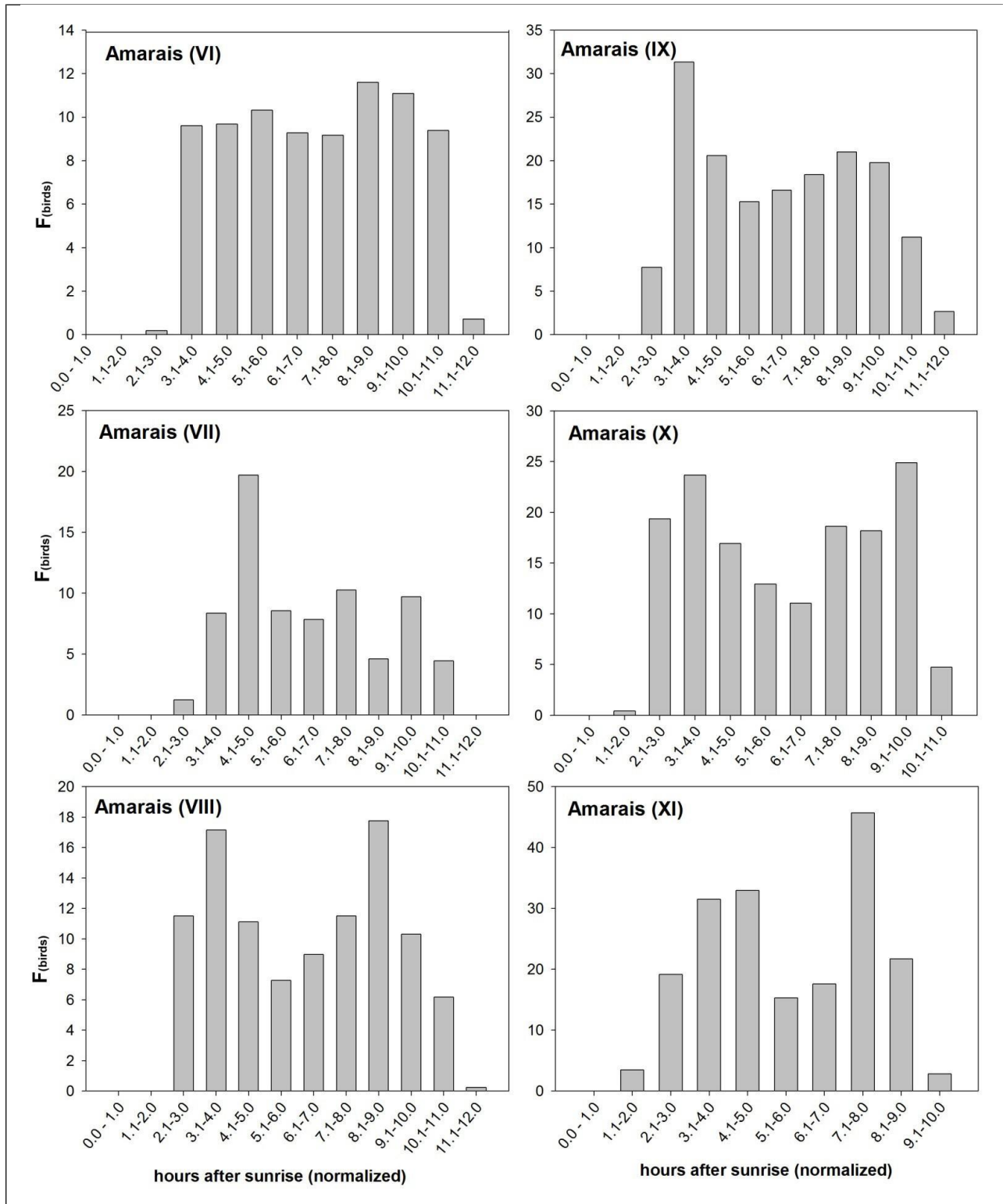


**Figure A.12 Daily variation in soaring activity of Black vultures at each month during the period of observation (Amarais, VI - XI) (Supplementary Files SF35)**

OY: Frequency of birds records ( $F_{\text{birds}}$ ) or a number of birds recorded during an hour of a month average over 13 viewpoints.

OX: Scale of time biological normalized to 12 hours. It shows the hours after sunrise. Value "0", "6", "12" of each month of this scale is equivalent to a local sunrise; noon and sunset, respectively.

....



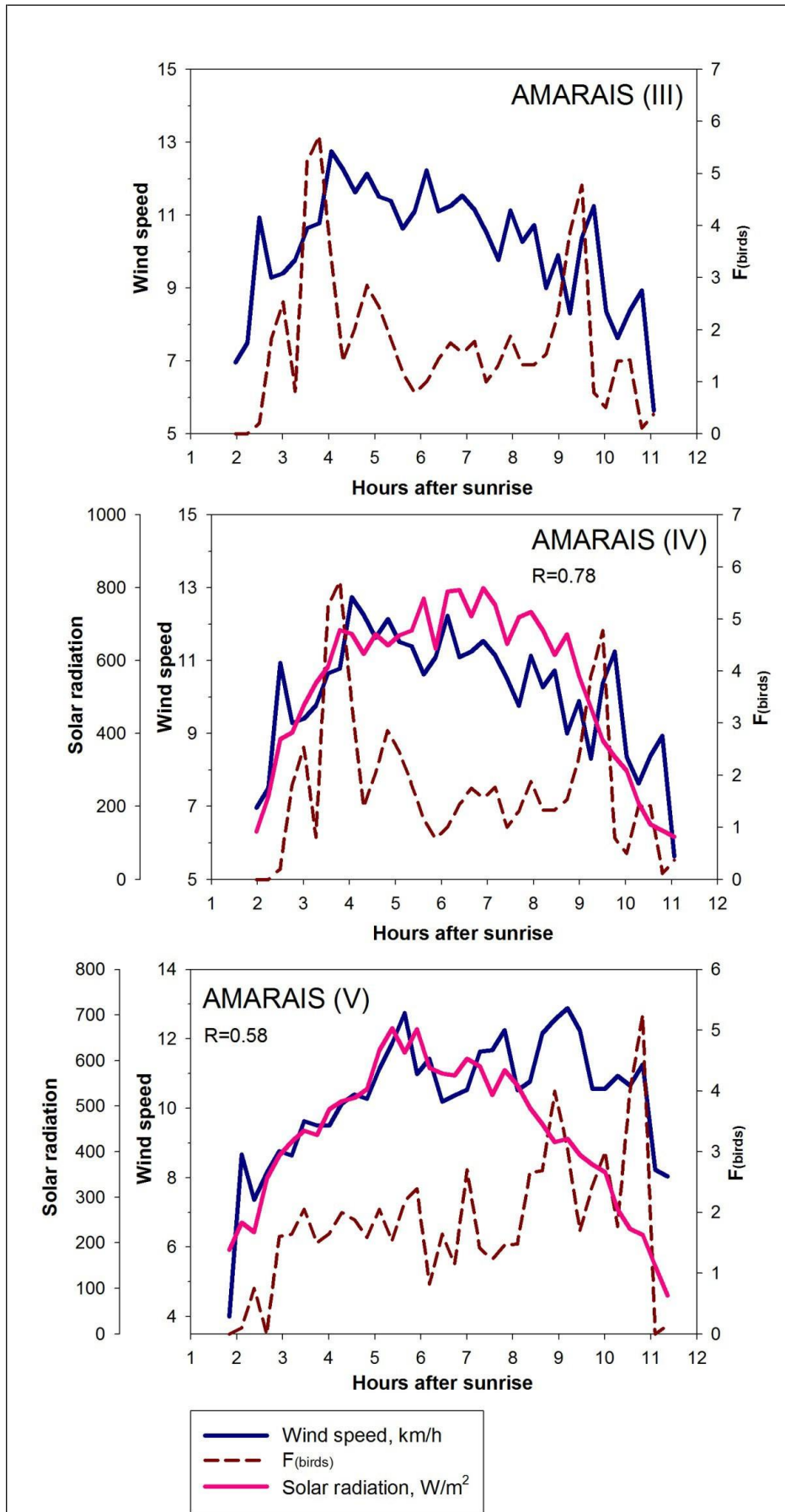


**Figure A.13(a)** Daily variation in soaring activity of Black vultures ( $F_{birds}$ ), wind speed and solar radiation for III, IV and V months of the period of study (Amaraais)



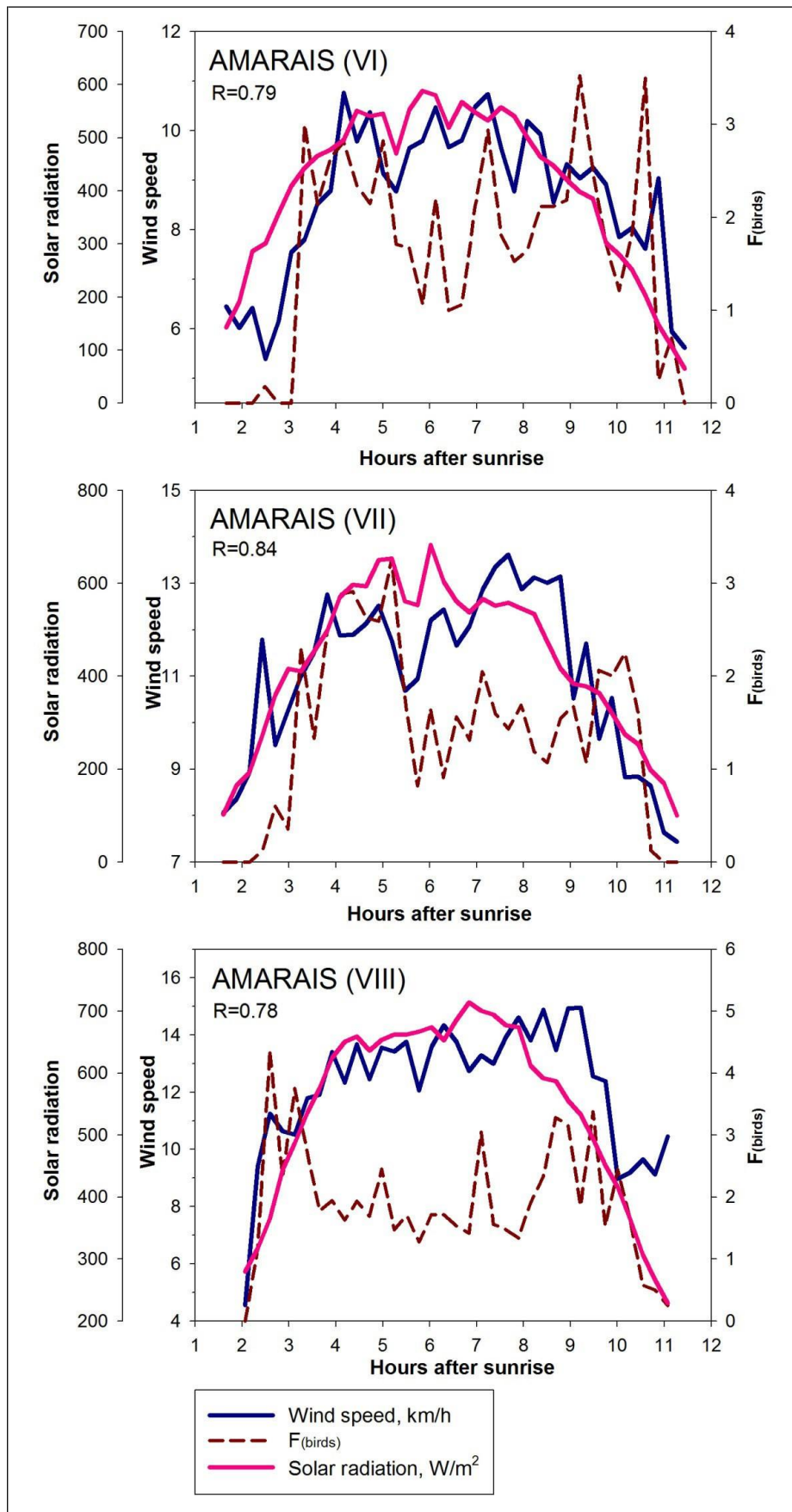


**Figure A.13(b) Daily variation in soaring activity of Black vultures ( $F_{birds}$ ), wind speed and solar radiation for VI, VII and VIII months of the period of study (Amarais)**

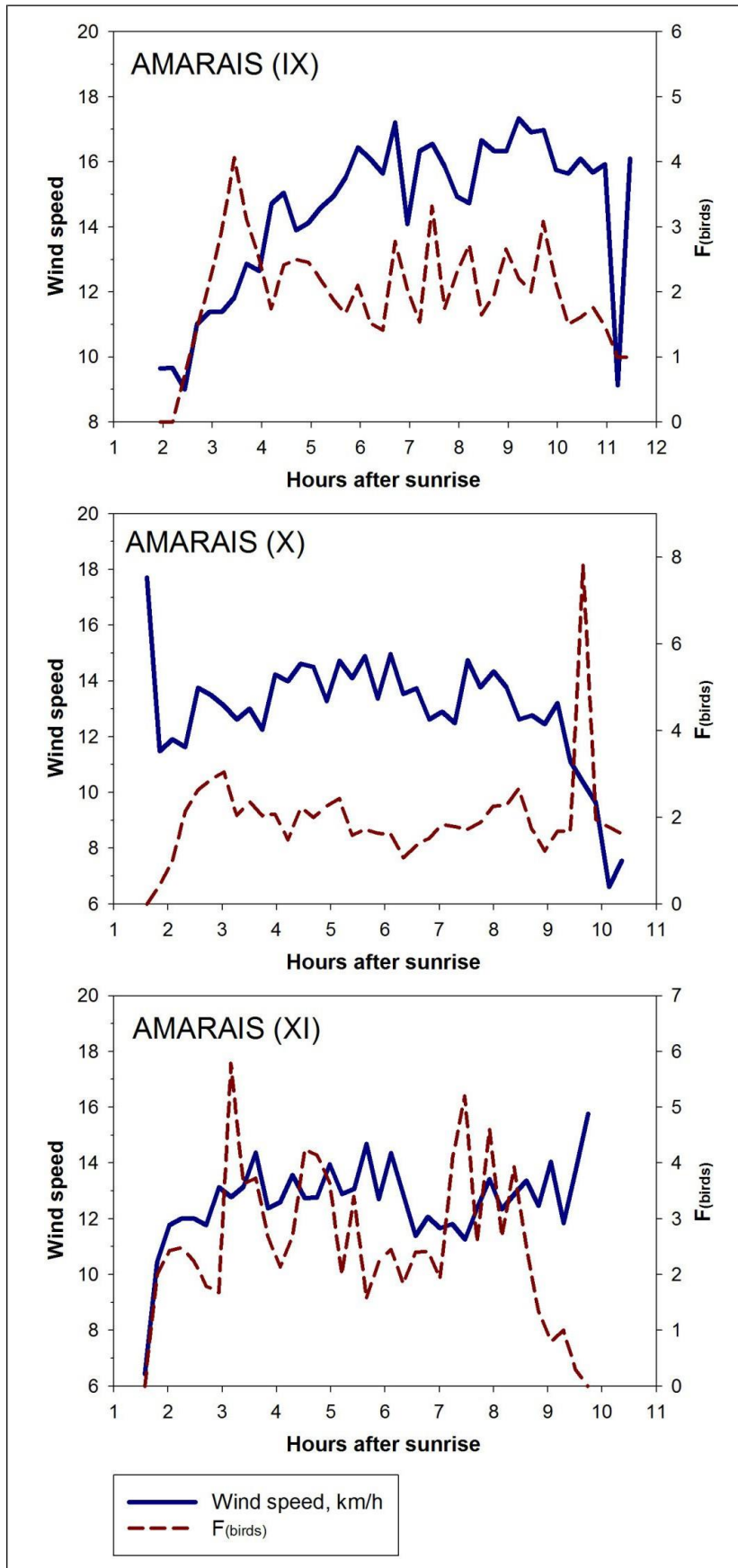
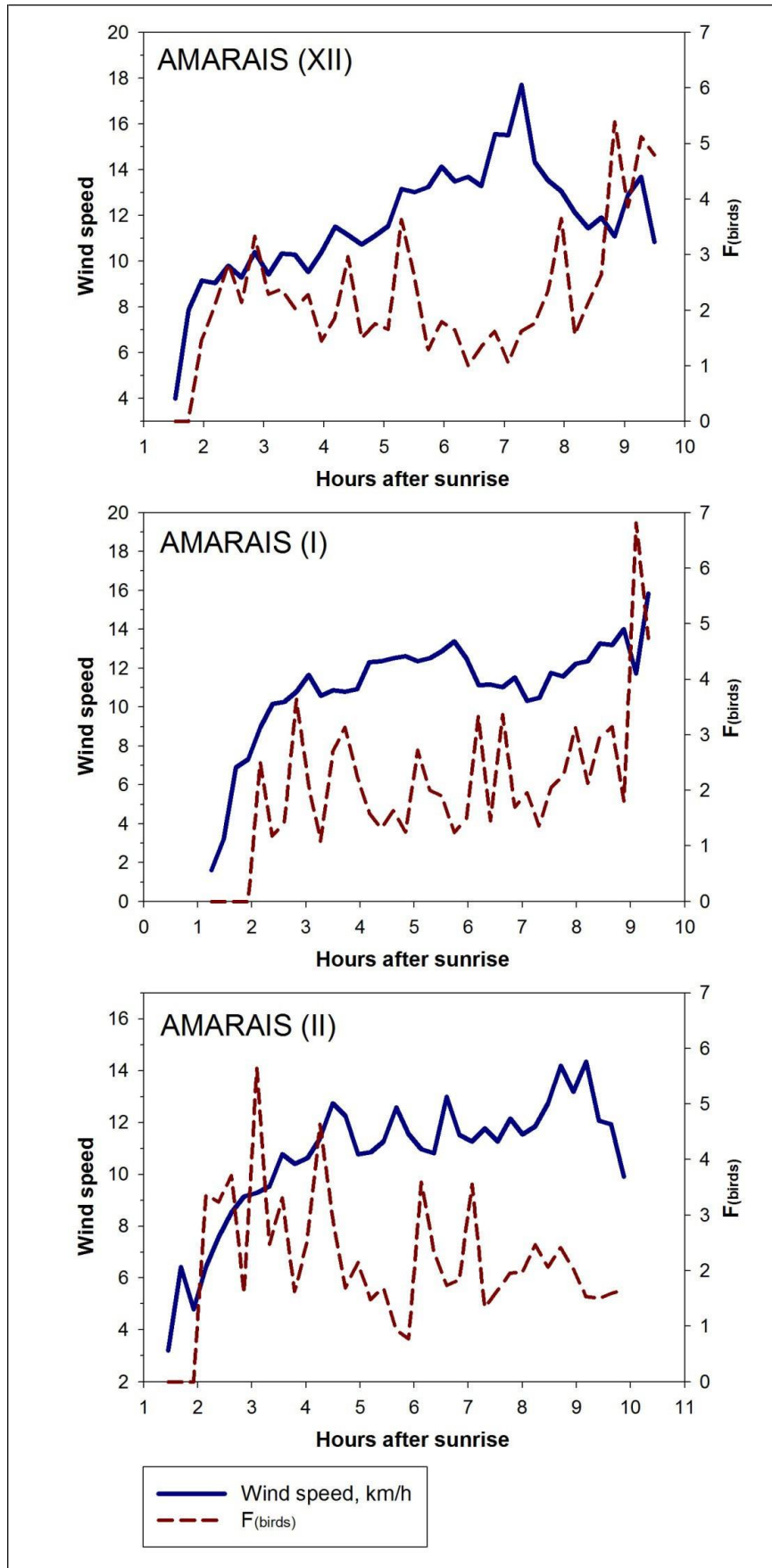
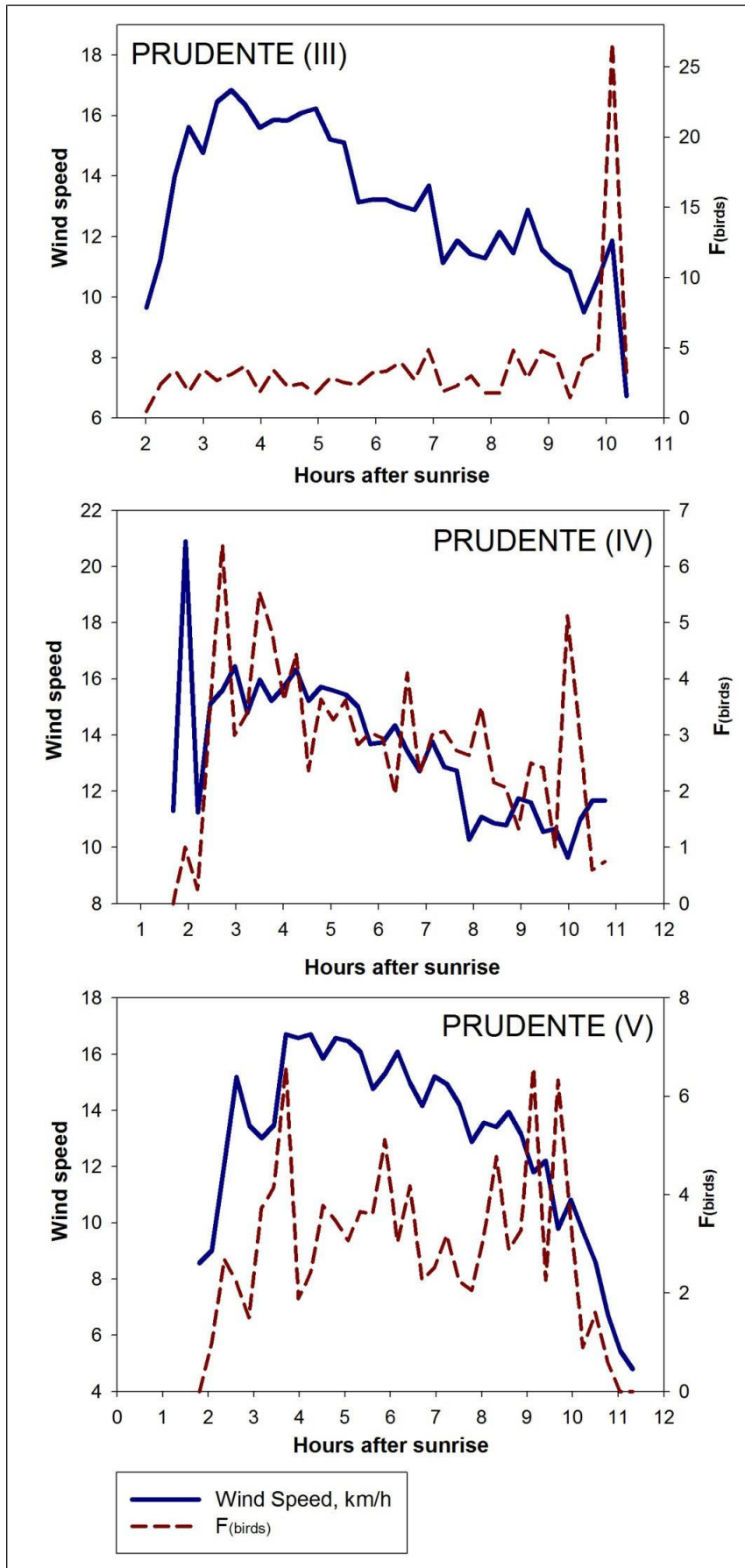


Figure A.13(c) Daily variation in soaring activity of Black vultures (Fbirds) and wind speed for IX, X and XI months of the period of study (Amarais)



**Figure A.13(d) Daily variation in soaring activity of Black vultures (Fbirds) and wind speed for XII, I and II months of the period of study (Amarais)**



**Figure A.14(a)** Daily variation in soaring activity of Black vultures (Fbirds) and wind speed for III, IV and V months of the period of study (Prudente)

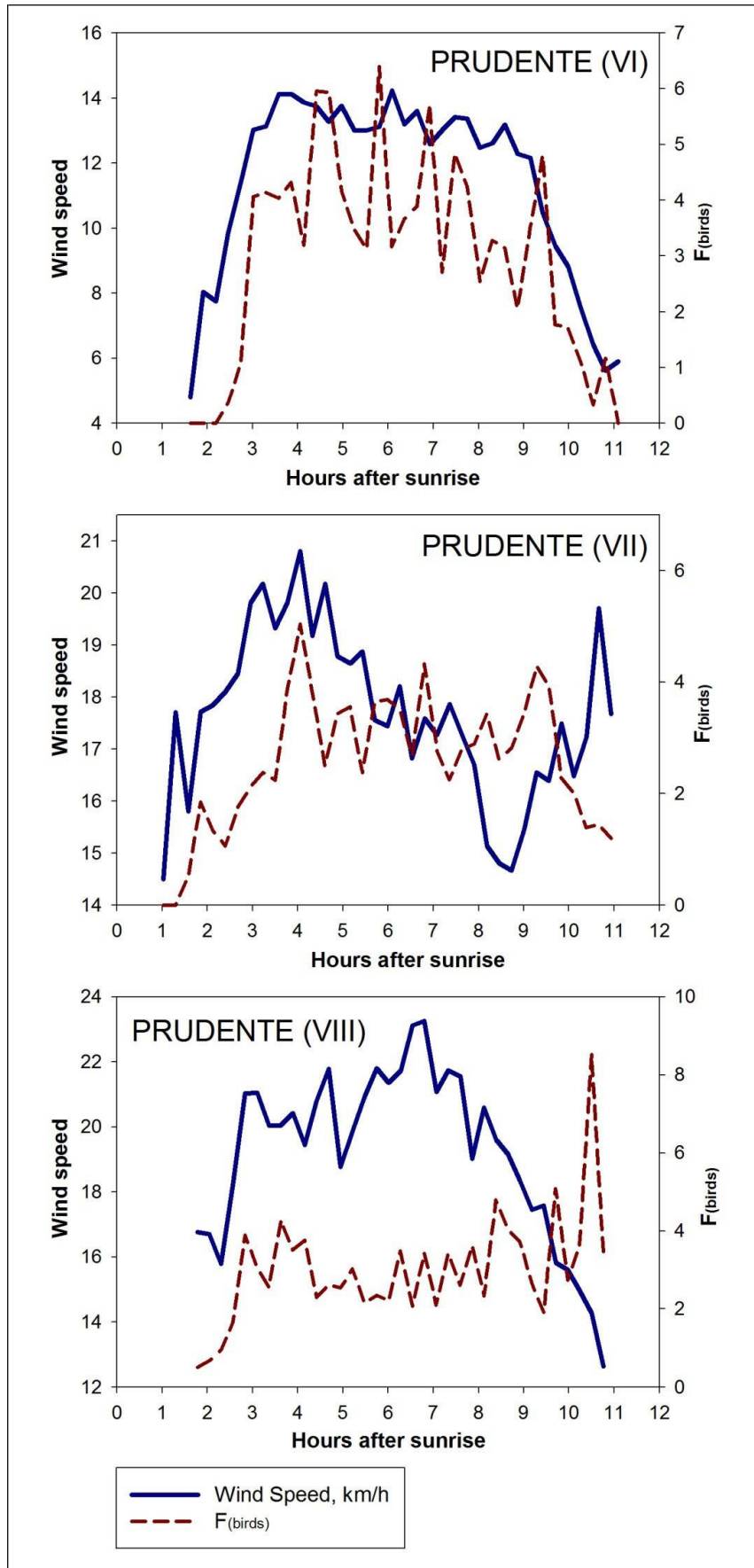


**Figure A.14(b) Daily variation in soaring activity of Black vultures (Fbirds) and wind speed for VI,VII and VIII months of the period of study (Prudente)**

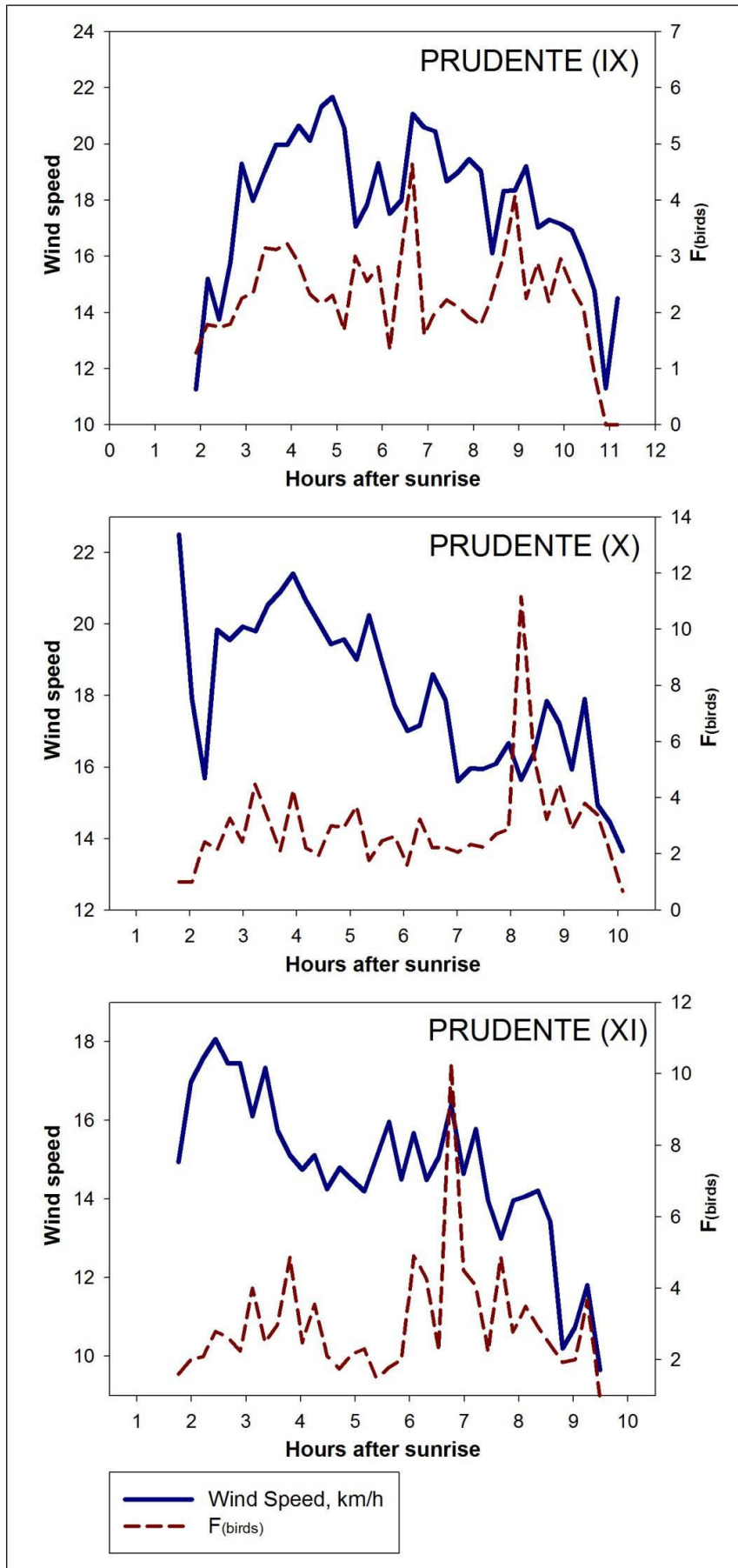


**Figure A.14(c)** Daily variation in soaring activity of Black vultures (Fbirds) and wind speed for IX, XI and XI months of the period of study (Prudente)



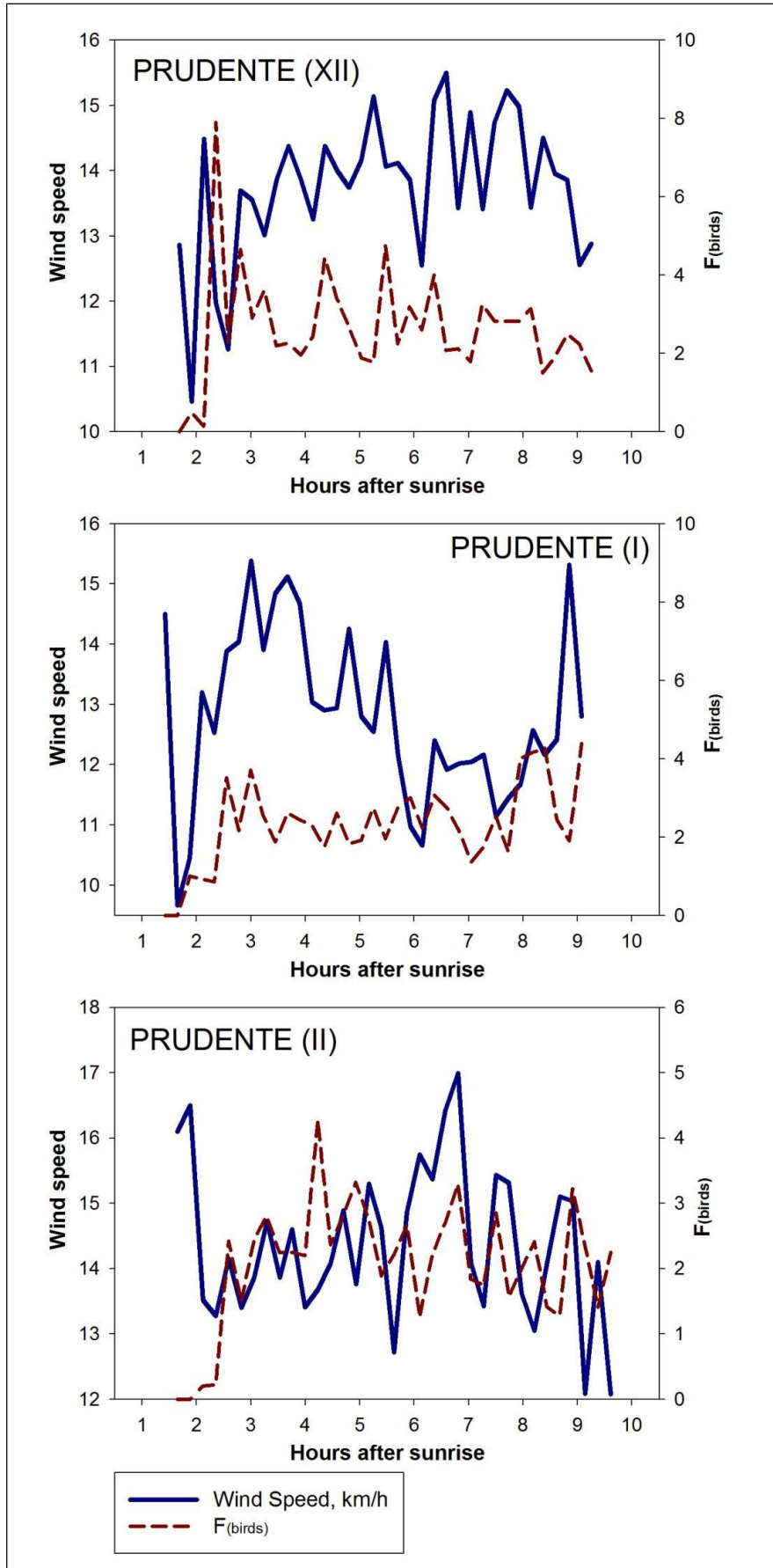


Figure A.14 (d) Daily variation in soaring activity of Black vultures ( $F_{birds}$ ) and wind speed for XII, I and II months of the period of study (Prudente)



## APPENDIX B – TABLES

**Table B.1 Geographical coordinates of the observation points (viewpoints) around the Amarais airport (Supplementary Files SF3)**

Number	Name	Latitude	Longitude
P1	Kraton	-22.744722	-47.134810
P2	Paulínia	-22.806000	-47.180269
P3	CPQBA	-22.798222	-47.113493
P4	LNLS	-22.805330	-47.055858
P5	ETE	-22.861451	-47.233998
P6	Marcelo Caminhos	-22.851343	-47.159462
P7	Amarais airport	-22.862927	-47.105279
P8	FAC	-22.862106	-47.045502
P9	San Conrado	-22.853790	-46.979896
P10	Wickbold	-22.901776	-47.188452
P11	PUCC	-22.919523	-47.122566
P12	Coração de Jesus	-22.906566	-47.037930
P13	Votorantim	-22.988791	-47.113591

**Table B.2 Geographical coordinates of the observation points (viewpoints) around the Presidente Prudente airport (Supplementary Files SF3)**

Number	Name	Latitude	Longitude
P1	Sabesp	-22.11833333	-51.471583333
P2	Pruden Pias	-22.12219444	-51.421527778
P3	Renato	-22.11677778	-51.367250000
P4	Represa	-22.17663889	-51.482055556
P5	Aeroporto Prudente	-22.17655556	-51.427388889
P6	Athia	-22.17358333	-51.370194444
P7	Fazenda 14	-22.21952778	-51.479250000
P8	Terra Parque	-22.24088889	-51.426694444
P9	Aeroclube	-22.22355556	-51.348750000
P10	Marocha	-22.04705556	-51.433027778
P11	Família	-22.16913889	-51.297888889
P12	Tosello	-22.29150000	-51.429861111
P13	Manoel	-22.17575000	-51.542222222

**Table B.3 Number of Black vultures registered around the viewpoints during each month and the whole period of observation (from September 2012 to August 2013) in Presidente Prudente study area (Supplementary Files SF34)**

Months\ viewpoints	Sept	Oct	Nov	Dec	Jan	Feb	Mar	Apr	May	Jun	Feb	Aug	Total in Pob
Pob1	300	211	158	279	123	142	243	218	313	346	249	397	<b>2979</b>
Pob2	60	100	53	117	26	45	75	7	94	59	75	96	<b>807</b>
Pob3	219	237	140	46	132	203	170	227	290	522	248	396	<b>2830</b>
Pob4	342	162	155	184	117	147	154	276	277	226	89	102	<b>2231</b>
Pob5	276	332	77	54	34	109	478	133	200	109	154	170	<b>2126</b>
Pob6	327	424	514	391	333	142	411	460	265	344	702	665	<b>4978</b>
Pob7	99	112	56	138	239	144	102	65	1	27	70	72	<b>1125</b>
Pob8	167	427	318	132	316	106	297	69	427	154	301	205	<b>2919</b>
Pob9	132	130	127	72	129	26	115	93	140	136	173	320	<b>1593</b>
Pob10	97	65	314	78	64	42	264	74	148	197	147	23	<b>1513</b>
Pob11	65	71	77	85	95	82	105	59	104	48	72	79	<b>942</b>
Pob12	66	63	55	158	64	46	65	86	43	126	68	66	<b>906</b>
Pob13	129	111	53	127	56	70	78	306	148	199	149	175	<b>1601</b>
Presidente Prudente in total	<b>2279</b>	<b>2445</b>	<b>2097</b>	<b>1861</b>	<b>1728</b>	<b>1304</b>	<b>2079</b>	<b>2073</b>	<b>2450</b>	<b>2493</b>	<b>2497</b>	<b>2766</b>	<b>26072</b>

**Table B.4 Number of Black vultures registered around the viewpoints during each month and the whole period of observation (from September 2012 to August 2013) in Amarais study area (Supplementary Files SF34)**

Months\ viewpoints	Sept	Oct	Nov	Dec	Jan	Feb	Mar	Apr	May	Jun	Jul	Aug	Total in Pob
Pob1	359	248	235	214	287	69	98	146	114	292	161	139	<b>2362</b>
Pob2	44	143	50	20	104	23	62	39	82	42	74	69	<b>752</b>
Pob3	248	74	140	112	35	70	104	53	75	43	30	85	<b>1069</b>
Pob4	99	99	132	149	55	36	17	40	24	23	38	41	<b>753</b>
Pob5	233	89	94	94	56	64	291	201	48	2	78	281	<b>1531</b>
Pob6	169	113	135	90	77	65	52	90	50	94	12	103	<b>1050</b>
Pob7	230	141	15	133	127	125	95	7	319	82	81	165	<b>1520</b>
Pob8	54	53	41	37	17	27	18	12	8	23	44	17	<b>351</b>
Pob9	81	101	76	43	49	104	17	36	1	23	78	38	<b>647</b>
Pob10	90	88	37	54	52	25	16	55	16	24	54	25	<b>536</b>
Pob11	270	437	1238	959	826	1097	304	591	241	177	203	203	<b>6546</b>
Pob12	50	104	25	71	47	21	36	37	78	98	14	87	<b>668</b>
Pob13	55	49	30	28	33	12	13	18	24	24	36	22	<b>344</b>
Amarais in total	<b>1982</b>	<b>1739</b>	<b>2248</b>	<b>2004</b>	<b>1765</b>	<b>1738</b>	<b>1123</b>	<b>1325</b>	<b>1080</b>	<b>947</b>	<b>903</b>	<b>1275</b>	<b>18129</b>

## APPENDIX C – TECHNICAL DESCRIPTIONS

### Algorithm C1

#### Preparation of the “Georeferenced birds and meteorological parameters” database as a base for implementation of analyses

The “*Georeferenced birds and meteorological parameters*” database is a point shapefile, which became the basis for both parts of our investigation. Its attribute table (entitled as the “*Birds and meteorological parameters*” merged dataset) was the basis for analyses, studying the relationship between soaring activity of Black vultures and meteorological conditions. The shapefile themselves was the intermediate stage of the data preparation for statistical analyses, studying the dependence of abundance of soaring vultures on superficial and anthropogenic characteristics. Also it was used for construction of maps, predicting the risk of collision with Black vultures over the territory.

The “Georeferenced birds and meteorological parameters” database was prepared in ArcGIS software using two datasets (tables in sheets of xlsx file of Excel), produced in the field observations: (i) *Number and locations of soaring birds dataset* (*vultures\_data*) containing census of ornithological objects and their registration parameters (i.e. number of viewpoint, geographical coordinates of viewpoint, quantity of birds, direction to bird, vertical angle to bird, distance to bird, date and time of observation), and (ii) *Values of meteorological parameters dataset* (*meteo\_data*) comprising meteorological characteristics (air temperature, relative humidity, wind speed, wind direction, atmospheric pressure, solar radiation, solar energy) registered synchronously with the birds observations in each viewpoint. Both datasets can be found in the Supplementary Files (Supplementary Files SF28).

Algorithm of the “Georeferenced birds and meteorological parameters” database preparation contained the following steps. At first, the *vultures\_data* and the *meteo\_data* datasets were linked with each other in a single table by the identical “time of observation” parameter. Then, the resulting merged table (entitled as the “Birds and meteorological parameters” merged dataset) was georeferenced in ArcGIS through the geographical coordinates of the viewpoints. Next, the geographical coordinates and the height of flight parameter were calculated for each registered bird. Finally, the “Birds and meteorological parameters” dataset was georeferenced again through the geographical coordinates of the registered birds.

#### Step 1. Linking of two datasets by the identical “time of observation” parameter

*The procedure was performed using Excel, ArcMap, Notepad*

1. In each table (*vultures\_data* and *meteo\_data*) the columns “Date” (ex. 02/04/2013) and “Time” (ex. 14:45:00) were joined with each other in a single column using the equation  $\text{=LEFT(D2;10) + LEFT(E2;10)}$  of Excel software. The resulting summary column (entitled here as “*date and time*” column) acquired “time of observation” parameter in the format of “date, time” (for example: 02/04/2013 14:45).
2. The “*date and time*” column was transformed in “text” format in both xlsx tables (*vultures\_data* and *meteo\_data*). For this the “text” format was previously set for an empty column of a sheet. Then, the “*date and time*” column was selected and saved in Excel and put in Notepad, saved there again, and put in the text column of xlsx file. As a result, *vultures\_data* and *meteo\_data* tables acquired the identical column with “time

of observation” parameter saved in “text” format. This column was entitled as `timevult_txt` and `timemeteo_txt` respectively.

3. The both tables (`vultures_data`, `meteo_data`) were added by “Add Data” option in ArcMap open project. For the `vultures_data` table the “Joins and Relates” option (which is launched directly from a layer) was applied by the following settings: In the graph “Choose the field in this layer that join will be based on”: `timevult_txt` was set. In the graph “Choose the table to join this layer”: `meteo_data` was set. In the “Choose the field in the table to base the join on”: `timemeteo_txt` was set. In the graph “Keep all records” – “ON” was set.
4. The resulting table (entitled here as “`jointdata`”) opened in ArcMap project contains data from both (`vultures_data` and `meteo_data`) tables linked with each other in a single table by the identical “time of observation” parameter. The “time of observation” parameter there was represented by two identical columns `timemeteo_txt` and `timevult_txt`. One of these columns was deleted from the table, another one was renamed as `dat_txt`.

## Step 2. Georeferencing of the merged dataset via observation points

*The procedure was performed using ArcMap*

The `jointdata` table was georeferenced (i.e. transformed to a point shapefile) via the geographical coordinates of observation points, i.e. columns `Lat_Pob` (latitude of viewpoint, degrees) and `Long_Pob` (longitude of viewpoint, degrees). For this, the “Display XY Data” option was launched directly from the `jointdata` table in ArcMap project. In the graph “Specify the fields for the X, Y and Z coordinates” the following was set: X field - `Long_Pob`; Y field - `Lat_Pob`. The resulting `Jointdata$Events` layer which was generated by ArcMap after considered operation, was exported to Shapefile format. For this directly from the layer `Jointdata$Events` it was set the following: `Data > Export Data`. In the graph “Use the same coordinate system as” the “this layer's source data” was set; in the graph “Output feature class” the destination folder and the Shapefile format of file were chosen. The resulting point shapefile (entitled here as `Jointdata.shp`) can be found in the Supplementary Files SF1). For each study site it represents the viewpoints as vector points on GIS map linked with datasets of vultures and meteorological data.

## Step 3. Calculation of the geographical coordinates of the registered birds

*The procedure was performed using ArcMap*

1. At first, the geographical coordinates (`Lat_Pob`, `Long_Pob`) of viewpoints in the prepared shapefile `Jointdata.shp` were transformed from degrees to metres. For this, the ArcMap project was transferred to UTM projection:  
View > Data Frame properties > Coordinate System > Projected Coordinate System - UTM - Southern Hemisphere  
- WGS 1984. UTM Zone 22S (Prudente); Zone 23S (Amarais)
2. Then, two new fields of “Double” type were created in the attribute table of `Jointdata.shp` and entitled as `LAT_PobM` and `LON_PobM`. The `Calculate Geometry` option was applied for calculation of the geographical coordinates of viewpoints in metres in those fields. It was conducted directly in the attribute table of `Jointdata.shp` by the following settings:  
The “Calculate Geometry” was launched for `LON_PobM` field > X Coordinate of Point > Use coordinate system of the data frame; Units Metres > OK.  
The “Calculate Geometry” was launched for `LAT_PobM` field > Y Coordinate of Point > Use coordinate system of the data frame; Units Metres; > OK.  
In the result of this operation, the `LAT_PobM` and `LON_PobM` fields acquired the geographical coordinates (latitude and longitude) of viewpoints expressed in metres.

3. Then, other three new fields of “Double” type were created in the attribute table of *Jointdata.shp*: *Pbird\_LatM* (for latitude), *Pbird\_LonM* (for longitude) and *ALT\_m* (for height of flight).
4. Finally, the latitude ( $X_a$  or *Pbird\_LatM*), longitude ( $Y_a$  or *Pbird\_LonM*) and height of bird's flight ( $h_a$  or *ALT\_m*) parameters were calculated for each ornithological object. The calculation were conducted by *Field Calculator* tool directly in attribute table of *Jointdata.shp* using the average values of registered intervals of distance ( $d$ ), compass direction ( $\alpha$ ), vertical angle expressed in radians ( $\beta$ ) and geographical coordinates of a viewpoint in metres ( $X_0$ ,  $Y_0$  or *LON\_PobM*, *LON\_PobM*) by the following equations:

$$X_a = X_0 + d_a \cdot \cos\alpha \cdot \cos\beta \quad (\text{Eq. c1.1})$$

$$Y_a = Y_0 + d_a \cdot \sin\alpha \cdot \cos\beta \quad (\text{Eq. c1.2})$$

$$h_a = d \cdot \sin\beta \quad (\text{Eq. c1.3})$$

As a result, the *Jointdata.shp* shapefile acquired columns of latitude, longitude and height of flight parameters (all of them are expressed in metres) for each ornithological object.

#### **Step 4. Georeferencing of the merged dataset via geographical coordinates of registered birds**

*The procedure was performed using ArcMap*

To represent the each ornithological object on GIS map as a vector point, the *Jointdata.shp* was exported to a new shapefile. For this, the attribute table of *Jointdata.shp* was exported to dbf (dBASE) table and added to ArcMap open project. Then, the operation of Georeferencing procedure was repeated by the scheme considered in the Step 2, but in the graph *Display XY Data* for X field *Pbird\_LonM* field was set; for Y field - *Pbird\_LatM* field was set.

The resulting point shapefile became the ready “*Georeferenced birds and meteorological parameters database and*”. You can find it for both study sites in the Supplementary Files SF2.

#### **Step 5. Preparation of the summary tables for statistical analyses, studying the relationships between soaring activity of Black vultures and meteorological conditions.**

*The procedure was performed using Excel, ArcMap*

The summary tables for implementation of three statistical tests studying the relationships between soaring activity of Black vultures and meteorological conditions (Principal component analysis, Multiple regression analysis and Pearson correlation analysis) were prepared from the attribute table of the “Georeferenced birds and meteorological parameters” database (Supplementary Data SF2). The summary tables were prepared by the following way. The  $F_{\text{birds}}$  index and the value of each meteorological parameter were calculated as an arithmetic mean for each time interval of 15 minutes and for each month over 13 viewpoints of both study sites. The obtained data were organized as a table. Those calculations were implemented in the ArcMap and Excel software within the attribute tables of shapefiles representing the “Georeferenced birds and meteorological parameters” georeferenced database. The resulting tables prepared for statistical analyses implementation you can find in the Supplementary Files SF39.

## Algorithm C2

### Transformation of timescale to the relative biological timescale and normalized relative biological timescale

To study the flying activity of birds during a day and throughout the year, the ordinary timescale used to record the time was transformed to a *relative biological timescale* where time of local sunrise was taken as a zero point. The ordinary time of the local sunrise, noon and sunset parameters were calculated for central viewpoints for each study site (point №7 for Amarais site and point №5 for Prudente site) for each day of the observation period. In those calculations, the Daylight Saving Time in Brazil (“summer time”) was taken into account: for both airports 1 hour was added to all data of sunrise, noon and sunset for the period from 21 October 2012 to 17 February 2013. To compare curves of daily activity by month, the parameters of sunrise, noon and sunset were averaged for each month.

To compare abundance of soaring birds by months, the relative biological time normalized to the day length of 12 hours was applied. This procedure allowed to compare the peaks and drops of the birds soaring activity, values of meteorological parameters and their dependence from sun position.

The converting to the normalized *relative biological timescale* was implemented by the following equation:

$$T_{\text{new}(i)} = \frac{T(i) - T_{\text{sunrise}(j)}}{T_{\text{sunset}(j)} - T_{\text{sunrise}(j)}} \cdot \frac{T_{\text{sunset}(23\text{sep})} - T_{\text{sunrise}(23\text{sep})}}{1} \quad (\text{Eq. c2.1})$$

Since  $T_{\text{sunset}(23\text{sep})} - T_{\text{sunrise}(23\text{sep})} = 12.14$  hours is equal to  $\sim 12$  hours, the resulting equation for time conversion is the following:

$$T_{\text{new}(i)} = 12 \frac{T(i) - T_{\text{sunrise}(j)}}{T_{\text{sunset}(j)} - T_{\text{sunrise}(j)}} \quad (\text{Eq. c2.2})$$

Where  $T(i)$  – time of the ordinary timescale;  $T_{\text{new}(i)}$  – the same time converted to the normalized *relative biological timescale*;  $T_{\text{sunrise}(j)}$ ,  $T_{\text{sunset}(j)}$  – times of local sunset and sunrise in a day to which the  $T(i)$  parameter belongs.

In the Supplementary Data SF29, SF30 you can find the .xlsx files representing all calculation procedures and tables with time of local sunrise, sunset and noon. Those values were calculated by the standard astronomic algorithm for each viewpoint and each day of the observation period for both studied territories.



## Algorithm C3

### Georeferencing of the birds through the projected polygons

The position of each flying bird in our study was registered as interval of values. This was determined by the complexity of the observed object (groups of birds flying at different altitudes) and the large studies areas. Both reasons provided the strict limitation of the applied techniques of birds' census and impossibility to register a position of flying bird as a point. For this reason, the georeferencing of the registered birds was conducted by two stages.

At first, the recorded birds were georeferenced as vector points with geographical coordinates calculated by the average values of its registered parameters (i.e. intervals of distance, vertical angle and direction) and geographical coordinates of a viewpoint from which it was observed. This procedure was considered in Algorithm C1. The resulting [Georeferenced birds and meteorological parameters database](#) (a point shapefile for each study site) combines all ornithological objects georeferenced as vector points. The attribute table of this shapefile represents each ornithological object as a series of the registered parameters and meteorological characteristics, measured synchronously with its observation<sup>48</sup>.

However, georeferencing of a recorded bird to a point determine only an approximate position of bird's location over the surface. To take into account the inaccuracy of the determined geographical position of a bird in analyses and map construction, the birds georeferenced as points (in point shapefile) were transformed to the birds georeferenced as polygons (in polygonal shapefile). Those polygons we entitled as the "*projected polygons*". Each projected polygon was constructed by the entire values of the registered parameters of a recorded bird (i.e. intervals of the distance, vertical angle and direction) and represents the projection on surface of three-dimension figure within which a recorded bird was located in the moment of registration. This transformation allows to determine the uncertainty of spatial position of flying birds caused by the interval character of the recorded parameters. Also it permits to include this uncertainty into analyses, which improved the accuracy of their results.

The georeference of ornithological objects by projected polygons was based on the point shapefile [Georeferenced birds and meteorological parameters database](#) and was implemented in two stages. At first, the projected polygons were constructed in the ArcGIS software. At second, for each projected polygon all ornithological objects, registered above it during the period of observation, were attributed. Both stages were implemented separately for Amarais and Prudente sites in ArcMap software by the technical algorithm considered below<sup>49</sup>.

#### Stage 1. Construction of projected polygons for a studied site

1. The [Georeferenced birds and meteorological parameters](#) database (point shapefile, Supplementary Files SF2) was used as the basis of construction of the projected polygons. The following parameters of each ornithological object (fields in the attribute table of point shapefile) were saved as a new point shapefile and applied for construction of projected polygons: number of viewpoint ( $P_{ob}$ ); latitude and longitude of each ornithological objects; latitude and longitude of viewpoint; quantity of birds, distance to bird ( $d$ ), vertical angle to bird ( $\beta$ ), direction to bird ( $\alpha$ ), time of observation. The resulting shapefile was entitled here [point\\_baseofpolygon.shp](#). It can be found in Supplementary Files SF6.

<sup>48</sup> The technical algorithm of preparation of the Georeferenced birds and meteorological parameters database is considered in the Algorithm C1. The shapefiles of this database you can find in the Supplementary Files (SF2).

<sup>49</sup> The algorithm considered all operations for one study site. These procedures were implemented identically for Amarais and Prudente sites. The most of titles of shapefiles, xlsx files and fields in the text are unreal, they are given only for simplicity of the technical description. The real titles of files and files themselves you can find in the Supplementary Files by links provided in the descriptions.



2. The maximum value of  $S$  ( $S_{\max}$ ) and the minimum value of  $S$  ( $S_{\min}$ ) were calculated for each combination of intervals of  $d$  (100-200 m, 200-400 m, 400-700 m, 700-6000 m) and  $\beta$  (2.5-7.5°, 7.5-12.5, 12.5-17.5... 82.5-87.5, 87.5-90°). The calculation was conducted in new fields within attribute table of [point\\_baseofpolygon.shp](#) by the following equations:

$$S_{\max} = \cos \beta_{\min} * d_{\max} \quad (\text{Eq. c3.1})$$

$$S_{\min} = \cos \beta_{\max} * d_{\min} \quad (\text{Eq. c3.2})$$

Where  $d$  - is a measured interval of distances between observer and bird (metres);  $\beta$  - a measured interval of vertical angles between observer and bird (degrees);  $S$  – a calculated interval of distances between viewpoint and projection of a bird on surface (metres).

For example, for interval of  $\beta$  (12.5-17.5°) and interval of  $d$  (100-200 m),

$$S_{\max} = \cos (12.5^\circ) * 200 = 195 \text{ m}$$

$$S_{\min} = \cos (17.5^\circ) * 100 = 95 \text{ m}$$

3. A new field of “double” type was created in the attribute table of [polygonbase.shp](#). It was entitled “Delta” and calculated by the Eq. 3 using the *Field Calculator tool* directly in the attribute table of [polygonbase.shp](#):

$$\text{Delta} = S_{\max} - S_{\min} \quad (\text{Eq. c3.3})$$

4. A new polygonal shapefile was constructed around each viewpoint by means of *Buffer tool* (Analysis toolbox, Proximity toolset). It was entitled [small\\_circles.shp](#) and consists from polygonal circles with centers in 13 viewpoints and radius equal to  $S_{\min}$ .

5. A new polygonal shapefile was constructed around each viewpoint by means of the *Buffer tool* (with the settings “Side Type” – “OUTSIDE\_ONLY”) by addition of “Delta” field to [small\\_circles.shp](#). The resulting polygonal shapefile was entitled [bagel.shp](#). It consists of circular objects with a shape of bagel, where the radius of empty inner circle equals to  $S_{\min}$  and the radius of large outer circumference equals to  $S_{\max}$ .

6. A new polygonal shapefile was constructed around each viewpoint. It consists from *sector triangles* with rays radiating from each viewpoint and directed at an angle equal to 22.5°, 67.5°, 112.5°, 157.5°, 202.5°, 247.5°, 292.5°. Each viewpoint has 8 resulting sectors triangles with central angles equal to intervals of [direction to a bird](#) parameter (i.e. 22.5-67.5° (sector №1), 67.5-112.5° sector №2, 112.5-157.5°, 157.5-202.5°, 202.5-247.5°, 247.5-292.5°, 292.5-337.5, 337.5 - 22.5° (sector №8)). The construction of sector triangles was implemented in two steps.

- At first, the geographical coordinates of two vertices of each triangle were calculated by the following equations:

$$X_b = X_0 + d \cdot \cos \alpha \cdot \cos \beta \quad (\text{latitude}) \quad (\text{Eq. c3.4})$$

$$Y_b = Y_0 + d \cdot \sin \alpha \cdot \cos \beta \quad (\text{longitude}) \quad (\text{Eq. c3.5})$$

Where  $X_0$ ,  $Y_0$  are the geographical coordinates of a viewpoint;  $\cos \beta = 1$  (since the vertical angle  $\beta = 0^\circ$ ), angle  $\alpha$  – equal to the values of the [direction to a bird](#) parameter (i.e. 22.5°, 67.5°, 112.5°, 157.5°, 202.5°, 247.5°, 292.5°);  $d > 6000\text{m}$  (equal to any constant number, which is a bit larger than the largest value of the [distance to a bird](#) parameter). Each triangle was constructed by 3 point (viewpoint and two vertices whose coordinate were calculated), by *Points*

*to line tool* (Data Management Toolset, Features). The resulting linear shapefile with constructed sector triangles was entitled as the *sectriangles1.shp*.

- At second, the linear *sectriangles1.shp* was transformed to a polygonal shapefile by the *Feature to Polygon tool* (Data Management Toolset). The resulting polygonal shapefile was entitled *sectriangles2.shp*. It consists from polygonal sector triangles of 13 viewpoints.

7. The intersection between *bagel.shp* (bagel looking objects) and *sectriangles2.shp* (polygonal sector triangles) were found by means of *Intersect tool* (Analysis Toolset, Extract, Overlay). The resulting polygonal shapefile was entitled *projected\_polygons.shp*. It contains the **final projected polygons** (Figs. 3.3-3.6). It can be found for both studied sites in Supplementary Files SF5.

The forms of projected polygons are defined by the geometry of a circle with observer in its center, which is caused by the specific of bird's census conduction from the viewpoints within radius of visibility. It looks like *annular sector* (when vertical angle to a bird was 5-85°), and *circle* (when the vertical angle to a bird was equal to 90°, i.e. bird was located exactly above the viewpoint)<sup>50</sup> (Fig. 3.5, Fig.3.6). The total number of projected polygons is determined by sum of all possible combinations of intervals of the recorded parameters (18 – by vertical angle; 8 - by direction and 4 - by distance), and taking into account that the vertical angle equal to 90° produces a circular projected polygon. Thus, the total number of projected polygons is the following: for each viewpoint:  $(18 \cdot 8 \cdot 4) - (4 \cdot 7) = 548$ ; for each airport:  $13 \cdot 548 = 7124$ ; in total  $= 7124 \cdot 2 = 14248$ . The projected polygons superpose each other (Fig. 3.5). This is caused by the geometry of their construction and by four distance intervals from a viewpoint to birds. The number of superposed polygons varies from three above the viewpoint to several dozen at the periphery of the studied zone.

## Stage 2. Georeference of ornithological objects through the projected polygons

8. The *identification index k* was calculated for each projected polygon using the parameters of its construction<sup>51</sup>: the number of viewpoint (**P<sub>ob</sub>**); the mean interval of vertical angle to bird (**β**); the direction to bird (**α**) expressed in the number of **sector** (for  $\alpha = 22.5-67.5^\circ$  sector = 1,  $\alpha = 67.5-112.5^\circ$  sector = 2,...  $\alpha = 337.5 - 22.5^\circ$  sector = 8); and the mean interval of distance to a bird (**d**). The calculation were implemented by the following equations and assigned to each projected polygon in a new “double” filed “*index\_k*”<sup>52</sup> created in the attribute table of *projected\_polygons.shp*.

$$k = \frac{P_{ob}}{100} + \frac{a}{1000} + \frac{Q}{100000} + d_{mean} \quad (\text{for } \beta < 90^\circ) \quad (\text{Eq. c3.6})$$

$$k^u = d_{mean} + \frac{P_{ob}}{100} \quad (\text{for } \beta = 90^\circ) \quad (\text{Eq. c3.7})$$

The resulting polygonal shapefile with indexed projected polygons can be found in the Supplementary Files SF7.

<sup>50</sup> When a vertical angle to a bird was 90° it was no value of “direction to a bird” parameter, because a bird was located exactly above the observer. In this case the projected polygon is a circle above the viewpoint with a radius equal to the height of a flying bird above the ground.

<sup>51</sup> At the same time they are the parameters of birds' registration.

<sup>52</sup> In the attribute table of shapefiles (SF6, SF7) this index entitled as “*Sum\_index*” for vertical angle < 90°, “*Sum\_ind90*” for vertical angle = 90° and “*index\_k*” – for all angles (this filed combines values of index from both previous fields) .

9. The same index was calculated for each ornithological object by the same equations in the attribute table of the point shapefile [point\\_baseofpolygon.shp](#) and placed in a new “double” field “*index\_k*”. As a result of both operations, the index k of each projected polygon was assigned to all ornithological objects which were registered above this polygon during the observation period. The resulting [point\\_baseofpolygon.shp](#) consisting of the “index k” field for the registered birds you can find in the Supplementary Files SF6.

10. In the [projected\\_polygons.shp](#) the unique ID number (ex. 1, 2, 3, 4....7123) was assigned to each projected polygon in a new “Short Integer” field “*UAid*”<sup>53</sup>. It was implemented by the “FID” field generated automatically in a shapefile and containing a numerical row. To attribute this numerical row to *UAid* field in a constant form<sup>54</sup>, the **FID+1** equation was calculated in it by the **Field Calculator** tool directly in attribute table of [projected\\_polygons.shp](#).

11. In the [point\\_baseofpolygon.shp](#) the *UAid* of each projected polygon was assigned to all ornithological objects which were registered above this polygon. It was implemented by linkage through the field “*index\_k*” using the option *Join attributes from a table* (directly from a layer: Joins and Relates > Join).

12. In the [point\\_baseofpolygon.shp](#) for each projected polygon (i.e. for each *UAid* number) the **sum of birds registered over this projected polygon during the period of observation** was calculated. It was conducted by means of *Dissolve tool* (Data Management, Generalization) with the following settings: in the *dissolve\_field* the “*UAid*” field was selected and in the statistics fields the “SUM” for quantity of birds (*Num\_vult*) field was set<sup>55</sup>. The calculated sum of birds was attributed to a new column entitled *SumVULT*.

The **SumVULT** field represents for each projected polygon (identified by a number in the *UAid* field) the **total amount of birds that were registered over this projected polygon during the period of observation**. We used this field in the subsequent data preprocessing.

The resulting point shapefile was entitled [point\\_birds\\_dissolve\\_sumvult.shp](#). It can be found for both studied site in the Supplementary Files SF8. This shapefile does not contain all registered birds. It is a “working file” which was created especially to assign for each number of *UAid* the total sum of birds (*SumVULT* field) registered over this polygon during the observation period.

13. The [point\\_birds\\_dissolve\\_sumvult.shp](#) was used to attribute the *SumVULT* field to the shapefile of projected polygons ([projected\\_polygons.shp](#)). The operation was implemented by the *Join attributes from a table* option. The joining was conducted by the *UAid*<sup>56</sup> field. The resulting shapefile of projected polygons was entitled [polygons\\_sumvult\\_all.shp](#). It can be found for both study sites in the Supplementary Files SF9. It consists from projected polygons constructed for four distance intervals (100-6000 m); each projected polygon of this shapefile contains the total sum of birds registered over it during the period of observation (*SumVULT* field). **This polygonal shapefile became the basis for preparation of summary tables for statistical and landscape analyses and for construction of risk assessment maps.**

The subsequent data preparation for analyses are considered in the Algorithm C4. The construction of risk assessment maps is described in the Algorithm C5.

<sup>53</sup> “*UAid\_amar*” for Amaraïs and “*UAid\_prud*” for Prudente

<sup>54</sup> We cannot use the FID itself, because it does not hold the numerical row in unchanged form in a shapefile. After saving of shapefile, the FID field generated again with a new numbering. The copy of numerical row of FID field into a new *UAid* field allowed to save of the identification number in a constant condition for each object of the shapefile.

<sup>55</sup> Each projected polygon has two unique parameters which were assigned to all ornithological objects registered over it in the [point\\_baseofpolygon.shp](#): *index\_k* and *UAid*. We dissolved by *UAid* field just for desire use this parameter as unique number of projected polygon and as index for linking projected polygon and birds which were registered over it. But we may did it without *UAid*, only by *index\_k*.

<sup>56</sup> We also can join using the *k\_index* field (see the previous footnote).

## Algorithm C4

### Preparation of the “ $W_{birds}$ and superficial parameters” georeferenced database for statistical analyses implementation

The `polygons_sumvult_all.shp`<sup>57</sup> became the basis for preparation of summary tables for statistical analyses, studying of relationships between abundance of soaring Black vultures and superficial characteristics. Preliminarily all polygons constructed within a distance to bird larger than 700 m (i.e. data of the fourth distance interval)<sup>58</sup> were excluded from this shapefile. In the resulting polygonal shapefile (`polygons_sumvult_700m.shp`, Supplementary Files SF10) each projected polygon contains the number of birds recorded over it during the year of observation in the field **SumVULT**.

The  $W_{birds}$  index was applied in analyses as a relative numerical measure of abundance of soaring birds over territory. In this regard, the “ $W_{birds}$  and superficial parameters georeferenced database” (or “ $W_{birds}$  database”) combining several polygonal shapefiles, was prepared in ArcGIS software. The attribute tables of those shapefiles (Supplementary Files SF15, SF16, SF17, SF18) became the basic tables for statistical tests implementation. Technical algorithms for preparation of  $W_{birds}$  database for statistical analyses are considered below.

#### Stage 1. Preparation of the $W_{birds}$ database for Principal component analysis and Multiple regression analysis

*The procedure was performed using ArcGIS (ArcMap)*

The Principal component analysis (PCA) and the Multiple regression analysis (MRA) were conducted to study the relationship between soaring activity of Black vultures expressed in  $W_{birds}$  index and superficial characteristics (`surface temperature`, `contrast of surface temperatures`, `altitude above sea level`, `slope inclination`, `slope exposure` and `level of anthropogenic pressure`<sup>59</sup>), revealed from the remote sensing products. The technical steps for preparation of summary tables for two statistical tests implementation were the following:

- ❖ Firstly, three relief parameters were assigned to a grid (entitled **Grid-1**) of square cells with a size of 30 m, which was created from the raster ASTER GDEM v2. Those parameters are `height`, which are the “native” parameter of ASTER GDEM v2, `aspect` and `inclination`, which were calculated from the altitude parameter by dint of Aspect and Slope ArcGIS tools respectively.

<sup>57</sup> The construction of `polygons_sumvult_all.shp` is considered in the Algorithm C3.

<sup>58</sup> The fourth distance interval (700 - 6000 m) was excluded from the analyses of superficial factors due to high uncertainty on determination of the number and geographical positions of flying birds (see details in "Assumptions and limitations" section of Chapter III).

<sup>59</sup> The obtainment of all superficial parameters from the remote sensing products is considered in the Chapter III, div. 2.2.1.1. The “level of anthropogenic pressure” parameter was detected together with the “landscape type” parameter according to the elaborated classification of landscape types (Chapter III, div. 2.2.1.2, Table 3.3). The landscape type is not a numerical parameter, since that it was not included in the statistical tests. The dependence of soaring activity of vultures from landscape type was studied separately in the “Landscape analysis”. The slope exposure did not reveal any significant influence on the soaring activity of birds, thus it was excluded from the statistical tests.

- ❖ Then, both surface temperature parameters were attached to the Grid-1. The *surface temperature* was detected directly from the raster AST\_08, while the *contrast of surface temperature* was recalculated from AST\_08 by *Slope tool* of ArcMap. Both parameters were assigned to a cell of the *Grid-1* by the method of simple averaging. For each cell belonging to the Grid-1 and overlapping with 2 or 4 pixels of AST\_08, a simple average of values in those pixels was assigned. The final grid (entitled *Grid-2*) acquired the relief and superficial temperature parameters.
- ❖ Next, the shapefile containing the *landscape type* and its *level of anthropogenic pressure* parameters was imposed on the Grid-2. Each cell of the resulting grid (entitled *Grid-3*) contains the whole cell of the Grid-2 or its part with a type of landscape attributed to it. Cells of the Grid-3 became the final “*spatial units*” of summary tables for statistical tests implementation. Each spatial unit has a size of 30 by 30 m or smaller, since a part of original cells was subdivided into smaller pieces. However, only spatial units with a side of about 30 m were used in the statistical tests. The smaller pieces were excluded from the analyses.
- ❖ Finally, the  $W_{birds}$  index was calculated for each “spatial unit” of the Grid-3<sup>60</sup>.

In the result, a polygonal shapefile containing of spatial units with attributed values of all superficial parameters and  $W_{birds}$  indices was acquired for each studied area. The attribute tables of those shapefiles became the summary tables for implementation of PCA and MRA. You can find those shapefiles and summary tables in the Supplementary Files SF15, SF40.

The surface parameters have the following accuracy of detection:

- The *level of anthropogenic pressure* parameter was detected without spatial distortion because it was attached to the final spatial units with its exact geographic position.
- Three *relief parameters* also were detected without spatial distortion because they belong to the raster of ASTER GDEM v2, which became the basis for the Grid-1, Grid-2, Grid-3 and for the creation of final spatial units.
- Two *surface temperature parameters* were determined with small spatial distortions because they were assigned to final spatial units by means of the simple averaging method. However, the spatial distortion of surface temperature parameters is not too large. A pixel size of the raster AST\_08 (from which the surface temperature parameters were detected) is of 100 by 100 m. When a pixel of AST\_08 overlaps a grid with cells of 30 by 30 metres or less, the averaged values of two or four neighboring pixels of AST\_08 pass to a negligible area comparing to its total sizes.

## Stage 2. Preparation of the $W_{birds}$ database for Spearman rank correlation analyses

The Spearman rank correlation analysis (SRCA) was conducted to clarify the links between abundance of soaring Black vultures expressed in  $W_{birds}$  index and two surface temperature parameters (*surface temperature* and *contrast of surface temperature*). The preparation of the  $W_{birds}$  database for this analysis included two steps:

At first, the  $W_{birds}$  database was constructed by the similar procedure as it was considered above for PCA and MRA. The spatial units of  $W_{birds}$  database were produced from the pixels of raster AST\_08, consisting from square cells with size of 100 by 100 m. In contrast with other statistical tests, the cells in SRCA did not change their size and

<sup>60</sup> The equation for  $W_{birds}$  index calculation is considered in the article 2 (Eq. 1) and in the text of dissertation (Eq. 7)



square shape during the  $W_{birds}$  database preparation. Both parameters (surface temperature, contrast of surface temperature) and  $W_{bird}$  index were assigned to each spatial unit of those shapefiles. The attribute tables of the resulting shapefiles became the basis for the preparation of the summary tables for SRCA implementation. Those shapefiles for both study sites can be found in the Supplementary Files SF16, SF17, SF18.

Next, both surface parameters were arranged in those summary tables and subdivided by values *in ascending* order, so that each rank comprised 10% of records.

Finally, for each rank the arithmetic mean of surface parameters and the weighted mean of  $W_{birds}$  index were calculated accounting for the area of each cell. This operation was implemented in Excel separately for each parameter in its own table. The resulted summary tables, presented in Tables 3.7- 3.10 and the Supplementary Files SF42 were processed with the Spearman correlation analysis between surface temperature and  $W_{birds}$ ; contrast of the surface temperature and  $W_{birds}$  index.

### Preparation of the $W_{birds}$ database for the landscape analyses

The landscape analysis was conducted to reveal the dependence of soaring activity of Black vulture and landscape type (i.e. type of surface covering coupled with its level of anthropogenic pressure). As in other spatial analyses, the study area of the landscape analysis was the circular zones with a radius of 700 m around 26 viewpoints of both airports' surroundings. The basis of implementation of landscape analysis was the  $W_{birds}$  database, prepared by the following algorithm in ArcGIS 10.0 (ArcMap) software.

- ❖ At first, the study area were manually digitized according to the elaborated classification of landscape types, consisting from 7 surface covering types coupled with 4 levels of anthropogenic stress (Table 3.3). The digitizing was conducted in ArcMap software basing on high-resolution DigitalGlobe imagery, obtained by fee-free option of the Basemap gallery of ArcMap. The resulting polygonal shapefile acquired "Landscape" text field, containing the title of landscape type. This shapefile was entitled here *landscape\_map.shp*. It can be found in the Supplementary Files SF19.
- ❖ Next, the **Dissolve tool** (Data Management - Generalization) was applied on *landscape\_map.shp* with the following settings: the "Landscape" field was set as a field for dissolve. The resulting polygonal shapefile (entitled here *landscape\_map\_dissolve.shp*) contains seven (for Amaraïs) and six (for Prudente) objects, each of each corresponds to a single landscape type.
- ❖ Finally, the *landscape\_map\_dissolve.shp* was joined by the "Join data from another layer based on spatial location" option (directly from a layer: Joins and Relates > Join) with shapefile of projected polygons *polygons\_sumvult\_700m.shp* (Supplementary Files SF10), containing the total sum of birds registered over each polygon during the observation period ( *SumVULT* field). In "How do you want the attributes to be summarized?" – the "Sum" was chosen.

The resulting polygonal shapefile acquired fields, representing the following parameters of each landscape type (i) *SumVULT* field - the total amount of birds that were registered above a landscape type during the observation period; (ii) *Area\_ha* field - the area in hectares of landscape type. It was calculated directly in the attribute table in the "double" type of field by "Calculate Geometry" tool; (iii) *SumVULT\_ha* field - the *SumVULT* parameter recalculated per 1 hectare of landscape type. It was calculated directly in the attribute table by the equation  $SumVULT / Area\_ha$  using the **Field Calculator tool**. This shapefile was entitled here *landscape\_Wbrds*. It can be found in Supplementary Files (SF20).

The attribute table of *landscape\_Wbrds* (Supplementary Files SF20) became the basis for subsequent data preparation for landscape analysis, which is considered in the text of dissertation and articles.

It is important to note, that in the landscape analysis the “Sum of birds recorded in each landscape type” parameter was applied as the numerical indicator of the abundance of soaring birds. It contrasts with statistical analyses and risk map construction, where the  $W_{\text{birds}}$  index was applied as a numerical indicator of the abundance of flying birds. We did not use  $W_{\text{birds}}$  index in the landscape analysis, because the objective of this analysis is to compare the landscape types by their attractiveness for vultures. For this purpose, it is more precisely to use a simple sum of registered birds counted in all polygons, instead of  $W_{\text{birds}}$  index.

Application of  $W_{\text{birds}}$  index allows to remove or smooth the incorrect increase of the number of registered birds attributed to some areas because of the geometry of projected polygons construction. For this reason, we used  $W_{\text{birds}}$  index for mapping (i.e. the detailed visual analysis of the territory) and statistical analysis, where landscapes were studied with other environmental characteristics. However, as any averaging,  $W_{\text{birds}}$  index increases the inaccuracy of the analysis studying the distribution of flying birds. Therefore, in the landscape analysis, where there was no need for such smoothing, we used a simple sum of birds registered.



## Algorithm C5

### The technique of cartographic visualization of the abundance of soaring Black vultures and the risk of collisions with these birds over the territory

The cartographic visualization of  $W_{\text{birds}}$  index allowed to construct maps, representing the numerical estimation of abundance of the recorded Black vultures over the airport's vicinities during the period of observation. At the same time those maps predict the risk of collision with these birds over each point of the studied territory. Those maps we entitled as the "*risk assessment maps*". We built them for the entire studied territory (i.e. for 13 km zone around each airport) and for circular zones of 700 m radius around the viewpoints.

The shapefile of projected polygons ([polygons\\_sumvult\\_all.shp](#)<sup>61</sup>, Supplementary Files SF9) containing the field **SumVULT** with the total amount of birds registered over each projected polygon during the observation period became the basis of creating of both maps. The construction of risk assessment maps was implemented in ArcGIS 10.0 (ArcMap) by the technique considered below.

#### Stage 1. The technique of construction of risk assessment maps for 13 km zone around airports

1. Firstly, a polygonal shapefile of grid consisting of equal square cells with size of 100 by 100 m and covering the entire studied territory (~13 km around airport) was created ([fishnet\\_polygon.shp](#), Supplementary Files SF11). Also the point shapefile consisting from net of points located in the centers of those square cells ([fishnet\\_points.shp](#), Supplementary Files SF12) was built. Both procedures were implemented by means of **Create Fishnet Tool** (Data Management - Feature Class - Create Fishnet) with settings: "geometry type" – polygon; the "Create Label Points" was marked).
2. Then, the polygonal grid [fishnet\\_polygon.shp](#) was joined by the "**Join data from another layer based on spatial location**" option (directly from a layer: Joins and Relates > Join) with the shapefile of projected polygons [polygons\\_sumvult\\_all.shp](#). In "**How do you want the attributes to be summarized?**" – the "**Average**" was chosen.

The resulting polygonal grid ([fishnet\\_polygon\\_all\\_Wbirds.shp](#), Supplementary Files SF11) acquired two fields: "**Count**", representing the number of overlapping projected polygons of the [polygons\\_sumvult\\_all.shp](#) in each cell of 100x100 m; and **AvgVULT** – representing the average number of birds registered in one of those polygons.

Next, values in the field **AvgVULT** were multiplied by 3 and written in a new field entitled **3AvgVULT**.

The field **3AvgVULT** represents the  $W_{\text{birds}}$  index<sup>62</sup>, which can be applied in analyses and mapping as a relative numerical measure of the abundance of soaring Black vultures over each point of the study territory. Also it can be interpreted and used as a numerical measure of hazard of collisions with these birds over the study territory.

3. In the next step we need to visualize the  $W_{\text{birds}}$  index on a map comprising the entire studied area, i.e. the 13 km zone around airport. It is impossible to visualize the  $W_{\text{birds}}$  index directly from the [fishnet\\_polygon\\_Wbirds.shp](#) for a large area in ArcMap, because the borders of cells do not allow to see the colors on a small scale. Thus, we constructed a raster from [fishnet\\_polygon\\_Wbirds.shp](#).

For this, the point shapefile [fishnet\\_points.shp](#), was joined by the "**Join data from another layer based on spatial location**" option (directly from a layer: Joins and Relates >

<sup>61</sup> The construction of [polygons\\_sumvult\\_all.shp](#) is considered in the Algorithm C3.

<sup>62</sup> The definition and equation of  $W_{\text{birds}}$  index con in the Chapter III (div. 2.2.4)

Join) with [fishnet\\_polygon\\_Wbirds.shp](#) (in the graph "Each point will be given all the attributes of the polygon that" the "it falls inside" option was set).

After this operation, the resulting point grid ([fishnet\\_points\\_Wbirds.shp](#), Supplementary Files SF12) acquired the **3AvgVULT** field representing the  $W_{birds}$  index.

4. Finally, the raster map visualizing the **3Avg\_VULT** or  $W_{birds}$  index was constructed using the Natural Neighbor method of [Interpolation tool](#) (Spatial Analyst) from the point shapefile [fishnet\\_points\\_Wbirds.shp](#). The resulting raster ([Wbirds\\_bigmap](#), Supplementary Files SF13) represents the final risk assessment map for the entire study area of airports surroundings. The color scale of a raster was adjusted for transmission of the general sense of the map. You can see the resulting map on the Fig 3.12, Fig.3.13.

## Stage 2. The risk assessment maps constructed for 700 m zone around viewpoint

The [polygons\\_sumvult\\_700m.shp](#) (Supplementary Files SF10), representing the projected polygons constructed for three distance intervals from 100 to 700 m (i.e. without data of the fourth interval), was implemented to build the small risk assessment maps. The algorithm of construction of map was similar to considered above, but small maps were created without interpolation, just by visualization the values of  $W_{bird}$  indices.

At first, the grid [fishnet\\_polygon.shp](#) was joined by the "Join data from another layer based on spatial location" option (directly from a layer: Joins and Relates > Join) with the [polygons\\_sumvult\\_700m.shp](#) (Supplementary Files SF10) containing the total sum of birds registered over each polygon during the year (**SumVULT** field). In the graph "How do you want the attributes to be summarized?" the "Average" was chosen. The resulting polygonal grid ([fishnet\\_polygon\\_700m\\_Wbirds.shp](#), Supplementary Files SF14) acquired two fields: "Count", which represents the number of overlapping polygons of the [polygons\\_sumvult\\_all.shp](#) in each cell of 100 by 100 m; and **AvgVULT**, which reveals the average number of birds registered in one selected polygon.

The  $W_{birds}$  index was calculated by multiplication of the **AvgVULT** field on 3 in a new "double" filed **3AvgVULT**. Then  $W_{birds}$  index was visualized directly on GIS maps. Examples of those maps constructed for two viewpoints of surroundings of the Amaraïs airport are presented in Fig. 3.14 (a), Fig. 3.15 (a).

The accuracy of the risk assessment maps is an important methodological issue. The records registered in the fourth distance interval (700- 6000 m) cover the significant areas within radius of 13 km around Amaraïs and Presidente Prudente airports. Whereas fourth interval has a large error in the determination of birds' number and geographical position, the maps are characterized by contrast precision. The areas mapped within 700 m zone around viewpoints reflect much more reliably the actual distribution of vultures and the hazard of collisions than the regions between 700 and 6000 m.

It is important to take into account our recommendation about the possibility of construction of risk assessment maps with high accuracy for all studied territory. Firstly, we recommend to reduce the distance between observation points up to 1400-1500 meters. In this case, areas of high-accuracy observations will connect with each other and the whole area will be covered by the high quality monitoring. Secondly, we suppose that the application of modern electronic equipment (*electronic laser range finders, video registration, radiolocation*) may allow to georeference the flying birds with higher accuracy than we did. However, we cannot say for sure that this equipment would allow recording quickly enough all birds flying around the observer; it should be tested. Also the use of these techniques will make the research more expensive.

## DESCRIPTION OF THE SUPPLEMENTARY FILES

The supplementary files you can find in the folder “SUPPLEMENTARY FILES\_NOVOSELOVA” by download it from the link (158 mb, zip):

<https://data.mendeley.com/datasets/74h7c74k8j/1>

Email for questions: [nataliceenov@gmail.com](mailto:nataliceenov@gmail.com)

Folder	File/Field	Type	№	Description of the Supplementary Files	Technical comments	Technical description: Appendix C
<b>Shapefiles</b>						
Preparation for analyses, studying the dependence of soaring activity of Black vultures on meteorological factors						
GIS_Shape	Amarais_FULldata.shp Prudente_FULldata.shp	point shapefile	SF1	The summary georeferenced database entitled as the “Georeferenced birds and meteorological parameters” database. AMARAIS, PRUDENTE The attribute table of this shapefile is the “Birds and meteorological parameters” merged database	In this shapefile each ornithological object is represented as a vector point, located in the viewpoint from which it was registered. The coordinates of viewpoint are presented in columns LAT_Pob (latitude) and LON_Pob (longitude). The coordinates of ornithological object itself are given in the fields Pbird_LatM (latitude) and Pbird_LonM (longitude).	Algorithm C1
GIS_Shape	Pbirds_FULL_Amarais.shp Pbirds_FULL_Prudente.shp	point shapefile	SF2	The summary georeferenced database entitled as the “Georeferenced birds and meteorological parameters” database. AMARAIS, PRUDENTE	These shapefile have the same attribute table as Amaraais_FULldata.shp, Prudente_FULldata.shp, but here each ornithological object is presented in GIS as a vector point with its own coordinates given in the fields Pbird_LatM, Pbird_LonM.	Algorithm C1
GIS_others	Amarais_Pobs.shp Prudente_Pobs.shp	point shapefile	SF3	Points of observation (viewpoints) of both study sites. The fields urbano, natural, agr_field, veget_nat present an approximate estimation of the area proportion for 4 landscape types (urban, natural, agricultural fields and	This simple assessment confirmed results of landscape analyses (which were more accurate and detailed, but considered smaller	

				natural vegetation) within a radius of 3340 m from each viewpoint. The assessment was carried out visually on the basis of high-resolution imagery of the Basemap gallery in ArcGIS.	areas - the 700 m radius zones around viewpoints). Both analyses showed that urban areas predominate in Amarais site, while in Prudente site natural and agricultural areas are more extensive.	
GIS_others	Amarais_Airport.shp PresPrudente_Airport.shp	point shapefile	SF4	Amarais Airport (Pob № 7 of Amarais site) Presidente Prudente Airport (Pob № 5 of Prudente site)		
<b>Projected polygons</b>						
GIS_Shape	GeorefpolygonsFULL_Amar. Shp GeorefpolygonsFULL_Prud. Shp	polygon shapefile	SF5	Georeferenced polygons constructed for all (four) distance ranges: 0-6000 m . AMARAIS, PRUDENTE		Algorithm C1
<b>Linking a projected polygon with birds registered over it by indexing. Construction of risk assessment maps</b>						
GIS_Shape	PbirdALL_indexed_UA_Amarais PbirdALL_indexed_UA_Prudente.shp	point shapefile	SF6	The resulting shapefile of indexed registered birds. Here each ornithological object has an identification index (field “index_k”) corresponding to the projected polygon above which it was registered. AMARAIS, PRUDENTE	The technical details about linking of the projected polygon and all birds which were registered over it by index_k you can find in the Algorithm C3.	Algorithm C3
GIS_Shape	PolygonsUA_indexed_Amarais.shp PolygonsUA_indexed_Prudente.shp	polygonal shapefile	SF7	The shapefile of indexed projected polygon. Here each ornithological object has an unique identification index (field “index_k”) calculated by the use of the certain parameters determined for each polygon (number of viewpoint, vertical angle, direction or sector and distance). AMARAIS, PRUDENTE	The technical details about linking of the projected polygon and all birds which were registered over it by index_k you can find in the Algorithm C3.	Algorithm C3
GIS_Shape	Pbirds_index_dissolv_SumVult_Amar.shp Pbirds_index_dissolv_SumVult_Prudente.shp	point shapefile	SF8	The resulting shapefile of birds’ observations after the Dissolve operation. This shapefile does not contain all registered birds. It is a “working file” which was created only to assign for each UAid (representing projected polygon) the total sum of birds (VULTsum field) which were registered over it during the year. This shapefile was used to attribute the VULTsum field to the shapefile of projected polygons by the identical field UAid. AMARAIS, PRUDENTE		Algorithm C3
<b>Cartographical representation of <math>W_{birds}</math> index. Construction of risk assessment maps</b>						
GIS_Shape	PolygonsUA_SumVult_ALL_Amar.shp PolygonsUA_SumVult_ALL_Prudente.shp		SF9	The resulting shapefile of projected polygons which contains the total sum of birds registered over it during the observation period (SumVULT field). This polygonal shapefile became the basis of preparing tables for statistical and landscape analyses and construction of the risk assessment maps. AMARAIS, PRUDENTE	The polygons with no registered birds were excluded from this shapefile	Algorithm C3

GIS_Shape	Georefpolygons700m_SumVultYear_Amar. Shp Georefpolygons700m_SumVultYear_Prud. shp	polygonal shapefile	SF10	Resulting shapefiles of projected polygons constructed for three distance ranges (0-700 m) with calculated SumVULT and DivSumVul8 parameters. (AMARAIS, PRUDENTE).	These shapefiles became the basis for preparing of data for statistical and landscape analyses and for construction of risk assessment maps of high accuracy for 700 m circular zones around viewpoints.	Algorithm C3
GIS_Shape	Fishnet_polygonal_Wbirds_Amarais.shp Fishnet_polygonal_Wbirds_Prudente.shp	polygonal shapefile	SF11	The polygonal shapefile of rectangular net consisting of square cells of 100x100 m covering the entire studied territory ( ~13 km around airport) It was created by dint of the Create Fishnet Tool of ArcGIS and used for construction of both types of risk assessment maps.		Algorithm C5
GIS_Shape	Fishnet_points_Wbirds_Amarais.shp Fishnet_points_Wbirds_Prudente.shp	point shapefile	SF12	The point shapefile of rectangular net consisting of points, located in the centres of square cells of Fishnet SF11. It was created by dint of the Create Fishnet Tool of ArcMap and used for construction of both types of risk assessment maps.		Algorithm C5
GIS_Raster\Amarais	wbird_amar wbird_prud	raster	SF13	The raster map created from the point shapefile of Fishnet (SF12), using the Natural Neighbor method of Interpolation tool (Spatial Analyst). This map visualizes the Wbirds index and represents the final risk assessment map for the entire airports surroundings (i.e. 13 km zone around each airport).		Algorithm C5
Risk assessment maps constructed for the area of 700 m radius around observation points (examples for Amaraïs site)						
GIS_Shape\riskmap700m_Amarais	Riskmap700m_Fishnet_Amarais.shp riskmap_amar11.shp riskmap_amar07.shp		SF14	Riskmap700m_Fishnet_Amarais.shp - is a polygonal shapefile of risk assessment maps, constructed for the area of 700 m radius around the 13 observation points of Amaraïs site. The map visualizes the Wbirds index (field 3AvgVULT), calculated for a year of observation for each spatial unit.  The riskmap_amar11.shp is this map, constructed around the viewpoint № 11 (PUCC) and riskmap_amar07.shp - around the viewpoint № 07 (Airport) of Amaraïs site.		Algorithm C5
Subsequent preparing shapefiles for analyses, studying the dependence of soaring activity of Black vultures on superficial and anthropogenic factors						
GIS_Shape	Surface_RegrModel_Amarais.shp Surface_RegrModel_Prudente.shp	polygonal shapefile	SF15	The "Wbirds and superficial parameters" georeferenced database (polygonal shapefile and its attribute table), which was used for preparing the summary tables for implementation of two statistical tests: Principal component analysis and Multiple regression analyses. The tests study the dependence of soaring activity of vultures from superficial (relief, surface temperature) and anthropogenic pressure parameters (AMARAIS, PRUDENTE).	The shapefile for each airport represent the studied area (i.e. 13 circular zones with a radius of 700 m around viewpoints) divided by small spatial units or cells (with size 30 x 30 m and smaller). For each cell the Wbirds index was calculated directly in the attribute table of shapefile (look WbirdsYear field below)	Algorithm C4

					and superficial parameters (surface temperature, contrast of surface temperatures, altitude above sea level, slope inclination, slope exposure, landscape type and level of anthropogenic stress) were attributed using the prepared georeferenced raster maps.	
GIS_Shape	Surftemp_gradtemp_vult_Amar.shp	polygonal shapefile	SF16	The “Wbirds and superficial parameters” georeferenced database (polygonal shapefile and its attribute table). It, was used for preparation of the summary tables for implementation of the Spearman rank correlation analysis between abundance of soaring vultures and two parameters of surface temperature (AMARAIS)		Algorithm C4
GIS_Shape	Surftemp_vult_Prud.shp	polygonal shapefile	SF17	The “Wbirds and superficial parameters” georeferenced database (polygonal shapefile and its attribute table). It was used for preparation of the summary tables for rimplementation of the Spearman rank correlation analysis between abundance of soaring vultures and surface temperature (PRUDENTE)		Algorithm C4
GIS_Shape	Gradsurftemp_vult_Prud.shp	polygonal shapefile	SF18	The “Wbirds and superficial parameters” georeferenced database (polygonal shapefile and its attribute table). It was used for preparation of the summary tables for rimplementation of the Spearman rank correlation analysis between abundance of soaring vultures and contrasts of surface temperature (PRUDENTE)		Algorithm C4
GIS_Shape	Landscape_map700m_Amar.shp Landscape_map700m_Prud.shp	polygonal shapefile	SF19	The landscape map (polygonal shapefile), produced by digitizing of the high-resolution DigitalGlobe image in ArcGIS according to the elaborated classification of seven landscape types and four levels of anthropogenic pressure. The landscape map were constructed for the circular zones of 700 m radius around the 13 observation points (AMARAIS, PRUDENTE)	The maps were used for implementation of two landscape analyses: for independent landscape analysis and for study the influence of anthropogenic pressure on soaring activity of vultures within PCA and MRA statistical tests..	Algorithm C4
GIS_Shape	Landscape700m_Wbirds_Amar.shp Landscape700m_Wbirds_Prud.shp	polygonal shapefile	SF20	The landscape map prepared for the Landscape analysis. It was produced from shapefiles Landscape_map700m_Amar.shp, Landscape_map700m_Prud.shp (F19). All digitized landscapes were merged in 6-7 objects (one object corresponds to one landscape type). For each landscape type the amount total of vultures registered over it in the observation period were calculated (fields Sum_SUMvul and Sum_Del8Vu).	Find description in Appendix C (Algorithm 4)	Algorithm C4

Raster maps of relief, surface temperature and gradient of surface temperature, created from the remote sensing products						
GIS_Raster	SlopeTsurfAm1.tif	raster	SF21(a)	Raster map representing the gradient or contrast of surface temperature parameter (angle degrees) for Amaraïs site (north part). It was built from AST_08 (derivative product of ASTER image) of 11.05.2013, 13:27: AST_L1A#00305112013132753_05132013034738.hdf by dint of Slope Tool of ArcGIS.	Look the parameters of the remote sensing products in the Chapter III, Table 3.1, Table 3.2.	
GIS_Raster/Amaraïs	SlopeTsurfAm2.tif	raster	SF21 (b)	Raster map representing the gradient or contrast of surface temperature parameter (angle degrees) for Amaraïs site (south part). It was built from AST_08 (derivative product of ASTER image) of 11.05.2013, 13:27: AST_L1A#00305112013132802_05132013034746.hdf by dint of Slope Tool of ArcGIS	Look the parameters of the remote sensing products in the Chapter III, Table 3.1, Table 3.2.	
GIS_Raster/Amaraïs	surfitem_moz.tif	raster	SF22	Raster map representing the surface temperature parameter (Celsius degrees) for Amaraïs site . It was built from AST_08 (derivative product of ASTER image) of 11.05.2013, 13:27: AST_L1A#00305112013132753_05132013034738.hdf (raster im1ast08_amar.tif) AST_L1A#00305112013132802_05132013034746.hdf (raster im2ast08_amar.tif)		
GIS_Raster/Amaraïs	astgdmaz_clip.tif	raster	SF23	Raster map representing the altitude above sea level parameter (metres) for Amaraïs site. It was obtained from two tiles of ASTER GDEM v2: ASTGTM.002:2088830049, ASTGTM.002:2088830127.		
GIS_Raster/Prudente	prud_ast08_clip.tif	raster	SF24	Raster map representing the surface temperature parameter (Celsius degrees) for Prudente site . It was built from the AST_08 (derivative product of ASTER image) of 20.08.2013, 13:46: AST_L1A#00308202013134626_08212013131509.hdf		
GIS_Raster/Prudente	prudgradtemp.tif	raster	SF25	Raster map representing the gradient or contrast of surface temperature parameter (angle degrees) for Prudente site. It was created from AST_08 (derivative product of ASTER image) of 20.08.2013, 13:46: AST_L1A#00308202013134626_08212013131509.hdf		
GIS_Raster/Prudente	Prud_astergdem.tif	raster	SF26	Raster map representing the altitude above sea level parameter (metres) for Prudente site. It was obtained from a tile of ASTER GDEM v2: ASTGTM.002:2088813568		
Datasets including the derived tables of shapefiles						
Datasets	FULLDATA_Amaraïs_Prudente.xlsx Sheet Amaraïs_FULLDATA	table.xlsx	SF27 (a)	"Birds and meteorological parameters" merged database. AMARAIS, PRUDENTE It is the copy of the attribute table of the		Algorithm C1



	Sheet Prudente_FULldata			Amarais_FULldata.shp, Prudente_FULldata.shp (SF1) in xlsx file		
Datasets\Meteo and vultures	AMARAIS_vult_meteo.xlsx Sheets: Vultures_Amarais Meteo_Amarais  PRUDENTE_vult_meteo.xlsx Sheets: Vultures_Prudente Meteo_Prudente	table xlsx	SF28	Two summary datasets: (i) Number and locations of soaring birds dataset, including census of ornithological objects and their registration parameters (i.e. the number of viewpoint, quantity of birds, direction, vertical angle, distance, and time of registration);(ii) Values of meteorological parameters dataset, with meteorological characteristics (air temperature, relative humidity, wind speed, wind direction, atmospheric pressure, solar radiation, solar energy) registered synchronously with the birds' observations in each viewpoint. Both tables have the identical time of observation parameter (dat_txt field). (AMARAIS, PRUDENTE)		Algorithm C1
Datasets\Biological timescal	Amarais_astromtime. xlsx Prudente_astromtime. xlsx	table xlsx	SF29	The basic tables of time of local sunrise, sunset and noon, calculated for each viewpoint of Amarais and Prudente sites by a special astronomic algorithm for each day of the observed period (September 2012 – August 2013)	By dint of this table the ordinary timescale was transformed to the relative biological timescale ("hours after sunrise" axis)	Algorithm C2
Datasets\Biological timescal	Amarais_aftersunrise_normalized Prudente_aftersunrise_normalized	table xlsx	SF30	Transformation of the ordinary timescale to the relative biological timescale and normalized relative biological timescale		Algorithm C2
Datasets\Biological timescal	Amarais_aftersunrise_normalized Sheet READYAmarNewTimeAxis-NORMAL(3) Prudente_aftersunrise_normalized Sheet READYPrud-NewTimeAxis-NORMAL(2)	table xlsx	SF31	The summary table for implementation of ANOVA test comparing months by Fbirds index, and for boxplot, representing the annual variation of Fbirds. This is an example of analysis where the normalized relative biological timescale was applied. (AMARAIS, PRUDENTE).		
Datasets\Height_Flight	Height of soaring flight.xlsx Sheet ALTITUDE OF FLIGHTS (amar)  Sheet ALTITUDE OF FLIGHTS (prud)	table xlsx	SF32	Summary table of the height of soaring vultures "height of flight" parameter, calculated from the observed parameters of birds position. Only data attributed to the distance to birds from 100 to 700 m were applied for calculations. AMARAIS, PRUDENTE		
Datasets\Height_Flight	Ranks_Height Flight.xlsx Sheet "Height & vult (50m) Amar"	table xlsx	SF33 (a)	Analysis of the height of vultures' flight parameter (AMARAIS).	The analysis studied the distribution of the recorded altitudes of soaring Black vultures nearby the Amarais airport during the year of observation	
Datasets\Height_Flight	Ranks_Height Flight.xlsx Sheet "Height & vult (50m) Prud"	table xlsx	SF33 (b)	Analysis of the height of vultures' flight parameter (PRUDENTE)	The analysis studied the distribution of the recorded altitudes of soaring Black vultures nearby Prudente Prudente airport during the year of	

					observation	
Datasets\Height_Flight	Height of flight & vultures number.jnb	sigma plot	SF33 (c)	Plots of analyses of the height of vultures' flight parameter (AMARAIS, PRUDENTE).	The analysis compared the real and the log-normal (theoretical) functional relationship between the "altitude of flight" and the "sum of birds recorded at this altitude" parameters	
Datasets\Monthly and daily soaring activity	Observed_vultures_by_month.xlsx sheet "Vultures Number (amar)"; sheet "Vultures Number (prud)"	table.xlsx	SF34	The number of Black vultures recorded during each month and the whole year of observation (AMARAIS, PRUDENTE).		
Datasets\Monthly and daily soaring activity	*PREP_Daily_Soaring_Amar.xlsx *PREP_Daily_Soaring_Prud.xlsx *Year_Amarais_F(birds).xlsx *F(birds) in Months_Prudente.JNB *F(birds) in Months_Amarais.JNB	table.xlsx sigma plot	SF35	The summary table for construction of plots, representing the daily variation in soaring activity of Black vultures at each month and the whole year of observations: from September 2012 to August 2013 (AMARAIS, PRUDENTE).	The plots were constructed using the "hours after sunrise" normalized axis.	
Datasets\Daily_meteo_vultures	AmarXII_ Meteo_F(birds)_aftersunrise.xlsx AmarXII_Meteo&F(birds).jnb	table.xlsx sigma plot	SF36 (a)	The summary table and the plot for graphical analysis studying the daily variation in soaring activity of Black vultures and meteorological characteristics in Amarais site (data averaged for each 15-min interval over 13 viewpoints for December 2012).		
Datasets\Daily_meteo_vultures	AmarVII_ Meteo_F(birds)_aftersunrise.xlsx AmarVII_Meteo&F(birds).jnb	table.xlsx sigma plot	SF36 (b)	The summary table and the plot for graphical analysis studying the daily variation in soaring activity of Black vultures and meteorological characteristics in Amarais site (data averaged for each 15-min interval over 13 viewpoints for July 2013).		
Datasets\Daily_meteo_vultures	PrudXII_ Meteo_F(birds)_aftersunrise.xlsx PrudXII_Meteo&F(birds).jnb	table.xlsx sigma plot	SF36 (c)	The summary table and the plot for graphical analysis studying the daily variation in soaring activity of Black vultures and meteorological characteristics in Prudente site (data averaged for each 15-min interval over 13 viewpoints for December 2012).		
Datasets\Daily_meteo_vultures	PrudVI_ Meteo_F(birds)_aftersunrise.xlsx PrudVI_Meteo&F(birds).jnb	table.xlsx sigma plot	SF36 (d)	The summary table and the plot for graphical analysis studying the daily variation in soaring activity of Black vultures and meteorological characteristics in Prudente site (data averaged for each 15-min interval over 13 viewpoints for June 2013).		
Datasets\Funcrel_Meteo_Soaring	Prud_Meteo_Vultures_funcrel.jnb Amar_Meteo_Vultures_funcrel.jnb		SF37	The summary tables and the plots for implementation of the graphical analysis studying the functional relationship between meteorological conditions and abundance of soaring Black vulture.		
Datasets	MonthDailyTemperature.jnb		SF38	Summary tables for constructing of plots, representing the average monthly temperature (for daily hours) for both studied sites. The plot's construction was based on the meteorological characteristics measured in our research		

				during the bird's observation.		
Datasets\Stat1_meteo_vult	Statanalyses_meteo_vult_Amar.xls x sheets "Amar_sumtab_meteostat"  Statanalyses_meteo_vult_Prud.xlsx sheets "Prud_sumtab_meteostat"		SF39 (a)	The summary tables for implementation of three statistical tests (Principal component analysis, Multiple regression analysis and Pearson correlation analysis) studying the dependence of soaring activity of Black vultures on meteorological conditions. The tables were prepared from the attribute table of the "Georeferenced birds and meteorological parameters" database (SF1, SF2), entitled the "Birds and meteorological parameters" merged database (SF27). AMARAIS, PRUDENTE		Algorithm C1
Datasets\Stat2_surfvult	Surf_regresfactor_amar.xlsx sheet "Prud_surf.reg.fact(3)Ready"  Surf_regresfactor_prud.xlsx sheet "Amar_surf.reg.fact(3)Ready"	table.xlsx	SF40	This is a summary table, which was the basis for implementation of two statistical analyses (Principal component analysis and Multiple regression analysis) studying the dependence of soaring activity of vultures from superficial (relief, surface temperature) and anthropogenic pressure characteristics AMARAIS, PRUDENTE	The tables were prepared from the attribute table of SF15.	Algorithm C4
Datasets\Landscape	Landscapeanalyses_amar.xlsx Sheet "Landscape_Amar_Ready"	table.xlsx	SF41 (a)	Preparing of the "Wbirds and superficial parameters" georeferenced database for implementation of the Landscape analysis studying the dependence of soaring activity of Black vultures on surface covering and anthropogenic pressure (AMARAIS).	It was created from the Landscape_WeightVult_Amar.shp	Algorithm C4
Datasets\Landscape	Landscapeanalyses_prud.xlsx Sheet "Landscape_Prud_Ready"	table.xlsx	SF41 (b)	Preparing of the "Wbirds and superficial parameters" georeferenced database for implementation of the Landscape analysis studying the dependence of soaring activity of Black vultures on surface covering and anthropogenic pressure (PRUDENTE)	It was created from the Landscape_WeightVult_Prud.shp	Algorithm C4
Datasets\Stat2_surfvult\Spearman	amar_gradsurftemp.xlsx amar_surftemperature.xlsx	table.xlsx	SF42 (a)	Preparation of the summary tables for the Spearman rank correlation analysis studying the relationship between soaring activity of vultures and gradient of surface temperature; soaring activity of vultures and surface temperature (AMARAIS).	They were prepared from the attribute table of Surftemp_gradtemp_vult_Amar.shp. (SF16)	Algorithm C4
Datasets\Stat2_surfvult\Spearman	prud_gradsurftemp.xlsx prud_surftemperature.xlsx	table.xlsx	SF42 (b)	Preparation of the summary tables for the Spearman rank correlation analysis, studying the relationship soaring activity of vultures and gradient of surface temperature; soaring activity of vultures and surface temperature (PRUDENTE)	They were prepared from the attribute tables of two shapefiles Gradsurftemp_vult_Prud.shp and Surftemp_vult_Prud.shp. (SF17, SF18)	Algorithm C4

Fields of the shapefiles and derived datasets						
Parameters of bird's registration						
	ID_amar, ID_prud	field		ID number of the bird's observation.		
	ID	field		ID number of the bird's observation with the first letters of the studied airport.		
	Nome_Pob Name_Pob	field		Title of a viewpoint (observation point)		
	N_Pob Npob_prud, Npob_amar	field		The number of the observation point (viewpoint)		
	Lat_Pob	field		Latitude of the observation point (degrees)	Was measured by GPS in the field	
	Long_Pob	field		Longitude of the observation point (degrees)	Was measured by GPS in the field	
	Num_vult Vultures	field		A number of Black vultures in an "ornithological object"		
	Ao_deg	field		Vertical angle to bird (as interval of values), degrees		
	DR_interv	field		Distance to a bird (as interval of values), metres		
	DR_medio	field		Mean value of the DR_interv		
	DD_max_m	field		This is the Smax parameter, which is calculated by the equation: $S_{max} = \cos \beta_{min} * d_{max}$	Where d is the interval of measured distance between observer and bird (metres); $\beta$ - the interval of measured vertical angle between observer and ornithological object (degrees); S - the interval of calculated	Algorithm C1_part2

					distances between viewpoint and projection of ornithological object on surface (metres).	
	DD_min_m	field		This is the Smin parameter, which is calculated by the equation: $S_{min} = \cos \beta_{max} * d_{min}$	The same as for "DD_max_m"	Algorithm C1_part2
	Delta_m	field		This is the Delta parameter, which is calculated by the equation: $\Delta = S_{max} - S_{min}$	The same as for "DD_max_m"	Algorithm C1_part2
	sector	field		The direction to a bird expressed in the sector number of a circle (for $\alpha = 45^\circ$ sector № 1, $\alpha = 90^\circ$ sector №2,... $\alpha = 315^\circ$ sector №7, $\alpha = 360^\circ$ sector №8. The sector parameter was used to construct the projected polygons and to calculate the index "index_k" linking each projected polygon with all birds recorded over it.		
	LAT_PobM	field		Latitude of the observation point (metres)	The values were calculated in ArcGIS from the field "Lat_Pob" for the WGS_1984_UTM_Zone_23S (Amarais) and WGS_1984_UTM_Zone_22S (Presidente Prudente).	Algorithm C1
	LON_PobM	field		Longitude of the observation point (metres)	The values were calculated in ArcGIS from the field "Long_Pob" for the WGS_1984_UTM_Zone_23S (Amarais) and WGS_1984_UTM_Zone_22S (Presidente Prudente).	Algorithm C1
	Pbird_LatM	field		Latitude of each ornithological object (metres)	Geographic coordinates (latitude, longitude) of a mid-point location of each recorded bird (ornithological object) in metres of WGS_1984_UTM_Zone_23S (Amarais), WGS_1984_UTM_Zone_22S (Presidente Prudente).	
	Pbird_LonM	field		Longitude of each ornithological object (metres)	Geographic coordinates (latitude, longitude) of a mid-point location of each recorded bird (ornithological object) in metres of WGS_1984_UTM_Zone_23S	

					(Amarais) and WGS_1984_UTM_Zone_22S (Presidente Prudente).	
	Data	field		Day, month, year of observation		
	dat_txt	field		Date (day, month, year) and Time (hours, minutes) with accuracy of 15 minutes of two types of observations, implemented at the same viewpoint simultaneously: the bird's census and the measurement of meteorological characteristics.	The data saved in column with "text" format. By means of "dat_txt" field the two datasets (Bird's observations and Meteorological characteristics) were linked with each other by ArcGIS tools in a single georeferenced database.	Algorithm C1
	time	field		Time (hours, minutes) of observation		
	month	field		month of observation (1-Jan, 2- Feb, etc)		
	Ao_deg	field		Vertical angle to the ornithological object (degrees)	The vertical angle to the ornithological object (from 0 to 90°) was measured by the inclinometer manual attached to the binoculars and assigned to one of 18 intervals: 2.5-7.5°, 7.5-12.5, 12.5-17.5... 82.5-87.5, 87.5-90°.	
	DR_interv	field		Distance between observer and ornithological object (by 4 intervals, metres)	Distance between the observer and the ornithological object (in meters) was measured using the 12-powered binoculars (CSR 12x50, 87m/1000m) and assigned to one of 4 intervals: 100-200 m, 200-400 m, 400-700 m, 700-6000 m. Birds did not approach to the observer closer than 100 metres, since that the interval from 0 to 100 m was not considered.	
	DR_medio_m	field		Average value of the interval in the "DR_interv" field		

	DD_m	field		Projection of the "DR_medio_m" (distance between the observer and the ornithological object) on the plane (metres)	The DD_m was calculated by the Eq. 2 (div 2.3.2 of Chapter II, Dissertation)	Algorithm C1
	ALT_m	field		The height of an ornithological object above the surface (metres)	The ALT_m was calculated by the Eq. 3 (div 2.3.2 of Chapter II, Dissertation)	Algorithm C1
	PC_deg	field		Direction to ornithological object (degrees)	Direction to the ornithological object (from 0 to 360°), was measured by a compass and attributed to one of 8 intervals (sectors of compass): 22.5-67.5°, 67.5-112.5°, 112.5-157.5°, 157.5-202.5°, 202.5-247.5°, 247.5-292.5°, 292.5-337.5°, 337.5-360°.	
	PC_rad	field		Direction to ornithological object (radian)	The field was calculated in ArcGIS from the PC_deg Filed. This calculation can be implemented also in Excel.	
	Aeroporto	field		Airport of study		
Meteorological parameters measured during the 15 minutes intervals (8:00-8:15; 8:16-8:30, 8:31-8:45.....17:46-18:00)						
	HiTemp	field		Maximum air temperature at a 15 minutes interval (degrees Celsius)		
	Out_Hum	field		Relative humidity at a 15 minutes interval (%)		
	HiWinSpeed Hi_Speed	field		Maximum wind speed at a 15 minutes interval (km/h)		
	Wind_Speed			Random wind speed parameter at a 15 minutes interval (km/h) (was not applied in the analyses)		
	HiWinDir Hi_Dir	field		Most frequent wind direction in a 15 minutes interval		
	BAR_hpa BAR	field		The atmospheric pressure in a 15 minutes interval (hPa)		



	HiSolarRad Hi_Solar_R	field		The maximum solar radiation at a 15 minutes interval (W/m <sup>2</sup> ). Was measured only for Amaraïs (April-August 2013).		
	Solar_Ener SolEnergy	field		The solar energy at a 15 minutes interval (Langley) It was measured only for Amaraïs site (April-August 2013).	1 Langley (Ly) = 11.622 Watt-hours per square meter = 41.84 kilojoules per square meter	
Projected polygons, $W_{birds}$ , $F_{birds}$						
	UAid_amar UAid_prud	field		The unique number of each projected polygon constructed with the maximum radius of 6000 m.		
	Fbirds F(birds) r_vult_amar r_vult_prud r_vult R(vult) Rvult	field		The Frequency of soaring birds records or Fbirds index calculated by the equation: $Fbirds = \sum birds / \sum reviews$ where $\sum birds$ represents the number of registered Black vultures in a set of viewpoints during a 15- or 60-minute interval and $\sum reviews$ is a total amount of sky reviews yielded in those viewpoints at the same time.		
	SUMvult_UA	field		The sum of birds registered in a single projected polygon with ID=UAid_amar during the period of observation		
	SumVULT	field		The sum of vultures, registered in all projected polygons above a given spatial unit (projected polygon, square cell, point, i.e. any polygonal or point object) during the whole year of observation.		
	DivSumVul8	field		The sum of vultures registered in all projected polygons above a given spatial unit (projected polygon, square cell, point, i.e. any polygonal or point object) during the whole year of observation. Unlike to the SumVULT parameter, the technical defect of improper increase the number of birds at a vertical angle equal of 90 degrees was considered here.  For projected polygons with $Ao = 90$ deg: $DivSumVul8 = SumVULT / 8$ ; For all other projected polygons ( $Ao = 5-85$ deg), $DivSumVul8 = SumVULT$		
	AvgVULT	field		The average number of birds, registered in a single projected polygon in a given spatial unit. It is calculated by the equation: $SumVULT / Conut$ Where SumVULT - here id=3, Count -here, id=4	It was calculated without division of the sum of birds recorded with angle = 90 deg on 8.	

	AvDiv8Vult, Avg_SUMvul Avg_Del8Vult	field		The average number of birds registered in a single projected polygon in a given cell. In other words, it is the WbirdsYear field divided by 3 or the Wbirds index calculated without multiplication by 3.	For calculation this parameter in all circular georeferenced polygons (i.e. with angle to a bird = 90 deg) the number of their registered birds was divided in 8.	
	WbirdsYear 3AvgVULT	field		The Weight of birds or Wbirds index, calculated for a year for a given spatial unit by the equation: $Wbirds = 3(\sum birds) / (\sum polygons)$ where $\sum birds$ represents a number of registered Black vultures in all three-dimensional shapes above the given point (i.e. in all overlapped projected polygons) and $\sum polygons$ is a total amount of their overlapping projections. The ratio was multiplied by 3 to bring the value of index at each point to position of viewpoint, representing the actual number of birds that were soaring over each point of the studied area during the observation hours.	The multiplication by 3 is not necessary for Wbirds index representation. We used it only to approximate the number of index to the real number of birds that were soaring over each point of the studied area during the observation hours. Since that, we used index only as ratio (without multiplication by 3) in statistical tests.	
	Wbird_1Ha	field		Wbirds index calculated for a year for a 1 hectare of a landscape type		
	SumDiv8Vul Sum_Del8Vu Sum_Del8Vult			Sum of "AvDiv8Vult" parameter in all georeferenced polygons overlapping over a given cell	For calculation this parameter in all circular georeferenced polygons (i.e. with angle to a bird = 90 deg) the number of their registered birds was divided in 8.	
	Count	field		The number of overlapping georeferenced polygons over a given cell	Cell - is a polygon object representing by a line of the attribute table of shape polygon theme.	
	index_k, Sum_index, Sum_ind90			The identification index, which was calculated for each projected polygon using the parameters of its construction: the number of viewpoint, vertical angle to bird, direction to bird (sector). The index was used for linking of each projected polygon with all birds recorded over it. The equation was different for vertical angle <90 degrees and vertical angle equal 90 degrees. In the attribute table of shapefiles this index is entitled as "Sum_index" for vertical angle < 90°, "Sum_ind90" for vertical angle = 90° and "index_k" – for all angles (this field combines values of index from both previous fields) .	The technique of linking of each projected polygon with all birds recorded over it by indexing and equations of index_k is considered in the Algorithm C3	Algorithm C3
	devPob, devSect, devAo			Parameters for calculation of "index_k": $devPob = N\_Pob / 100$ ; $devSect = sector / 1000$ ; $devAo = Ao\_deg / 100000$		

Superficial parameters						
	TempSuf_C	field		Surface temperature (degrees of Celsius)	The parameter was obtained directly from AST_08 (the derivative product of ASTER image)	
	Avg_TempSuf_C Avg_TempSu	field		The mean value of surface temperature parameter (TempSuf_C field) within a spatial unit (Celsius degrees)	It was calculated in ArcGIS as the average temperature of all overlapping "temperature cells" of field "TempSuf_C" in a 30x30 m cell	
	Min_TempSu Max_TempSu			The minimum and maximum value of surface temperature parameter (TempSuf_C field) within a spatial unit (Celsius degrees) (Were not applied in the analyses)		
	Height_m	field		Altitude above sea level (metres)	The parameter was obtained directly from ASTER GDEMv2 (the derivative product of ASTER imagery)	
	Aspect	field		Exposure, aspect or slope direction (0-360 degrees)	The parameter was calculated by Aspect Tool of ArcGIS	
	SlopeRelGr	field		Inclination or slope angle, 0-90 degrees	The parameter was calculated by Slope Tool of ArcGIS	
	Landscape			A type of surface covering or landscape type, according to the elaborated classification.		
	LandDetail			Details of landscape description. For "heavy urbanized" zone this field marks a landscape type – "dense residential area" or "industrial area". In the analyses both types were considered separately.		
	StressAnth			Level of anthropogenic stress inherent to a landscape type according to the elaborated classification.		
	Details	field		details of surface covering		
	GradFoc n2GradFoc ("GradTemp1" in tables)	field		The gradient (or contrast) of surface temperature, calculated with the help of Focal Statistics Tools of ArcGIS. (method 1). It was not used in the analyses.	It was calculated from TempSuf_C field in ArcGIS by dint of Focal Statistic.	

	Avg_GradFoc	field		The Mean of the gradient of surface temperature parameter obtained by the method1 It was not used in analyses.	It was calculated in ArcGIS as the averaged value of field GradFoc	
	SlopTemGR or GradSlopTg ("GradTemp_slope_deg" or "GradTempSlop_deg" in tables)	field		The gradient (or contrast) of surface temperature, calculated in the Slope Tool of ArcGIS (angle degrees). The statistical analyses were conducted using only this variant of calculation of the gradient of surface temperature parameter. (method 2)	It was calculated in ArcGIS by Slope Tool. The final analyses were conducted using only this variant of calculation of gradient of surface temperature parameter.	
	Avg_SlopeTemGR Avg_GradSl Avg_SlopTe	field		The mean of the gradient or contrast of surface temperature parameter. It was calculated in ArcGIS as the averaged value of SlopTemGR field (angle degrees)		
	Min_GradSl Max_GradSl			The Minimum and Maximum values of the gradient or contrast of surface temperature parameter calculated in ArcGIS by SlopTemGR field (angle degrees) They were not used in analyses.		
	Area	field		Area of a spatial unit, square meters		
	SumArea	field		Sum of area of all polygonal cells		
	SumBirds	field		Sum of "AvDiv8Vult" parameter over each landscape type	AvDiv8Vult - parameter which reflects the number of registered vultures	
	SumBirds(i), %	field		The percent of total amount of birds registered in each landscape type (100% - the total sum of all registered birds)		
	SumArea(part_i)	field		The percent of area of each landscape type		
	SumBirds(i)/ SumArea(part_i)	field		Normalization by area or bringing all to the area equal to "1" (i.e. this value shows the number of birds in case the object occupies the area equal to 1.)		

Technical Descriptions (Appendices C)						
Article 1 (Chapter II)						
	Algorithm C1			Preparation of the “Georeferenced birds and meteorological parameters” database as a base for implementation of analyses		
	Algorithm C2			Transformation of timescale to the relative biological timescale and normalized relative biological timescale		
Article 2 (Chapter III)						
	Algorithm C3			Georeferencing of the recorded birds through the projected polygons		
	Algorithm C4			Preparation of the “Wbirds and superficial parameters” georeferenced database for statistical analyses implementation		
	Algorithm C5			The technique of cartographic visualization of the abundance of soaring Black vultures and the risk of collisions with these birds over the territory		

## APPENDIX D – DECLARATIONS



COORDENADORIA DE PÓS-GRADUAÇÃO  
INSTITUTO DE BIOLOGIA  
Universidade Estadual de Campinas  
Caixa Postal 6109, 13083-970, Campinas, SP, Brasil  
Fone (19) 3521-6378. email: cpgib@unicamp.br



### DECLARAÇÃO

Em observância ao §5º do Artigo 1º da Informação CCPG-UNICAMP/001/15, referente a Bioética e Biossegurança, declaro que o conteúdo de minha Dissertação de Mestrado, intitulada ***"Análise do efeito das condições meteorológicas, superficiais e antropogênicas sobre atividade de voo do Urubu-de-cabeça-preta (Coragyps atratus, Cathartidae) por meio de SIG e sensoriamento remoto e suas implicações para a redução do risco de colisões com aeronaves"***, desenvolvida no Programa de Pós-Graduação em Biociências e Tecnologia de Produtos Bioativos do Instituto de Biologia da Unicamp, não versa sobre pesquisa envolvendo seres humanos, animais ou temas afetos a Biossegurança.

Assinatura: \_\_\_\_\_

Nome do(a) aluno(a): Natalia Novoselova

Assinatura: \_\_\_\_\_


Nome do(a) orientador(a): Wesley Rodrigues Silva

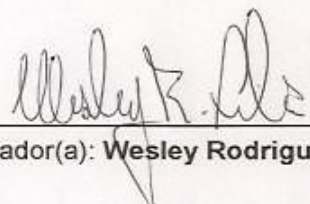
Data: 28.06.2016

**Profa. Dra. Rachel Meneguello**  
Presidente  
Comissão Central de Pós-Graduação  
**Declaração**

As cópias de artigos de minha autoria ou de minha co-autoria, já publicados ou submetidos para publicação em revistas científicas ou anais de congressos sujeitos a arbitragem, que constam da minha Dissertação/Tese de Mestrado/~~Doutorado~~, intitulada **Análise do efeito das condições meteorológicas, superficiais e antropogênicas sobre atividade de voo do Urubu-de-cabeça-preta (Coragyps atratus, Cathartidae) por meio de SIG e sensoriamento remoto e suas implicações para a redução do risco de colisões com aeronaves**, não infringem os dispositivos da Lei n.º 9.610/98, nem o direito autoral de qualquer editora.

Campinas, 28.06.2016

Assinatura :   
Nome do(a) autor(a): **Natalia Novoselova**  
RG n.º V796951A

Assinatura :   
Nome do(a) orientador(a): **Wesley Rodrigues Silva**  
RG n.º